12-1-2012

Cannabinoid 2 receptor (CB2R) agonists modulate neuropathic pain and cytokine expression

Jenny Wilkerson

Jenny L. Wilkerson
Candidate

Biomedical Sciences- Department of Neurosciences
Department

This dissertation is approved, and it is acceptable in quality and form for publication:

Approved by the Dissertation Committee:

Erin D. Milligan, PhD, Chairperson

James Wallace, PhD

Lee Anna Cunningham, PhD

Oscar Bizzozero, PhD

CANNABINOID 2 RECEPTOR (CB2R) AGONISTS MODULATE NEUROPATHIC PAIN AND CYTOKINE EXPRESSION

by

JENNY L. WILKERSON

B.S. Biology, Northwest Missouri State University, 2004

DISSERTATION

Submitted in Partial Fulfillment of the
Requirements for the Degree of

Doctor of Philosophy
Biomedical Sciences

The University of New Mexico
Albuquerque, New Mexico

November, 2012

Acknowledgements

There are so many people that have helped me throughout my life, making my journey towards obtaining my doctorate possible. First, I need to recognize all those teachers that inspired and encouraged me throughout my schooling. In particular, my first grade teacher, Mrs. Trutzel, stands out, as she spent countless hours privately tutoring me in lesson areas where I needed help. Her tireless dedication to her students is both commendable and honorable in so many ways, and her contribution in my life is truly immeasurable. Secondly, I must acknowledge the team of physicians that mended a physically broken newborn so many years ago, and allowed me the chance of a normal life. It is those physicians, and the medical researchers that developed the life-saving surgical and critical care skills that allowed me to live, that has inspired me to dedicate my professional career towards medical research.

My family has been so supportive in me reaching for my dreams throughout the years, even though I know it was bittersweet for them to watch me fly away. Thank you so much for always believing in me, and encouraging me to follow my dreams. My mother is truly amazing, as she allowed me the freedom to become my own person, and to find my own passions in life. I also owe my love of reading and books to my mom, as she ritually took me to our local library to participate in their summer reading program. Both my parents sacrificed so much, so that I may have a good life, and of which, I will never forget. In this time of remembrance, I must honor my late grandmother, Myra Lynn. I was blessed to have her a part of the first 15 years of my life. She was truly an inspiring,

remarkable, thoughtful and kind person with incredible inner strength, and she is my most important role model. I count myself as blessed to have such phenomenal experiences from being in Girl Scouts, and special thanks goes out to my extended Girl Scout family- you are all amazing women. I am so thankful to both my family and my friends for the love, support, well-wishes, shoulders that were leaned on, and ears that were talked nearly off, throughout this process. My wonderful husband, Jesse, has been my rock and source of strength. Through the years we have been together, he has stood by me, comforted me, and put me and my goals first. He has been willing to follow me wherever I go in life, and does so many little things to help, to make me laugh, and to show his undying love, devotion and support. I cannot express in words how thankful I am to him, and I am excited to see where life takes us from here.

The mentoring that I have received at the University of New Mexico has been terrific. I cannot say thank you enough to Dr. Maggie Warner-Washburne, and the UNM Initiatives to Maximize Student Diversity (IMSD) program for the financial support of my first two years of graduate work, and for the mentoring that did not cease after the program. Dr. Linda Saland and Dr. Jim Wallace are both incredible scientists and amazing people in the department of Neuroscience at UNM. They have provided so much guidance in my development as a scientist, and their dedication to teaching the next generation of physicians and basic scientists is evident in the interactions that I have had with each of them. My committee on studies has provided both wonderful praises, as well as a critical eye in my progress, and I greatly thank the members of my committee for

both. Above all, I owe my P.I. and primary mentor, Erin Milligan, for molding and making me into the scientist that I have become. She has been a wonderful role model through the years. She has believed in me, guided me, and both mentally and financially supported me throughout my years in her laboratory. She pushed me to perform beyond my own initial expectations of myself, towards my true potential. Also, she has taught me to personally accept only the highest standards of excellence in my professional development. I am so grateful to have had her has my mentor. I also am very much indebted to all the past and present laboratory personnel that I have had the pleasure to work with and come to know. Each one of you, in your own way, left an indelible mark on me, and I thank you for helping me grow as a person, as a scientist, and where appropriate, as a mentor. I must acknowledge the aid that I received from Dr. Clark Bird from UNM department of Neuroscience in his assistance in designing my CB1R primers. I also must thank the marvelous support staff at UNM for so many 'behind the scenes' contributions. Thank you to the BSGP staff and the Neurosciences department staff for the administrative support that you have shown me through the years. Thank you to Buz Tyler, who has provided so much invaluable I.T. support, and the Cancer Resource Facility microscopy suite personnel for their expertise on microscopy. Also, a big thank you goes out to the Animal Resource Facility and its staff in doing what you all do, because without it I would not have been able to complete my dissertation.

Table of Contents

Cannabinoid 2 Receptor Agonists Modulate Neuropathic Pain and Cytokine Production

By

Jenny Linn Wilkerson

Abstract

The focus of the work in this dissertation is to elucidate the efficacy of cannabinoid 2 receptor agonists, specifically targeting the spinal cord, for the treatment of chronic neuropathic pain. Chemical structures for all cannabinoid compounds utilized are displayed (Supplemental Figure A-1). As an orientation for the reader, the organization of this dissertation consists of five components; chapters 1 through 5. In the first chapter, a background is developed to acquaint one with the topics of chronic pain, and the use of cannabinergic compounds for chronic pain relief. This chapter is in the form of a review, and specifically addresses (1) the underlying differences in physiological processes during periods of acute pain compared to chronic pain, (2) the role of spinal cord glial cells under conditions of chronic inflammation, reflecting what is seen under chronic pain conditions, (3) the endogenous cannabinoid system, (4) evidence that specifically targeting the cannabinoid 2 receptor in the spinal cord may eventually be ideal for the treatment of chronic pain, and (5) the current clinical trial endeavors utilizing cannabinoid 2 receptor agonists. Following the review,

evidence will be presented in support of the stated specific aims. Specific aim 1 of this dissertation will be in the form of two published manuscripts.

The first manuscript, Chapter 2, explores the efficacy of one of the most widely utilized cannabinoid 2 receptor agonists, AM1241 following a peri-spinal, intrathecal injection. I display a dose-dependent effect, and the timecourse of the compound's ability to reverse pain symptoms. Further, using immunohistochemical techniques I detail a novel method of quantifying discrete anatomical changes in the immunostaining of inflammatory markers via the use of a computer assisted analysis of the entire spectral range of a variety of fluorescently-tagged antibodies. I refer to this method as 'spectral analysis'. This spectral analysis approach is more sensitive and accuate than conventional methods. Finally, this manuscript examines changes in critical factors known to mediate pathological pain in both the dorsal horn of the spinal cord and the dorsal root ganglia.

The second manuscript, Chapter 3, explores the efficacy of a novel cannabinoid 2 receptor agonist AM1710 belonging to a chemically distinct classification of cannabinoid-like compounds following a peri-spinal, intrathecal injection. As in the first manuscript, for this compound, I display a dose-dependent effect, and the time course of the compound's ability to reverse pain symptoms. Additionally, spectral analysis methods are utilized to examine AM1710's ability to alter levels of critical factors known to mediate pathological pain, in both the spinal cord dorsal horn and the dorsal root ganglia. Finally, this manuscript characterizes

AM1710's ability to act through anti-inflammatory pathways via peri-spinal glial cells within the meninges surrounding the spinal cord to block the development of neuropathic pain in a purely immune-mediated model of chronic pain.

Specific aim 2 is in the form of a fourth manuscript to be submitted for peer-review in The Journal of Pain. The studies presented here within Chapter 4, are completed and provide evidence for AM1710's specificity to act via a restricted cannabinoid type 2 receptor, and not on the other classical cannabinoid receptor, the cannabinoid type 1 receptor. Further, the use of transgenic mice that lack functional cannabinoid 1 receptors uncovers a potentially novel and protective role of the endocannabinoid system under chronic pain conditions.

Chapter 5 consists of a discussion of the main points from all the prior chapters to support the overarching thesis that the use of cannabinoid 2 receptor agonists is effective for the treatment of neuropathic pain. Additionally presented is a critique of some of the methods used to conduct experiments, and a supporting rationale for why these methods were selected. This dissertation concludes with potential future directions of this work, to further elucidate the endocannabinoid system for pain control.

List of Figures

Abbreviations

2-AG = 2-Arachidonylglycerol

AEA = Anandamide

ALS = Amyotrophic lateral sclerosis

AMPA = α-amino-3hydroxyl-5methyl-4-isoxazolepropionic acid

ATP = Adenosine triphosphate

BL = Baseline

CB_1R = Cannabinoid 1 receptor

CB_2R = Cannabinoid 2 receptor

CCI= Chronic constriction injury

CFA = Complete Freund's adjuvant

CNS = Central nervous system

CSF = Cerebral spinal fluid

DAPI = 4',6-diamidino-2-phenylindole

DRG = Dorsal root ganglia

EDTA = Ethylenediaminetetraacetic acid

ERK = Extracellular signal-regulated kinase-1

FAAH = Fatty acid amide hydrolase

GFAP = Glial fibriliary acidic protein

Gp120 = Glycoprotein 120

Het = Heterozygous

IBA-1 = Ionized calcium binding adaptor molecule – 1

IHC = Immunohistochemistry

IL-1β = Interleukin 1 beta

IL-10 = Interleukin 10

iNOS = Inducible nitric oxide

I.p. = Intraperitoneal

IR = Immunoreactivity

ISH = In situ hybridization

I.t. = Intrathecal

JNK = C-Jun N-terminal kinase

KO = Knockout

LPS = Lipopolysaccharide

MAGL = Monoacylglcerol lipase

MCP-1 = Monocyte chemoattractant protein-1 (CCL2)

mGluR = Metabotrophic glutamate receptor

MKP = Mitogen-activated kinase-phosphatase

MS = Multiple sclerosis

NDS = Normal donkey serum

NF-H = Neurofilament heavy

NK1 = Neurokinin 1

NMDA = N-Methyl-D-Aspartic acid

NO = Nitric oxide

PBS = Phosphate buffered saline

p-p38MAPK = Phosphorylated p38 MAPK

ROI = Region of interest

SNL= Sciatic nerve ligation

TNF-α = Tumor necrosis factor alpha

TLR4 = Toll-like receptor 4

TRPV-1 = Transient receptor potential cation channel subfamily V member 1

TSPO = Translocator protein

WDR = Wide dynamic range neuron

WT = Wild type

1. The central role of glia in pathological pain and the potential of targeting the cannabinoid 2 receptor for pain relief

ISRN Anesthesiology

Review

Authors: Jenny L. Wilkerson* and Erin D. Milligan

Department of Neurosciences, School of Medicine, University of New Mexico, Albuquerque, NM 87131

JLWilkerson@salud.unm.edu, EMilligan@salud.unm.edu

* Corresponding Author:
Jenny L. Wilkerson
University of New Mexico, HSC
Dept. of Neurosciences
MSC08- 4740
1 University of New Mexico
Albuquerque, NM 87131
Email: JLWilkerson@salud.unm.edu

Abstract

Under normal conditions, acute pain processing consists of well-characterized neuronal signaling events. When dysfunctional pain signaling occurs, pathological pain ensues. Glial activation and their released factors participate in the mediation of pathological pain. The use of cannabinoid compounds for pain relief is currently an area of great interest for both basic scientists and physicians. These compounds, bind mainly either the cannabinoid receptor subtype 1 (CB_1R) or cannabinoid receptor subtype 2 (CB_2R), and are able to modulate pain. Although cannabinoids were initially only thought to modulate pain via neuronal mechanisms within the central nervous system, strong evidence now supports that CB_2R cannabinioid compounds are capable of modulating the activity or function of glia, (e.g. astrocytes and microglia) for pain relief. However, the mechanisms underlying cannabinoid receptor-mediated pain

relief remain largely unknown. An emerging body of evidence supports that CB_2R agonist compounds may prove to be powerful novel therapeutic candidates for the treatment of chronic pain.

Keywords: review, endocannabinoid, MAGL, DRG, IL-1β, spinal cord, microglia, astrocytes, CB_2R

Chronic pathological pain is one of the most common reasons to seek medical attention and is reaching worldwide epidemic proportions [1]. Chronic pain becomes pathological as a consequence of abnormal pain signaling and is often manifested in numerous diseases, such as diabetes, arthritis, amyotrophic lateral sclerosis (ALS), multiple sclerosis (MS), and cancer [2-6]. Glial cells, which include oligodendrocytes, astrocytes and microglia, have been found to play key roles when chronic pain becomes pathological. Given less is known about the involvement of oligodendrocytes, this review will focus primarily on astrocytes and microglial cells in chronic pain processing.

Cannabinoid compounds are emerging as novel therapeutic targets for the treatment of chronic neuropathic pain [7]. These compounds, with subsequent CB1 and CB2 receptor (CB_1R and CB_2R, respectively) activation, are able to modulate pain through a number of mechanisms involving alterations in microglial functions [8]. This review will first discuss how normal pain becomes pathological and the role of activated glia in mediating such pain. These sections will be followed by addressing cannabinoid-mediated modulation of glial proinflammatory factors, which are known to produce chronic neuropathic pain in

animal models. An emphasis will be made on the CB_2R. Given this review focuses on the action of the CB_2R, a discussion is included on the current states of clinical trials examining the potential efficacy of CB_2R agonists as pain therapeutics.

1.1 Normal vs. pathological pain

1.1.1 Acute Pain Signaling

Acute pain processing is distinct from the etiology underlying chronic pathological pain. Distinguishing the cellular responses and underlying signaling cascades that are unique to pathological pain may prove critical in understanding why many neuronally-targeted treatments do not prove to be effective in relieving chronic pathological pain in the clinical setting. In acute pain, such as that caused by high intensity stimuli from mechanical stimulation (e.g. pinprick), unmyelinated C and lightly myelinated Aδ nociceptive nerve fiber terminals in the body depolarize and transduce this information into action potentials that travel through the peripheral axon to the dorsal root ganglia (DRG). The centrally projecting terminals of these nociceptors predominantly enter the spinal cord dorsal horn to reach the superficial (laminae I - II) and deeper lamina IV-V, and synapse onto second order pain projection neurons located in lamina I, IV and V [9-11]. The classical neurotransmitter primarily responsible for synaptic communication between nociceptors and pain projection neurons is the excitatory amino acid glutamate. Glutamate then binds and activates the ionotropic α-amino-3hydroxyl-5-methyl-4-isoxazolepropionic acid (AMPA) and kainate receptors as well as metabotropic glutamate receptors (mGluR 1, 3, 5

and 7) [12]. Additionally, a number of nociceptive-related neuropeptides acting in the spinal cord dorsal horn have been identified to play key roles in pain neurotransmission. For example, the classic neuropeptide, substance P, is released from primary nociceptive afferents [13]. Substance P then binds and activates its receptor, neurokinin 1 (NK1), which is present in high concentrations on dorsal horn lamina I neurons. Both substance P and its NK1 receptor are widely known to play a significant role in nociceptive processing [14]. These spinal cord nociceptive neurotransmitters, along with their receptors, are critical for activating second order neurons, which communicate to supraspinal pain-processing centers and elicit reflexive and protective responses to avoid potential or further tissue damage.

1.1.2 Central Sensitization

However, under some circumstances, incoming nociceptive signaling is prolonged leading to clinical manifestations of pathological neuronal signaling. Examples of such pathological states are hyperalgesia, which is decreased threshold to nociceptive stimuli, and dynamic tactile allodynia, which is increased sensitivity to non-nociceptive light touch. Both pain states often occur in regions beyond the tissue-injured site. The underlying neurobiological events initiated by prolonged nociceptive signaling include increased synaptic function triggered within the central nervous system. Specifically, these events are known to occur within the dorsal horn of the spinal cord, and culminate in a process termed, spinal sensitization of pain projection neurons [15, 16]. Once triggered, this central sensitization is sustained despite the termination of noxious input.

Experimentally, continued activity is substantially extended following the end of the stimulus application [17, 18]. These seminal early studies suggested that pain may be experienced even in the absence of peripheral noxious stimuli.

Pathological pain results from inflammation and/or trauma to peripheral nerve(s), tissue(s), or the central nervous system (CNS), and may arise as a complication to numerous medical conditions. Various animal models have been developed to induce conditions similar to those observed clinically. Neuropathic pain is commonly studied in models of peripheral nerve injury/inflammation. Models of diabetic neuropathy, chemotherapy-induced pain, post-surgical pain, and osteoarthritis pain are well-established examples, and reports of these are cited throughout this review. Although distinct in disease etiology, peripheral neuropathies share in the manifestation of pathological pain. This pathological processing is initially triggered by incoming noxious signals from nociceptors leading to central sensitization. One classically known mechanism for spinal sensitization involves excitation of pain projection neurons in the superficial laminae of the spinal cord dorsal horn as well as wide dynamic range neurons (WDR) located in deeper lamina IV and V that process the rapid and intense nerve depolarizations. Following prolonged and significant depolarization by the actions of glutamate and substance P, spinal pain projection neurons become sensitized, leading to the activation of N-Methyl-D-Aspartic Acid (NMDA) receptors that are normally inactive due to a Mg^{2+} plug within the cation channel. Prolonged depolarization induces Mg^{2+} release followed by enhanced influx of Ca^{2+} [19, 20]. A cascade of intracellular events occurs, which ultimately leads to

post-synaptic enhancement of AMPA and mGlu receptor action, thereby increasing synaptic efficacy [21].

1.1.3 Sensory Changes in Pathological Pain

Increasing synaptic efficacy exerts profound changes in dorsal horn sensory processing [16, 22]. Indeed, enhanced synaptic efficacy, initiated by low intensity mechanosensitive Aβ fibers, occurs at synapses on pain projection neurons in the dorsal horn [23], creating the perceptual equivalent of a noxious stimulus. Activated low-intensity Aβ fibers, that carry non-painful information such as light touch, are now capable of activating high intensity nociceptive neurons resulting in the clinical phenomenon known as allodynia. That is, non-painful light touch is coded as painful, leading to a pain sensation that occurs in the absence of noxious input. Despite the fact that the stimulus is initiated in the periphery, its manifestation is a consequence of central changes like sensitization in the spinal cord [15]. Both allodynia and hyperalgesia are a hallmark of pathological pain [15, 16].

1.2 The role of glia in pathological pain

1.2.1 Glial activation

While it is clear that neuronal processes are critical for spinal sensitization leading to pathological pain signaling, non-neuronal glial mechanisms are also important [24]. Under persistent pathological conditions, the availability of neuropeptides, such as substance P and amino acid neurotransmitters like glutamate are increased and able to bind their receptors not only on neurons, but

also on astrocytes as well as parenchymal and perivascular microglia. Glial "activation" ensues and sets in motion a cascade of excitatory signaling events [25].

At the onset and during pathological pain conditions, multiple signaling cascades within glia are triggered including the activation of p38 mitogen activated protein kinase (p-p38MAPK) and the c-Jun N-terminal kinase (JNK) pathways via phosphorylation events. Consequently, downstream cascades are initiated, including NF-κβ activation, a cytokine nuclear transcription factor, and lead to the subsequent production of pro-inflammatory cytokines such as interleukin-1β (IL-1β) and tumor necrosis factor-α (TNF-α), as well as chemokines (chemo-attractant cytokines) [25-30]. It is important to note that multiple signaling pathways can activate NF-κβ leading to altered gene expression. For example, glially released TNF-α, when bound to its receptor, leads to phosphorylation of p38MAPK (p-p38MAPK) and NF-κβ activation. Alternatively, IL-1β, when bound to its receptor, can directly activate NF-κβ [31, 32]. In the spinal cord, IL-1β and TNF-α can further directly excite neurons because neurons express receptors for these cytokines. Indirect neuronal stimulation occurs by cytokine-induced release of additional excitatory mediators such as prostaglandins and nitric oxide (NO). It has been reported that spinal p38MAPK, JNK and the extracellular signal-regulated kinase, ERK1/2, also referred to as MAPK3/1, are critical mediators of pathological pain in animal models [33-37]. For example, sciatic nerve ligation (SNL), a well characterized rodent model of peripheral nerve injury, leads to increased p38MAPK in spinal astrocytes and microglia, and upon spinal

pharmacological blockade with the p-p38MAPK inhibitor SB203580, p38MAPK activation with associated neuropathic pain is diminished [34]. Although very little is known about oligodendrocyte signaling in chronic pain, emerging evidence suggests that these cells are not merely passive observers to chronic pain, but rather these cells may also up-regulate (phosphorylated) p-AKT, a factor that has been found to mediate apoptosis, cell migration and motility in the dorsal horn of the spinal cord. Phosphorylated-AKT may be critical to the previously discussed spinal cord neuronal sensitization process [38].

It is notable that activated microglia respond to and produce inducible nitric oxide synthase (iNOS), and likewise activated astrocytes release NO [39, 40]. The production of NO by both neurons and glia is characteristic of neuroinflammation [41-44]. Thus, upon spinal glial activation from NO (among several other activating factors), intracellular signaling cascades lead to increases in cytokines and diffusible factors that further activate neighboring neurons and glia. That is, IL-1β and TNF-α lead to a feed-forward loop of further JNK and MAPK signaling, NF-κβ activation, and increased NO, cytokine, and chemokine production, which all contribute to ongoing pathological pain.

While microglia and immune-like astrocytes respond to spinal IL-1β and TNF-α resulting in pathological pain, increased peripheral immune cell (neutrophils, lymphocytes, monocytes, macrophages) migration to critical regions of nociceptive processing, such as the DRG and the spinal cord dorsal horn also occurs in response to cytokines [39, 45-47]. The specific underlying mechanisms

are poorly understood. What is known, however, is that cellular enrichment at these critically important anatomical sites takes place via increased immune cell actin remodeling and proliferation in response to chemotactic signaling [45, 48, 49].

1.2.2 Glial morphology and activation markers

Activated glial cells typically undergo changes in morphology, proliferation and migration, termed gliosis. For example, astrocytes up-regulate vimentin and glial fibrillary acidic protein (GFAP), and become highly arborized with thickened processes [50]. These changes in morphology and increased GFAP expression are often considered a sign of spinal cord pathogenesis during the expression of neuropathic pain in animal models, and are thought to be indicative of CNS inflammatory processes [26, 50, 51]. A report examining cellular enrichment of the spinal cord in a peripheral nerve injury rat-model of pain identified that microglial cells are more proliferative and undergo more clustering than astrocytes [52]. Microglia, when activated, typically up-regulate the cellular makers, ionized calcium binding adaptor molecule-1 (Iba-1), and CD11b/c, also known as OX42 [52-57]. However, the up-regulation of these proteins is not always indicative of proinflammatory phenotypic processes of glial cells. For example, activated microglia can additionally express ED2, a classic anti-inflammatory marker, suggesting that activated microglia are not solely engaged in proinflammatory processes [58, 59].

Although these cellular changes have been widely documented in animal models of chronic pain, less is known about whether glial activation always reflects inflammation and whether it contributes to chronic pain in humans. What is known is that gliosis occurs within the spinal cord of patients with neuroimmune diseases such as ALS, MS, and spodylytic myopathy [60, 61]. It is noteworthy that these patients often report chronic pain symptoms [4, 6]. Furthermore, post mortem tissue analysis from these patients often reveals gliosis concominant with the disease, and as such, these glial changes may contribute to chronic pain in these patients. However, the role of these cellular markers in animal models of chronic pain are not fully understood, as reports show a disconnection between glial marker up-regulation, proinflammatory signaling markers, and behavior associated with pain. For example, while fluorocitrate attenuated up-regulation of GFAP in mice with the chronic constriction injury of the sciatic nerve (CCI), another commonly used model of chronic neuropathic pain, chronic pain symptoms remained unchanged [53]. Additionally, in separate studies utilizing a paw incision model of postsurgical pain, chronic morphine administered subcutaneously delayed the normal resolution of allodynia and hyperalgesia, which was observed with saline-injected controls. Tissues from the corresponding groups in this study were analyzed for GFAP, Iba-1, p-ERK and p-p38MAPK, with saline injected animals showing clear behavioral resolution, which was absent in the morphine treated groups. Strikingly, no differences in GFAP or Iba-1 immunoreactivity were observed between saline or chronic morphine-treated groups. However, p-ERK and p-38MAPK were increased in the

chronic morphine treated groups, corresponding to their behavioral profile [62]. Conversely, perivascular microglia have been shown to remain in an activated state as assessed by immunohistochemical detection of ED2 during the presence of pain reversal [63]. From these studies, and as noted previously, the presence or absence of glial activation, per se, is too simplistic to fully understand a glial role in chronic pain. It is possible that microglia can remain activated while producing and releasing anti-inflammatory factors that ultimately lead to pain suppression [64, 65].

1.2.3 Downstream glial signaling of cytokines

Both IL-1β and TNF-α induce chemotactic activity on CNS microglia and astrocytes. Indeed, once activated, microglia and astrocytes are well known to undergo migration and proliferation in the spinal cord under conditions of chronic pain [52]. Recently, it has been shown that an increase in glial cell numbers occurs within the ipsilateral dorsal horn of the spinal cord following unilateral peripheral nerve injury [66].

During pathological pain states, peripheral immune cells additionally migrate to critical CNS pain processing sites. However, the contribution of peripheral vs. CNS immune cell actions with subsequent cytokine signaling to neuropathic pain is not fully understood. Rat spinal cord meninges contain peripheral immunocompentent cells such as macrophages, and following in vitro stimulation of isolated meninges with the administration of the HIV-1 envelope glycoprotein gp120, IL-1β and TNF-α were released [67]. These data suggest that meningeal

cells, characterized to include peripheral immune cells like macrophages, contribute to ongoing spinal cord glial activation via proinflammatory cytokine actions. Given these compelling data, we explored the possibility that anatomically intact meninges contain macrophages that express IL-1β. Here, we utilized immunofluorescent histochemical procedures followed by detection with confocal microscopy and demonstrated that IL-1β is indeed present within the meningial layers surrounding the spinal cord of neuropathic rats (Figure 1.1. A,B,C). Histologically, these data confirm prior reports showing, via in situ hybridization, that IL-1β mRNA was co-labeled with Iba-1 [68], indicating infiltrating monocytes/ macrophages. Within deeper dorsal horn laminae, IL-1β is co-labeled with Iba-1 that also identifies microglia (Figure 1.1 D, E, F). While we found some co-labeling of IL-1β with GFAP, no co-labeling with NF-H (data not shown) within the dorsal horn of the spinal cord was observed. Given the evidence that immune cell and glial-derived IL-1β (as well as other cytokines discussed, above) has a critical role in animal models of pathological pain, treatments focused on targeting neurons alone is now thought to be an incomplete approach. Immune and glial cells within the CNS may serve as novel targets to modulate enduring pathological pain.

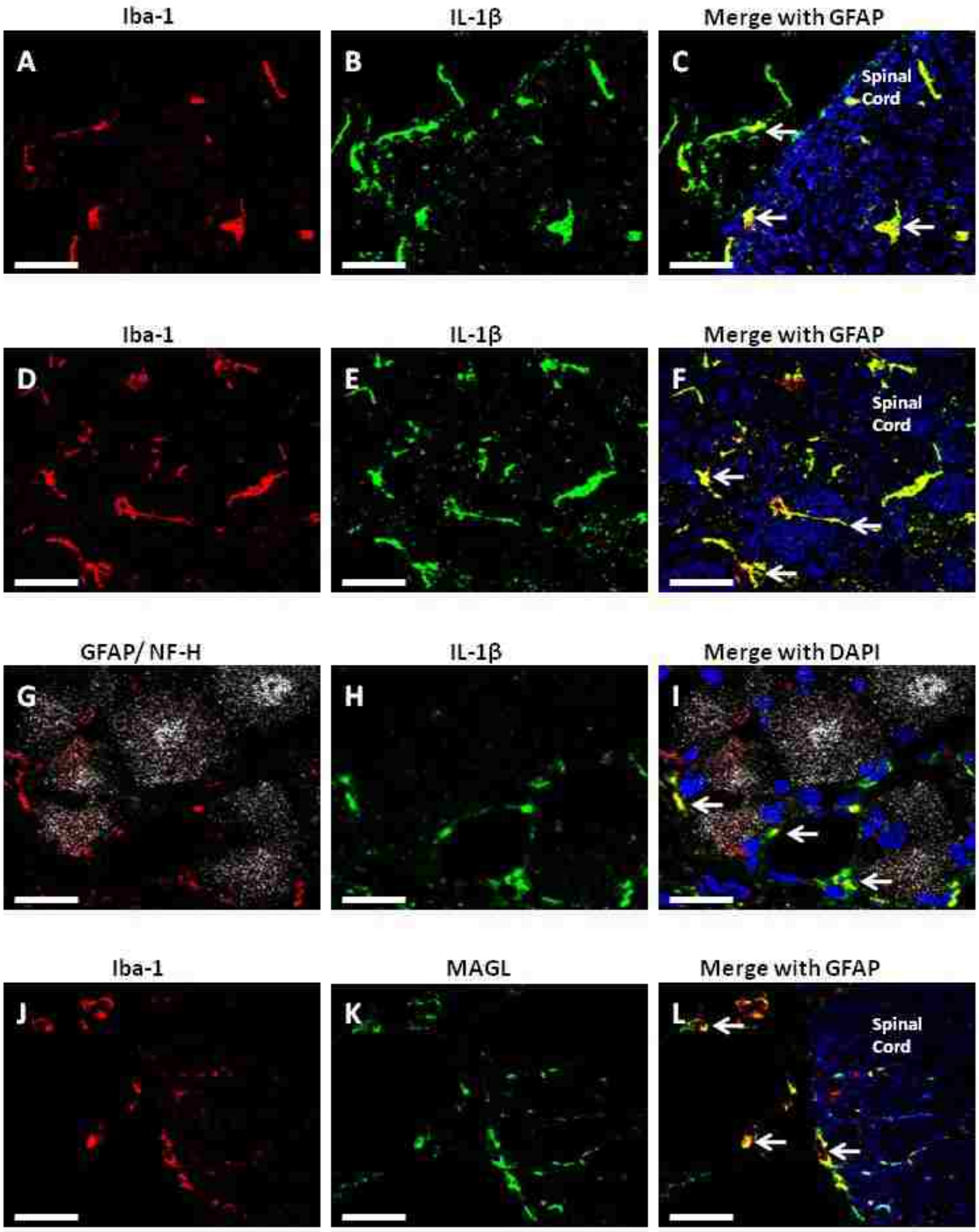

Figure 1.1 Qualitative confocal images of cellular immunostaining.

A, Immunostaining of Iba-1 (red) for infiltrating macrophages and microglia in the meninges and superficial white matter of the spinal cord in a rat with ongoing neuropathy. **B**, Immunostaining with IL-1β (green). **C**, Arrows indicate yellow co-labeling of IL-1β and Iba-1 positive cells and not with GFAP (blue). **D**, Immunostaining of Iba-1 (red) in the deeper laminae of the spinal cord dorsal horn in a rat with ongoing neuropathy. **E**, Immunostaining with IL-1β (green). **F**, Arrows indicate yellow co-labeling of IL-1β and Iba-1 positive cells and not with GFAP (blue). **G**, DRG immunostaining of GFAP positive satellite cells (red) and neurons stained for neurofilament-heavy (NF-H, white) from a rat with ongoing neuropathy. **H**, DRG immunostaining for IL-1β

(green). **I**, Arrows indicate yellow DRG IL-1β and GFAP colabeling with DAPI nuclear labeling (blue). **J**, Immunostaining of Iba-1 (red) in meninges and superficial laminae of the dorsal horn spinal cord in a rat with ongoing neuropathy. **K**, Immunostaining of MAGL (green). **L**, Arrows indicate yellow co-labeling of MAGL and Iba-1 positive cells, and not with GFAP (blue). Scale bars for all images indicate 20 μm.

1.2.4 Glia in DRG

Glial satellite cells in the DRG are also important in mediating pathological pain in addition to spinal cord glial cytokine actions. Satellite glia completely surround DRG neurons and together form a functional unit [69]. Glial satellite cells become activated and contribute to pathological pain in response to peripheral injury by several possible mechanisms [69-72]. For example, glial satellite cells generate cytokines, including IL-1β, and TNF-α, which have been characterized to activate peripheral immune cells [70, 72-74]. DRG invasion by peripheral immune cells [75-77] occurs as a consequence of peripheral nerve injury [29, 78, 79]. Neuro-immune activity is a potential mechanism because DRG neurons have receptors for these cytokines, and when stimulated, lead to the production of the chemokine monocyte chemotractant protein -1 (MCP-1), which induces peripheral immune cell migration to the DRG [49, 79]. In addition, neuroactive IL-1β and other immune signals released from satellite glia act in a paracrine fashion to stimulate neighboring sensory ganglia and their axons, creating allodynia [69, 72, 80-82]. Indeed, stimulating sensory neurons in the DRG with IL-1β leads to further axonal release of substance P [83] within the dorsal horn of the spinal cord. IL-1β acts in a p-p38MAPK dependent manner in the DRG [80], and increased p-p38MAPK expression is well-characterized in the DRG following peripheral nerve injury that produces pathological pain [80, 84, 85]. Here we show an example of DRG IL-1β in close proximity with sensory neurons. IL-1β is

co-labeled with GFAP-positive satellite cells within a DRG from an animal with ongoing CCI-induced neuropathy is shown (Fig. 1 G,H,I). The actions of glially-released cytokines such as IL-1β on nearby neuronal processing in both spinal cord and DRG indicate that, not only neuronal, but also glial systems are altered during conditions that lead to and promote chronic pain. These data strongly suggests that in order to efficiently control chronic or pathological pain associated with numerous disease states, including diabetic neuropathy and cancer, promising therapeutics will need to address this underlying glial contribution.

1.2.5 Modulating glial activation for pain relief

Several compounds specifically targeting glial activation have been developed with the potential for the treatment of pain. While a full discussion of such compounds is beyond the scope of this review (for review, see [86]), one example drug is discussed here to underscore the supposition that altering glial activation states is a highly promising approach to control pathological pain. An example of a compound that targets microglial activation is minocycline, a well-characterized microglial inhibitor [87]. In numerous animal models, minocycline robustly produces anti-allodynia and analgesia [53, 87-89]. However, globally disrupting the function of microglia as well as peripheral immune cells may produce unintended side-effects, such as increased susceptibility to CNS infection [90]. An alternative approach using cannabinoid-related compounds appears to be very promising for clinical pain relief. Cannabinoids may act in an anti-inflammatory manner, and these anti-inflammatory actions may have a glial role [7, 91]. Intriguingly, the cannabinoid receptor subtype 2, CB_2R, has been

identified primarily on microglia [92]. Published reports strongly suggest that activation of this receptor subtype leads to pain control [93, 94]. In the remainder of this review we will provide a brief overview of cannabinoids, specifically discussing published data in support of cannabinoid-related compounds for pain control with a glial-centric view.

1.3 The endocannabinoid system

1.3.1 Components of the endocannabinoid system

The endogenous cannabinoid (endocannabinoid) system is comprised of multiple components, including receptors, ligands, and degradative enzymes. Each will be discussed in turn, below. Within the past 6 years, an explosion of reports has occurred on the endocannabinoid system and its potential role in modulating numerous disease processes, including those associated with pathological pain conditions. This is due, in part, following the identification of cells that express cannabinoid receptors and subsequent signaling mechanisms. In general, endocannabinoid signaling was thought to involve only neurons [95-97]. Glia in the CNS had no role. However, immune cells, including microglia are now known to be involved in endocannabinoid signaling cascades (discussed further, below). While the underlying mechanisms involved in mediating the therapeutic effects of the endocannabinoid system are still a mystery, new breakthroughs have elucidated the bioavailability of endocannabinoids and cannabinoid receptor action with regard to the mediation of pain processing.

The two widely acknowledged cannabinoid receptors are the CB_1R and the CB_2R. Both have shown great potential for the development of therapeutics targeted at pain control. The putative cannabinoid receptor subtype of the 'orphan' receptor, GPR55 [98], remains controversial as several reports indicate opposite pharmacological profiles [99-102]. Research targeting this receptor with cannabinoid ligands has just begun to gain momentum, [99, 103-105]. However, there are reports that at least five distinct cannabinoid receptors have been identified [8]. The most well-characterized cannabinoid receptor, the CB_1R is primarily found on neurons within the heart, small intestine, urinary bladder and vas deferens in the periphery and, within the CNS, has the highest concentrations in the cerebellum, hippocampus, basal ganglia and cerebral cortex [106-108]. However, the CB_2R has a distinctly different distribution and is primarily found on immune cells [109-111]. Current evidence demonstrates that the endocannabinoid system may have potential as a target for pain control, and thus the remainder of this review will focus on the endocannabinoid system relative to pain therapeutics.

1.3.2 Classical cannabinoid receptor signaling

Both the CB_1R and CB_2R belong to the G-protein coupled receptor (GPCR) superfamily, and couple to the inhibitory Gi/o and Gi, respectively. Activation of either receptor leads to p42/44 MAPK signaling and inhibits adenylate cyclase, limiting the ATP production of cyclic AMP (cAMP), and leading to lessened activity of protein kinase A (PKA) [106, 112, 113]. CB_1R activation, but not CB_2R activation, can modulate ionic Ca2+ and K+ channels, which is blocked with

pertussis toxin, indicating that the CB_1R Gi/o proteins are directly responsible for modulation of these ion channels [106, 114-116]. Evidence exists that CB_1R activation can activate p38MAPK in vitro [117, 118]. However, this is a paradoxical finding- because activation of p38MAPK can lead to increased pain signaling, which opposes the therapeutic efficacy of CB_1R agonists for pain control. A mechanism for these findings has not been elucidated, but may include or be wholly dependent on, non-cannabinoid receptor signaling cascades. No similar *in vivo* report exists detailing p38MAPK activation from CB_1R activation.

Although a few of the above mentioned signaling properties of the CB_1R have proven to be sufficient in leading to pain control, the practical implications of CB_1R agonists in a clinical setting are limited. The CB_1R was first discovered as the receptor for the major psychoactive ingredient in Cannabis sativa, Δ^9-tetrahydrocannabinol (THC) which was first isolated in 1965 [119-121]. The attractiveness for clinical application of compounds selectively acting on the CB_1R is limited by the development of tolerance [122] and its psychotropic effects [7, 123], which include cognitive impairment [124], catalepsy [125-127], hypothermia [127-129], and negative impacts on learning and memory [128, 129]. This is in contrast to the effects of cannabidiol, another active compound of marijuana [130]. Cannabidiol does not produce unwanted CNS side-effects by itself, but it is not widely thought to act robustly at either the CB_1R or the CB_2R due to low binding affinities observed *in vitro* [130]. Despite low CB_1R and CB_2R binding properties that cannabidiol possesses, it remains as a promising therapeutic for chronic pain treatment based on its anti-inflammatory actions.

In vivo, cannabidiol within the CNS may still produce CB_2R activation resulting in anti-inflammatory properties. It was recently demonstrated in a mouse model of diabetic neuropathy that intranasal administration of cannabidiol produces anti-inflammatory actions via down-regulation of p-p38MAPK in spinal glia [131]. In this animal model, spinal glia are characterized to become activated and contribute to neuropathic conditions resulting in mechanical sensitivity and thermal hyperalgesia through the activation of proinflammatory signaling cascades like p38MAPK [132-134]. Cannabidiol is sufficient to produce neuropathic pain relief that is dependent on CB_2R activation [131]. These data demonstrate that there is a critical link between cannabidiol's therapeutic action, which includes a CB_2R role, to spinal glial activation and pain control.

1.3.3 Cannabinoid 2 receptors

The CB_2R is predominantly found on immune cells, such as lymphocytes, neutrophils, and macrophages, with the highest peripheral concentrations in the spleen, lymph nodes and testes [92, 109-111]. Within the CNS, the CB_2R is found primarily on microglia, and some neurons specifically within the hippocampus, cortex and substantia nigra [108, 135, 136]. However, the spinal cord and DRG distribution of the CB_2R is an area of much debate, as the current literature frequently reports conflicting data. One report suggests the CB_2R is expressed only on neurons [139], while a separate report reveals CB_2R expression on microglia, and to a lesser extent on neurons [96], and yet another report demonstrates CB_2R on microglia with no neuronal expression [138]. The discrepancy between studies identifying the CB_2R expression on specific cell

types may be partially due to the recent discovery of two separate isoforms of the CB_2R. The most prevalent isoform of the CB_2R within the periphery, termed “CB2B”, is found extensively within the spleen, and to a lesser degree, in the liver, intestines, and leukocytes. The shorter isoform, “CB2A”, is predominately found within the brain, testes, and to a lesser degree in the spleen, kidney, muscle and leukocytes [137]. As most commercially available antibodies for the CB_2R utilize CB_2R isolated from spleen, it is possible that the CB2B isoform, found in much greater abundance within the spleen than the CB2A isoform, is the isoform recognized by most commercially available antibodies for immunohistochemistry. For example, Wotherspoon and colleagues, utilizing immunohistochemistry and CB_2R null mice, showed that CB_2R expression was induced by nerve ligation and was localized to the spinal cord superficial lamina ipsilateral to the nerve damage, while null CB_2R mice revealed no up-regulation [138]. The authors suggest that CB_2R was expressed on sensory afferent terminals because co-localization with growth associated protein-43 and the neuropeptide galanin, was observed. However, Romero-Sandoval and colleagues demonstrated, also through immunohistochemistry, that the CB_2R was primarily found on parenchymal and perivascular microglial cells. The authors additionally noted very limited and sparse staining in neurons [91, 94, 139]. Lastly, in a study using in situ hybridization (ISH), CB_2R mRNA was present on immunohistochemically-identified microglia [135].

Based on the above-noted discrepancies of the cellular localization of the CB_2R in the spinal cord, one possible consideration should be the animal model that is

utilized. It has been demonstrated that the CB_2R may not be up-regulated in the dorsal horn of the spinal cord in inflammatory pain models, but rather in chronic neuropathic pain models [135]. This suggests that the degree of CB_2R up-regulation in chronic pain is heavily dependent on the model. The type of the injury induced in a specific model may dictate the overall receptor up-regulation and the cellular co-localization of the CB_2R. The CB_2R isoform distribution within the spinal cord and DRG under basal and chronic inflammatory pain conditions has not been systematically examined. Given these potential confounds, identifying the cellular distribution of the CB_2R within the spinal cord remains elusive.

1.3.4 Bioavailability of endocannabinoids

The endogenous cannabinoid system is also comprised of a number of endogenous ligands for the CB_1R and CB_2R, which includes anandamide (AEA), 2-arachadonyl glyercol (2-AG), as well as degradative enzymes [140-143]. The endocannabinoids AEA and 2-AG are produced and released from neurons and microglia [92], which are controlled by enzymatic hydrolysis of fatty acid amide hydrolase (FAAH) and monoacylglycerol lipase (MAGL), respectively [140, 142]. The enzyme MAGL has been identified on presynaptic axon terminals in brain, suggesting it can terminate 2-AG activity in presynaptic nerve terminals [141, 143] of centrally projecting afferent nociceptors in the spinal cord dorsal horn. Interestingly, it has been found that microglia release 2-AG, and functional MAGL has been described in primary microglial cell cultures [144]. Recently, a novel isoform of MAGL has been described in BV-2 microglial cell cultures, although it

is uncertain if this isoform occurs within microglial cells in vivo [145]. To date, MAGL cellular co-expression utilizing immunohistological techniques has not been performed on pain-relevant spinal cord dorsal horn regions or spinal cord tissue. We show here, utilizing confocal microscopy, that within the meningial layer surrounding the spinal cord taken from behaviorally verified neuropathic rats, MAGL is co-labeled with Iba-1 positive infiltrating monocytes. In superficial laminae, MAGL is co-labeled with either resident microglia or infiltrating monocytes/macrophages (Figure 1.1 J,K,L). We additionally observed in the deeper dorsal horn laminae, that MAGL is co-labeled with Iba-1 positive microglia, and morphologically identifiable neuronal cell bodies (data not shown).

1.3.5 The implications of the endocannabinoid system in pain modulation

Following peripheral nerve or tissue injury, increased expression of endocannabinoids, CB_2R, FAAH and MAGL occurs in DRG and spinal cord [92, 107, 146]. For example, AEA and 2-AG are up-regulated in DRG following L5 spinal nerve ligation (SNL), a well-described animal model that leads to neuropathic pain [107]. Additionally, in a paw incision model of pain, 2-AG, widely characterized to produce analgesia, was found to be up-regulated in the ipsilateral lumbar spinal cord on days 3 and 9, and in the contralateral lumbar spinal cord on days 1 and 9 after surgery [63]. These data suggest that endocannabinoid compounds may act to counterbalance the cytokine actions known to mediate neuropathic pain.

Recent studies show that exogenous application of the endocannabinoids, AEA and 2-AG, lead to pain control. Exogenous AEA administered spinally reverses carageenan-induced nociception [147], and exogenous 2-AG injected into the hindpaw blocks nociceptive responses due to formalin injection [148, 149]. Paradoxically, administration of exogenous AEA to the hindpaw or high intrathecal doses, produces nociceptive behavior, and in both cases, is mediated by the ionotropic transient receptor potential cation channel, superfamily V subtype 1 (TRPV-1) [147, 150]. Several reports detail that the actions of AEA may be mediated by TRPV-1, and as such, caution must be taken when assigning endocannabinoid actions to only the CB_1R or the CB_2R.

Manipulating the enzymes responsible for the bioavailability of AEA or 2-AG is additionally effective for pain control. Altering endocannabinoid levels by inhibiting the actions of MAGL and/or FAAH increases available endogenous AEA and 2-AG and results in therapeutic actions. Following localized administration of MAGL inhibitors (JZL184, URB602) into rat hindpaws increases local levels of 2-AG, with simultaneous attenuation of formalin-induced pain in rats [148, 149]. Additionally, systemic administration of FAAH inhibitors (PF-3845, URB597), MAGL inhibitors (JZL184, URB602) or the dual FAAH/MAGL inhibitor, JZL195, increases CNS levels of AEA and 2-AG, with attenuation of CCI-induced pain in mice [151, 152]. Specifically, the pharmacological FAAH inhibitor, PF-3845 decreased allodynia and hyperalgesia in CCI-induced neuropathic mice without the development of tolerance [127]. Numerous studies have demonstrated that MAGL inhibitors increase 2-AG accumulation [127, 151,

153]. However, recent studies indicate that following challenge with CB_1R agonists, increased 2-AG availability leads to CB_1R down-regulation, desensitization and lessened CB_1R effects [125, 127]. These data suggest that significantly increasing the levels of 2-AG may not be a clinically viable approach for treating chronic pain conditions.

Although pain behavior is suppressed following exogenous administration of 2-AG and AEA or by increased levels of endocannabinods via enzyme inhibitors, the exact mechanisms of these cannabinoids underlying the modulation of inflammation and pain is not well understood. Studies are currently underway by several groups to elucidate the mechanisms whereby the endocannabinoid system is able to lead to pain control [63, 127, 151, 152]. Alkaitis and colleagues, utilizing dual CB_1R and CB_2R antagonists, AM281 and AM630 respectively, recently found that the endocannabinoid system plays critical roles in the resolution of allodynia from surgical hindpaw incision, an animal model of post-surgical pain [63]. In addition, blocking the activation of both the CB_1R and the CB_2R resulted in increased p-p38MAPK levels in this model of post-surgical pain, suggesting that constitutive endocannabinoid actions play a role in modulating p-p38MAPK. These findings support that the endocannabinoid system alters factors which are critical mediators of inflammatory processes underlying pain responses in a wide range of medical conditions where chronic pain is a component. Although speculative, CB_2R actions during chronic pain may be primed for enhanced activity to ultimately produce pain modulation following CB_2R stimulation, as down-regulation and desensitization previously noted to

occur with the CB_1R has not been observed with the CB_2R [7, 93, 154]. Numerous synthetic CB_2R agonists are currently being explored as potential therapeutic interventions for the treatment of chronic pain.

1.4 Well-characterized CB_2R synthetic compounds

Growing evidence that CB_2R agonism appears to lack the adverse CNS effects that activated CB_1R exerts has fueled the development of clinically-viable CB_2R agonists. Therefore, a strong research effort in pursuit of the development and characterization of synthetic CB_2R agonists with modified chemical structures to facilitate selective binding to the CB_2R over the CB_1R is ongoing. The remainder of this review will address the current evidence of synthetic CB_2R selective compounds for the treatment of different animal models of pathological pain. This is not an exhaustive review of all studies, but rather an overview. Additional reviews detailing the chemistry, bioavailability, efficacy, and kinetics of specific drug compounds are available elsewhere [7, 155, 156].

Synthetic agonists selective for CB_2R have been shown to produce anti-inflammatory effects with modulation of signaling cascades favorable for controlling chronic pain. Caution must be used in assuming that specific anti-inflammatory effects seen with a particular CB_2R agonist will additionally be seen with all other CB_2R agonists, as the binding site for different compounds may not be the same. This factor may further influence the cellular signaling pathways that occur downstream of cannabinoid receptor binding, and the compound's ultimate intracellular fate, such as degradation by MAGL as opposed to FAAH.

Therefore, each selected CB_2R agonist and its observed actions are presented in a table (Table 1.1). The most recent findings for each compound are summarized. JWH-015 is a CB_2R selective agonist from the aminoalkylindole classification of CB_2R agonists with a 27-fold affinity for the CB_2R over the CB_1R [157, 158]. Collectively, the aminoalkylindoles represent the most studied group of synthetic CB_2R agonists. Romero-Sandoval and colleagues have recently used a well-characterized *in vitro* model of inflammation to examine the anti-inflammatory actions of JWH-015. Lipopolysaccharide (LPS), an outer cell-wall particle of gram-negative bacteria which strongly activates innate immune cells, was given to macrophages in cell culture. It was demonstrated that incubation with JWH-015 leads to a decrease in phosphorylated extracellular signal-regulated kinase-1 (P-ERK) that is mediated by mitogen-activated kinase-phosphatase (MKP) 1 and 3 [91]. MKP-3 is a selective negative modulator of the ERK-2 signaling pathway through negative feedback loop mechanisms, while in the same in vitro studies, neither JNK nor p38MAPK signaling was affected [159]. CB_2R agonist treatment failed to suppress LPS-stimulated increases in p-ERK-2 in the presence of MKP-3 inhibitors, supporting the possibility that CB_2R agonists exert anti-inflammatory actions via MKP-3 signaling [91]. These data support that CB_2R activation, by binding highly selective synthetic agonists, may control proinflammatory processes.

Other CB_2R agonists that produce therapeutic effects to control chronic pain are described below. The compound AM1241, a CB_2R selective agonist also from the aminoalkylindole class, has a 36-fold affinity for the $CB_2R>CB_1R$ [156, 160,

161]. Despite the fact that it has been described as a protean agonist because it exerts different inverse agonist properties [161], it is widely characterized as an effective compound for pain suppression. For example, AM1241 has been found to be effective in treating experimental models of bone cancer pain. Acute and sustained intraperitoneal (i.p.) administration of AM1241 to mice decreased pain symptoms and additionally lessened the amount of bone loss during bone cancer-induced neuropathic pain. The authors suggest that these observations were mediated via the CB_2R, as acute behavioral effects observed were not present with the addition of SR144528, a CB_2R antagonist [162]. In a separate study using two models of bone cancer pain, systemic administration of AM1241 was efficacious in reducing pain symptoms and was reliant on spinal CB_2R. Interestingly, the authors concluded that the actions of opioid receptors were necessary to achieve these analgesic effects, as the administration of naloxone, a short-acting opioid antagonist in a replicate experiment, blocked the development of AM1241-mediated analgesia [163]. The involvement of endogenous opioids was further supported in mediating CB_2R analgesia by an earlier study using non-neuropathic naïve rats [164]. However, Rahn and colleagues have recently demonstrated that the anti-nociceptive effects of systemic AM1241 in naïve rats are not dependent on the actions of opioid receptors or downstream effects [165]. In this study, the reported dose of AM1241 utilized by Ibrahim and colleagues, 0.1 mg/kg i.p, did not achieve reliable effects, and so higher doses of AM1241, up to 1 mg/kg were evaluated. Additionally, in the SNL model of neuropathic pain, the effects of AM1241

following i.p. administration were not blocked by naloxone suggesting that AM1241 does not act via opioid receptors to exert analgesic effects [166] (Table 1.1). The discrepancy between these studies suggests that bone cancer pain may uniquely involve endorphin-endocannabinoid interactions while other discrete peripheral nerve lesions or naïve conditions may involve only the endocannabinoid system.

Spinal sensitization is a key component of chronic pathological pain. Thus, compounds developed for chronic pain control will require centrally-mediated actions and may be insufficient if they do not cross the blood brain barrier because their actions will be sequestered to peripheral sites of pain processing. A growing body of evidence supports that spinal administration of AM1241 produces significant control over pathological pain in several models using peripheral manipulations. For example, intrathecal (peri-spinal, i.t.) AM1241 reverses allodynia induced by either SNL or intra-paw injection of complete Freund's adjuvant (CFA), a model of local inflammatory pain [166]. Additionally, i.t. AM1241 has been found to reverse CCI-induced allodynia [167] and leads to a corresponding decrease in spinal cord astrocyte activation of these previously neuropathic animals [168]. In separate studies that used SNL to induce peripheral neuropathy in rats, both astrocyte and microglial phenotypic markers of activation were decreased following either i.t. administration of JWH-015 [94] or i.p. administration of GW405833 [169], a partial CB_2R agonist. Taken together, these reports demonstrate that CB_2R agonists are able to alter spinal glial

activation states and create in vivo anti-inflammatory effects suitable for pain control.

The ability for CB_2R agonists to be administered without the development of tolerance or reliance on μ-opioid actions within the spinal cord has been studied utilizing GW405833. This compound is also classified as an aminoalkylindole, and is additionally known as L-768,242. Conflicting reports of GW405833's affinity for the CB_2R over the CB_1R exist [156]. However, it is generally accepted that at the human CB_2R the compound displays a 1,200-fold affinity for the CB_2R over the CB_1R, and at the rat CB_2R there is a 78-fold affinity for the CB_2R over the CB_1R [170]. Leichsenring and colleagues recently demonstrated that chronic repeated i.p. injection of GW405833 was able to provide sustained reversal from allodynia following SNL. That is, animals did not develop tolerance to this compound, which was in stark contrast to treatment with the mixed CB_1R/CB_2R agonist, WIN55,212-22 [169]. Additionally, allodynia returned after intermittent treatment of GW405833. The authors also performed immunohistochemistry and, as previously noted, found diminished astrocyte and microglial activation. However, after cessation of GW405833 treatment, astrocyte and microglial activation returned, which occurred in parallel with the return of allodynia. In addition to the above mentioned benefits of CB_2R agonist actions, it has recently been reported that GW405833 can reverse CCI-induced increased helplessness responses, as assessed in the forced swim test for rats, which is a model that may elucidate depression-like symptoms in animals [171]. Furthermore, GW405833 is efficacious in treating knee pain, however, these studies indicate

that GW405833 may have partial agonist actions at the TRPV-1 [172]. While endocannabinoids are capable of acting at the TRPV-1 receptor at high doses that subsequently lead to TRPV-1 desensitization [173, 174], the report by Schuleret and colleagues is the first electrophysiological demonstration of CB_2R agonist actions on neuronal TRPV-1 ion channels. Further research is needed to understand if the downstream signaling following GW405833 binding to neuronal TRPV-1 may enhance this CB_2R agonist compound's anti-nociceptive actions.

1.5 Newer CB_2R agonist compounds

Several newer classes of CB_2R agonists have been developed to examine therapeutic efficacy for chronic pain relief. AM1714 and AM1710 are members of the novel cannabilactone classification [156, 175]. AM1710's pharmacological profile has recently been characterized both in vitro and in vivo [168, 176]. AM1710 does not cross the blood brain barrier, and is 57-fold more selective for the CB_2R over the CB_1R [176]. Systemic i.p. AM1710 in naïve rats was able to produce anti-nociceptive mechanical responses when a 100-fold dose range (from 0.1mg/kg – 10mg/kg) was examined. At the 0.1 mg/kg dose, AM1710's effects were altered only by the administration of a CB_2R antagonist, but not the administration of a CB_1R antagonist. However, at the dose of 5 mg/kg, both CB_1R and CB_2R antagonists diminished AM1710's anti-nociceptive actions. The doses of either 0.1 mg/kg or 10 mg/kg AM1710 did not produce behaviors typically associated with CB_1R activation. This was in stark contrast to the observed CB_1R induced effects from the mixed CB_1R/CB_2R agonist, WIN 55,212-2. Anti-nociceptive effects of 5 mg/kg AM1710 were observed for as long as 120

minutes after i.p. injection, while no effects at 0.1 mg/kg were observed at the same timepoint, showing a dose effect on the duration of AM1710 efficacy [176]. In separate studies, i.t. injection of AM1710 reverses CCI-induced allodynia for approximately 3 hours [167, 168]. Additionally i.t. pretreatment with AM1710 blocks the development of allodynia in a rat model of sterile spinal cord inflammation using i.t. administration of the HIV-1 envelope glycoprotein, gp120 [168]. Separately, Rahn and colleagues have shown that AM1714 is capable of reversing chemotherapy-induced pain [176] while AM1710 prevented pain in the same model [177]. NESS400, a novel CB_2R agonist, decreased spinal astrocyte and microglial activation and reversed signs of neuropathic pain behavior following i.p. administration [178]. MDA19 is also a novel CB_2R agonist with moderate selectivity for the CB_2R over the CB_1R (approximately 14-fold), and displays properties of a protean agonist *in vitro* [179], like AM1241. MDA19 was found to reverse both the spinal nerve ligation and chemotherapy-induced models of chronic pain (Table 1).

Abbott Laboratories has developed two novel compounds, A-796260 and A-836339, both of which are selective for the CB_2R over the CB_1R [180-182]. A-796260, when given to rats i.p., was able to produce relief from local inflammatory pain, neuropathic pain, postoperative pain, and osteoarthritis pain. These effects were due only to the actions of the CB_2R, and not CB_1R or μ-opioid receptor actions, and without the development of CB_1R mediated psychotropic effects. It was found *in vitro* that A-836339 could act as a CB_1R agonist, and studies in vivo revealed that high doses of A-836339 produced CB_1R mediated

psychotropic effects [182]. Further studies with A-836339 reveal that this compound was also efficacious in animal models of inflammatory, neuropathic, postoperative, and osteoarthritis pain, when administered locally to the hindpaw, intra-DRG, and intrathecally. As before, the actions of A-836339 at these sites were due primarily to the CB_2R, and not μ-opioid receptor agonism [166] (Table 1.1).

Compound/ Produced By	Classification	CB_2R > CB_1R Selective	CB_2R Compound Route of Administration	*In Vivo* Models of Pain	Tested Efficacy	Glial Effects	References
A-796260 Abbott Laboratories	Alkylindole	h = 206-fold r = 26-fold	i.p.	CFA, CCI, PSP, Knee joint osteoarthritis	Mechanical allodynia, Grip force	Unknown	- (Frost et al., 2008) - (Yao et al., 2008) - (Yao et al., 2009)
A-836339 Abbott Laboratories	Iminothiazole	h = 421-fold r = 189-fold	i.p., plantar hindpaw, intra-DRG, i.t.	CFA, CCI, PSP	Thermal hyperalgesia, Mechanical allodynia	Unknown	- (Frost et al., 2008) - (Yao et al., 2008) - (Yao et al., 2009) - (Hsieh et al., 2011)
AM1241 Cayman Chemicals, Sigma-Aldrich, Enzo Life Sciences, A. Makryannis (Northeastern University)	Amino-alkylindole	h = 125-fold r = 36-fold protean agonist	i.p., i.t., intra-DRG, plantar hindpaw	Bone cancer, SNL, CCI	Mechanical allodynia, Thermal hyperalgesia	↓ astrocyte activation	- (Mukherjee et al., 2004) - (Yao et al., 2006) - (Thakur et al., 2009) - (Lozano-Ondoua et al., 2010) - (Wilkerson et al., 2009) - (Wilkerson et al., 2010) - (Hsieh et al., 2011)
AM1710 A. Makryannis (Northeastern University)	Cannabilactone	r = 57-fold	i.t., i.p.	i.p. paxlitaxol, CCI, i.t. gp120	Mechanical allodynia, Thermal hyperalgesia	Prevented macrophages/ microglial mediated induction of i.t. gp120	- (Khanolkar et al., 2007) - (Thakur et al., 2009) - (Wilkerson et al., 2009) - (Wilkerson et al., 2010) - (Rahn et al., 2010a) - (Rahn et al., 2011)
AM1714 A. Makryannis (Northeastern University)	Cannabilactone	r = 490-fold	i.p.	i.p. paxlitaxol	Mechanical allodynia, Thermal hyperalgesia	Unknown	- (Khanolkar et al., 2007) - (Rahn et al., 2008) - (Thakur et al., 2009)
***Cannabinor** Pharmos Scientific	Bicyclic	h ~ 80-90-fold	i.p., oral, s.c.	Hindpaw carrageenan, i.p. acetic acid, CCI	Thermal hyperalgesia, Mechanical allodynia, Cold allodynia	Unknown	- (Bar-Joseph et al., 2003) - (Bar-Joseph et al., 2004) - (Beltramo, 2009)
CBS0550 S. Saito (Taisho Pharmaceutical Co.)	Imine Derivative	h = 1000-fold	oral	Hindpaw yeast cell wall	Mechanical hyperalgesia	Unknown	- (Ohta et al., 2008)

Compound/ Produced By	Classification	CB_2R > CB_1R Selective	CB_2R Compound Route of Administration	*In Vivo* Models of Pain	Tested Efficacy	Glial Effects	References
***GRC10693** Glenmark Pharmaceutical Limited	Unknown	Species unknown >4700-fold	oral	CFA, CCI, SNL	Unknown	Unknown	- Glenmark Pharmaceuticals website
GW405833 Sigma-Aldrich, Tocris Bioscience, Santa Cruz Biotechnology Inc, Enzo Life Sciences	Amino-alkylindole	h = 1200-fold r = 78-fold	i.p., chronic i.p.	SNL, CCI, Knee joint osteoarthritis	Mechanical allodynia	↓ astrocyte activation, ↓microglial activation	- (Valenzano et al., 2005) - (Leichsenring et al., 2009) - (Schuelert et al., 2010)
***GW842166X** Glaxo-Smith-Klein	Pyrimidine Ester	h ~ 500-fold	oral	CFA	Paw weight bearing	Unknown	- (Giblin et al., 2007)
JWH-015 Cayman Chemicals, Sigma-Aldrich, Tocris Bioscience	Amino-alkylindole	h = 27-fold	plantar hindpaw, i.t.	CCI, PSP	Thermal hyperalgesia, Mechanical allodynia, Cold allodynia	↓ microglial activation, ↓ astrocyte activation i.t., prevented microglial activation (*in vitro*)	- (Showalter et al., 1996) - (Huang et al., 2001) - (Romero- Sandoval et al., 2009) - (Hervera et al., 2010)
MDA19 M. Naguib (University of Texas)	N-alkyl isatin acylhydrazone Derivative	h ~ 14-fold r ~ 70 fold protean agonist	i.p.	SNL, i.p. paxlitaxol	Mechanical allodynia	Unknown	- (Xu et al., 2010)
O-3223 A. Lichtman (Virginia Commonwealth University)	Ethyl Sulfonamide Derivative of THC	h = 80-fold	i.p.	LPS, SNL	Edema, Thermal hyperalgesia	Unknown	- (Kinsey et al., 2010)

Table 1.1

CB_2R agonist effects from animal and clinical studies. For the compound/ produced by column, * indicates compounds that are also examined in clinical trials. For the CB_2R >CB_1R selective column, human binding (h), rat binding (r). For in vivo models of pain, the abbreviations are as follows: local inflammatory pain models of lipopolysaccharide (LPS), complete Freund's adjuvant (CFA). The systemic visceral model of pain: intraperitoneal acetic acid (i.p. acetic acid). Neuropathic pain models: chronic constriction injury (CCI), sciatic nerve ligation (SNL), intraperitoneal chemotherapy induced pain (i.p. paxlitaxol), bone cancer induced pain (bone cancer), osteoarthritis induction via knee joint synovium injection (knee joint osteoarthritis). Other models of pain utilized are noted as: post-operative model of surgical pain (PSP), and intrathecal administration of the HIV-1 envelope glycoprotein, gp120 (i.t. gp120).

Several independent groups have developed and characterized additional promising CB_2R selective compounds. The Lichtman laboratory has recently synthesized an ethyl sulfonamide THC analog: O-3223. This compound is also a

novel CB_2R agonist with a 79-fold affinity for the CB_2R over the CB_1R, and administration of this compound in naïve mice did not produce the psychotropic effects associated with CB_1R activation [183]. *In vivo* anti-nociceptive effects of this compound were determined to be reliant on CB_2R, but not CB_1R function. Pre-treatment with i.p. O-3223 was efficacious in lowering the amount of edema in the paws of mice given the immune stimulant LPS, and i.p. O-3223 reversed hyperalgesia in a mouse model of sciatic nerve ligation [183]. CBS0550 is a novel CB_2R agonist with high selectivity for the CB_2R, and when given orally to rats, was efficacious in reversing yeast cell-wall induced local inflammatory pain [184]. Taken together, these studies reflect just a sample of the efforts being made toward identifying optimal CB_2R compounds for pain therapeutics (Table 1.1).

1.6 Clinical use of CB_2R agonists

The current clinical trials using cannabinoid compounds for the treatment of chronic pain have examined mixed CB_1R/ CB_2R agonists, or CB_1R agonists. Sativex, Marinol/Dronabinol, and Nabilone, all containing THC derivatives, have reached late stage or regulatory approval in various countries [185, 186]. To date, only three CB_2R compounds have entered into clinical trials for human evaluation. First noted by Beltramo [155], the progress of CB_2Rs in clinical trials has not been swift. Glenmark Pharmaceuticals reported in a press release (April 13th, 2009), that its CB_2R compound, GRC10693, successfully completed a phase I clinical trial, showing good tolerance and no serious adverse events in the 80 healthy patients enrolled. This safety profile of GRC10693 was observed

with the highest dose of GRC10693 evaluated – 1200 mg. Glenmark Pharmaceuticals states that GRC10693 shows a CB_2R selectivity of >4700-fold over the CB_1R. Additionally, peripheral and oral administration of GRC10693 showed efficacy in modulating the *in vivo* animal models of systemic acetic acid-induced visceral pain and hindpaw carageenan-induced local inflammation, as well as CCI [187, 188]. However, the company has decided to not move forward with phase II clinical trials, as it is currently contemplating licensing the compound to other pharmaceutical companies (http://www.glenmarkpharma.cz/clin2.php?lang=en). Early clinical trials showed a safety and tolerability profile of Pharmos Scientific's Cannabinor CB_2R selective compound, but it lacked reliable analgesia. Cannabinor is no longer being developed as an i.v. therapeutic (http://www.pharmoscorp.com/development/cannabinor.html). Glaxo-Smith-Klein reports numerous phase I and II trials for its CB_2R agonist GW842166X. GW842166X was described as highly selective for the CB_2R over the CB_1R, with the ability to cross the blood brain barrier in animals. Additionally, this compound showed efficacy in the CFA inflammatory model of pain, without the development of tolerance [189] (Table 1.1). Interestingly, the only completed phase I clinical trial examined the distribution of radiolabeled GW842166X (specifically, [11c]GW842166X) via positron emission tomography (PET) analysis, (http://clinicaltrials.gov/ct2/show/NCT00511524?term=GW842166X&rank=2).

The rationale was to identify whether this compound was able to cross the blood brain barrier in 6 healthy males. All other phase I studies of this compound were

terminated prior to study completion. Glaxo-Smith-Klein reports a total of 3 phase II clinical studies, all aimed at oral dosing, with all reaching completion. The first phase II study examined molar tooth extraction with enrollment in European sites. The other two studies, also with European enrollment sites, examined GW842166X efficacy in osteoarthritis pain (Table 1.1). Reports from these studies have not been released, and all were completed by September, 2009.

The outcomes from the above-noted early clinical trials, specifically those of Cannabinor from Pharmos Scientific, suggest that there may be intrinsic differences between the cellular mechanisms within the human patient that has suffered with pain for an indeterminate amount of time. Further, intrinsic physiological differences may also exist, even in a closely monitored animal model of pain. One potential explanation may lie within the previously described spinal cord mechanisms underlying the maintenance of chronic pain. The clinical studies described did not administer these CB_2R agonist compounds to the spinal cord. The restriction of these compounds to peripheral sites, (i.e., poor blood brain barrier permeability) is desired to ensure that even minuscule CB_1R non-specific binding within the CNS does not occur. This is thought to be an optimal approach to avoid off-target (i.e., CB_1R) psychotropic effects. However, it may be that the administration of these compounds to reach the spinal cord is necessary to produce enduring pain relief due to the potential spinal glial mechanisms underlying chronic pathological pain. Indeed, the argument can be made that these compounds, lipophilic in nature, do possess the ability to penetrate the blood brain barrier. Additionally, it may be that these compounds,

acting as very weak CB_1R agonists within the CNS, at levels that do not produce psychotropic or motor side effects, are beneficial in producing pain relief.

1.7 Summary

CB_2R agonists are emerging as favorable therapeutics over CB_1R for the treatment of chronic pain, as these compounds produce relief from pain symptoms without the commonly reported CB_1R-related side-effects, like catalepsy and motor ataxia. CB_2R agonists may exert their actions independently from μ-opioid receptor actions, and no evidence currently exists related to the development of tolerance or addiction following CB_2R agonist administration. While CB_2R agonists appear to be highly promising as a new avenue for pain therapeutics, the actual direct CNS and DRG effects of CB_2R agonists on the endocannabinoid system are largely unknown. In addition, the CNS role in pain modulation of the endocannabinoid system is itself currently not fully understood and is an area of intense research. The findings discussed in this review suggest that CB_2R ligands hold promise as future therapeutics to treat chronic pain problems. However, greater research efforts are required to yield new clinically useful CB_2R ligands, as the evidence and outcomes from clinical trials is limited regarding the efficacy of these compounds. Although speculative, spinal CB_2R activation in humans may be necessary to reverse ongoing chronic pathological pain. This approach would preferentially target activated glia which are critical modulators of chronic neuropathic pain. Targeting glial cells, including microglial cells, with CB_2R ligands may hold the key to unlocking an efficacious treatment for chronic pain patients.

2. Immunofluourescent spectral analysis reveals the intrathecal cannabinoid agonist, AM1241, produces spinal anti-inflammatory cytokine responses in neuropathic rats exhibiting relief from allodynia.

Brain Behavior and Immunity

Abbreviated Title: Intrathecal AM1241 controls allodynia and cytokines.

Authors: Jenny L. Wilkerson*[1], Katherine R. Gentry[2], Ellen C. Dengler[1], James A. Wallace[1], Audra A. Kerwin[1], Megan N. Kuhn[1], Alexander M. Zvonok[3], Ganesh A. Thakur[3], Alexandros Makriyannis[3], and Erin D. Milligan[1]

Affiliation(s):

Department of Neurosciences, Health Sciences Center, School of Medicine, University of New Mexico, Albuquerque, NM 87131

Department of Anesthesiology and Critical Care Medicine, Health Sciences Center, School of Medicine, University of New Mexico, Albuquerque, NM 87131

Center for Drug Discovery, Northeastern University, Boston, MA 02115

* Corresponding Author:

Jenny L. Wilkerson
University of New Mexico, HSC
Dept. of Neurosciences
MSC08- 4740
1 University of New Mexico
Albuquerque, NM 87131
Email: JLWilkerson@salud.unm.edu
Phone: +1(505)272-4441
Fax: +1(505)272-8082

Figures: 7, Tables: 1
Number of pages: 46
Number of words for Whole Manuscript: 14,127
Number of words for Abstract: 202
Number of words for Introduction: 728

Abstract

During pathological pain, the actions of the endocannabinoid system, including the cannabinoid 2 receptor, leads to effective anti-allodynia and modifies a variety of spinal microglial and astrocyte actions. Here, following spinal

administration of the cannabinoid 2 receptor compound, AM1241, we examined immunoreactive alterations in proinflammatory markers, activated p38 mitogen-activated protein kinase, interleukin-1 β, the anti-inflammatory cytokine, interleukin-10, as well as degradative endocannabinoid enzymes, and markers for activated glia in neuropathic rats. In these studies the dorsal horn of the spinal cord and dorsal root ganglia were examined. AM1241 produced profound anti-allodynia and correspondingly restored basal immunoreactive levels of p38-mitogen activated kinase, interleukin-1β, interleukin-10, and the endocannabinoid enzyme monoacylglycerol lipase. In addition, astrocyte activation markers in the dorsal root ganglia and the spinal cord were reset to basal values. In contrast, spinal AM1241 did not suppress the increased microglial activation observed in neuropathic rats. The differences in fluorescent markers were determined within discrete anatomical regions by applying spectral analysis methods, which virtually eliminated non-specific signal during the quantification of specific immunofluorescent intensity. These findings provided reliable expression profiles and support that intrathecal AM1241 controls pathological pain though anti-inflammatory mechanisms by modulating critical glial factors, and additionally decreases expression levels of endocannabinoid degradative enzymes.

Keywords: CCI, paraffin immunohistochemistry, MAGL, DRG, pain

2.1 Introduction

Microglia and astrocytes (glia) play a crucial role in the development and maintenance of chronic neuropathic pain in various animal models [24]. Increased glial activation is well known to occur in the dorsal horn of the spinal cord in animal models of peripheral neuropathy, as demonstrated by increased production of glial fibrillary acidic protein (GFAP) in astrocytes and ionized calcium binding adaptor molecule -1 (Iba-1) in microglia [50, 93]. When strongly activated, glia can increase expression of proinflammatory factors such as phosphorylated p38 mitogen-activated protein kinase (p-p38MAPK) that can lead to production and release of proinflammatory cytokines such as interleukin-1β (IL-1β) and tumor necrosis factor- α (TNF-α), which subsequently bind and activate their respective receptors on nearby neurons and glia [25, 29, 190]. The cellular anatomical localization of p-p38MAPK is predominantly expressed and is functionally important in spinal cord microglia and corresponding satellite cells in dorsal root ganglia (DRG) during neuropathic pain [191-195]. IL-1β mRNA and protein are upregulated within spinal cord homogenates of rats with pathological pain [196]. However, immunohistochemical detection of increased IL-1β protein, as well as alterations in the anti-inflammatory cytokine, interleukin-10 (IL-10), in intact spinal cord dorsal horn from rats with peripheral neuropathy has not yet been characterized. One goal of these studies is to quantify immunoreactivity (IR) for IL-1β as well as IL-10 in sections of the intact dorsal horn from rats with chronic peripheral neuropathy. In addition, changes in immunoreactive p-p38MAPK levels were examined to verify prior reports that increases in p-

p38MAPK occurs in combination with increased proinflammatory cytokine expression. Peripheral neuropathy is assessed by the presence of allodynia, characterized as a sensitivity to light mechanical touch that is not present under healthy conditions.

AM1241 is a widely characterized cannabinoid agonist that controls hyperalgesia (exaggerated nociceptive thresholds) and allodynia following intraperitoneal [197, 198], intravenous [199], intra-dorsal root ganglia (DRG), or intrathecal (i.t.) [166] injection. In the current studies, we sought to determine the timecourse and dose-dependent changes in allodynia produced by unilateral chronic constriction injury (CCI) of the rat sciatic nerve following i.t. AM1241 administration to avoid known peripheral actions of the compound. The development of bilateral allodynia following unilateral CCI has been documented in numerous studies [200-206]. We therefore followed not only bilateral sensory behavioral changes, but also quantitative changes in the bilateral immunoreactivity of: (1) cytokines, (2) p-p38MAPK, (3) enzymes responsible for the bioavailability of endocannabinoids characterized to exert analgesic properties [151, 207, 208], and (4) activated astrocytes and microglia in spinal cord and DRG.

Existing evidence shows that AM1241 acts as an agonist at the cannabinoid type 2 receptor (CB_2R) that results in suppression of nociceptive responses [165], and prevents neuropathic and inflammatory pain [155, 198, 209, 210], with selectivity demonstrated not only by utilizing pharmacological CB_2R antagonists, but also by examining AM1241 analgesic efficacy in CB_2R knockout mice [197, 211]. CB_2R's

are characterized on microglia and macrophages in cell culture [92, 212, 213] and in the rodent spinal cord following peripheral nerve damage [94, 135] or in transgenic mice over-expressing the CB_2R [93], as well as in the human central nervous system (CNS) under inflammatory diseased conditions. Given AM1241 can act on CB_2R's expressed on spinal microglia, the potential additional (1) cytokine and (2) p-p38MAPK role in AM1241's efficacy in producing spinal anti-inflammatory actions concurrent with anti-allodynia may be identified in these studies.

Related to these goals, we examined two methods to analyze immunofluorescent images of spinal cord tissue sections to identify the most sensitive procedure for detecting and quantifying differences in specific immunoreactive protein markers. In this context, an alternative method that utilizes spectral analysis procedures, demonstrated here, can be advantageous over conventional methods of image analysis.

2.2 Materials and methods

2.2.1 Animals

A total of 52 pathogen-free adult male Sprague Dawley rats (300-400 gram; Harlan Labs, Madison, WI) were used in all experiments. Rats were double-housed in a temperature and light-controlled (12 hour light/dark; lights on at 6:00 AM) environment, with standard rodent chow and water available ad libitum. All procedures were approved by the Institutional Animal Care and Use Committee (IACUC) of the University of New Mexico Health Sciences Center.

2.2.2 Drugs

The CB_2R agonist used in these experiments was (R,S)-(2-iodo-5-nitrophenyl)-(1-[(1-methylpiperidin-2-yl)methyl]-1H-indol-3yl)-methanone (AM1241) from the aminoalkyndole classification [161]. Water soluble hydrochloride salt of racemic AM1241 was generously gifted (A. Makriyannis, Center for Drug Discovery, Northeastern University). Initial doses of AM1241 were based on those previously reported for intravenous (i.v.) injection [199] and pilot studies. A 1000-fold dose range of AM1241, dissolved in sterile saline (Hospira Inc, Lake Forest, IL) was tested (10 µg - .01 µg in 10 µl) or equivolume sterile saline as vehicle. Of note, fully solubilized AM1241 resulted in a clear solution.

2.2.3 Behavioral assessment of allodynia

Baseline (BL) responses to light mechanical touch were assessed using the von Frey test after animals were habituated to the testing environment, as previously described [214, 215]. Briefly, rats were placed atop 2 mm bars with 8 mm spacing between parallel bars for approximately 45 minutes for 5 days. All behavioral testing was performed during the first half of the light cycle in a sound, light, and temperature controlled room. The von Frey test utilizes a series of calibrated monofilaments, (3.61 – 5.18 log stimulus intensity; North Coast Medical, Morgan Hills, CA) applied randomly to the left and right plantar surface of the hindpaw for 8 seconds. Lifting, licking or shaking the paw was considered a response. Following chronic constriction injury (CCI) or sham surgery, animals were behaviorally tested on Day 3 and 10. On Day 10 post-surgery after behavioral assessment, all animals received an i.t. AM1241 or vehicle injection

followed by behavioral reassessment at 30 min intervals for 5 hr and again at 24 hrs. Testing was performed in a blinded fashion.

2.2.4 Chronic constriction injury (CCI) surgery

Following BL behavioral assessment, the surgical procedure for chronic constriction of the sciatic nerve was completed as previously described [216]. Briefly, isoflurane (induction 5% vol. followed by 2.5% in oxygen), anesthetized rats had their mid- to lower back and the dorsal left thigh shaved and cleaned with diluted Bacti-Stat AE, (EcoLab HealthCare Division, Mississauga, Ontario, Canada). Using aseptic procedures, the sciatic nerve was carefully isolated, and loosely ligated with 4 segments of chromic gut sutures (Ethicon, Somerville, NJ) with each suture approximately 1mm apart. Sham surgery was identical to CCI surgery but without the nerve ligation. The overlying muscle was sutured closed with two 3-0 sterile silk sutures (Ethicon, Somerville, NJ), and animals recovered from anesthesia within approximately 5 minutes.

2.2.5 Intrathecal (i.t.) injection

AM1241 was administered via acute i.t. catheter. Injections were performed as previously described [217]. Briefly, rats were anesthetized with isoflurane and an 18-gauge sterile, hypodermic needle, with the plastic hub removed was inserted between lumbar vertebrae L5 and L6. The PE-10 injection catheter was marked between 7.7-7.8 cm from an open end, with the other end inserted into a 30-gauge needle. A sterile Hamilton syringe was fitted with the 30-gauge needle and the attached PE-10 catheter, and collectively referred to as an injection catheter.

Either 10 µl drug or equivolume vehicle was withdrawn from respective vials via the open end of the PE-10 injection catheter, which was gently inserted into the L5 and L6-placed 18-gauge needle and threaded rostrally to the 7.7 cm marking on the injection catheter. The resulting position of the inserted tip of the PE-10 catheter occurs at the i.t. lumbosacral enlargement (~L4-L5). During this time, light tail twitching and a small amount of cerebrospinal fluid efflux from the 18-gauge needle was typically observed indicating successful i.t. catheter placement. Drug or vehicle was injected during a 10 second interval. Upon completion of injection, the PE-10 i.t. catheter was removed followed by removal of the 18-gauge needle. A 100% motor recovery rate was observed from this injection procedure.

2.2.6 Immunohistochemical procedures

Following behavioral assessment at indicated timepoints (Figure 2.3, 2.4) animals were overdosed with an intraperitoneal injection (8 - 1.3 cc) of sodium phenobarbital (Sleepaway, Fort Dodge Animal Health, Fort Dodge, IA) and perfused transcardially with saline followed by 4% paraformaldehyde. Whole vertebral columns with intact spinal cords (cervical 2 through sacral 1 spinal column segments) were removed, and underwent overnight fixation in 4% paraformaldehyde at 4°C. This tissue collection procedure ensured that all relevant anatomical components, including the spinal cord, DRG, and related meninges, were intact within the vertebral column, allowing important spatial relationships to remain for examining corresponding functional interactions at individual and specific spinal cord levels. All specimens underwent EDTA (Sigma

Aldrich, St. Louis, MO) decalcification for 30 days, and spinal cord sections were subsequently paraffin processed and embedded in Paraplast Plus Embedding Media (McCormick Scientific, St. Louis, MO) as previously described [218]. Four adjacent tissue sections (7μm) were mounted on a vectabond-treated slide (Vector Labs, Burlingame, CA), and allowed to adhere to the slide overnight at 40°C.

Approximately 130 slides per L4-L6 lumbar spinal cord, and 40 slides per lumbar L5 DRG, were generated in this manner for each animal. Two slides from an animal's lumbar spinal cord and two slides of DRG were randomly chosen for each staining procedure. The 7-um sections then underwent deparaffinization, and rehydration via descending alcohols to PBS (1X, pH 7.4). Sections were then processed with microwave antigen retrieval procedures (citrate buffer pH 6.0, or tris-based buffer, pH 9.0; BioCare Medical, Concord, CA).

2.2.7 Antibody staining

Slides were incubated with 5% normal donkey serum (NDS), in PBS (1X, pH 7.4) for 2 hours, followed by overnight primary antibody (Table 1) incubation in a humidity chamber at 3° C. Slides underwent secondary antibody incubation (Table 1) for 2 hours in a humidity chamber at room temperature, rinsed in PBS, and then coverslipped with Vectashield containing the nuclear stain 4',6-diamidino-2-phenylindole (DAPI) (Vector Labs, Burlingame, CA). For detection of MAGL, phosphorylated p38MAPK, and IL-10 protein, sections were incubated overnight with primary antibodies, incubated with biotinylated secondary antibody (Table 1) for 1 hour, and then treated with Vectastain ABC Elite kit (Vector Labs,

Burlingame, CA) and stained using TSA Plus Fluorescein System (PerkinElmer Life Sciences, Waltham, MA) and finally coverslipped with Vectashield containing DAPI. Stained section orientation was kept consistent throughout for proper identification of ipsilateral and contralateral spinal cord and DRGs. For lumbar spinal cord, sections were taken from L4-L6, and the dorsal horn analyzed (Fig. 1 A). For DRG material, sections were taken containing the DRG with the projection to L5, and the most distal portion of the DRG was analyzed (Fig. 1 B). Low magnification photomicrographs were obtained (Figure 1 A, B) using a Nikon Optiphot fluorescent microscope equipped with a DP2-BSW (Olympus) camera.

Primary antibody	Antibody clone	Indication	Anatomical region	Vendor/ Catolog Number	Host	Dilution used	Antigen retrieval	TSA Used	Secondary Antibody*
GFAP	Polyclonal	Astrocyte	Dorsal Horn Spinal Cord	Millipore/ AB5804	Rabbit	1:1000	Tris Buffer	No	Rhodamine Red Donkey anti- Rabbit (1:200)
GFAP	Monoclonal	Satellite cell	DRG	Progen/ 65011	Rabbit	1:10	Citrate Buffer	No	Rhodamine Red Donkey anti- Rabbit (1:200)
Iba-1	Polyclonal	Microglia	Dorsal Horn Spinal Cord	Wako/ 019-19741	Rabbit	1:300	Tris Buffer	No	Rhodamine Red Donkey anti- Rabbit (1:200)
FAAH	Polyclonal	Ecb enzyme	Dorsal Horn Spinal Cord	Cayman Chemical/ 101600	Rabbit	1:100	Tris Buffer	No	Rhodamine Red Donkey anti- Rabbit (1:200)
MAGL	Polyclonal	Ecb enzyme	Dorsal Horn Spinal Cord	Abcam/ AB24701	Rabbit	1:100	Citrate Buffer	Yes	Biotinylated Donkey anti- Rabbit (1:1300)
p-p38	Polyclonal	Phospho-p38 MAP Kinase	Dorsal Horn Spinal Cord, DRG	Cell Signaling/ 45112	Rabbit	1:800	Citrate Buffer	Yes	Biotinylated Donkey anti- Rabbit (1:1300)
IL-10	Polyclonal	IL-10 Protein	Dorsal Horn Spinal Cord, DRG	R&D Systems/ AF519	Goat	1:250	Citrate Buffer	Yes	Biotinylated Donkey anti- Goat (1:1300)
IL-1β	Polyclonal	IL-1 Beta Protein	Dorsal Horn Spinal Cord, DRG	Santa Cruz/ SC-7884	Rabbit	1:300	Tris Buffer	No	FITC, Rhodamine Red Donkey anti- Rabbit (1:200)

Table2. 1. List of all antibodies used in this study and designated under the appropriate column heading. Primary antibodies for polyclonal GFAP (astrocyte specific glial fibrillary acidic protein, Millipore, Billerica, MA), monoclonal GFAP (astrocyte specific glial fibrillary acidic protein, Progen, Heidelberg, Germany) previously used in (Achstatter *et al.*, 1986), Iba-1 (microglia, monocyte specific calcium channel protein, Wako Chemicals, Osaka, Japan)., FAAH (fatty acid amide hydrolase, endocannabinoid degredgative enzyme, Cayman Chemicals, Ann Arbor, MI), IL-1β protein (proinflammatory cytokine, Santa Cruz Biotechnology, Santa Cruz, CA), MAGL (monoacylglyerol lipase, endocannabinoid dregradative enzyme, Abcam, Cambridge, MA), phosphorylated p38MAPK (activated proinflammatory cytokine signaling pathway, Cell Signaling Technology, Beverly, MA), and IL-10 protein (anti-inflammatory cytokine, R&D Systems, Minneapolis, MN) were used. Secondary antibody incubation was performed with the indicated fluorophore conjugated secondary antibody. For MAGL, phosphorylated p38MAPK, and IL-10 protein, after overnight primary incubation, sections were instead incubated with biotinylated secondary antibody. *All secondary antibodies are from Jackson Immunoresearch (West Grove, PA).

2.2.8 Immunohistochemical image analysis

2.2.8.1 Image J software analysis

Fluorescent images for standard fluorescence analysis were obtained in the same manner as detailed above, with DAPI omitted from the Vectasheild mounting media. This was to ensure that DAPI staining did not potentially

obscure the fluorescence intensity. Images were taken on an Olympus BX51 microscope (Center Valley, PA) equipped with an Olympus DP72 camera. Images were then converted to grey scale and analyzed using Image J software available for free download at http://rsb.info.nih.gov/ij/. Briefly, an outline of the dorsal horn gray matter was drawn on an image, and holding the area within this outline consistent, the fluorescent intensity was obtained within this area for each image. This value was generated for each given tissue section (e.g. ipsilateral dorsal horn spinal cord) and averaged together (total of 4 tissue sections from a single animal) for an overall value. Therefore, for each anatomical location (e.g., ipsilateral and contralateral dorsal horn spinal cord and DRG), the 4 values (fluorescent intensity average count/second/ mm2) were averaged to obtain an individual animal's overall fluorescent intensity, with 3 animals in each experimental treatment group, to generate an average for that experimental condition. Likewise, background values were generated from control tissues incubated with PBS and the given secondary antibody, and averaged together. The average background was then subtracted from the above mentioned average of each experimental treatment group.

2.2.8.2 Spectral analysis of images

All images of the spinal cord dorsal horn and DRGs were captured by a Zeiss Axioscope Microscope at 20x magnification with a Nuance Spectral Camera (Cambridge Research & Instrumentation, Woburn, MA). Utilizing the Nuance computer software, the fluorescent wavelength emission spectra was initially determined for each fluorophore utilized in the detection of the primary antibody

of interest (DAPI, 488 nm +/- 10nm; FITC, 575 nm +/- 5nm; Rhodamine Red 600 nm+/- 5nm) by using a control slide with only a drop of the pure fluorophore. This was performed in the absence of a tissue specimen that may potentially obscure the measurement of the fluorophore's emission spectra. Two sets of additional control slides with tissue sections, one with only PBS without primary but with secondary antibody treatment, and the other, with primary but without secondary antibody treatment, were then used to objectively eliminate low intensity fluorescence and autofluorescence background 'noise' from our measurements (Figure2.1 C). Using control slides, the Nuance software allows the user to set an acceptable threshold of low-level emission fluorescent intensity (as opposed to the software's "autothreshold" option) within and outside the defined wavelength of interest between tissue samples. The experimenter determined low-level emission intensity by closely replicating the composite computer image with that observed through the eyepiece. Emission values that fall below this acceptable threshold of low-level emission, within and outside the defined wavelength of interest, were eliminated from our measurements (Figure 2.1 D). This level of fluorescent threshold for each protein marker was determined by the user finding the most appropriate wavelength of interest that captures the specific FITC or Rhodamine Red staining for each protein marker within a tissue (e.g., dorsal horn spinal cord or DRG). Once the optimal level of fluorescent threshold was determined for a particular protein marker, this level was held consistent throughout all of the treatment groups for the image analysis (Figure 2.1 D). These steps were followed by software conversion of fluorescent wavelength

intensity for each fluorophore to a numerical value. Autofluorescence was defined as that emission outside the defined wavelength of interest (e.g. DAPI, 488 nm +/- 10nm; FITC, 575 nm +/- 5nm; Rhodamine Red 600 nm+/- 5nm). These specific autofluorescent and low-level background emission values were subtracted from the image (Figure 2.1 E,F), yielding a numerical value of true fluorescent emission intensity for each fluorophore [219, 220].

Primary antibody staining procedures remained consistent to minimize intensity variations of each fluorophore (FITC or Rhodamine Red) used to detect the different primary antibodies of interest. To ensure that fluorophore binding was not impeded through possible steric hindrance of other proximal fluorophores, sections were labeled for only one cellular marker of interest on a slide.

The user also determined the minimum number of connected pixels on the computer screen for image analysis, counted as a region of interest (ROI) defined in the Nuance software system, which resulted in a software image containing distinctive morphology (i.e., of cellular bodies and processes, pattern of protein expression) that was virtually identical to the morphology observed through the microscope. The number of minimum connected pixels would therefore be set higher for a protein expressed abundantly by a cell (i.e., GFAP) than a protein expressed sparsely, leading to a punctuate pattern (i.e., IL-1β). These conditions resulted in a ROI, and were held consistent for both the ipsilateral and contralateral tissues in every experimental condition and for each antibody stain. The total area of each ROI, as measured by mm2, is calculated and is factored into the overall measurement of fluorescent intensity per second

of exposure. The average count of fluorescent emission intensity per second exposure, per mm^2 is the analyzed value that we report here. That is, fluorescent intensity average count/second/mm^2, which takes into account the density as well as the intensity of the fluorophore detected. A total of 4 sections per animal (N=3) were randomly selected and analyzed in this manner. By applying this novel method of data acquisition and analysis, experimenter bias is greatly minimized or even eliminated, yielding greater consistency and objectivity to fluorescent quantification.

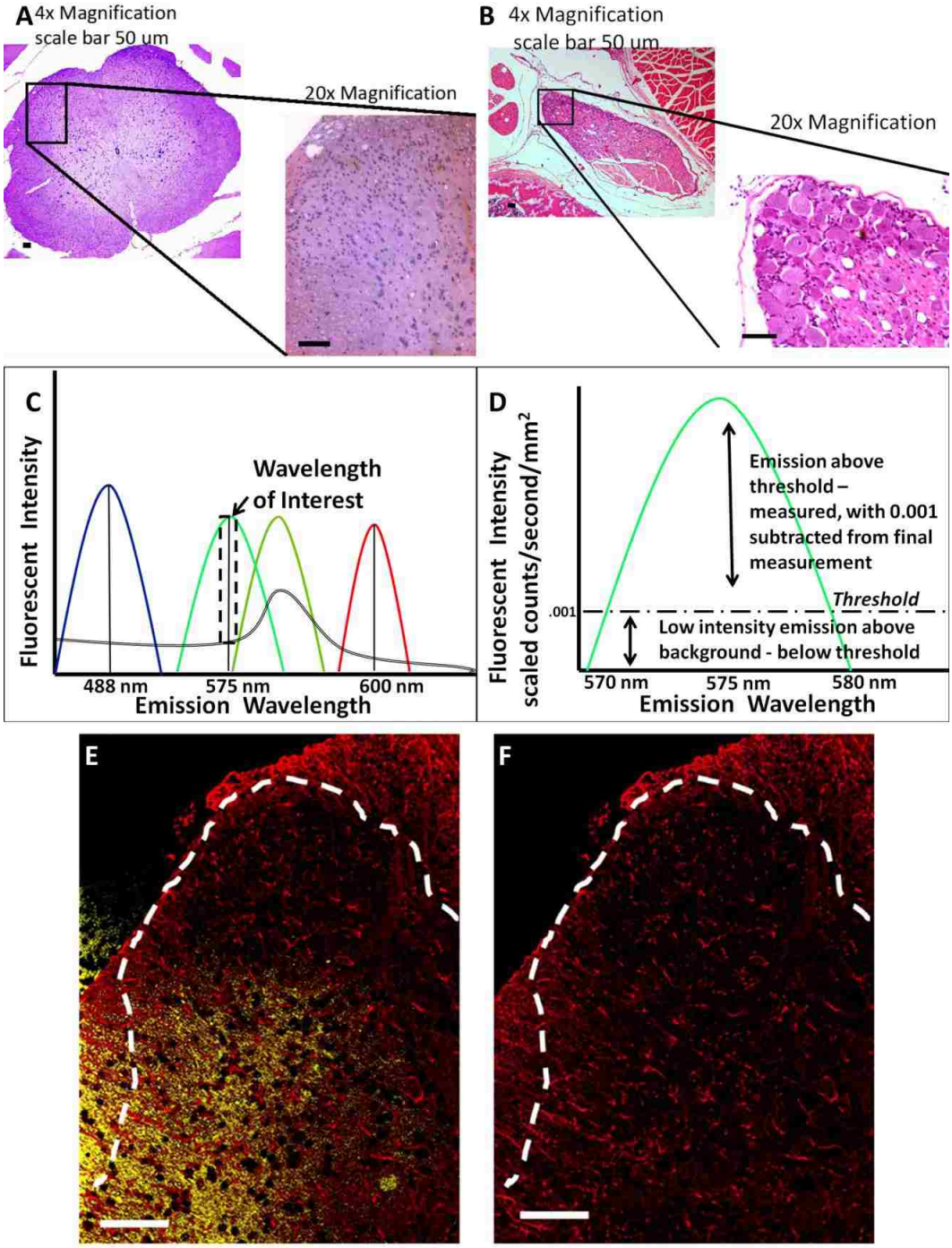

Figure 2.1 Anatomical location of images acquired and spectral analysis allows for discrete fluorescence signal detection and analysis.

Anatomical location of images acquired and spectral analysis allows for discrete fluorescence signal detection and analysis. **A**, Hematoxylin and eosin staining of the dorsal horn of the spinal cord and **B**, dorsal root ganglion (area within black box) is displayed in context to relevant anatomical structures (the entire spinal cord and partial cauda equina, respectively) at 4x magnification, and then at 20x magnification. **C**, Representative fluorescent emission for DAPI (blue) FITC (light green), GFP (dark green) Rhodamine Red (red) and autofluorescence (double black). Selection of narrow fluorescent peak emission bands (dotted black box around FITC

wavelength) allows for analysis of only FITC signal, without autoflourescent or GFP signal contaminating fluorescent analysis. **D**, Representative fluorescent emission threshold level of FITC defined and expanded from dotted black box in **A**, with the fluorescent threshold of intensity set (dashed black line), above autofluorescent levels. **E,** Representative spectral image of dorsal horn spinal cord as stained for GFAP (red), with autofluorescent signal defined in yellow. **F**, Same image in **E**, with autofluorescent signal removed. In all images the scale bar is equal to 50 μm.

2.2.9 Data analysis

Psychometric behavioral analysis was performed as previously described [215] to compute the log stiffness that would have resulted in the 50% paw withdrawal rate. Briefly, thresholds were estimated by fitting a Gaussian integral psychometric function to the observed withdrawal rates for each of the tested von Frey hairs, using a maximum-likelihood fitting method [221]. Estimated thresholds derived from a Gaussian integral function yield a mathematical continuum and thus are appropriate for parametric statistical analyses [215, 221]. The computer program PsychoFit may be downloaded from L.O. Harvey's website (http://psych.colorado.edu/~lharvey). All other data analysis was performed using the computer program GraphPad Prism version 4.03 (GraphPad Software Inc., San Diego, CA). For behavioral analysis to assess BL values, a one-way ANOVA was applied. To examine the presence of allodynia, a repeated-measures ANOVA was used at BL, 3 and 10 days after CCI, and indicated times note above (Behavioral assessment of allodynia). For the initial evaluation of fluorescence fading (Fig. 3 A, B), the student's t test with a 95% confidence interval was utilized. For all other statistical analysis, a two way ANOVA with a 95% confidence interval was performed. Statistical significance was determined with P-values <0.05. All data is expressed as mean +/- SEM. For post hoc analysis Bonferroni's test was performed.

2.3 Results

2.3.1 Intrathecal injection of AM1241 reverses CCI-induced allodynia in a dose-dependent manner

Limited evaluation exists for i.t. spinal application of CB_2R agonists to control allodynia produced by CCI, a widely used and well-characterized rodent model of chronic peripheral neuropathy with related pain-like behaviors [216]. We first examined if the putative CB_2R agonist from the aminoalkylindole class, AM1241 (36-fold CB_2>CB_1) [156, 161], could reverse ongoing allodynia produced by CCI. Prior to surgical manipulation, all groups exhibited similar bilateral (ipsilateral and contralateral) BL thresholds (ANOVA, $F_{(6,36)}$ =1.105; p=0.3764 ANOVA, $F_{(6,36)}$ =2.632; p=0.5884, respectively), (Figure 2.2 A,B). Following CCI, clear bilateral allodynia developed by Day 3 and continued chronically through Day 10 compared to sham-operated rats (ANOVA, $F_{(6,36)}$ =73.23; p< 0.0001, ANOVA, $F_{(6,36)}$ = 71.32; p<0.0001 respectively). On Day 10, compared to i.t. control injected neuropathic rats, AM1241 produced a dose-dependent reversal of allodynia, with maximal reversal observed at 1.5 hours following the highest injected dose (10 µg). However, allodynia fully returned by 3 hours after i.t. AM1241 treatment, with allodynia remaining constant through 24 hours. While 0.1 µg produced attenuated allodynia, 0.01 µg did not alter allodynia for either the ipsilateral (Figure 2.2 A), (ANOVA, $F_{(6,36)}$ = 138.8; p<0.0001), or contralateral (Figure 2.2 B) hindpaws (ANOVA, $F_{(6,36)}$ =131.6; p<0.0001). Post hoc analysis revealed 10 µg AM1241 yielded maximal reversal similar to pretreatment BL values at 1.5 hours after injection (p>.05).

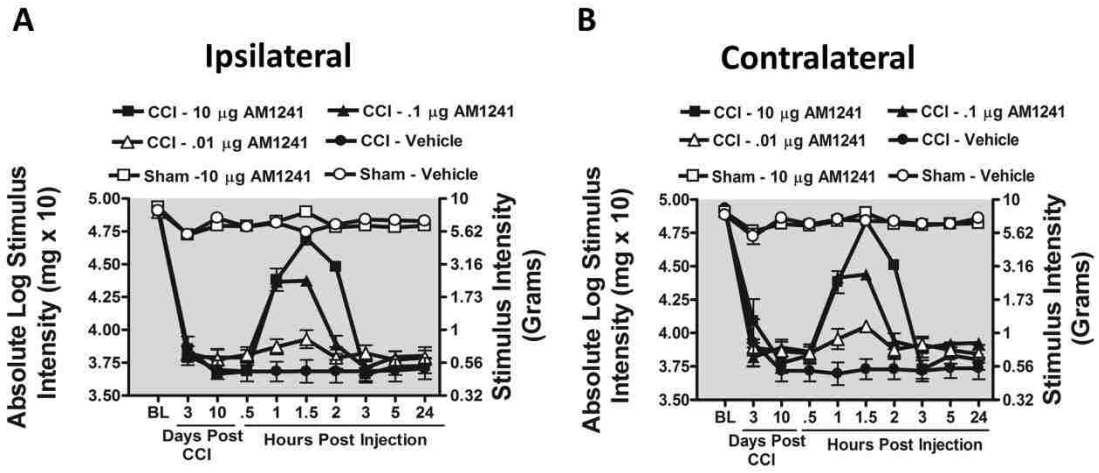

Figure 2.2 Intrathecal AM1241, a cannabinoid 2 receptor agonist reverses CCI-induced allodynia.

Intrathecal AM1241, a cannabinoid 2 receptor agonist reverses CCI-induced allodynia. A, B, AM1241 reverses CCI-induced allodynia in a dose-dependent manner. Before surgical manipulation, all AM1241 BL values of experimental groups exhibited similar ipsilateral and contralateral BL thresholds CCI surgery produced significant bilateral allodynia at days 3 and 10 following injury compared to sham-treated animals. Responses from AM1241 (10 μg) maximally reversed CCI-induced allodynia, (black squares), at 1.5 hours with allodynia fully returning by 3 hours after intrathecal administration.

2.3.2 Spectral Analysis vs. Standard Image J Fluorescent Analysis

Although previous reports detail an observed increase of IL-1β IR within the dorsal horn of the spinal cord after nerve ligation with chromic gut or silk sutures [26], detecting statistically significant changes in IL-1β IR has been problematic. Meanwhile, the use of spectral analysis procedures in other studies has demonstrated increased accuracy and sensitivity for the detection of cell specific markers [220, 222]. We therefore made direct comparisons between standard fluorescent analysis with Image J software and spectral image analysis software to identify the most sensitive method to quantify immunoreactive proteins of interest. Identical slides for both analysis procedures were used to eliminate potential fluorescent intensity variance between slides. Additionally, FITC-conjugated secondary antibody was examined as well as Rhodamine-conjugated

secondary antibody to identify whether intrinsic differences between different fluorophores (red vs. green) could yield false positive group differences.

IL-1β IR was examined with standard FITC fluorescent analysis utilizing NIH Image J software procedures (Figure 2.3 A). While a trend toward differences was present using Image J software, no statistically significant increase in IL-1β IR in either the ipsilateral or contralateral dorsal horn was found between non-neuropathic (Sham-Vehicle) and neuropathic CCI-treated rats (student T test p=0.0620 and p=0.5142, respectively). We utilized FITC-tagged secondary antibody in these studies because FITC tends to fade at a greater rate than Rhodamine Red, providing a stringent assessment of potential observed differences between experimental groups following a subsequent exposure. We therefore exposed the same tissue sections analyzed in Figure 2.3 A for a second time (Figure 2.3 B) with double the exposure-duration, but with the light sensitivity held consistent. Doubling the exposure time provides a rigorous test to determine whether fading can influence quantitative results. In using Image J, marginal non-significant fading of fluorescent intensity (Fig. 3 A vs. B) (student T test p= 0.7418 and p=0.9060, respectively) was present, and no difference in IL-1β IR between non-neuropathic and neuropathic rats was detected (student T test p=0.0648 and p=0.4874, respectively). In the same context, marginal fading was observed with spectral microscopy exposure between an initial exposure and a subsequent exposure (data not shown).

Given fluorophore fading was not present upon subsequent exposures, a new set of FITC stained IL-1β tissues from non-neuropathic (Sham-Vehicle) and

neuropathic rats (CCI-Vehicle) treatment groups were examined with standard Image J fluorescence analysis followed by spectral analysis. With Image J, we found no significant effect of surgery in either ipsilateral or contralateral dorsal horn (student T test p=0.5604 and p=0.6988, respectively)(Figure 2.3 C). However, spectral analysis of the identical sections revealed statistically significant differences in ipsilateral IL-1β IR due to surgical treatment (student T test p=0.0482 and p=0.0635, respectively) (Figure 2.3 D).

We found similar effects following comparison with a new set of slides from L4-L6 lumbar spinal cord tissue sections treated with IL-1β primary antibody, but incubated with a secondary antibody conjugated to the Rhodamine Red fluorophore (Figure 2.3 E,F). That is, the quantitative results between FITC or Rhodamine Red fluorescent intensity were similar within each method of image analysis. Specifically, no significant effect from surgical treatment was found utilizing standard Image J Rhodamine Red fluorescence analysis between treatment groups, either ipsilaterally or contralaterally (student T test p=0.2918 and p=0.2023, respectively) (Figure 2.3 E), while incorporating spectral analysis methods of the same tissues revealed strong increases in ipsilateral but not contralateral IL-1β IR in CCI treated rats (chronic neuropathy) (student T test p=0.0096 and p=0.1047, respectively) (Figure 2.3 F). Representative tissue staining for sham and CCI IL-1β are shown, as acquired with standard fluorescent microscopy (Figure 2.3 G,H) and with spectral fluorescent microscopy (Figure 2.3 I J). Thus, these findings demonstrate that the use of

spectral analysis may yield quantitative differences that may have previously gone undetected utilizing standard immunohistochemistry analysis techniques.

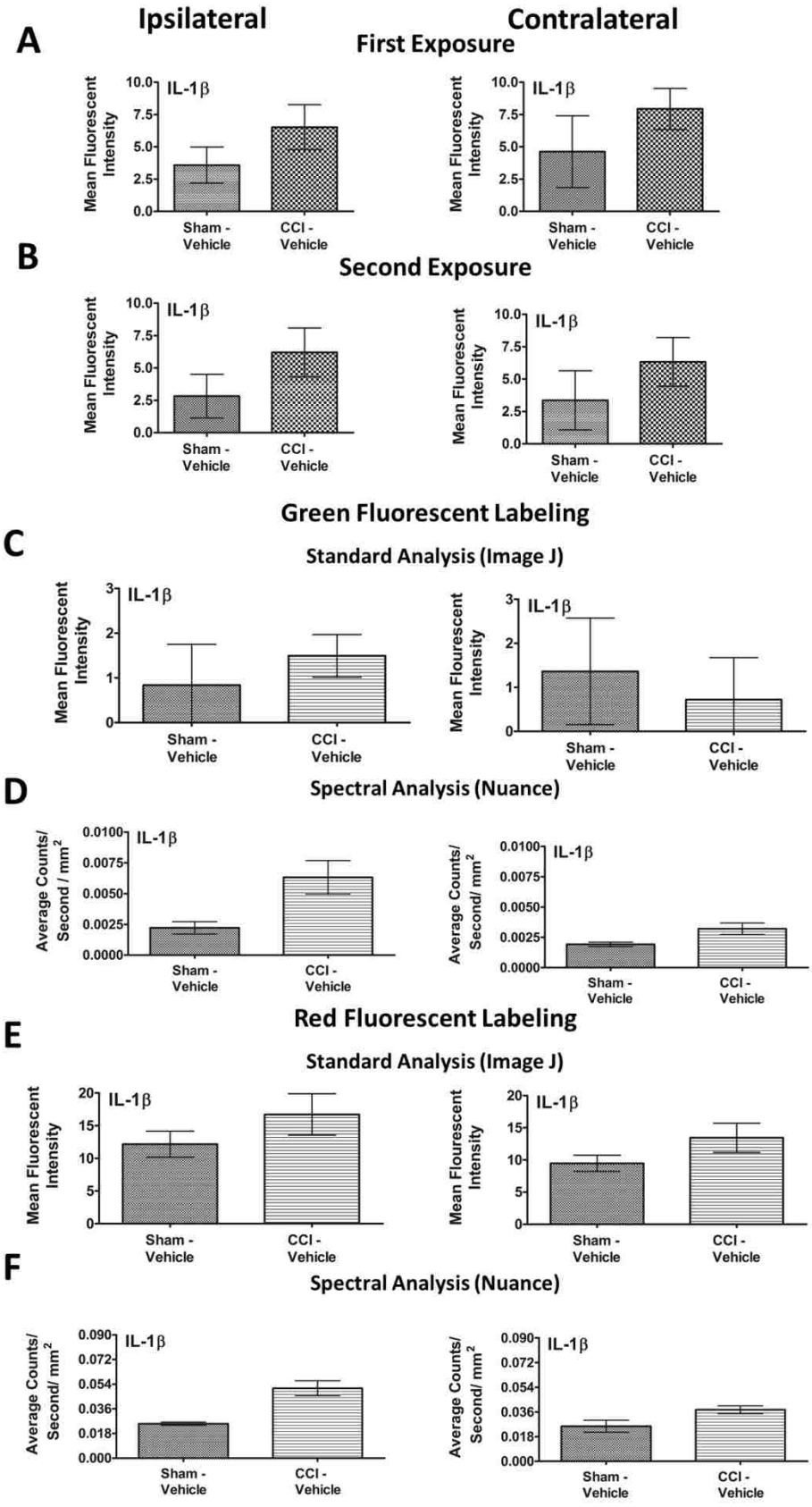
A
Ipsilateral
Contralateral
First Exposure
IL-1β
Mean Fluorescent Intensity
10.0
7.5
5.0
2.5
0.0
Sham - Vehicle
CCI - Vehicle
B
Second Exposure
C
Green Fluorescent Labeling
Standard Analysis (Image J)
Mean Flourescent Intensity
3
2
1
0
D
Spectral Analysis (Nuance)
Average Counts/ Second / mm2
0.0100
0.0075
0.0050
0.0025
0.0000
Average Counts/ Second/ mm2
E
Red Fluorescent Labeling
20
15
10
5
F
0.090
0.072
0.054
0.036
0.018
0.000

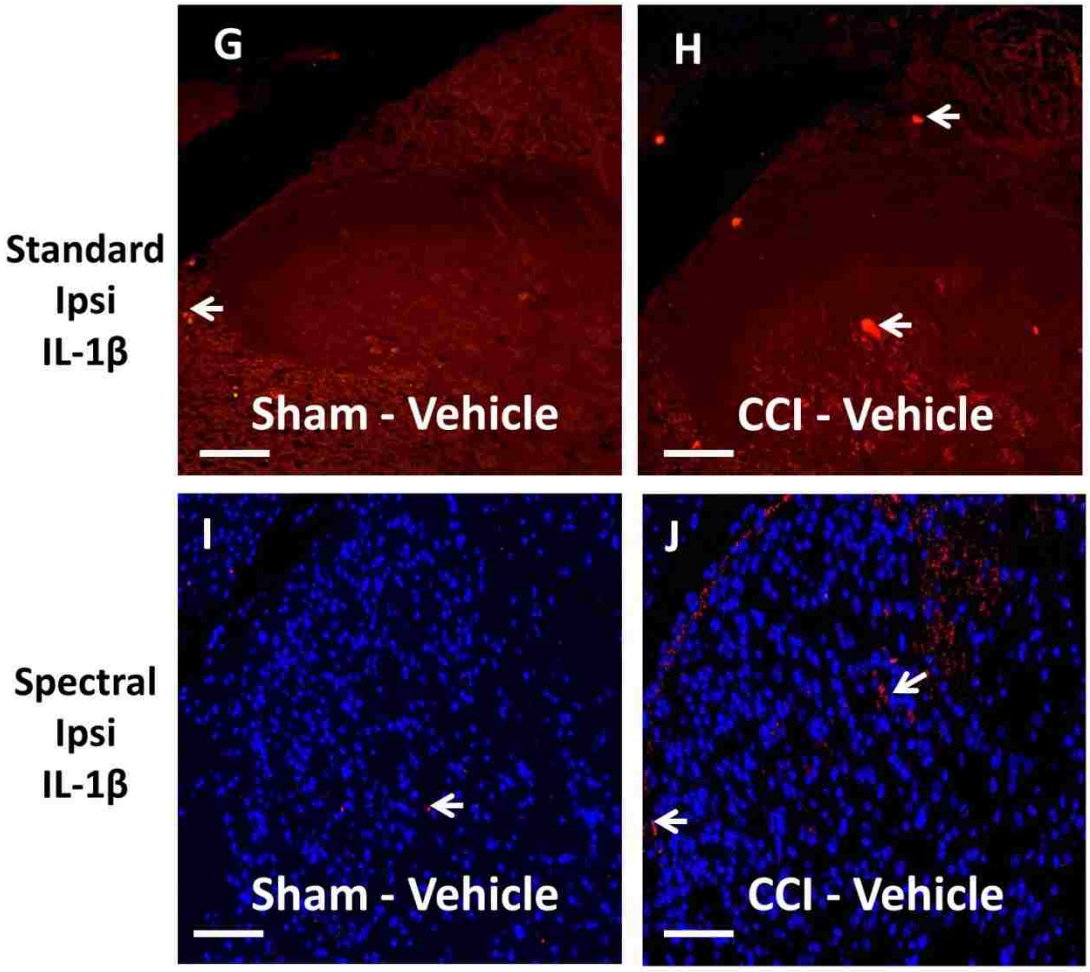

Figure 2.3 Spectral vs. standard Image J immunofluorescent intensity quantification comparision.

Spectral vs. standard Image J immunofluorescent intensity quantification comparision. **A,** Utilizing standard Image J immunofluorescent quantification, no significant IL-1β IR differences between CCI-induced neuropathy or non-neuropathic sham-treated rats in either the ipsilateral or contralateral dorsal horn of the spinal cord. IL-1β IR was observed by FITC labeled secondary antibody. **B**, Following a second exposure for image capture, fluorophore fading was virtually absent thereby lacking potential artificial IR intensity differences between experimental conditions. **C**, A comparison of sham and CCI-treated rats with i.t. vehicle using Image J immunofluorescent quantification resulted in no significant fluorescent intensity differences of labeled IL-1β IR between groups, in either the ipsilateral or contralateral dorsal horn. **D**, Utilizing spectral immunofluorescent quantification, significant differences of fluorescent intensity from FITC-labeled IL-1β between sham- and CCI-treated rats given i.t. vehicle was observed in the ipsilateral, but not contralateral dorsal horn spinal cord. **E**, An examination of fluorescent intensity between groups with a flourophore of a different spectral signature, Rhodamine Red (600 nm), using standard Image J immunofluorescent quantification revealed no significant group differences between sham- and CCI-treated rats despite a trend of increased IL-1β IR in CCI-treated rats with i.t. vehicle in either the ipsilateral or contralateral dorsal horn. **F**, Spectral immunofluorescent quantification of Rhodamine Red-labeled IL-1β yielded significant group differences between non-neuropathic sham rats and CCI-treated rats with vehicle in the ipsilateral

dorsal spinal cord. IL-1β IR increases were absent in the contralateral dorsal horn. **G**, **H**, Representative fluorescent images analyzed with Image J at 20x magnification of IL-1β fluorescent labeling (red). **I**, **J**, Representative spectrally unmixed images at 20x magnification of IL-1β fluorescent labeling (red) with DAPI nuclear stain (blue). In all images the scale bar is equal to 50 μm. All sections were 7 □m thick, and collected 1.5 hours after i.t. vehicle administration 10 days after CCI or sham surgery.

2.3.3 Behavioral verification of i.t. AM1241 for subsequent spinal cord immunohistochemistry

In a separate group of rats, intrathecal (i.t.) injection of AM1241 again produced robust bilateral reversal from allodynia (Figure 2.4 A,B), similar to that observed in Figure 2.2, Prior to CCI, all groups exhibited similar ipsilateral and contralateral BL thresholds (ANOVA, $F_{(3,11)}$ =0.9006; p=0.4821, ANOVA, $F_{(3,11)}$ =0.8916; p=0.4860, respectively). CCI produced significant bilateral allodynia at Day 3 and continued to Day 10 compared to sham-treated animals (ANOVA, $F_{(3,11)}$ =135.8; p< 0.0001 and ANOVA, $F_{(3,11)}$ = 149.9; p=0.0001, respectively). Behavioral responses following i.t. AM1241 (10 μg) produced maximal bilateral reversal of allodynia (ANOVA, $F_{(3,11)}$ =150.4; p<0.0001 and ANOVA, $F_{(3,11)}$ =72.36; p<0.0001, respectively). At peak reversal, animals were sacrificed and spinal tissue was collected to examine bilateral immunoreactivity for proteins including cytokines p-p38MAPK, glial activation markers, and endocannabinoid degradative enzymes.

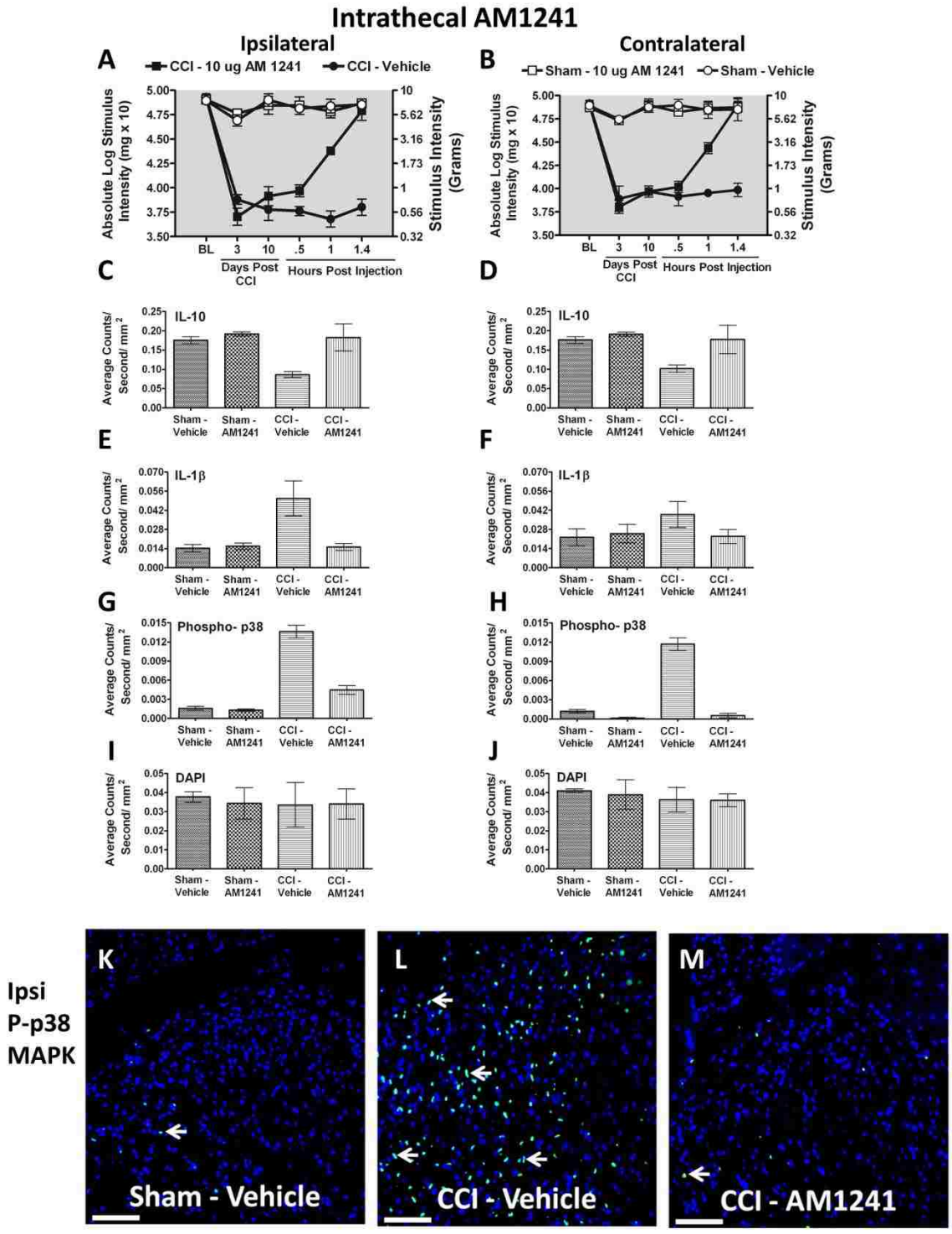

Figure 2.4 Cytokine, p-p38MAPK, DAPI Immunofluorescent intensity quantification of Tissues from AM1241-treated rats

Immunofluorescent intensity quantification from 7 µm thick sections of dorsal horn spinal cord from behaviorally verified rats following i.t. vehicle or AM1241. **A, B,** Prior to CCI, all groups exhibited similar ipsilateral and contralateral BL thresholds. CCI produced significant bilateral allodynia at days 3 and 10 following injury compared to sham-treated animals. Behavioral

responses following AM1241 (10 µg) produced maximal bilateral reversal of allodynia followed by tissue collection of immunofluorescent intensity quantification. **C**, **D**, IL-10 expression was bilaterally decreased in CCI-treated rats that received i.t. vehicle compared to control sham-treated rats given either vehicle or AM1241, while IL-10 IR recovered to sham levels in CCI neuropathic rats given i.t. AM1241. **E**, **F**, Compared to sham controls, IL-1β expression was increased ipsilaterally, but not contralaterally in CCI-treated animals given i.t. vehicle of AM1241. However, i.t. AM1241 in CCI-treated rats robustly suppressed increases in IL-1β IR. **G**, **H**, Phospho-p38 expression was bilaterally increased in CCI-induced neuropathic rats treated with i.t vehicle of AM1241. Increased bilateral p-p38MAPK was significantly suppressed in CCI-treated rats given i.t. AM1241. **I**, **J**, No differences in DAPI nuclear stain fluorescent intensity was observed in either sham control or CCI-treated rats given either i.t. vehicle or AM1241. **K**, **L**, **M**, Representative spectrally unmixed images at 20x magnification of P-p38 MAPK fluorescent labeling (green) with DAPI nuclear stain (blue). In all images the scale bar is equal to 50 µm.

2.3.4 Immunohistochemical analysis of dorsal spinal cord

2.3.4.1 IL-10

While spinal CB_2R activation controls pain-related behaviors and glial activation in neuropathic rats [93, 94, 135, 139, 223], the underlying spinal immunoregulatory signals remain unclear. One of the most effective anti-inflammatory cytokines characterized to control pathological pain processing to date is IL-10 [202, 204, 217, 224-230]. Here, we examined changes in IL-10 IR at the time of peak AM1241 efficacy. Bilateral IL-10- immunoreactivity (IR) in the dorsal horn spinal cord was dramatically decreased in CCI-induced neuropathic rats compared to sham-treated rats (ANOVA, $F_{(1,8)}$=10.09; p=0.0131; ANOVA, $F_{(1,8)}$=7.548; p=0.0252, respectively), (Figure 2.4 C,D). In stark contrast, treatment with AM1241 resulted in basal levels of IL-10 IR, for both the ipsilateral and contralateral dorsal spinal cord (ANOVA, $F_{(1,8)}$ =13.19; p=0.0067; ANOVA, $F_{(1,8)}$ =7.903; p=0.0228, respectively).

2.3.4.2 IL-1β

To replicate our results described in Figure 2.3 (D, F), separate L4-L6 lumbar spinal cord tissue sections were processed and analyzed. Compared to non-

neuropathic sham-operated rats given i.t. AM1241 or equivolume vehicle, CCI-induced neuropathy produced a robust unilateral increase in dorsal horn IL-1β IR (ANOVA, $F_{(1,8)}$ =10.46; p=0.0120), while compared to controls, no differences in contralateral IL1β were observed (ANOVA, $F_{(1,8)}$ =1.627; p=0.2379), (Figure 2.4 E,F). Conversely, following AM1241 administration, significantly lower levels of IL-1β IR were detected (ANOVA, $F_{(1,8)}$ =9.431; p=0.0153). IL-1β IR observed in the contralateral dorsal horn was not substantially elevated when compared to vehicle injected animals (ANOVA, $F_{(1,8)}$ =1.321; p=0.2836).

2.3.4.3 p38-MAPK and DAPI

Spinal p-p38MAPK is widely characterized to mediate allodynia through the actions of spinal IL-1β [27, 194, 231]. Therefore, p-p38MAPK was examined. Compared to non-neuropathic sham-operated rats given i.t. AM1241 or equivolume vehicle, CCI-induced neuropathy produced a robust p-p38MAPK bilateral IR increase in the spinal cord dorsal horn (ANOVA, $F_{(1,8)}$ =223.1; p<0.0001; ANOVA, $F_{(1,8)}$ =148.0; p<0.0001, respectively), (Figure 2.4 G,H). In contrast, tissues from rats treated with i.t. AM1241 revealed dramatically lower levels of p-p38MAPK IR that were close to or similar to spinal cord tissues from non-neuropathic sham-treated rats (ANOVA, $F_{(1,8)}$ =85.82; p<0.0001; ANOVA, $F_{(1,8)}$ =187.1; p<0.0001, respectively) . Representative fluorescent images are presented corresponding to the image analysis of either sham treated with i.t. vehicle (Figure 2.4 K), CCI treated with i.t. vehicle (Figure 2.4 L), or CCI treated with AM1241 (Figure 2.4 M).

It is possible that overall changes in spinal cord cell numbers could dramatically alter dorsal horn immunofluorescent intensity quantification, as proliferation of microglia [232], astrocytes [233], or leukocyte CNS extravasation [76] have been reported. Consequently, cells could simply be constitutively expressing low-levels of proteins, thus diminishing interpretation that a protein-specific cellular response has occurred following either CCI and/or i.t. AM1710. However, we observed no change in cell numbers as assessed by quantification of nuclear-specific DAPI fluorescence intensity as a consequence of either CCI procedures (ANOVA, $F_{(1,8)}$=0.1076; p=0.7514, ANOVA, $F_{(1,8)}$=0.7780; p=0.4035, respectively) or i.t. drug injections (ANOVA, $F_{(1,8)}$=0.04328; p=0.8404, ANOVA, $F_{(1,8)}$ =0.06960; p=0.7986, respectively), (Figure 2.4 I,J).

2.3.5 Microglial and astrocyte activation

2.3.5.1 Iba-1 to identify altered microglial responses

Based on reported evidence that CB_2Rs are present on microglia, we examined whether bilateral dorsal spinal microglial responses during CCI-induced allodynia were altered subsequent to i.t. administration of AM1241. To examine microglia in the dorsal horn of the spinal cord, expression of the microglial marker, Iba-1 was examined. Compared to non-neuropathic sham-operated rats given i.t. AM1241 or equivolume vehicle, CCI-induced neuropathy produced a robust bilateral increase in spinal cord dorsal horn Iba-1 IR (ANOVA, $F_{(1,8)}$ =212.0; p<0.0001, ANOVA, $F_{(1,8)}$=62.28; p<0.0001, respectively), (Figure 2.5 A,B). Surprisingly, AM1241 did not alter increased levels of spinal dorsal horn Iba-1 IR in behaviorally reversed rats (ANOVA, $F_{(1,8)}$ =2.767; p=0.1348, ANOVA, $F_{(1,8)}$

=0.1346; p=0.7232, respectively), (Figure 2.5 A,B). Representative images taken from the spinal cord dorsal horn following i.t. vehicle injection in sham and CCI treated rats are provided (Figure 2.5 C,D).

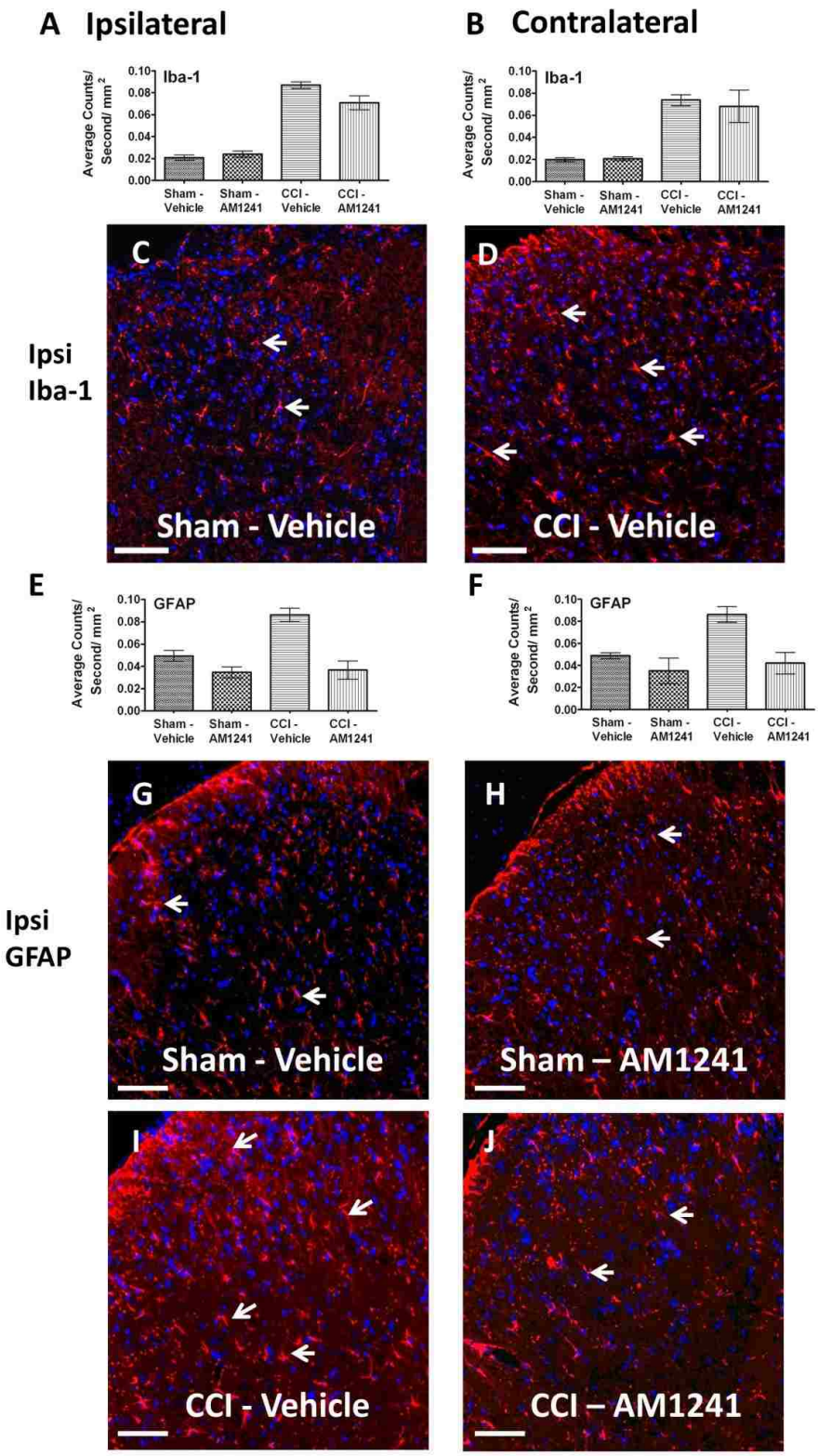

Figure 2.5 Glial Immunofluorescent intensity quantification in tissues from rats treated with AM1241

Immunofluorescent intensity quantification of the spinal cord dorsal horn reveals differences in astrocyte activation but not microglial activation in neuropathic rats treated with AM1241. **A**, **B**,

Iba-1 expression increased within the ipsilateral and contralateral dorsal horn of the spinal cord following CCI manipulations compared to control sham treatment, irrespective of i.t. vehicle or AM1241. **C**, **D**, Representative spectrally unmixed images at 20x of Iba-1 fluorescent staining (red) and DAPI nuclear stain (blue). **E**, **F**, GFAP immunofluorescent intensity in the dorsal horn of the spinal cord was significantly increased in neuropathic rats following CCI given i.t. vehicle, while GFAP IR in neuropathic rats given i.t. AM1241 was greatly attenuated. **G**, **H**, **I**, Representative spectrally unmixed images at 20x magnification of GFAP fluorescent labeling (red) with DAPI nuclear stain (blue). In all images the scale bar is equal to 50 µm. All sections were 7 □m in thickness.

2.3.5.2 GFAP to identify altered astrocyte responses

In the superficial dorsal horn, where incoming signals from pain fibers are processed, histological observation reveals that astrocytes make intimate contact with microglia that express CB_2Rs [94]. Prior reports additionally show that following spinal CB_2R activation in neuropathic rats, superficial dorsal horn GFAP IR is significantly reduced [91]. Therefore, we examined GFAP IR in the dorsal horn of the spinal cord following i.t. administration of AM1241. Compared to non-neuropathic control animals, neuropathic rats demonstrated a robust bilateral increase in dorsal horn GFAP IR (ANOVA, $F_{(1,8)}$ =15.00; p=0.0047; ANOVA, $F_{(1,8)}$ =10.45; p=0.0120, respectively) (Figure 2.5 E,F). In stark contrast, lower values of bilateral GFAP IR were observed from tissues of rats treated with i.t. AM1241 (ANOVA, $F_{(1,8)}$=41.38; p=0.0002; ANOVA, $F_{(1,8)}$=17.63; p=0.0030, respectively) (Figure 2.5 E,F). Corresponding representative fluorescent images used for analysis are shown; sham-operated rats treated with i.t. vehicle (Figure 2.5 G,), or CCI-treated rats injected with either i.t. AM1241 or equivolume vehicle (Figure 2.5 H,I).

2.3.5.3 MAGL and FAAH

Endocannabinoids known to produce anti-allodynic effects are metabolized via enzymatic hydrolysis by fatty acid amide hydrolase (FAAH) and/or monoacylglycerol (MAGL) [234]. Inhibition of FAAH or MAGL increases the bioavailablity of CNS endocannabinoids with a corresponding attenuation of neuropathic pain rats [151, 152]. Whether FAAH and MAGL IR expression levels are altered in the dorsal horn following i.t. CB_2R agonist injections in neuropathic rats, is unknown. Therefore, we examined potential changes in MAGL and FAAH IR in tissue sections from rats given i.t. AM1241. Compared to non-neuropathic control rats, neuropathic rats showed a robust ipsilateral (ANOVA, $F_{(1,8)}$ =34.19; p=0.0004) and contralateral (ANOVA, $F_{(1,8)}$ =27.51; p=0.0008) increase in dorsal horn MAGL IR (Figure 2.6 A,B). In contrast, spinal tissue collected from rats given an i.t. AM1241 injection revealed significantly lower bilateral MAGL IR (ipsilateral ANOVA, $F_{(1,8)}$=8.356; p=0.0202, and contralateral ANOVA, $F_{(1,8)}$ =4.146; p=0.0761, respectively) (Figure 2.6 A,B). Interestingly, no interpretable or meaningful change in FAAH IR between non-neuropathic and neuropathic CCI rats was observed following surgical manipulation (ipsilateral ANOVA, $F_{(1,8)}$ =8.072; p=0.0218, and contralateral ANOVA, $F_{(1,8)}$ =0.09666; p=0.7638), or following i.t. AM1241 or vehicle treatment (ANOVA, $F_{(1,8)}$ =0.5436; p=0.4820; ANOVA, $F_{(1,8)}$ =2.174; p=0.1786, respectively) (Figure 2.6 C,D).

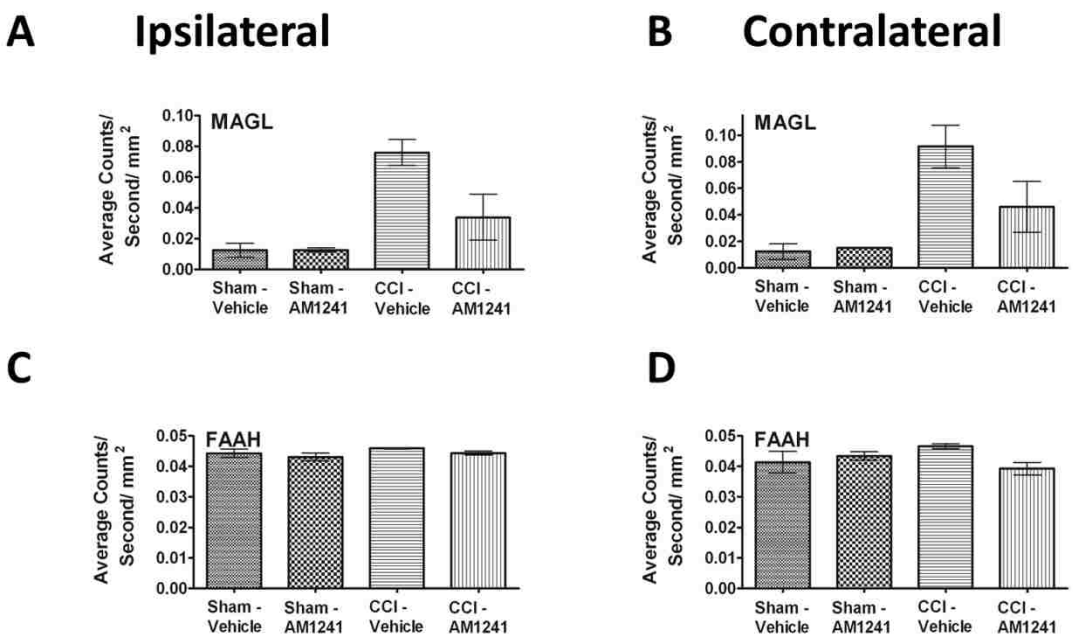

Figure 2.6 Endocannabinoid degradative enzyme immunofluorescent intensity from rats treated with AM1241

Immunofluorescent intensity quantification of the spinal cord dorsal horn reveals AM1241 reduces the expression of the endocannabinoid degragative enzyme, MAGL but does not alter FAAH. **A**, **B**, Compared to control rats, MAGL IR expression was increased ipsilaterally, with strong trends contralaterally in CCI-treated neuropathic rats that received i.t vehicle of AM1241, while spinal MAGL IR in CCI-treated rats given i.t. AM1241 was substantially reduced. **C**, **D**, No changes in FAAH IR expression in ipsilateral and contralateral dorsal horn of either sham or CCI-neuropathic rats given either i.t. vehicle or AM1241 was observed. All sections were 7 □m in thickness.

2.3.6 Dorsal Root Ganglia Immunohistochemical analysis: GFAP, IL-1β, p-p38MAPK and IL-10

Immunohistochemical detection of GFAP, IL-1β, p-p38MAPK, and anti-inflammatory IL-10 in L4-L5 DRG that correspond to the ipsilateral and contralateral spinal cord segments was quantified. Results revealed that compared to non-neuropathic control rats, CCI-induced neuropathic rats displayed a robust bilateral increase in GFAP IR in DRG (ipsilateral ANOVA, $F_{(1,8)}$ =9.133; p=0.0165, and contralateral ANOVA, $F_{(1,8)}$ =8.443; p=0.0197, respectively), (Figure 2.7 A,B). However, i.t. AM1241 injection robustly blocked bilateral increases in GFAP IR (ipsilateral ANOVA, $F_{(1,8)}$ =27.19; p=0.0008, and

contralateral ANOVA, $F_{(1,8)}$ =5.223; p=0.0516, respectively), (Figure 2.7 A,B). Intriguingly, DRG changes in levels of p-p38MAPK IR occurred in the ipsilateral (ANOVA, $F_{(1,8)}$ =6.885; p=0.0305), but not the contralateral DRG (ANOVA, $F_{(1,8)}$ =0.2013; p=0.6656) to the sciatic nerve damage (Figure 2.7 C,D), and, i.t. AM1241 injection revealed p-p38MAPK IR that was similar to controls (ANOVA, $F_{(1,8)}$ =15.92; p=0.0040, ANOVA, $F_{(1,8)}$ =2.051; p=0.1900, respectively). This unilateral change was also observed with IL-1β IR due to CCI surgery (ipsilateral ANOVA, $F_{(1,8)}$ =6.414; p=0.0351; contralateral ANOVA, $F_{(1,8)}$ =0.3111; p=0.5923), and AM1241 treatment resulted in levels similar to controls (ipsilateral ANOVA, $F_{(1,8)}$ =52.03; p<0.0001; contralateral ANOVA, $F_{(1,8)}$ =0.2221; p=0.6500) (Figure 2.7 E,F). An intriguing unilateral decrease in IL-10 IR was measured in CCI-treated only (ipsilateral ANOVA, $F_{(1,8)}$ =17.42; p=0.0031, and contralateral ANOVA, $F_{(1,8)}$ =1.583; p=0.2438), while an i.t. AM1241 injection (ipsilateral ANOVA, $F_{(1,8)}$ =22.83; p=0.0014, and contralateral ANOVA, $F_{(1,8)}$ =1.327; p=0.2826), (Figure 2.7 G,H) resulted in increased IL-10 IR levels that were similar to controls. Collectively, these data show that while GFAP-positive satellite cells in bilateral DRG are a target of AM1241, only ipsilateral IL-1β, p-p38MAPK and IL-10 IR levels are altered.

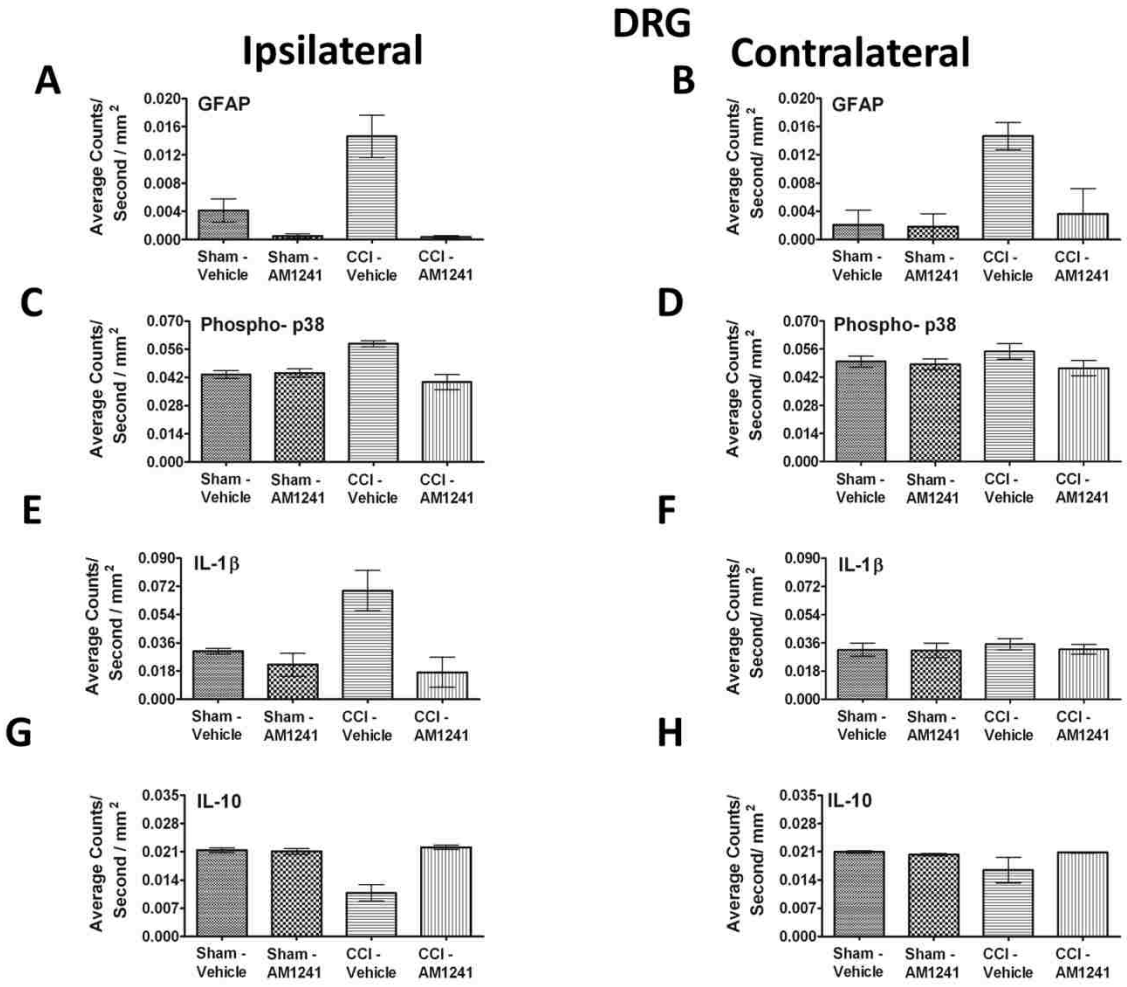

Figure 2.7 Immunofluorescent intensity quantification DRG

Immunofluorescent intensity quantification of 7 µm in thick sections from the dorsal root ganglion reveals significant differences in satellite cell activation, phosphorylated p38MAPK, IL-1β and IL-10 in i.t. AM1241 injected rats. **A**, **B**, GFAP (satellite cell activation) expression was increased in animals with CCI compared to sham-treated rats, given i.t. vehicle ipsilaterally as well as contralaterally, and robust bilateral suppression of GFAP IR was observed in rats given i.t. AM1241. **C**, **D**, A small but significant unilateral increase in phospho-p38 (activated) IR was detected on the side ipsilateral to the CCI treatment with i.t. vehicle , while i.t. AM1241 attenuated increased p-p38MAPK IR in CCI-treated rats. **E, F,** Unilateral IL-1β IR was increased in DRG on the side ipsilateral to the CCI manipulation compared to sham-treated controls, while IL-1β expression was substantially decreased in CCI-treated rats with i.t. AM1241. **G, H**, Ipsilateral, but not contralateral, IL-10 IR was significantly decreased in CCI-treated neuropathic rats given i.t. vehicle of AM1241 compared to sham controls given either i.t. vehicle or AM1241. However, a robust increase in IL-10 IR in the DRG of CCI neuropathic rats given i.t. AM1241 was detected.

2.4 Discussion

In the present study, we examined the efficacy of an i.t. CB_2R agonist, AM1241, on chronic bilateral allodynia produced by unilateral sciatic nerve CCI. We

present evidence that AM1241 produced robust bilateral reversal from allodynia in a dose-dependent manner that may act via anti-inflammatory mechanisms. While prior reports show that peripheral administration of AM1241 controls pathological pain [182, 198, 199, 209], peripheral neuropathy induced by spinal nerve ligation [182, 211] and cancer chemotherapeutic agents [165, 210], the current results extend these findings by showing that peri-spinal i.t. AM1241 injection acts to reverse CCI-induced allodynia. Importantly, AM1241 itself did not alter normal basal sensory threshold responses at any dose when administered intrathecally, which is distinct from reports showing an anti-nociceptive action at peripheral nerve terminals following peripheral administration of AM1241 that produced increased BL sensory thresholds [165, 175, 197].

In this study, we additionally present evidence for distinct profiles of anti-inflammatory protein expression patterns in the dorsal horn of the spinal cord and DRG. In the dorsal horn of neuropathic rats, bilateral IL-10 IR was significantly lower compared to non-neuropathic rats. While a reduction of peripheral nerve or DRG IL-10 mRNA or protein has been reported [74, 191, 235, 236], to date, no prior reports have demonstrated decreased dorsal horn IL-10 IR in adult rats during chronic allodynia from peripheral neuropathy. Additionally, greater bilateral p-p38MAPK, astrocyte GFAP, microglial Iba-1 and MAGL IR levels were measured in neuropathic rats compared to non-neuropathic controls. Further, an increase in unilateral spinal IL-1β IR was measured on the side ipsilateral to CCI. However, following an i.t. AM1241 injection, not only was behavioral allodynia reversed, but IL-10, p-p38MAPK, astrocyte GFAP, MAGL and IL-1β IR levels

were similar to those observed in non-neuropathic animals. The corresponding L4-L5 DRG immunofluorescent analysis from neuropathic rats revealed similar changes in protein expression patterns, however, bilateral DRG changes were observed only with GFAP IR. These data extend prior reports that AM1241 acts in a general anti-inflammatory manner by identifying specific in vivo spinal and DRG changes of elevated IL-10, with concurrently diminished IL-1β and p-p38MAPK IR in the dorsal horn of the spinal cord.

The pattern of bilateral allodynia reported in the current study supports a number of prior reports demonstrating a similar behavioral pattern from CCI [200-203, 217, 226, 237-239]. Bilateral biochemical changes in the spinal cord and the DRG have been examined that may, in part, characterize underlying contralateral allodynia from CCI. These studies reported decreased α2-adrenergic receptor mRNA expression [240], increased neuronal Fos protein [241], increased TNF-α protein [191], and increased IL-6 mRNA expression [239]. Additionally, very recent reports have demonstrated increases in unilateral spinal IL-1β mRNA expression [242], or increased IL-1β spinal immunohistochemical detection [243] following unilateral sciatic nerve ligation or transection. Further, endogenous IL-1β receptor antagonist IL-1RA contributes to the anti-inflammatory effects of activated CB2 receptors [244]. Here, we demonstrate the unique findings that an ipsilateral increase in IL-1β IR is observed in anatomically intact spinal cord following CCI that produces bilateral allodynia. It is notable that the actions of spinal IL-1β are necessary for allodynia produced from CCI [204, 217]. Together, these data suggest that ipsilateral IL-1β is important for initiating changes that

ultimately spread to the contralateral spinal cord resulting in contralateral allodynia. Given astrocytes can communicate via gap junctions, it is possible that ipsilateral IL-1β-to-astrocyte communication leads to the spread of contralateral astrocyte activation via gap junctions inducing signals that result in contralateral allodynia. In support of this hypothesis, a model of localized unilateral sciatic nerve inflammation was demonstrated to critically involve spinal astrocyte gap-junctional communication underlying bilateral allodynia, which was mediated, in part, by spinal IL-1β [237]. Given the indirect role that ipsilateral IL-1β may play in contralateral allodynia, the key biochemical difference between ipsilateral and contralateral spinal cord may be in IL-1β expression patterns.

In the current data reported here, we have identified significant increases of IL-1β IR in anatomically discrete regions of the spinal cord in CCI-induced neuropathic rats as a consequence of identifying and omitting autofluorescence and low-level background emission intensities from tissue samples. This was achieved by applying relatively straightforward spectral analysis, using the Nuance software, to quantify immunofluorescent levels in anatomically intact spinal cord that eliminates unwanted autofluorescence occurring at nearby wavelengths, which is not discernable using conventional methods of immunofluorescence detection and quantification. Furthermore, we report that i.t. AM1241 resulted in low-level immunoreactivity for IL-1β similar to non-neuropathic control levels that corresponds to anti-allodynia. This discrete IL-1β difference between experimental groups was lost when applying standard Image J analysis methods.

The most striking feature of this approach is that autofluorescent emission-peaks at nearby wavelengths can be determined from control tissue specimens not stained for the protein marker under examination. The identified autofluorescent wavelengths with corresponding intensity can be subtracted from images derived from tissues that have undergone specific immunohistochemical fluorescence staining procedures. This feature of subtracting ‘noise’ is advantageous when considering that sections between animals within a single experimental group can display variations in peak autofluorescence intensity. Of critical importance is that low-level fluorescence emission within a discrete 10 nm fluorescent wavelength range being analyzed (e.g. FITC 575 nm, +/- 5 nm) can occur in the absence of targeted immunofluorescence protein staining thereby contributing to background ‘noise’. This noise is detected by applying the consistent use of both a fixed contiguous pixel number and fluorescent threshold during image capture. The identified endogenous fluorescent intensity is then omitted from quantification of specific markers in the image. These additional steps ensure experimenter bias is eliminated. A practical consideration is that the spectral analysis software is easily learned and fluorescence intensity quantification can be conducted in a timely manner. An additional advantage applying immunofluorescent quantification following spectral analysis of intact spinal cord is greater sensitivity to detect specific protein markers compared to other protein quantification procedures that require relatively high amounts of tissue samples (e.g. 100 µg). These traditional methods often translate into the necessity for greater animal numbers to achieve detectable results.

Proinflammatory factors were examined in this report that extend beyond IL-1β in an attempt to provide a broad characterization of the anti-inflammatory effects of CB_2R agonists like AM1241. The mitogen-activated protein kinase (MAPK) family consists of three major members that includes p38, which as noted above, contributes to pain sensitization following peripheral nerve injury [27, 34, 192, 193, 195, 232, 245-248] via the actions of spinal IL-1β and other proinflammatory cytokines [249, 250]. The current data support these prior reports in that increased p-p38MAPK IR is present in the dorsal horn of the spinal cord and DRG in neuropathic rats, and extend AM1241 characterization as an anti-inflammatory CB_2R agonist by demonstrating that AM1241 robustly suppresses p-p38MAPK IR in pain-reversed rats with peripheral neuropathy.

Microglial and astocytic glial markers in the spinal cord dorsal horn in neuropathic rats, as assessed by immunofluorescent detection, reveal increased glial responses in support of prior reports [251, 252]. Dorsal horn spinal cord astrocyte and microglial responses are recognized to mediate pathological pain in a variety of animal models via the actions of p-p38MAPK and IL-1β [24, 194, 253]. CB_2R mRNA and immunohistochemically identified protein expression is present mostly in spinal microglia [94, 135, 139, 212]. CB_2Rs in the CNS have been identified mostly on microglia [94], and prior studies reported decreased microglial activation following i.t. administration of CB_2R agonists [94, 139, 254] . Studies examining spinal cords of transgenic CB_2R knock-out mice exposed to partial sciatic nerve injury with concurrent neuropathic pain-like behaviors [93] also revealed increased bilateral dorsal horn microglial activation compared to

wild-type controls. These results suggest that CB_2Rs play a regulatory role in microglial activation during peripheral neuropathic conditions. However, we report that i.t. AM1241 does not inhibit dorsal spinal microglial activation, as assessed by Iba-1 staining, despite full behavioral reversal of CCI-induced allodynia. Upregulation of Iba-1 is widely known to indicate active microglia [57, 255, 256]. The differences in the data results may be that the aminoalkylindole, AM1241, acts in a distinctly different manner than other CB_2R agonist compounds, perhaps by inhibiting general spinal proinflammatory processes while leaving microglial function intact. Importantly, increased expression of microglial Iba-1 is indicative of ongoing microglial activity, but cannot distinguish anti-inflammatory vs. proinflammatory phenotypes. Thus, it is possible that the increased microglial Iba-1 reported here may be a consequence of increased IL-10 and/or mitogen-activated protein-phosphatase production, which are negative regulators to several proinflammatory MAPKs [91].This notion is supported by a prior in vitro study that demonstrated CB_2R ligands enhance IL-10 release from immune stimulated macrophages [257].

Intriguingly, microglia are an important additional source of the endocannabinoid, 2-arachidonylglycerol (2-AG) [8]. Endocannabinoids such as anandamide and 2-AG are produced and released from neurons and microglia [92]. Increased endocannabinoid ligand expression and activity in regions such as the spinal cord are characterized to inhibit pain-like behaviors in rats [208, 258].

In contrast to persistent microglial activity, i.t. AM1241 reduced bilateral GFAP IR in spinal cord astrocytes and robustly suppressed satellite GFAP-IR in the

corresponding DRGs. These results support that CB_2R activation reverses chronic bilateral allodynia, in part, by suppressing astrocyte activation. In other studies using immunohistochemical examination of astrocytes and microglia, it is notable that astrocyte endfeet frequently make intimate contact with microglia [259, 260], providing a potential mechanism by which microglia, albeit activated but in an anti-inflammatory manner, can influence astrocyte activation.

The enzyme, MAGL, has been identified on presynaptic axon terminals in brain, suggesting it can terminate 2-AG activity following ligand-receptor internalization in presynaptic neurons [143]. The current report supports, but is not limited to, the presynaptic localization of MAGL because immunofluorescent levels were dramatically increased by neuropathy in the superficial dorsal horn where afferent nociceptive fiber terminals communicate to spinal cord pain processing neurons. These data extend prior reports by showing a strong decrease in spinal MAGL IR following i.t. AM1241 that is concurrent with complete reversal of allodynia. Indeed, MAGL inhibitors decrease allodynia in CCI-induced neuropathic mice [151], resulting in an increase in 2-AG accumulation that is widely characterized to produce analgesia [153]. Microglia also release 2-AG, and MAGL activity has been described in microglia [145]. Together, these data support that decreased MAGL IR may be a result of a generalized decrease in proinflammatory factors following AM1241 treatment.

Surprisingly, an unremarkable unilateral alteration of FAAH was observed following CCI-neuropathy compared to sham controls, and these levels remained unchanged following i.t. AM1241 injection. As such, it is not clear from these data

whether FAAH plays an important role in chronic pain produced by CCI-peripheral neuropathy given these levels remained unchanged during pain reversal. However, only a single biochemical marker was used to ascertain FAAH expression levels. Further, activity of FAAH may not be reflected in its levels of expression. In support of this possibility, reports have demonstrated that blockade of FAAH actions results in anti-allodynia in inflammatory pain models, or following peripheral nerve transection [146] or CCI [151]. Thus, virtually unchanged spinal FAAH IR levels should be cautiously interpreted until further assays verify FAAH expression and activity in models of peripheral neuropathy. Distinct from data in the current report, increased FAAH IR was observed in large diameter DRG neurons following sciatic nerve axotomy or L5 spinal nerve transection [146]. However, animal models of peripheral axotomy can result in different protein expression profiles in spinal cord and DRG compared to intact damaged axons, as is the case with CCI. These observed differences are frequently reported in different animal models of pathological pain [24].

DRG satellite cells form a distinct sheath that completely surround sensory neurons, and together with the neuron, create a discrete morphological [71] and a functional unit [69]. Satellite DRG glia have gained increasing recognition for altering nociceptive transmission by expressing and responding to several proinflammatory cytokines including IL-1β [69, 72, 261]. Indeed, IL-1β rapidly activates nociceptive cells in a p38MAPK-dependent manner [80]. The current report supports these reports, as increased expression of p-p38MAPK and IL-1β, in addition to GFAP, were present in the DRG of neuropathic animals. We

demonstrate that ipsilateral DRG IL-10 expression is significantly decreased during CCI-induced chronic neuropathy. Conversely, i.t. treatment with AM1241 resulted in greater p-p38MAPK, IL-1β and IL-10 IR levels that are similar to non-neuropathic control basal values. No IL-10, IL-1β and p-p38MAPK IR changes in contralateral DRG were observed during CCI-induced chronic allodynia, suggesting these immune signals in contralateral DRG do not play a significant role in CCI-induced contralateral allodynia.

Although AM1241's behavioral effects occur within a relatively short therapeutic half-life (~1.5 hr), these data reveal crucial findings which may support the development of longer lasting, 'next generation' CB_2R agonists to produce therapeutic pain control. An advantage of a short therapeutic half-life is the capability to tightly regulate drug loading doses and potential unwanted side-effects. Oral formulations easily allow for repeated dosing at discrete intervals. Additionally, a short half-life for i.t. efficacy localized to the spinal cord may be advantageous as it may remain localized to spinal canal, avoiding potential global inhibition of important immune function. Prior reports together with the data presented here support that the actions of AM1241 are highly effective to control pathological pain when delivered either peripherally or by i.t. administration. Additionally, this report supports that pathological pain states, which can include contralateral allodynia ("mirror image" body part) is mediated by significant shifts in ipsilateral and contralateral pro- and anti-inflammatory spinal cord cytokine milieu, as well as shifts in p38MAPK and the endocannabinoid degradative enzyme, MAGL. The implication of these results is

that compounds capable of acting on cytokines in the CNS, can therapeutically control clinically relevant centrally and peripherally mediated pathological pain conditions.

2.5 Acknowledgements

The authors would like to thank Genevieve Phillips at the University of New Mexico Cancer Center Shared Microscopy Center for her valuable input and training on the spectral software utilized. This work was supported by NIH grants: NIDA 018156, GM60201. This project was also funded in part by the Dedicated Health Research Funds from the University of New Mexico School of Medicine.

The authors would like to disclose a conflict of interest. A.M. is a consultant for MAK Scientific.

3. Intrathecal cannabilactone CB_2R agonist, AM1710, controls pathological pain and restores basal cytokine levels

Pain

Authors: Jenny L. Wilkerson[1*], Katherine R. Gentry[2], Ellen C. Dengler[1], James A. Wallace[1], Audra A. Kerwin[1], Leisha M. Armijo[1], Megan N. Kuhn[3], Ganesh A. Thakur[4], Alexandros Makriyannis[4], and Erin D. Milligan[1*]

Affiliation(s):

Department of Neurosciences, Health Sciences Center, School of Medicine, University of New Mexico, Albuquerque, NM 87131

Department of Anesthesiology and Critical Care Medicine, Health Sciences Center, School of Medicine, University of New Mexico, Albuquerque, NM 87131

Health Sciences Center, School of Medicine, University of New Mexico, Albuquerque, NM 87131

Center for Drug Discovery, Northeastern University, Boston, MA 02115

* Corresponding Authors:

Jenny L. Wilkerson
University of New Mexico, HSC
Dept. of Neurosciences
MSC08- 4740
1 University of New Mexico
Albuquerque, NM 87131
Email: JLWilkerson@salud.unm.edu
Phone: +1(505)272-4441
Fax: +1(505)272-8082

Erin D. Milligan
University of New Mexico, HSC
Dept. of Neurosciences
MSC08- 4740
1 University of New Mexico
Albuquerque, NM 87131
Email: Emilligan@salud.unm.edu
Phone: +1(505)272-8103
Fax: +1(505)272-8082

Number of total pages: 37
Number of tables and figures: 9
Keywords : cannabinoid; CCI; paraffin immunohistochemistry; rat; spectral analysis; gp120

Abstract

Spinal glial and proinflammatory cytokine actions are strongly implicated in pathological pain. Spinal administration of the anti-inflammatory cytokine interleukin (IL)-10 abolishes pathological pain and suppresses proinflammatory IL-1β and tumor necrosis factor alpha (TNF-α). Drugs that bind the cannabinoid type-2 receptor (CB_2R) expressed on spinal glia reduce mechanical hypersensitivity. To better understand the CB_2R-related anti-inflammatory profile of key anatomical nociceptive regions, we assessed mechanical hypersensitivity and protein profiles following intrathecal application of the cannabilactone CB_2R agonist, AM1710, in 2 animal models; unilateral sciatic nerve chronic constriction injury (CCI), and spinal application of human immunodeficiency virus-1 glycoprotein 120 (gp120), a model of peri-spinal immune activation. In CCI animals, lumbar dorsal spinal cord and corresponding dorsal root ganglia (DRG) were evaluated by immunohistochemistry for expression of IL-10, IL-1β, phosphorylated p38-mitogen-activated-kinase (p-p38MAPK), a pathway associated with proinflammatory cytokine production, glial cell markers, and degradative endocannabinoid enzymes, including monoacylglycerol lipase (MAGL). AM1710 reversed bilateral mechanical hypersensitivity. CCI revealed decreased IL-10 expression in dorsal spinal cord and DRG, while AM1710 resulted in increased IL-10, comparable to controls. Adjacent DRG and spinal sections revealed increased IL-1β, p-p38MAPK, glial markers, and/or MAGL expression, while AM1710 suppressed all but spinal p-p38MAPK and microglial activation. In spinal gp120 animals, AM1710 prevented bilateral mechanical

hypersensitivity. For comparison to immunohistochemistry, IL-1β and TNF-α protein quantification from lumbar spinal and DRG homogenates was determined, and revealed increased DRG IL-1β protein levels from gp120, that was robustly prevented by AM1710 pretreatment. Cannabilactone CB_2R agonists are emerging as anti-inflammatory agents with pain therapeutic implications.

3.1 Introduction

Spinal sensitization of pain projection neurons is a critical process underlying pathological pain. Unilateral chronic constriction injury (CCI) of the sciatic nerve as well as spinal inflammation following i.t. HIV-1 glycoprotein-120 (gp120) are utilized here as animal models of pathological pain. While distinctly different in etiology, both models are characterized to involve activated spinal glia and proinflammatory cytokine activity [262]. Astrocytes and microglia produce interleukin-1β (IL-1β) and tumor necrosis factor-alpha (TNF-α) which mediate pathological pain in a variety of animal models [24, 253]. Glia in spinal cord dorsal horn and dorsal root ganglia (DRG) [80, 250] show increases in phosphorylated p38 mitogen-activated kinase (p-p38MAPK), a MAPK strongly associated with IL-1β and TNF-α expression [27]. DRG are home to glial satellite cells that generate IL-1β and TNF-α, additionally contributing to pathological pain in response to peripheral injury [69-74, 263]. Conversely, interleukin-10 (IL-10) is a critical pleiotropic anti-inflammatory cytokine that suppresses IL-1β and TNF-α actions and blocks phosphorylation of factors that activate MAPK pathways resulting in the inhibition of MAPK actions [264]. Lumbosacral intrathecal (i.t.) administration of the IL-10 transgene or protein leads to robust suppression of

light touch hypersensitivity (allodynia) produced by CCI as well as spinal inflammation following i.t. gp120 [204, 217, 265].

Two cannabinoid receptor subtypes, CB_1R and CB_2R, are characterized to produce analgesic effects [232]. CB_1R are present on neurons throughout the CNS and their activation within the brain corresponds to a variety of effects beyond pain control [7]. However, CB_2R are primarily expressed on microglia [139] and peripheral immune cells including macrophages [266]. Activation of CB_2Rs lack the known central nervous system (CNS) side effects produced by CB_1R activation [7, 135, 139, 212]. Following peripheral nerve injury, increased expression of CB_2Rs, endocannabinoids, and related degradative enzymes occur in DRG and spinal cord [92, 107, 146]. Reports demonstrate that the effects of CB_2R activation reduces pathological pain with a corresponding decrease in activation markers for spinal cord astrocytes, microglia, and factors associated with proinflammatory pathways [131, 241, 254, 267]. Given the newly characterized cannabilactone, AM1710, binds CB_2R with greater affinity than CB_1R (54-fold $CB_2R>CB_1R$) [160, 175], and its antinociceptive action is selectively blocked by CB_2R antagonists [176], i.t. administration of AM1710 was examined here for its potential actions to reverse or prevent allodynia produced by CCI and i.t. gp120, respectively. While prior reports reveal that spinal CB_2R activation controls pathological pain responses in neuropathic rats [93, 94, 135, 223, 241], the underlying spinal immunoregulatory signals in parallel with endocannabinoid degradative enzymes remain unclear.

The aim of the present study was to determine alterations in IL-10 immunoreactivty with concurrent reduction in immunoreactivity of CNS glial activation markers, IL-1β, p-p38MAPK, and the widely characterized endocannabinoid degradative enzymes, monoacylglycerol lipase (MAGL) and fatty acid amine hydrolase (FAAH) in the dorsal horn and DRG in behaviorally-verified CCI neuropathic rats following i.t. application of AM1710 [175, 176]. Bilateral allodynia was examined, as prior reports have documented this change from normal sensory responses [200, 201, 217, 238]. Following i.t. gp120, cytokine protein levels surrounding the injection site and DRG were quantified by enzyme-linked immunosorbent assay (ELISA) procedures.

3.2 Methods

3.2.1 Animals

A total of 76 pathogen-free adult male Sprague Dawley rats (300-400 gram; Harlan Labs, Madison, WI) were used in all experiments. Rats were double-housed in a temperature and light-controlled (12 hour light/dark; lights on at 6:00 AM) environment, with standard rodent chow and water available ad libitum. All procedures adhered to the guidelines of the Committee for Research and Ethical Issues of the International Association for the Study of Pain and were approved by the Institutional Animal Care and Use Committee (IACUC) of the University of New Mexico Health Sciences Center.

3.2.2 Drugs

The CB_2R agonist, 3-1(1',1'-Dimethylheptyl)-1-hydroxy-9-methoxy-6H-benzo[c]-chromene-6-one (AM1710) [160, 175] was used in these experiments. AM1710 was generously gifted by A.M. and G.T. AM1710 was first dissolved in 100% ethanol and diluted in sterile water (Hospira Inc, Lake Forest, IL) for a final of concentration 1 mg/ mL containing 5% ethanol. The vehicle of AM1710 was sterile water containing 5% ethanol. Pilot studies determined the dose range of AM1710, with a 100-fold dose range tested (10 µg - .1 µg in 10 µl or equivolume vehicle). Immediately prior to intrathecal (i.t.) injections, frozen (-80°C) recombinant gp120 (product 1021-2; lot number 7A3I20; ImmunoDiagnostics, Bedford, MA) was thawed, and diluted to 0.5 µg/µl with 0.1% rat serum albumen in sterile PBS, pH 7.4 (Life Technologies, Gaithersburg, MD. Three (3) µg in 6 µl or equivolume vehicle was prepared on ice as detailed in prior reports [196, 215, 237, 268].

3.2.3 Behavioral assessment of allodynia

Baseline (BL) responses to light mechanical touch were assessed using the von Frey test after animals were habituated to the testing environment, as previously described [214, 215]. Briefly, rats were placed atop 2 mm-thick parallel bars, spaced 8 mm apart and habituated for approximately 45 minutes for 5 days. All behavioral testing was performed during the first half of the light cycle in a sound, light, and temperature controlled room. The von Frey test utilizes a series of calibrated monofilaments, (3.61 – 5.18 log stimulus intensity; North Coast Medical, Morgan Hills, CA) applied randomly to the left and right plantar surface

of the hindpaw for 8 seconds. Lifting, licking or shaking the paw was considered a response. For all behavioral testing, threshold assessment was performed in a blinded fashion by J.L.W.

3.2.4 Chronic constriction injury (CCI) surgery

Following BL behavioral assessment, the surgical procedure for chronic constriction of the sciatic nerve was completed as previously described [216]. Briefly, in isoflurane- (induction 5% vol. followed by 2.5% in oxygen) anesthetized rats, the mid- to lower back and the dorsal left thigh shaved and cleaned with diluted Bacti-Stat AE, (EcoLab HealthCare Division, Mississauga, Ontario, Canada). Using aseptic procedures, the sciatic nerve was carefully isolated, and loosely ligated with 4 segments of chromic gut sutures (Ethicon, Somerville, NJ). Sham surgery was identical to CCI surgery but without the nerve ligation. The overlying muscle was sutured closed with (2) 3-0 sterile silk sutures (Ethicon, Somerville, NJ), and animals recovered from anesthesia within approximately 5 minutes. Animal placement into either CCI or sham surgical groups was randomly assigned.

3.2.5 Chronic indwelling catheter surgery used for i.t. gp120 administration

Following BL assessment for light mechanical touch, chronic indwelling i.t. catheterization was performed as previously described in experiments utilizing gp120 for the induction of allodynia [215, 268, 269]. All animals recovered from this procedure within 5 minutes without overt signs of motor weakness or discomfort. Verification of lumbar PE-10 catheter placement was conducted at

the time of tissue collection. One hundred percent of catheters were successfully placed within the intrathecal L5 lumbar region.

3.2.6 Intrathecal injection for chronic indwelling catheters

For chronic indwelling catheters in gp120 experiments, all drugs were pre-filled into an 'i.t. injection catheter' as detailed previously [269]. A 3-minute i.t. injection was administered in alert, conscious rats with light towel restraint. No overt motor weakness was observed. Six microliters of gp120 followed by an 8 µl sterile saline flush during a 10 second interval was injected.

3.2.7 Acute intrathecal injection used in CCI-related experiments

In rats with CCI, all drugs were administered via acute i.t. catheter placement. Injections were performed as previously described [215]. Either 10 µl drug or equivolume vehicle was withdrawn into the injection catheter, which was gently inserted and threaded rostrally to the 7.7 cm marking to achieve a catheter-tip position at the i.t. lumbosacral enlargement (~L4-L5). During this time, light tail twitching and a small amount of cerebrospinal fluid efflux from the 18-gauge needle was typically observed indicating successful i.t. catheter placement. Drug or vehicle was injected during a 10 second interval. Drug treatment was randomly assigned to animals. Upon completion of injection, the PE-10 i.t. catheter was removed followed by removal of the 18-gauge needle. A 100% motor recovery rate was observed from this injection procedure.

3.2.8 Immunohistochemical procedures from CCI-treated rats

Following behavioral assessment, animals were overdosed with an intraperitoneal injection sodium phenobarbital (Sleepaway, Fort Dodge Animal Health, Fort Dodge, IA), then perfused transcardially with saline followed by 4% paraformaldehyde. Whole vertebral columns with intact spinal cords (cervical 2 through sacral 1 spinal column segments) were removed, and underwent overnight fixation in 4% paraformaldehyde at 4°C. This tissue collection approach ensured that all relevant anatomical components, including the spinal cord, DRG, and overlying meninges, were intact within the vertebral column, allowing important spatial relationships to remain for examining corresponding functional interactions at individual and specific spinal cord levels. All specimens underwent EDTA (Sigma Aldrich, St. Louis, MO) decalcification for 30 days, and spinal cord sections were subsequently paraffin processed and embedded in Paraplast Plus Embedding Media (McCormick Scientific, St. Louis, MO) as previously described [93]. Adjacent tissue sections (7 µm) were mounted on vectabond-treated slides (Vector Labs, Burlingame, CA), and allowed to adhere to slides overnight at 40°C, followed by deparaffinization, and rehydration via descending alcohols to PBS (1X, pH 7.4). Sections were then processed with microwave antigen retrieval procedures (citrate buffer pH 6.0, or tris-based buffer, pH 9.0; BioCare Medical, Concord, CA).

Slides were incubated with 5% normal donkey serum (NDS), in PBS (pH 7.4) for 2 hours, followed by overnight primary antibody (Table 3.1) incubation in a humidity chamber at 3° C. Slides underwent secondary antibody incubation

(Table 3.1) for 2 hours in a humidity chamber at room temperature, rinsed in PBS, and then coverslipped with Vectashield containing the nuclear stain 4',6-diamidino-2-phenylindole (DAPI) (Vector Labs, Burlingame, CA). For detection of MAGL , phosphorylated p38MAPK, and IL-10 protein, sections were incubated overnight with primary antibodies, incubated with biotinylated secondary antibody (Table 3.1) for 1 hour, and then treated with Vectastain ABC Elite kit (Vector Labs, Burlingame, CA) and stained using TSA Plus Fluorescein System (PerkinElmer Life Sciences, Waltham, MA) and finally coverslipped with Vectashield containing DAPI. Stained section orientation was kept consistent throughout for proper identification of ipsilateral and contralateral spinal cord and DRGs. For lumbar spinal cord, sections were taken from L4-L6, and the dorsal horn analyzed (Supplemental Figure A-2 A). The intact meninges overlying the ipsilateral dorsal horn of the spinal cord were analyzed separately to discern possible immunoreactive changes between surgical and drug treatments groups that may be different from quantified values obtained for the entire ipsilateral dorsal horn. For meningeal analysis, those sections revealing clear identification of the meninges vs.

Primary antibody	Antibody clone	Indication	Anatomical region	Vendor	Host	Dilution used	Antigen retrieval	TSA Used	Secondary Antibody*
GFAP	Polyclonal	Astrocyte	Dorsal Horn Spinal Cord	Millipore	Rabbit	1:1000	Tris Buffer	No	Rhodamine Red Donkey anti- Rabbit (1:200)
GFAP	Polyclonal	Astrocyte	Dorsal Horn Spinal Cord	Abcam	Chicken	1:1000	Tris Buffer	No	AMCA, CY-5 Donkey anti-Chicken (1:200)
GFAP	Monoclonal	Astrocyte	DRG	Progen	Rabbit	1:10	Citrate Buffer	No	Rhodamine Red Donkey anti- Rabbit (1:200)
Iba-1	Polyclonal	Microglia	Dorsal Horn Spinal Cord	Wako	Rabbit	1:300	Tris Buffer	No	Rhodamine Red, FITC Donkey anti- Rabbit (1:200)
FAAH	Polyclonal	Ecb enzyme	Dorsal Horn Spinal Cord	Cayman Chemical	Rabbit	1:100	Tris Buffer	No	Rhodamine Red Donkey anti- Rabbit (1:200)
MAGL	Polyclonal	Ecb enzyme	Dorsal Horn Spinal Cord	Abcam	Rabbit	1:100	Citrate Buffer	Yes	Biotinylated Donkey anti- Rabbit (1:1300)
p-p38	Polyclonal	Phospho-p38 MAP Kinase	Dorsal Horn Spinal Cord, DRG	Cell Signaling	Rabbit	1:800	Citrate Buffer	Yes	Biotinylated Donkey anti- Rabbit (1:1300)
IL-10	Polyclonal	IL-10 Protein	Dorsal Horn Spinal Cord, DRG	R&D Systems	Goat	1:250	Citrate Buffer	Yes	Biotinylated Donkey anti- Goat (1:1300)
IL-1β	Polyclonal	IL-1 Beta Protein	Dorsal Horn Spinal Cord, DRG	Santa Cruz	Rabbit	1:300	Tris Buffer	No	Rhodamine Red Donkey anti- Rabbit (1:200)
NF-H 200	Monoclonal	Neuron	Dorsal Horn Spinal Cord, DRG	Millipore	Mouse	1:100	Citrate Buffer	No	Rhodamine Red Donkey anti- Mouse (1:200)

Table 3. 1

List of all antibodies used in this study and designated under the appropriate column heading. Primary antibodies for polyclonal GFAP (astrocyte specific glial fibrillary acidic protein, Millipore, Billerica, MA, and Abcam, Cambridge, MA), monoclonal GFAP (astrocyte specific glial fibrillary acidic protein, Progen, Heidelberg, Germany), Iba-1 (microglia, monocyte specific calcium channel protein, Wako Chemicals, Osaka, Japan), FAAH (fatty acid amide hydrolase endocannabinoid degredgative enzyme, Cayman Chemicals, Ann Arbor, MI), IL-1β protein (proinflammatory cytokine, Santa Cruz Biotechnology, Santa Cruz, CA), NF-H 200KDa (neurofiliament heavy chain clone 3G3, Millipore, Billerica, MA), MAGL (monoacylglyerol lipase endocannabinoid dregradative enzyme, Abcam, Cambridge, MA), phosphorylated p38MAPK (activated proinflammatory cytokine signaling pathway, Cell Signaling Technology, Beverly, MA) and IL-10 protein (anti-inflammatory cytokine, R&D Systems, Minneapolis, MN) were used. Secondary antibody incubation was performed with the indicated fluorophore conjugated secondary antibody. For MAGL, phosphorylated p38MAPK, and IL-10 protein, after overnight primary incubation, sections were instead incubated with biotinylated secondary antibody. *All secondary antibodies are from Jackson Immunoresearch (West Grove, PA).

superficial spinal cord were chosen. As such, meninges of tissue sections comprising complete groups stained for IL-10, Iba-1 and MAGL were analyzed. For DRG material, sections were taken containing the DRG corresponding to L5 spinal cord segment, and the most distal portion of the DRG was analyzed (Supplemental Figure A-2 B). Low magnification photomicrographs were obtained (Supplemental Figure A-2 A, B) using a Nikon Optiphot fluorescent microscope equipped with a DP2-BSW (Olympus) camera.

3.2.9 Confocal microscopy

All tissue processing, slicing, and procedures for immunohistochemistry were identical to that described above. However, in these studies more than one primary antibody was used and examined under confocal microscopy. Therefore, after the first antibody staining procedure, the slides went through subsequent staining procedures. This took place over multiple days to account for the times needed for individual antibody incubation and staining. Confocal microscopy at 63x magnification was then performed on a Zeiss AxioObserver inverted LSM510 META confocal microscope utilizing Zen 2009 software (Carl Zeiss, AG, Germany). Final images were generated from collapsed z-stacks comprised of 17 images taken 0.393 µm apart on the z axis.

3.2.10 Immunohistochemical spectral image analysis

All images of the spinal cord dorsal horn, overlying meninges and DRGs were captured by a Zeiss Axioscope Microscope, at 20x magnification, with a Nuance Spectral Camera (Cambridge Research & Instrumentation, Woburn, MA).

Utilizing the Nuance computer software, the fluorescent wavelength emission spectra range was initially determined for each fluorophore utilized in the detection of the primary antibody of interest (DAPI, 488 nm +/- 10nm; FITC, 575 nm +/- 5nm; Rhodamine Red 600 nm+/- 5nm) by using a control slide with only a drop of the pure fluorophore. This was performed in the absence of a tissue specimen that may potentially obscure the measurement of the fluorophore's emission spectra. Two sets of additional control slides with tissue sections were prepared, one with only PBS without primary or secondary antibody treatment, and the other without primary but with secondary antibody treatment. These control slides were used to objectively eliminate low intensity fluorescence and autofluorescence background 'noise' from our measurements (Supplemental Figure A-2 C). Using the control slides, the Nuance software allows the user to set an acceptable threshold of low-level emission fluorescent intensity (as opposed to the software "autothreshold" option) within and outside the defined wavelength range of interest between tissue samples. Emission values that fall below this acceptable threshold of low-level emission, within and outside the defined wavelength range of interest, were eliminated from our measurements (Supplemental Figure A-2 D). The fluorescent intensity threshold for each protein marker was determined by the user finding the most appropriate threshold that captures the specific FITC or Rhodamine Red staining for each protein marker within a tissue (e.g., dorsal horn spinal cord or DRG). Once the optimal level of fluorescent threshold was determined for a particular protein marker, this level was held consistent throughout all of the treatment groups for the image analysis

within each protein marker of interest (Supplemental Figure A-2 D). These steps were followed by software conversion allowing fluorescent wavelength intensity for each fluorophore to be converted to a numerical value. Autofluorescence was defined as that emission outside the defined wavelength of interest (e.g. DAPI, 488 nm +/- 10nm; FITC, 575 nm +/- 5nm; Rhodamine Red 600 nm+/- 5nm) as well as low-level emission that fell below the acceptable threshold of low-level emission fluorescent intensity. These specific autofluorescent and low-level background emission values were subtracted from the image (Supplemental Figure A-2 E,F), yielding a numerical value of true fluorescent emission intensity for each fluorophore [219, 220].

Primary antibody staining procedures remained consistent to minimize intensity variations of each fluorophore (FITC or Rhodamine Red) used to detect the different primary antibodies of interest. To ensure that fluorophore binding was not impeded through possible steric hindrance of other proximal fluorophores, sections were labeled for only one cellular marker of interest on a slide.

The user also determined the minimum number of connected pixels on the computer screen for image analysis, counted as a region of interest (ROI) defined in the Nuance software system, which resulted in a software image containing distinctive morphology (i.e., of cellular bodies and processes, pattern of protein expression) that was virtually identical to the morphology observed through the microscope for each protein marker. The minimum number of connected pixels would therefore be set higher for a protein expressed

abundantly by a cell (i.e., GFAP) in comparison to a protein expressed sparsely, leading to a punctuate pattern (e.g., IL-1β). These conditions resulted in a ROI, and were held consistent for both the ipsilateral and contralateral tissues in every experimental condition and for each antibody stain. The total area of each ROI, as measured by mm^2, is calculated and is factored into the overall measurement of fluorescent intensity per second of exposure. The average count of fluorescent emission intensity per second exposure, per mm^2 is the analyzed value that we report here. That is, fluorescent intensity average count/second/mm^2, which takes into account the density as well as the intensity of the fluorophore detected. A total of 4 sections per animal (N=3) were randomly selected and analyzed in this manner. By applying this novel method of data acquisition and analysis, experimenter bias is eliminated, yielding greater consistency and objectivity to fluorescent quantification.

3.2.11 Protein quantification by ELISA

Twenty minutes after i.t. gp120 and subsequent behavioral verification, rats were given an overdose i.p. injection (0.8-1.3 cc) of sodium phenobarbital (Sleepaway, Fort Dodge Animal Health, Fort Dodge, IA) and perfused transcardially with ice cold saline followed by exposure of the lumbosacral enlargement by laminectomy. After verifying subdural intrathecal catheter placement and cerebral spinal fluid (CSF) collection, the dorsal portion of the lumbosacral spinal cord and the corresponding bilateral L4-L6 dorsal root ganglia were collected separately into tubes and flash frozen in liquid nitrogen. Tubes were then stored at -80°C

until assay. ELISA procedures were performed for IL-1β and TNF-α according to manufacturer's instructions (R&D Systems, Minneapolis, MN).

Experimental Paradigms

Behavioral efficacy of i.t AM1710 following CCI. Behavioral assessment of BL thresholds was conducted prior to CCI or sham surgical manipulation. Hindpaw threshold responses were assessed 3 and 10 days after surgery. Immediately following behavioral assessment, rats (N=6/group) were given an i.t. injection of AM1710 or vehicle. Hindpaw threshold responses were reassessed during the following 24 hr at discrete timepoints.

Immunohistochemical detection of spinal and DRG changes. In a separate group of rats (N=3/group), identical BL threshold assessment and surgical procedures were followed, as just described. I.t. AM1710 was injected at the dose (10 ug) identified to produce maximal reversal from allodynia produced by CCI. At the time of maximal efficacy (~3 hr), rats were deeply anesthetized followed by procedures for IHC analysis of tissue sections. Thus, all tissue sections from the dorsal horn of the spinal cord and the corresponding intact DRG were analyzed from behaviorally verified rats from different experimental manipulations (sham vs. CCI + vehicle vs. AM1710).

Behavioral efficacy of i.t AM1710 following i.t. gp120.

A separate group of rats were behaviorally verified for BL thresholds followed by chronic i.t. catheterization. Threshold values were reassessed 6 days later.

Immediately thereafter, rats received i.t AM1710 or vehicle, and hindpaw threshold responses were reassessed 3 hr later (at maximal AM1710 efficacy). At this time, i.t. gp120 was injected, followed by threshold assessment at 20 min (N=6 rats/group), and immediately followed by anesthetic overdose and tissue collection for protein quantification.

3.2.12 Data analysis

Psychometric behavioral analysis was performed as previously described [215] to compute the log stiffness that would have resulted in the 50% paw withdrawal rate. Briefly, thresholds were estimated by fitting a Gaussian integral psychometric function to the observed withdrawal rates for each of the tested von Frey hairs, using a maximum-likelihood fitting method [221]. For behavioral statistical analysis to assess the presence of allodynia, a 1-way ANOVA was used at BL, and a 2-way repeated measures ANOVA was used at 3 and 10 days after CCI/sham surgery in CCI-related experiments. To determine AM1710 drug efficacy following i.t. injection on Day 10, a 3-way repeated-measures ANOVA was applied at 0.5, 1, 2, and 2.95 hr timepoints. For experiments utilizing i.t. gp120, a 1-way ANOVA was used at BL, and a 2-way repeated-measures ANOVA was used at 6 days after indwelling catheter surgery, and immediately prior to i.t. gp120. A two-way repeated-measures ANOVA was applied to assess AM1710 efficacy 20 minutes after i.t. gp120. All other data analysis was performed using a one-way ANOVA. A p-value of <0.05 was considered statistically significant. The computer program GraphPad Prism version 4.03 (GraphPad Software Inc., San Diego, CA) was used in all statistical analyses. All

data is expressed as mean +/- SEM. For post hoc analysis Bonferroni's test was performed.

3.3 Results

3.3.1 Intrathecal injection of AM1710 dose-dependently reverses CCI-induced allodynia

The CB_2R cannabilactone agonist, AM1710, reversed allodynia produced by CCI. Prior to surgical manipulation, all groups exhibited similar bilateral (ipsilateral and contralateral) BL behavioral thresholds (Figure 3.1 A,B). Following CCI, clear bilateral allodynia developed by Day 3 and 10 compared to sham-operated rats. On Day 10, following i.t. AM1710 or vehicle injection in sham-operated rats, AM1710 did not alter normal sensory threshold responses to light touch, as well as throughout the entire timecourse. However, in rats with CCI, i.t. AM1710 produced reversal from allodynia, with maximal efficacy observed at 3 hr following the highest dose (10 µg) injected, whereas a 10-fold lower dose (1.0 µg) attenuated allodynia. The lowest dose examined (0.1 µg) did not significantly alter threshold responses, with allodynia remaining stable through the last timepoint tested (24 hr). All CCI-treated rats revealed full allodynia at 5 hr after i.t. AM1710 treatment.

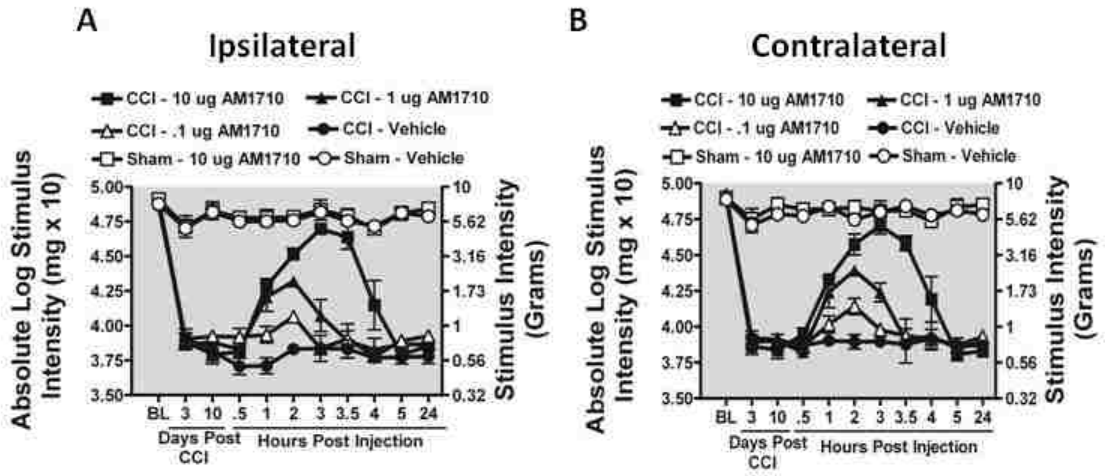

Figure 3.1 Selective i.t. cannabinoid 2 receptor agonist AM1710 reverses CCI-induced allodynia.

Selective i.t. cannabinoid 2 receptor agonist AM1710 reverses CCI-induced allodynia. **A**, **B**, AM1710 reverses CCI-induced allodynia in a dose-dependent manner. A total of 36 animals were used in this experiment. Prior to surgical manipulation, all groups exhibited similar bilateral (ipsilateral and contralateral) BL thresholds (ANOVA, $F_{(5,35)}$ =1.982 ; p=0.1124, ANOVA, $F_{(5,35)}$ =1.142; p=0.3616, respectively). Following CCI, clear bilateral allodynia developed by Day 3 and continued chronically through Day 10 compared to sham-operated rats. On Day 10, compared to i.t. control injected rats, AM1710 produced a dose-dependent reversal from allodynia, with maximal reversal observed at 3 hours following the highest injected dose (10 µg). However, allodynia fully returned by 5 hours after i.t. AM1710 treatment, with allodynia remaining stable through 24 hours (ipsilateral paw ANOVA, $F_{(15,84)}$ = 187.6; p<0.0001; and contralateral paw, ANOVA, $F_{(15,84)}$=403.7; p<0.0001). While 1.0 µg produced attenuated allodynia, 0.1 µg did not alter allodynia for either the ipsilateral or contralateral hindpaws. Post hoc analysis revealed that 1µg AM1710 produced a robust reversal from allodynia at 2 hours following i.t. injection, while all AM1710 treated animals returned to allodynia by 4 hours (p<0.001).

3.3.2 Immunohistochemical analysis of spinal cord dorsal horn

Peak behavioral efficacy after i.t. AM1710 injection was again observed at ~ 3 hr compared to neuropathic vehicle-injected rats (Figure 3.2 A,B), which is in support of the behavioral dose-response characterization above (Figure 3.1 A,B). Bilateral IL-10 immunoreactivity (IR) in the spinal cord dorsal horn is dramatically decreased in CCI-induced neuropathic rats compared to sham-treated rats (Figure 3.2 C,D). However, treatment with AM1710 rescued IL-10 IR bilaterally, similar to levels found in non-neuropathic controls. The intact meninges surrounding the ipsilateral spinal cord revealed a trend toward decreased IL-10

IR in CCI animals treated with vehicle, however, no changes between treatment groups were observed (Inset, Figure 3.2 C). Representative fluorescent images of either sham treated with i.t. vehicle (Figure 3.2 K), CCI treated with i.t. vehicle (Figure 3.2 L), or with AM1710 (Figure 3.2 M) corresponding to the quantitative image analysis data are presented. Moreover, confocal microscope examination reveals IL-10 expression in astrocytes (Figure 3.6 C,F) within superficial (Lam I-II) and deeper dorsal horn laminae (Lam III-V), and microglia (Figure 3.6 I; Lam I-III). It is notable that when IL-10 returns to non-neuropathic basal levels, allodynia is correspondingly reversed.

For IL-1β IR analysis, compared to non-neuropathic sham-operated rats given i.t. AM1710, or equivolume vehicle, CCI-induced neuropathy produced a robust unilateral increase in IL-1β IR in i.t. vehicle injected animals (Figure 3.2 E,F). Conversely, i.t. administration of AM1710 completely suppressed increased dorsal horn IL-1β IR. Representative fluorescent images are of sham-treated rats with i.t. vehicle (Figure 3.2 N), CCI-treated rats with i.t. vehicle (Figure 3.2 O), or CCI treated-rats with AM1710 injection (Figure 3.2 P) that correspond to data examined by microscopy analysis. Interestingly, in comparison to IL-10 IR in CCI animals, IL-1β IR observed in the contralateral dorsal spinal cord was not substantially elevated when compared to non-neuropathic control animals.

We also examined dorsal horn p-p38 MAPK IR. Compared to sham-operated rats given i.t. AM1710, or equivolume vehicle, CCI-induced neuropathy produced a robust bilateral increase in the dorsal horn of p-p38MAPK IR (Figure 3.2 G,H).

Unexpectedly, AM1710 did not alter ipsilateral or contralateral increases in p-p38MAPK IR. Again, representative fluorescent images are presented, which correspond to image analysis of either sham-treated rats with i.t. vehicle (Figure 3.2 Q), CCI-treated rats with i.t. vehicle (Figure 3.2 R), or CCI-treated rats with AM1710 (Figure 3.2 S).

Upon close examination of the nuclear specific dye, DAPI, no differences in fluorescence intensity as a consequence of either CCI procedures or i.t. drug injections were observed, suggesting that local lumbar cellular numbers remained relatively unchanged (Figure 3.2 I, J).

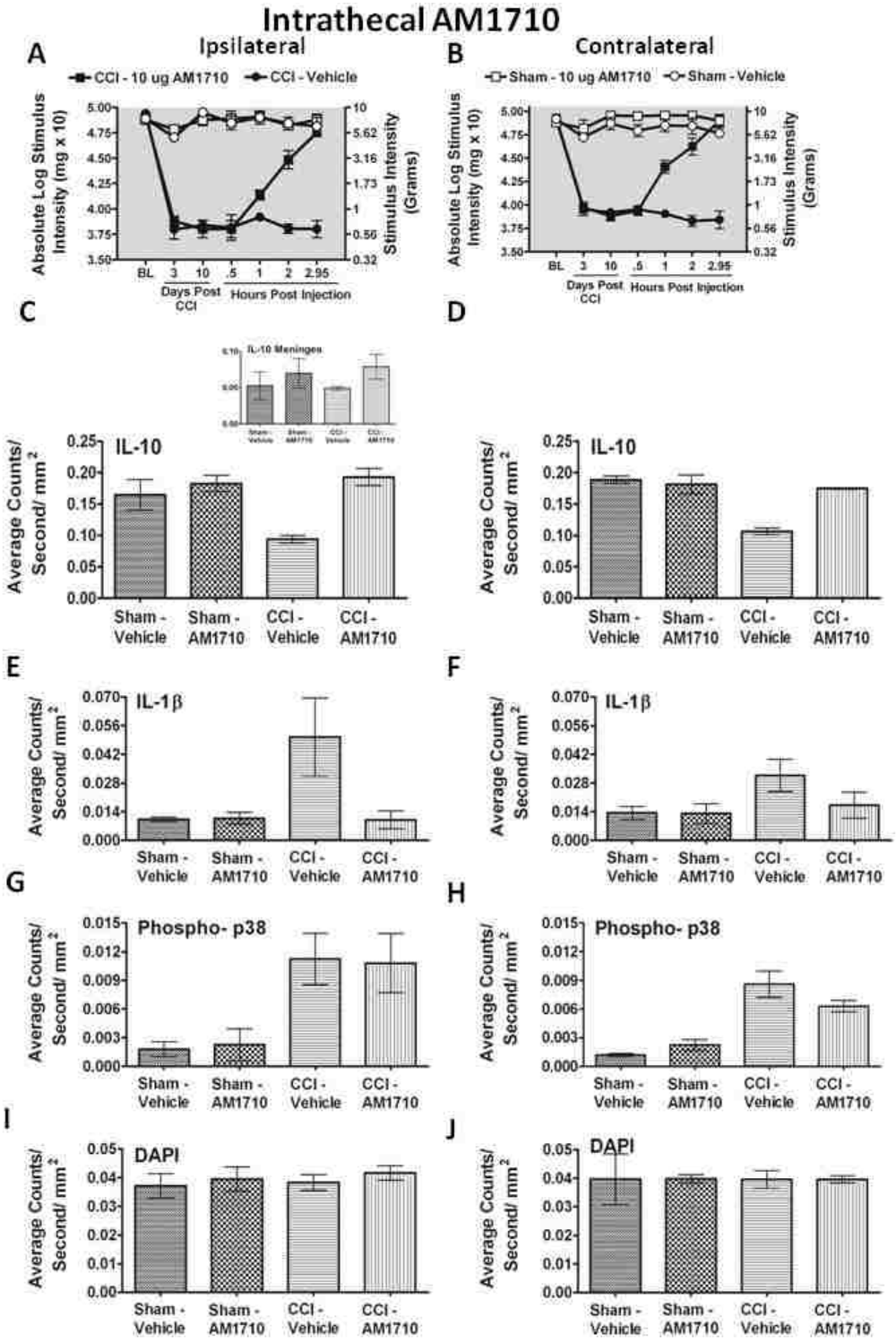
Intrathecal AM1710
A
Ipsilateral
CCI - 10 ug AM1710
CCI - Vehicle
Absolute Log Stimulus Intensity (mg x 10)
Stimulus Intensity (Grams)
BL
Days Post CCI
Hours Post Injection
B
Contralateral
Sham - 10 ug AM1710
Sham - Vehicle
C
IL-10
Average Counts/ Second/ mm 2
Sham - Vehicle
Sham - AM1710
CCI - Vehicle
CCI - AM1710
D
E
IL-1β
F
G
Phospho- p38
H
I
DAPI
J

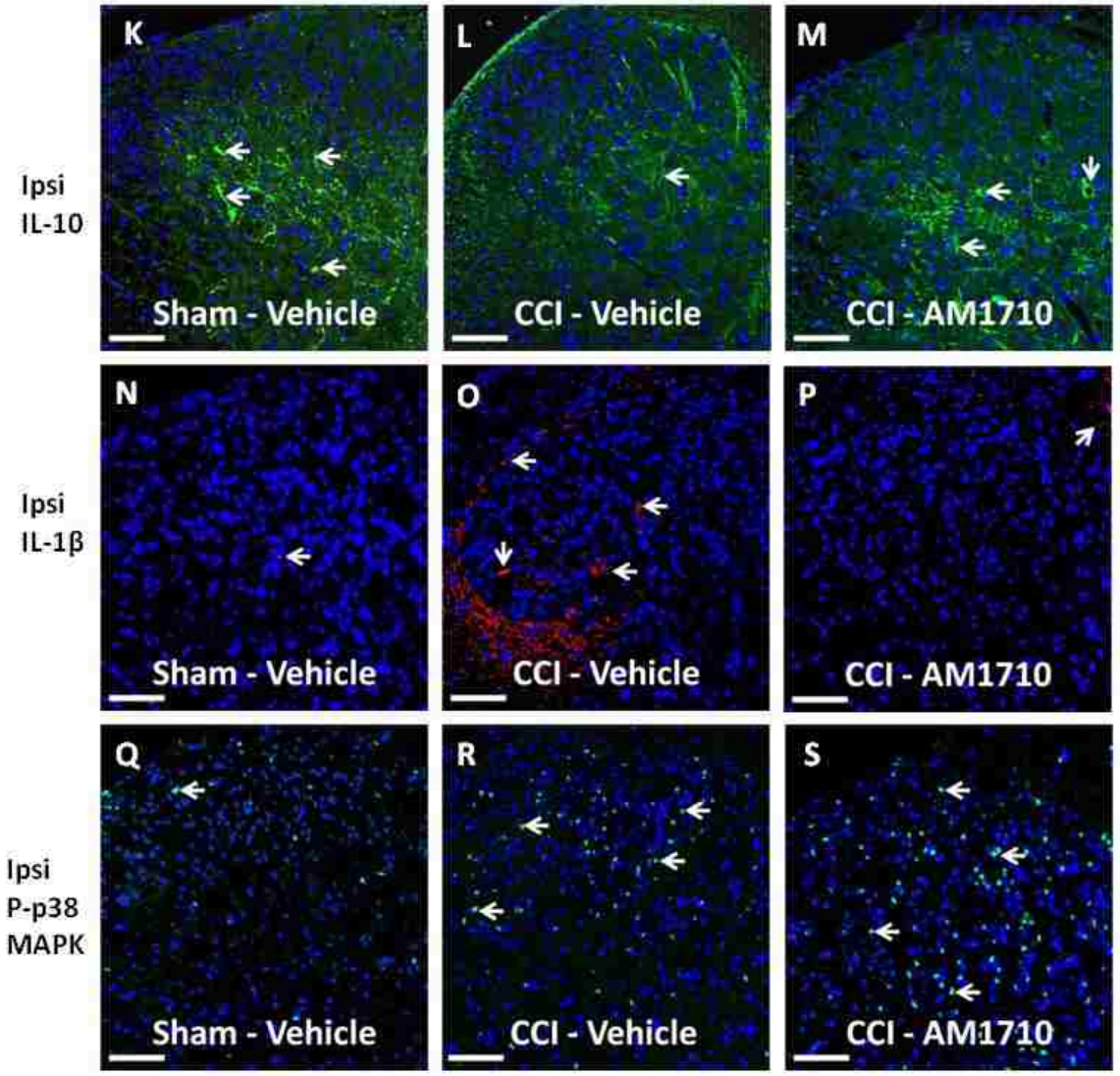

Figure 3.2 Immunofluorescent intensity quantification cytokines

Immunofluorescent intensity quantification following AM1710 –induced reversal of allodynia. A total of 12 animals were used for both the behavioral experiment reported here and tissues from these animals were analyzed in the reported immunohistochemical experiments. **A**,**B**, Prior to CCI, all groups exhibited similar ipsilateral and contralateral BL thresholds (ANOVA, $F_{(3,11)}$ =2.396; p=0.1438, and ANOVA, $F_{(3,11)}$ =1.432; p=0.3036, respectively). CCI produced significant bilateral allodynia at Day 3 and continued to Day 10 compared to sham-treated animals (ANOVA, $F_{(1,8)}$ =284.8; p< 0.0001, and ANOVA, $F_{(1,8)}$=222.9; p=0.0001, respectively). Behavioral responses following i.t. AM1710 (10 µg) produced maximal bilateral reversal of allodynia (ANOVA, $F_{(1,8)}$= 269.7; p<0.0001 and ANOVA, $F_{(1,8)}$=146.0; p<0.0001, respectively). At peak reversal, animals were sacrificed and spinal tissue was collected. **C**, **D**, Bilateral IL-10- immunoreactivity (IR) in the dorsal horn spinal cord was dramatically decreased in CCI-induced neuropathic rats compared to sham-treated rats. In stark contrast, treatment with AM1710 rescued IL-10 IR to basal levels in both the ipsilateral and contralateral dorsal spinal cord (ANOVA, $F_{(3,11)}$=12.36; p=0.0023; ANOVA, $F_{(3,11)}$=30.68; p<0.0001, respectively). **Inset, C,** No changes in expression of meningeal IL-10 IR between non-neuropathic sham and neuropathic CCI rats following i.t. AM1710 or equivolume vehicle were observed (ANOVA, $F_{(3,11)}$=1.109; p=0.4008). **E, F,** Compared to non-neuropathic sham-operated rats given i.t. AM1710 or equivolume vehicle, CCI-induced neuropathy produced

a robust unilateral increase in IL-1β IR in i.t. vehicle injected animals. Conversely, i.t. administration of AM1710 reversed increased dorsal horn spinal IL-1β IR. IL-1β IR observed in the contralateral dorsal horn spinal cord was not substantially elevated when compared to non-neuropathic control animals. (ANOVA, $F_{(3,11)}$= 6.240; p=0.0172; ANOVA, $F_{(3,11)}$=3.354; p=0.0.760, respectively). **G, H**, Compared to non-neuropathic sham-operated rats given i.t. AM1710 or equivolume vehicle, CCI-induced neuropathy produced a robust p-p38MAPK bilateral IR increase in dorsal horn spinal cord tissues following i.t. vehicle injection. AM1710 administered i.t. did not reverse CCI- induced increases in p38MAPK IR. (ANOVA, $F_{(3,11)}$=4.221; p=0.0459; ANOVA, $F_{(3,11)}$=22.26; p=0.0003, respectively). **I**, **J**, No differences in DAPI nuclear stain fluorescent intensity were observed in AM1710 ipsilateral or contralateral dorsal horn (ANOVA, $F_{(3,11)}$=0.4571; p=0.7197, ANOVA, $F_{(3,11)}$=0.0006230; p=1.0, respectively). **K, L, M,** Representative spectrally unmixed images at 20x magnification of IL-10 fluorescent staining (green) with DAPI nuclear stain (blue). **N, O, P**, Representative spectrally unmixed images at 20x magnification of IL1β fluorescent staining (red) and DAPI nuclear stain (blue). **Q**, **R**, **S**, Representative spectrally unmixed images at 20x magnification of phospho-p38 fluorescent staining (green) with DAPI nuclear stain (blue). In all images the scale bar is equal to 50 μm.

While non-neuropathic sham-operated animals given i.t. AM1710 or equivolume vehicle exhibited similar Iba-1 IR levels, a marker for altered microglial activity, AM1710 did not modify the increased dorsal horn Iba-1 IR in CCI-treated rats during AM1710-induced reversal from allodynia compared to CCI-treated treated rats with ongoing allodynia (Figure 3.3 A,B). Therefore, despite robust suppression of dorsal horn IL-1β expression and full reversal of allodynia, local administration of AM1710 does not inhibit increased levels of spinal Iba-1 IR. Meningeal Iba-1 IR was significantly elevated in CCI-treated compared to non-neuropathic sham-treated rats (Figure 3.3 A Inset). While a trend toward decreased Iba-1 IR was observed in meninges of CCI-treated rats given i.t. AM1710, this decrease was insignificant.

Bilateral dorsal horn GFAP IR expression in adjacent Iba-1 stained sections was examined. Compared to non-neuropathic sham-operated rats given i.t. AM1710, or equivolume vehicle, a robust bilateral increase in dorsal horn GFAP was demonstrated in neuropathic rats (Figure 3.3 C,D). However, clear suppressive effects of AM1710 on astrocyte activation were observed. Intrathecal AM1710

strikingly reduced the bilateral increases in dorsal horn GFAP IR seen in CCI vehicle-treated rats (Figure 3.3 C,D). Corresponding representative fluorescent images used for analysis are shown; sham-operated rats treated with either i.t. vehicle or AM1710 (Figure 3.3 E,F), or CCI-treated rats injected with either i.t. AM1710 or equivolume vehicle (Figure 3.3 G,H).

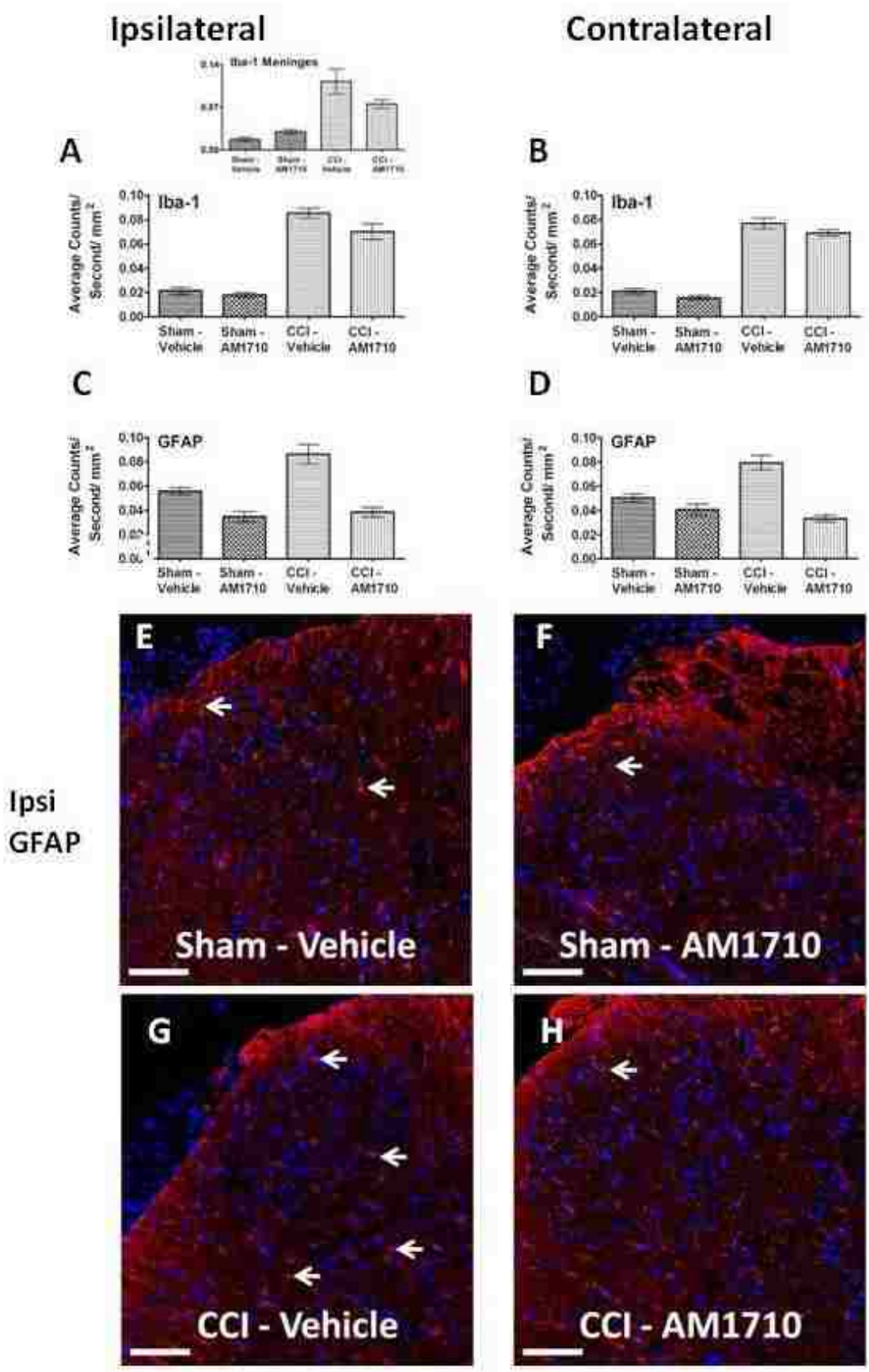
Ipsilateral
Contralateral
A
B
C
D
Iba-1 Meninges
Iba-1
GFAP
Average Counts/ Second/ mm²
Sham - Vehicle
Sham - AM1710
CCI - Vehicle
CCI - AM1710
Ipsi GFAP
E
F
G
H
Sham - Vehicle
Sham - AM1710
CCI - Vehicle
CCI - AM1710

Figure 3.3 Immunofluorescent intensity quantification glia

Immunofluorescent intensity quantification of the spinal cord dorsal horn reveals differences in astrocyte but not microglial activation in neuropathic rats treated with AM1710. **A**, **B**, Compared to non-neuropathic sham-operated rats given i.t. AM1710 or equivolume vehicle, CCI-induced neuropathy produced a robust bilateral increase in spinal cord dorsal horn Iba-1 IR in rats given i.t. vehicle (ANOVA, $F_{(3,11)}$=58.94; p<0.0001, ANOVA, $F_{(3,11)}$=175.5; p<0.0001, respectively). **Inset, A,** significant changes in expression of meningeal Iba-1 IR between non-neuropathic sham and neuropathic CCI rats following i.t. AM1710 or equivolume vehicle were observed (ANOVA, $F_{(3,11)}$=22.55; p=0.0003). **C**, **D**, Compared to non-neuropathic sham-operated rats given i.t. AM1710 or equivolume vehicle, neuropathic rats demonstrated a robust bilateral increase in dorsal horn GFAP IR given i.t. vehicle (ANOVA, $F_{(3,11)}$=30.32; p=0.0001, ANOVA, $F_{(3,11)}$=31.57; p<0.001, respectively). **E**, **F**, **G**, **H**, Representative spectrally unmixed images at 20x magnification of GFAP fluorescent staining (red) and DAPI nuclear stain(blue). In all images the scale bar is equal to 50 µm.

FAAH and MAGL IR were examined at maximal anti-allodynic efficacy of AM1710. Surprisingly, no changes were observed in FAAH IR between non-neuropathic sham and neuropathic CCI rats following i.t. AM1710 or equivolume vehicle (Figure 3.4 A,B). However, the exact opposite was observed with MAGL IR. That is, neuropathic rats given i.t. vehicle showed a robust bilateral increase in dorsal horn MAGL IR compared to non-neuropathic sham-operated rats given i.t. AM1710, or equivolume vehicle (Figure 3.4 C,D). These observed MAGL IR increases were robustly and ipsilaterally suppressed in spinal cords of rats treated with i.t. AM1710 (Figure 3.4 C,D). The intact meninges overlying the ipsilateral spinal cord were also separately analyzed. Different from dorsal spinal analysis, a significant increase in MAGL IR was observed from non-neuropathic sham rats given i.t. AM1710 compared to non-neuropathic rats given i.t. vehicle (Inset, Figure 3.4 C). Like dorsal spinal analysis, a clear increase in MAGL IR from CCI-treated rats given vehicle was measured. Representative corresponding fluorescent images of analyses from whole dorsal horn spinal cord are shown from sham-operated rats injected with either i.t. vehicle or AM1710 (Figure 3.4 E,F), or CCI-treated rats with either i.t. vehicle or AM1710 (Figure 3.4

G,H). While MAGL has been identified in neuronal and microglial cultures, we show that MAGL can be expressed in microglia *in vivo* (Figure 3.6 J,K,L)

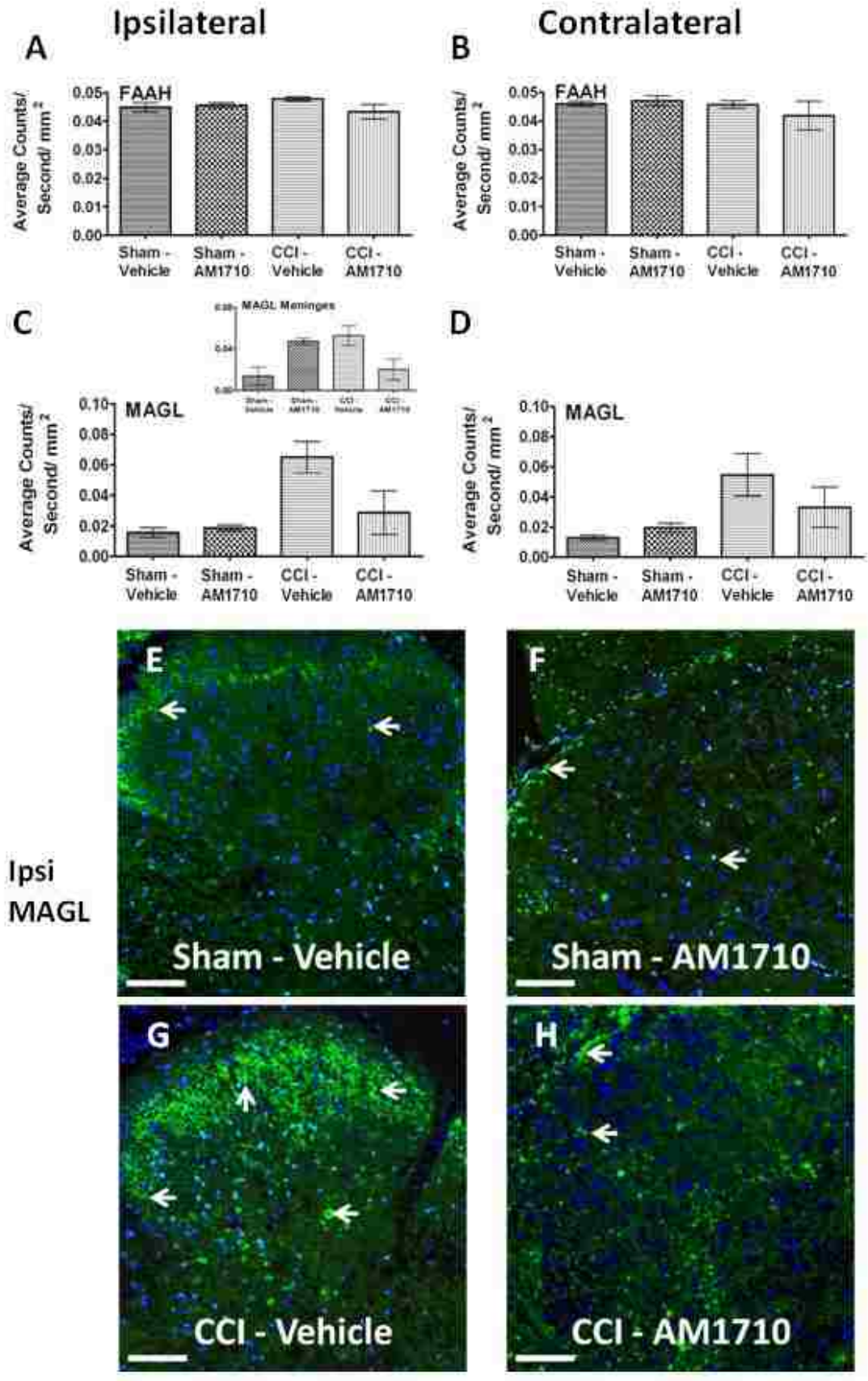
Ipsilateral
Contralateral
A
B
C
D
FAAH
MAGL
MAGL Meninges
Average Counts/ Second/ mm²
Sham - Vehicle
Sham - AM1710
CCI - Vehicle
CCI - AM1710
Ipsi MAGL
E
F
G
H
Sham - Vehicle
Sham - AM1710
CCI - Vehicle
CCI - AM1710

Figure 3.4 Immunofluorescent intensity quantification endocannabinoid degragative enzymes

Immunofluorescent intensity quantification of the spinal cord dorsal horn reveals i.t. AM1710 reduces the expression of the endocannabinoid degragative enzyme, MAGL. **A**, **B**, No changes in expression of FAAH IR between non-neuropathic sham and neuropathic CCI rats following i.t. AM1710 or equivolume vehicle were observed (ANOVA, $F_{(3,11)}$=1.967; p=0.1976; ANOVA, $F_{(3,11)}$=3.068; p=0.0910, respectively) **C**, **D**, Compared to non-neuropathic sham operated rats given i.t. AM1710 or equivolume vehicle, neuropathic rats given i.t. vehicle showed a robust bilateral increase in dorsal horn MAGL IR. In contrast, an i.t. AM1710 injection robustly suppressed bilateral increases in dorsal spinal MAGL IR (ANOVA, $F_{(3,11)}$=11.38; p=0.0029, ANOVA, $F_{(3,11)}$=5.444; p=0.00247, respectively). **Inset, C,** non-neuropathic sham rats given i.t. AM1710 as well as neuropathic rats given i.t. vehicle showed an increase in meningeal MAGL IR compared to non-neuropathic rats given i.t. vehicle (ANOVA, $F_{(3,11)}$=8.153; p=0.0081). **E**, **F**, **G**, **H**, Representative spectrally unmixed images at 20x magnification of MAGL fluorescent staining (green), and DAPI nuclear stain (blue). In all images the scale bar is equal to 50 µm

3.3.3 Immunohistochemical analysis of dorsal root ganglia

Non-neuropathic sham-operated rats given i.t. AM1710, or equivolume vehicle, revealed low GFAP IR, a marker for satellite cells. In striking contrast, a robust bilateral increase in GFAP IR was observed in the DRG from CCI-induced neuropathic rats given i.t. vehicle (Figure 3.5 A,B). However, AM1710 robustly blocked bilateral GFAP IR increases in DRG (Figure 3.5 A,B). Ipsilateral, and not contralateral, DRG increases in levels of p-p38MAPK (Figure 3.5 C,D), IL-1β (Figure 3.5 E,F) and decreases in IL-10 (Figure 3.5 G,H) were observed in vehicle injected neuropathic rats. However, following i.t. AM1710, these immunoreactive changes in p-p38MAPK, IL-1β and IL-10 significantly recovered to non-neuropathic controls levels. Representative corresponding p-p38MAPK and IL-10 immunofluorescent images of these analyses are shown from ipsilateral DRG of sham-operated rats treated with i.t. vehicle (Figure 3.5 I,L), or CCI-treated rats given either i.t. vehicle (Figure 3.5 J,M) or AM1710 (Figure 3.5 K,N).

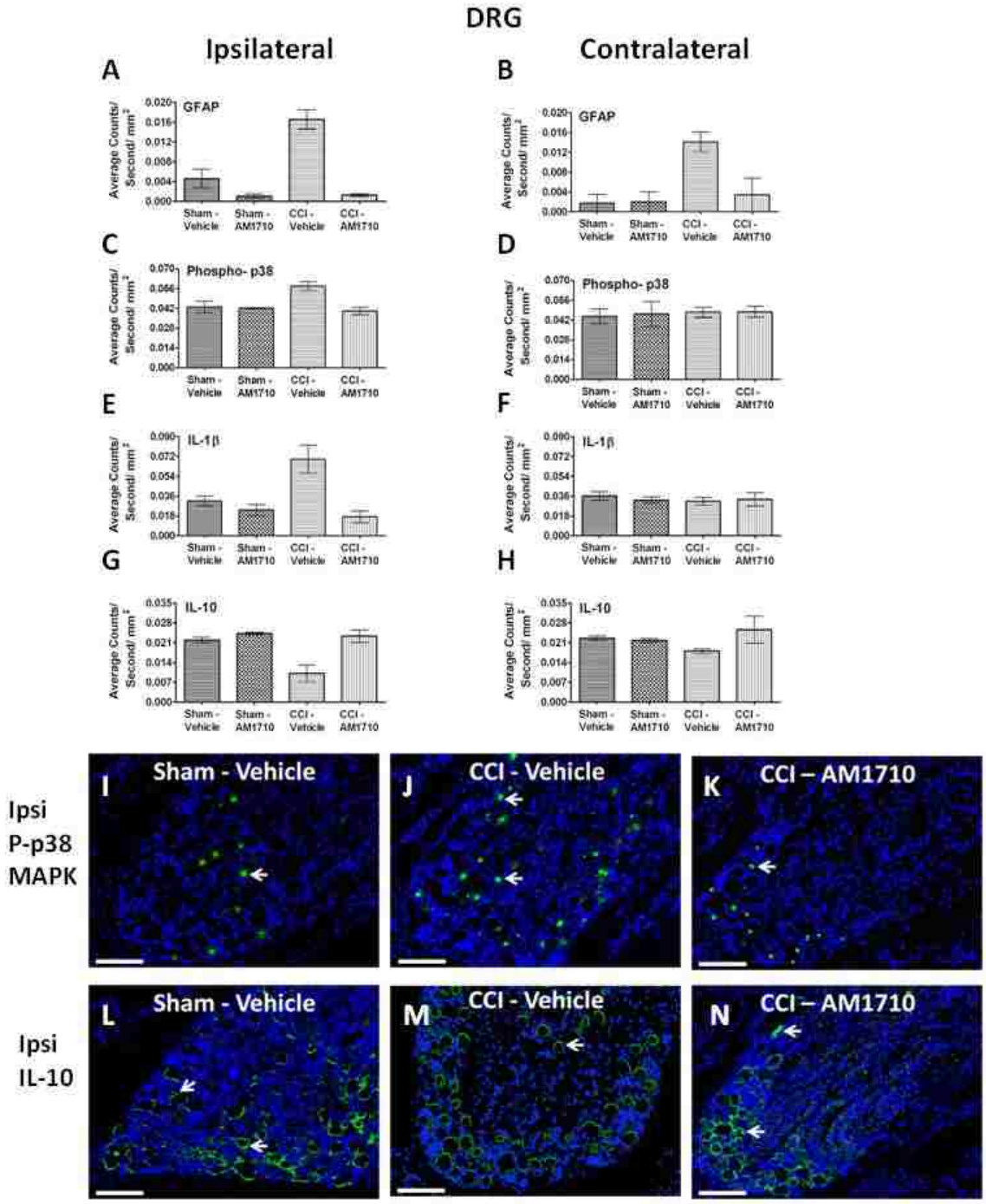

Figure 3.5 Immunofluorescent intensity quantification DRG

Immunofluorescent intensity quantification of the dorsal root ganglion reveals differences in astrocyte activation levels, phosphorylated p38MAPK, IL1β and IL-10. **A**, **B**, Compared to non-neuropathic sham operated rats given i.t. AM1710 or equivolume vehicle, CCI-induced neuropathic rats given i.t. vehicle revealed a robust bilateral increase in GFAP IR. However, i.t. AM1710 injection robustly blocked bilateral increases in GFAP IR (ANOVA, $F_{(3,11)}$=28.56; p=0.0001, ANOVA, $F_{(3,11)}$=6.067; p=0.0186, respectively). **C**, **D**, DRG changes in levels of p-p38MAPK IR occurred in the ipsilateral (ANOVA, $F_{(3,11)}$=8.097; p=0.0083), but not the contralateral (ANOVA, $F_{(3,11)}$=0.01644; p=0.9969) spinal cord to the sciatic nerve damage. **E, F,**

Unilateral change was also observed with IL-1β IR (ipsilateral ANOVA, $F_{(3,11)}$=9.291; p=0.0055, contralateral ANOVA, $F_{(3,11)}$=0.2395; p=0.8664). **G, H**, IL-10 IR was also unilaterally decreased in neuropathic animals following CCI surgery given i.t. vehicle treatment of AM1710 (ipsilateral ANOVA, $F_{(3,11)}$=12.01; p=0.0025, contralateral ANOVA, $F_{(3,11)}$=1.612; p=0.2618). **I, J, K**, Representative spectrally unmixed images of phospho-p38 at 20x magnification, phospho-p38 fluorescent staining (green) and DAPI nuclear stain (blue). **L**, **M**, **N**, IL-10 representative spectrally unmixed images at 20x, IL-10 fluorescent staining (green) and DAPI nuclear stain (blue). In all images the scale bar is equal to 50 µm.

3.3.4 Identification of IL-10 expressed in dorsal horn astrocytes and microglia

Within the superficial laminae, IL-10 is not co-labeled with GFAP positive cells (Figure 3.6 A,B,C). However, within the deeper laminae of the dorsal spinal cord, IL-10 is extensively co-labeled with GFAP, (Figure 3.6 D,E,F) while co-labeling with NF-H (neurons) was completely absent (data not shown). Additionally, Iba-1 positive cells (macrophages and/or resident microglia) express IL-10 protein in laminae I-III (Figure 3.6 G,H,I).

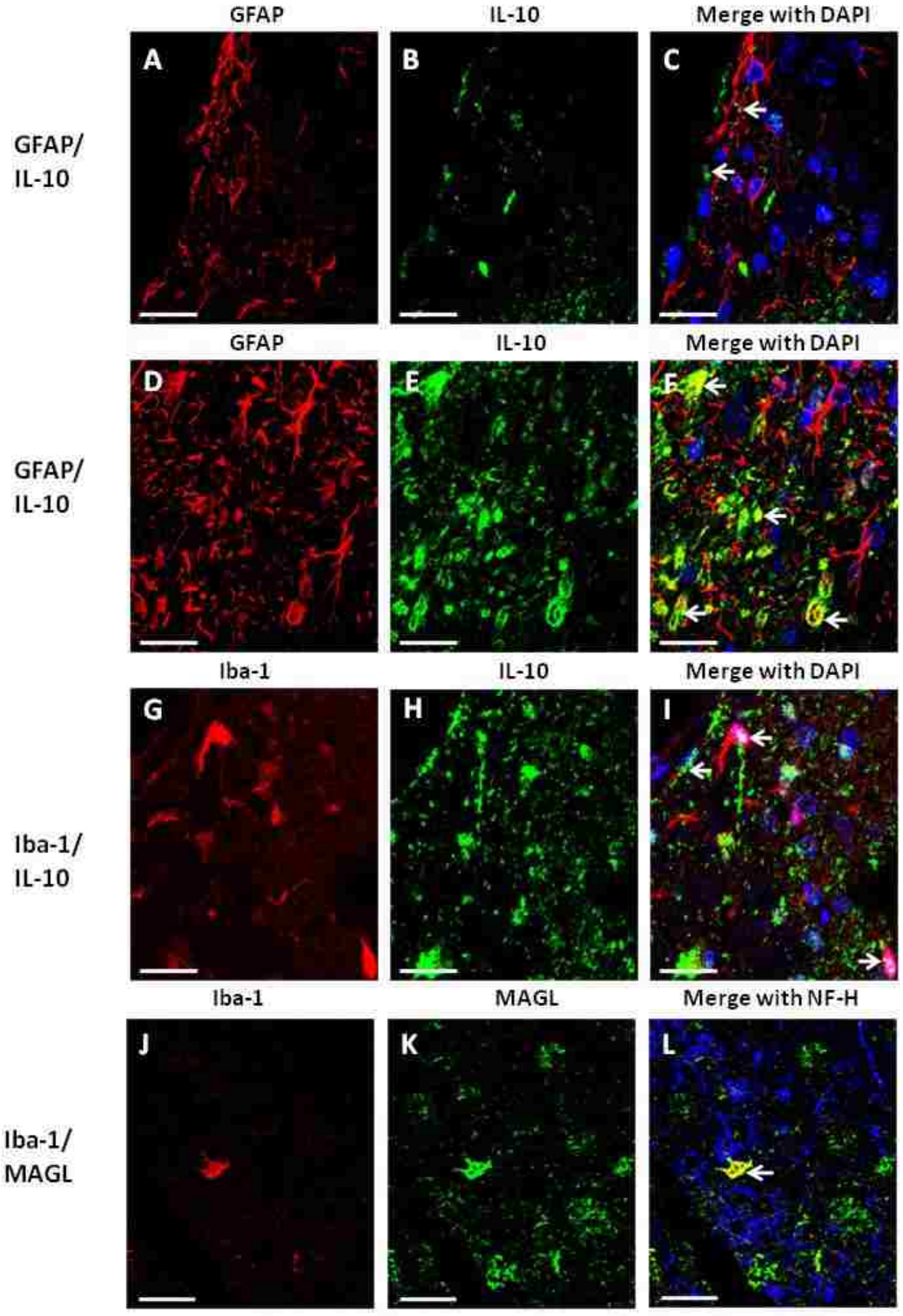

Figure 3.6 Qualitative confocal images of cellular immunostaining of IL-10 in spinal cord.

Qualitative confocal images of cellular immunostaining of IL-10 in spinal cord. **A**-**I,** Spinal cord tissue from rats with CCI-AM1710 treatment. **A**, **B**, **C**, Immunostaining of IL-10 (green) in meninges and superficial laminae of the spinal cord dorsal horn is not co-labeled with GFAP (red)

positive cells. DAPI nuclear labeling is blue. Arrows indicate IL-10 in the superficial laminae. **D**, **E**, **F,** Immunostaining of IL-10 (green) in the deeper laminae of the dorsal horn spinal cord is co-labeled yellow with GFAP (red) positive cells, with DAPI nuclear labeling (blue). Arrows indicate co-labeling of IL-10 and GFAP positive cells. **G**, **H**, **I**, Immunostaining of IL-10 (green) in the meninges and superficial laminae of the dorsal horn spinal cord is co-labeled (yellow) with Iba-1 (red) positive cells, with DAPI nuclear labeling (blue). Arrows indicate co-labeling of IL-10 and Iba-1 positive cells. **J**, **K**,**L**, Immunostaining of MAGL (green) in the deeper laminae of the dorsal horn is co-labeled yellow with Iba-1 (red) positive cells, with NF-H neuronal labeling (blue). An arrow indicates co-labeling of MAGL and an Iba-1 positive cell. In all images the scale bar is equal to 20 µm.

3.3.5 Blockade of gp120-induced allodynia and DRG IL-1β production

Pilot data determined the timecourse in which AM1710 blocked the ability of gp120 to induce allodynia. We found that 10 µg of AM1710 was sufficient in blocking the initial development of gp120-induced allodynia, with the anti-allodynic effects gone by 60 minutes (data not shown). All animals revealed similar BL responses prior to i.t. lumbar cannula implantation, i.t. AM1710 or equivolume vehicle injection (Day 6), and immediately prior i.t. gp120 (Figure 3.7 A, B). As expected, a robust bilateral allodynia was observed in animals given i.t. pretreatment with the vehicle for AM1710 followed ~3 hrs later by i.t. gp120. In stark contrast, i.t. pretreatment with AM1710 completely prevented the initiation of the bilateral gp120-induced allodynia (Figure 3.7 A, B). Tissue collected from these animals 20 minutes after gp120 administration revealed a robust increase in IL-1β protein levels and a strong trend toward increased TNF-α protein production in the L4-L6 DRG corresponding to L4-L6 spinal segments exposed to i.t gp120 compared to controls (Figure 3.7 C, D). However, IL-1β protein was significantly suppressed in animals given i.t. AM1710 pretreatment followed by gp120, while a strong trend toward blunted TNF-α protein production was measured. Expectedly, changes in IL1-β and TNF-α within either the CSF or the dorsal horn spinal cord was not observed at this early post-i.t. gp120 timepoint.

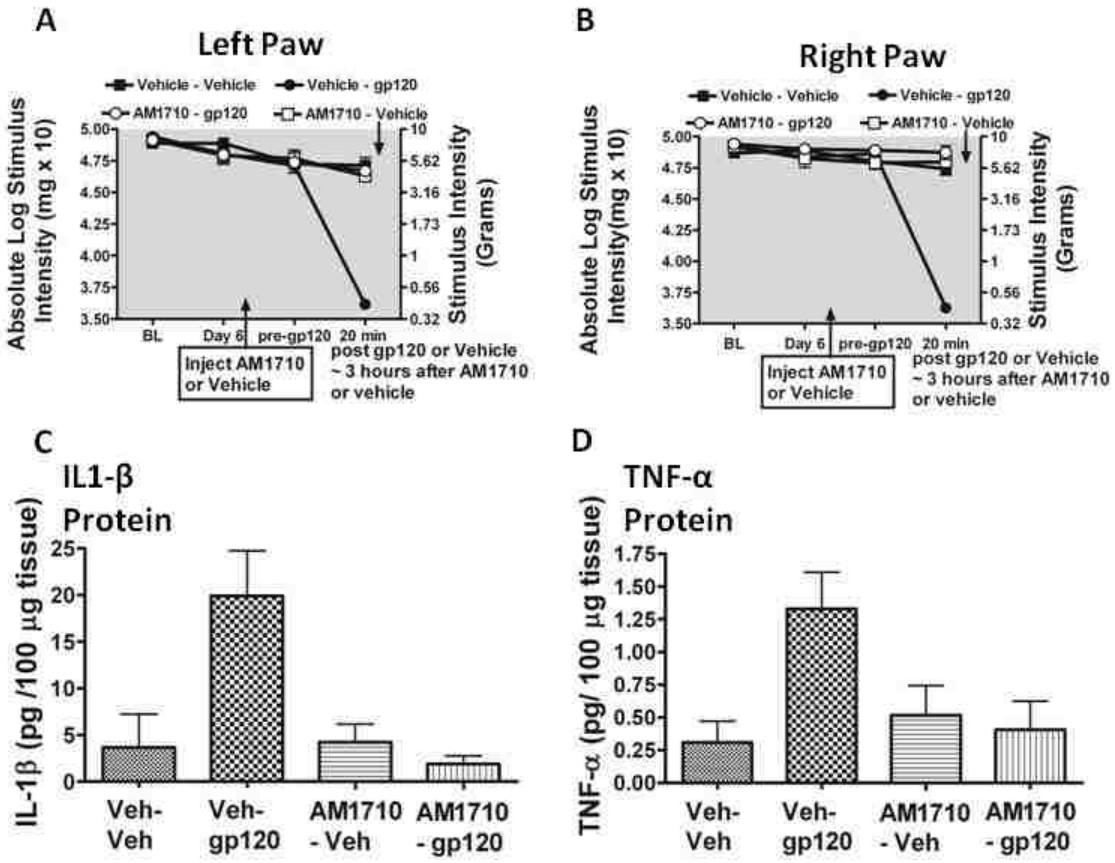

Figure 3.7 AM1710 pre-treatment blocks gp120-induced allodynia and IL-1β cytokine production.

AM1710 pre-treatment blocks gp120-induced allodynia and IL-1β cytokine production. A total of 24 animals were used for both the behavioral experiment reported here and tissues from these animals were analyzed in the reported ELISA experiments. **A**, **B**, Prior to surgical manipulation, all groups exhibited similar bilateral (ipsilateral and contralateral) BL thresholds (ANOVA, $F_{(3,23)}$ =1.781; p=0.1833; $F_{(3,23)}$ =2.311; p=0.1072, respectively). Following indwelling catheter implantation, there was no major effect of surgery on Day 6 after surgery thresholds when compared to BL thresholds or following the i.t. pretreatment of either AM1710 or vehicle (ANOVA, $F_{(6,60)}$ = 0.9381; p=0.1311; ANOVA, $F_{(6,60)}$=2.415 ; p=0.1648, respectively). Animals given i.t. gp120 developed strong allodynia in both left and right paws at 20 min compared to pre-gp120 threshold values (ANOVA, $F_{(3,20)}$=61.72; p<0.0001 ANOVA, $F_{(3,20)}$=75.73; p<0.0001, respectively). **C**, Quantification of IL-1β protein by ELISA revealed IL-1β was significantly increased in left DRG of allodynic rats following i.t. gp120 given a pretreatment with i.t. vehicle of AM1710 (ANOVA, $F_{(3,13)}$= 7.785; p=0.0057). **D**, a trend in the levels of TNF-α protein, although not statistically significant (ANOVA, $F_{(3,14)}$ = 2.977; p=0.0741).

3.4 Discussion

In this study, we present evidence that a distinct anti-inflammatory response is induced following spinal (i.t.) administration of the recently characterized cannabinoid CB_2R agonist compound from the cannabilactone class, AM1710,

which either prevents or reverses allodynia induced in two distinguishable animal models. The findings of each animal model will be discussed in turn. In the CCI model, a transitory bilateral reversal of allodynia from chronic unilateral CCI is observed following i.t. AM1710 administration. While AM1710 was previously shown to increase nociceptive thresholds following peripheral administration in naïve rats [175, 176], this study reports that normal light touch sensory thresholds are not altered following i.t. AM1710 in non-neuropathic rats. Additionally, immunoreactivity (IR) for IL-10, significantly decreased in CCI-treated rats. In striking contrast, i.t. AM1710 in CCI neuropathic animals reset bilateral IL-10 IR to basal levels. Overlying meninges revealed similar, albeit insignificant, trends in IL-10. Furthermore, using confocal microscopy, dorsal horn localization of IL-10 is observed in astrocytes and microglia in superficial and deeper laminae (III-V). Together, these findings suggest that spinal parenchyma IL-10 regulate glia to induce pain relief.

It is critical to note that in response to peripheral nerve injury, CNS cellular populations can increase by proliferation of microglia [232], astrocytes [270], or by influx of bone marrow derived perivascular microglia and macrophages [85]. Thus, increased immunoreactivity of specific proteins in the lumbar spinal cord could simply be due to a general increase in cell numbers constitutively expressing these markers. However, DAPI IR of cellular nuclei remained constant in all experimental conditions, supporting the possibility that cellular specific responses to CCI and AM1710 occurred.

Indeed, alterations in several proinflammatory markers were observed in the spinal cord dorsal horn following CCI. Bilateral increases in p38MAPK IR were observed, supporting prior work demonstrating that p38MAPK plays a critical role in mechanical allodynia that involves the action of proinflammatory cytokines including IL-1β in models of peripheral nerve lesions [27, 194, 271]. While increased ipsilateral spinal IL-1β mRNA was recently reported following sciatic nerve ligation [242], the current data in this study is the first demonstration of increased unilateral IL-1β IR in anatomically intact spinal cord dorsal horn of rats with CCI-induced allodynia. As with IL-10, AM1710 reset IL-1β to basal levels, but p-p38MAPK remained completely unaltered by AM1710, suggesting that basal levels of IL-10 are not sufficient to suppress activated p-p38MAPK IR. In addition, the data reported here show bilateral increases in GFAP IR were observed in neuropathic rats. Prior work suggests that increased GFAP expression may not simply be a cellular marker co-incident with neuropathy, as has been frequently reported [93, 252, 272], but rather, may play a critical role mediating neuropathic pain [273]. Interestingly, CB_2R activation in neuropathic rats resulted in significantly reduced superficial dorsal horn GFAP IR [94], which may occur via microglial alterations because astrocytes make contact with microglia.

CB_2R expression has been identified mostly in spinal microglia [93, 135, 139, 212, 241]. While AM1710 blunted increases in GFAP IR, Iba-1 IR remained unaltered. Iba-1 is one of several immunohistochemical markers used to identify active microglia [274, 275]. Spinal cord microglial activation, identified by Iba-1

IHC staining, was reversed by 3 hours following treatment with a microglial-specific inhibitor [134]. Other markers include the CD11b/CD18 [268], or translocator protein (TSPO), formerly known as the peripheral benzodiazepine receptor [276] preferentially expressed in CNS macrophage/microglia. However, in contrast to prior reports revealing decreased microglial activation following i.t. CB_2R activation [131, 241, 254], we show increased Iba-1 IR persists following i.t. AM1710 and during reversal from allodynia. However, interpretations of these results are limited, given only a single microglial marker was used to examine microglial activation. Nevertheless, microglia produce the anti-inflammatory endocannabinoid, 2-arachidonyl glycerol (2-AG) during pathological CNS conditions [8, 144]. Notably, microgla may also be a source of IL-10 [277] in the spinal cord. Indeed, co-localization of IL-10 in microglia within superficial and deeper spinal cord laminae (III-IV) in behaviorally reversed CCI-treated rats is shown in this report.

The bioavailability of endocannabinoids such as anandamide and 2-AG produced and released from neurons and microglia [8, 144] are primarily controlled through enzymatic metabolism by FAAH and MAGL [140, 142, 234]. Inhibitors of FAAH and MAGL that result in increased CNS levels of AEA and 2-AG, suppress pathological pain [151, 152, 208, 258]. The current study uniquely shows increased dorsal horn MAGL IR of neuropathic rats that is reduced following i.t. AM1710 in allodynic-reversed rats. As noted above, microglia are a known source of 2-AG [8], where the actions of MAGL have been described [145]. We additionally show that MAGL expression is co-localized in superficial dorsal horn

microglia using confocal microscopy. Interestingly, no change in FAAH-IR was observed.

Satellite glial cells in the DRG form a clear sheath around individual large and small sensory neurons, and when activated under neuropathic conditions, reveal enriched GFAP and IL-1β expression [69, 72, 80, 81, 273]. IL-1β released from satellite glia further stimulates sensory neurons. Notably, DRG p-p38MAPK expression is well-characterized following peripheral nerve injury associated with pathological pain [84, 85]. Here, examination of DRG revealed increased unilateral p-p38MAPK, IL-1β, and bilateral peri-neuronal (satellite cells) GFAP-IR in neuropathic animals, while i.t. AM1710 abolished all of these changes. Like that observed in spinal cord dorsal horn, DRG IL-10 expression was significantly diminished during chronic neuropathy, in support of prior reports [191, 208, 273], and AM1710 resulted in basal IL-10 IR levels.

Bilateral allodynia induced by unilateral sciatic nerve CCI is demonstrated in this study supporting previous findings [200, 201, 203, 217, 226, 237-239]. Reports demonstrating bilateral biochemical changes in lumbar spinal cord substantiate these behavioral observations. Prior demonstrations include, a decrease in α2-adrenergic receptor mRNA expression [240], greater Fos protein in neurons [91], and IL-6 mRNA upregulation [239]. However, unique findings from the present work reveal unilateral spinal cord dorsal horn IL-1β IR increases. Thus, the spinal actions of IL-1β must be critical for inducing ipsilateral biochemical changes that in turn alter contralateral spinal cord activity. One possible mechanism may

involve ipsilateral IL-1β mediated astrocyte activation that spreads to the contralateral spinal cord via astrocyte gap-junctional communication. Evidence for a critical role of spinal gap-junctional communication leading to contralateral allodynia that is partly mediated by IL-1β has been reported in a model of localized sciatic nerve inflammation [237].

Intrathecal HIV-1 gp120 is an informative model of pathological pain because the spinal actions of IL-1β, p38MAPK and other proinflammatory factors are necessary for allodynia to develop [196, 204, 215, 217, 226, 265, 268, 278]. Here, the onset of gp120-induced allodynia replicated previously characterized allodynia [67, 196, 204, 215, 217, 226, 265, 268, 278]. However, an early timepoint analysis of IL1-β reveals no changes in CSF or dorsal horn, in support of prior reports [268, 278], while increases in DRG IL1-β are observed. Allodynia and increased protein levels of DRG IL-1β following i.t. HIV-1 gp120 was completely prevented by i.t. AM1710 pretreatment, supporting immunofluorescent quantitative IL-1β changes observed from DRG in CCI neuropathic animals. This data supports that rapid changes in allodynia may primarily be an aspect of altered DRG activity.

CB_2Rs can modulate various signal transduction pathways involved in controlling allodynia in the animal models utilized in this report; CCI and i.t. gp120. While each model initiates spinal glial responses with subsequent proinflammatory cytokine production by different pathways, their downstream intracellular pathways converge. In CCI, enhanced central terminal and dorsal horn

neurotransmitter (glutamate, substance P), ATP and chemokine release occurs, activating their cognate receptors on surrounding microglia, astrocytes and neurons [79, 253, 279-281]. Separately, i.t. gp120 activates microglia and astrocytes in their role as immunocompetent cells that release neuroactive substances culminating in allodynia [282]. However, for both models, activated MAPKs, such as extracellular signal-regulated kinases (ERK1/2), p38 and c-Jun N-terminal Kinase (JNK), are critical contributors of glial intracellular signaling leading to IL-1β and TNF-α synthesis and pathological pain [27, 196, 268, 280]. Additionally, spinal nitric oxide (NO), highly reactive through secondary reactions creating reactive oxygen species, activates MAPKs [283] and mediates allodynia in both models [67, 196, 280]. CB_2R activation impacts signaling pathways involving cAMP, ERK1/2, JNK, p38-MAPKs and NO production [257, 284] by several potential mechanisms. First, CB_2R activation induces the expression of MAPK phosphatase-1 (MKP-1) in microglial cells, which acts to de-activate ERK1/2 and decrease NO production [284]. Second, CB_2R activation induces IL-10 production that is well-established to suppress IL-1β TNF-α and NO production [277]. While CB_2R-mediated IL-10 production requires p38-, ERK1/2 and JNK-MAPK activation [257], concurrent inhibition of downstream translocation to the nucleus of the transcription factor, nuclear factor-kappaB (NFκB) that triggers IL-1β and TNF-α transcriptional activation, occurs by disrupting cytoplasmic IkB important for NFκB translocation [257]. The recently recognized key glial receptor participating in pathological pain, toll-like receptor 4 (TLR4), may become activated not only by its classic ligand, lipopolysaccharaide,

but also by factors released from i.t. gp120- or CCI-activated glia and damaged neurons [262, 285]. An intriguing possibility is that CB_2R activation may exert anti-inflammatory effects through the ceramide pathway [286], as ceramide analogs and TLR4 activation in microglia act synergistically to produce IL-10 via the p38MAPK pathway [287, 288].

Together, the implication of these results is that CB_2R compounds capable of acting independently on both the spinal cord and DRG glial cytokines can control clinically relevant pathological pain conditions.

3.5 Acknowledgements

The authors would like to thank Genevieve Phillips at the University of New Mexico Cancer Center Shared Microscopy Center for her valuable input and training on the spectral software utilized. This work was supported by NIH grants: NIDA 018156, GM60201. This project was also funded in part by the Dedicated Health Research Funds from the University of New Mexico School of Medicine.

The authors would like to disclose a conflict of interest. A.M. is a consultant for MAK Scientific.

4. The selective cannabinoid receptor 2 (CB_2R) agonist AM1710 acts independently of cannabinoid receptor 1 (CB_1R) responses in neuropathic mice

Journal of Pain

Authors: Jenny L. Wilkerson[1*], Lauren B. Alberti[1], Pamela S. Platero[1], James A. Wallace[1], Audra A. Kerwin[1], Daniel Moezzi[1], Sergio Torres[1], Catherine A. Ledent[2], Ganesh A. Thakur[3], Alexandros Makriyannis[3], and Erin D. Milligan[1*]

Affiliation(s):

Department of Neurosciences, Health Sciences Center, School of Medicine, University of New Mexico, Albuquerque, NM 87131

Universite libre de Bruxelles, B-1070 Brussels, Belgium

Center for Drug Discovery, Northeastern University, Boston, MA 02115

*** Corresponding Authors:**

Jenny L. Wilkerson
University of New Mexico, HSC
Dept. of Neurosciences
MSC08- 4740
1 University of New Mexico
Albuquerque, NM 87131
Email: JLWilkerson@salud.unm.edu
Phone: +1(505)272-4441
Fax: +1(505)272-8082

Erin D. Milligan
University of New Mexico, HSC
Dept. of Neurosciences
MSC08- 4740
1 University of New Mexico
Albuquerque, NM 87131
Email: Emilligan@salud.unm.edu
Phone: +1(505)272-8103
Fax: +1(505)272-8082

Abstract

Chronic constriction injury (CCI) of the rodent sciatic nerve causes light touch mechanical sensitivity (allodynia) and leads to activation of spinal cord astrocytes, microglia and dorsal root ganglia (DRG) satellite cells. The

endocannabinoid system includes the cannabinoid receptor 1 (CB_1R) present on neurons and the cannabinoid receptor 2 (CB_2R) present on immune cells like microglia. CB_2R agonists, like AM1710, are effective in controlling pathological pain states in animal models. Activation of the CB_1R could be responsible for the analgesic effects of AM1710 through non-specific binding. Thus, we sought to determine whether spinal or peripheral AM1710 could lead to anti-allodynia and produce changes in spinal and DRG pro- and anti-inflammatory protein expression in mice with a CB_1R genetic deletion. Following CCI, CB_1R KO mice displayed allodynia similar to their wild-type and heterozygous littermates. AM1710, given either spinally or peripherally reversed CCI-induced allodynia in CB_1R KO mice to sham control levels. Immunohistochemical procedures followed by fluorescent microscope analysis were performed for the anti-inflammatory cytokine IL-10, the pro-inflammatory cytokine IL-1β, and the chemokine monocyte chemoattractant protein 1 (MCP-1/CCL2) in these tissues. Mouse macrophage culture supernatants revealed suppressed factors following exposure to AM1710 under pro-inflammatory stimulating conditions.

Part of this work was presented in abstract form at the 2012 American Pain Society meeting held in Honolulu, HI.

Perspective

Overall, the results support the selective CB_2R agonist AM1710 may act independently of CB_1R actions in spinal cord and DRG. Absence of the CB_1R under neuropathic conditions reveals increases in neuroprotective IL-10 in both

the DRG and spinal cord. Removal of CB_1R actions coupled with CB_2R agonists may produce heightened anti-inflammatory effects, and may be clinically relevant in the treatment of chronic, neuropathic pain.

Keywords: cannabinoid; mouse; paraffin immunohistochemistry; spectral analysis; MCP-1/CCL-2

4.1 Introduction

Both the dorsal root ganglia (DRG) and dorsal horn of the spinal cord are well characterized to house neurons critical for processing information underlying chronic pain. It is well established that glia, (i.e., astrocytes, microglia, as well as DRG satellite cells) mediate chronic pathological pain signaling [25, 289-292]. Under healthy conditions, glial activation is correlated to immune surveillance, and is critical for the maintenance of homeostasis. However, unrelenting, continous activation of glial cells without a homeostatic function often leads to aberrant, pathological activation, resulting in the release of proinflammatory cytokines such as tumor necrosis factor alpha (TNF-α), and interleukin (IL)-1β. Proinflammatory cytokines are known to be a critical components of chronic neuropathic pain [29, 202]. The chemokine CCL2 (C-C motif ligand 2), also known as monocyte chemo-attractant protein-1 (MCP-1), exists as a neuron to glia signal. MCP-1 is released from pre-synaptic neurons in the superficial lamina of the dorsal horn of the spinal cord, binds to its receptor CCR2 on glia, leading to glial activation and pathological pain [77, 293-295]. It has been established that the actions of the anti-inflammatory cytokine IL-10 reverses neuropathic pain

in several animal models [202, 229, 230, 296, 297]. Although anatomically distinct, the relative contribution of spinal cord glia compared to DRG glia in the ongoing maintenance of chronic pain conditions is not well understood.

The most widely understood receptors of the endocannabinoid system are the cannabinoid 1 receptor (CB_1R), predominately found on peripheral nociceptor cell bodies within the DRG and on pre- and post synaptic neurons in the superficial lamina of the dorsal horn, including GABA-urgic interneurons [298], and the cannabinoid 2 receptor (CB_2R) predominately found on immune cells such as microglia. Activation of either the CB_1R or CB_2R has been extensively characterized to produce analgesia [91, 94, 139, 148, 155, 162-164, 177, 210, 211, 258, 261, 299-302]. However, actions at the CB_1R produce a number of effects other than analgesia, which diminishes its potential clinical application. Alternatively, CB_2R specific compounds that do not produce the unintended effects that activation of the CB_1R produces, have been pursued. We previously found that the novel CB_2R agonist AM1710 from the cannabilactone classification [175, 176] was efficacious in preventing and reversing allodynia, light touch mechanical sensitivity, a significant and frequent manifestation of neuropathic pain [300]. In correlation with behavioral reversal, we found a distinct anti-inflammatory effect after intrathecal administration of AM1710 in both the dorsal horn spinal cord as well as corresponding DRG. However, CB_1Rs may be greater in number than CB_2Rs in the spinal cord. Antibodies for CB_2R have been problematic, leading to difficulty in quanifying numbers of CB_1R vs. CB_2R under normal and pathological conditions. Although AM1710 has a ~54-fold greater

affinity for the CB_2R over the CB_1R [175], non-specific actions at the CB_1R cannot be dismissed as a major factor contributing to the anti-allodynic effects of AM1710.

The goal of these studies was to examine whether AM1710 controls pathological pain via CB_2R specific actions that involves a role for cytokines in the spinal cord and DRG. The use of transgenic animals lacking functional CB_1R was employed to examine the specificity of AM1710. Here we sought to tease out the discrete anatomical influences of critical protein mediators of chronic pain, such as the cytokines IL-1β, IL-10 and the chemokine MCP-1 on the reversal of neuropathic pain. Intriguingly, with the constitutive removal of the CB_1R in CB_1R KO mice, we find a novel interplay between the endogenous actions of CB_1R and the expression of the neuroprotective protein IL-10 under neuropathic conditions.

4.2 Methods

4.2.1 Animals

A total of 173 pathogen-free adult male mice on a CD1 genetic background (24-39 grams) were used in all experiments. The weight difference in the mice utilized was due to both the age range (1 month to 3 months old) as well as the genotype differences due to the CB_1R KO. That is, with the genetic deletion of the CB_1R, these mice tend to weigh less than age matched controls, but this did not lead to observable differences in withdrawal responses during behavioral testing. Mice were housed in a temperature and light-controlled (12 hour light/dark; lights on at 6:00 AM) environment, with standard rodent chow and

water available ad libitum. All procedures adhered to the guidelines of the Committee for Research and Ethical Issues of the International Association for the Study of Pain and were approved by the Institutional Animal Care and Use Committee (IACUC) of the University of New Mexico Health Sciences Center.

Heterozygous CB_1R knockout mice were generated on a CD1 background and were generously gifted from the laboratory of Dr. C. Ledent [303]. Of note, it has been established that this strain of knockout mice do not display typical behavioral endpoints observed with CB_1R agonists. Heterozygous (CB_1R-/+) and Knockout (CB_1R-/-) mice, along with their Wildtype (CB_1R+/+) littermates, were used in all experiments.

The following primer sequences were used in PCR for genotyping:

GGG TGA GGA GAC ATG CCT GGT GA ---------- CB_1R Wildtype Forward primer
AGA GGT GCC AGG AGG GAA CCC TA ---------- CB_1R Wildtype Reverse primer
CCT TGC GCA GCT GTG CTC GA ---------- CB_1R Knockout Forward primer
GAA CAG TTC GGC TGG CGC GA ---------- CB_1R Knockout Reverse primer

4.2.2 Drugs

The CB_2R agonist, 3-1(1',1'-Dimethylheptyl)-1-hydroxy-9-methoxy-6H-benzo[c]-chromene-6-one (AM1710) [175, 176, 300, 304] was used in these experiments. AM1710 was generously gifted by A.M. and G.T. AM1710 was first dissolved in 100% ethanol and diluted in sterile water (Hospira Inc, Lake Forest, IL) for a final of concentration 1 mg/ mL containing 5% ethanol. The vehicle of AM1710 consisted of sterile water containing 5% ethanol, as described previously [300]. The selective CB_2R antagonist, 6-Iodo-2-methyl-1-[2-(4-morpholinyl)ethyl]-1H-indol-3-yl](4-methoxyphenyl)methanone, (AM630) was purchased (cat # 1120,

Tocris Bioscience, Minneapolis, MN). As described for AM1710, AM630 was first dissolved in 100% ethanol and diluted in sterile water (Hospira Inc, Lake Forest, IL) for a final of concentration 1 mg/ mL containing 5% ethanol. The vehicle of AM630 was made up of sterile water containing 5% ethanol.

4.2.3 Behavioral assessment of allodynia

Baseline (BL) responses to light mechanical touch were assessed using the von Frey test after animals were habituated to the testing environment, as described elsewhere [305]. Briefly, mice were placed atop 2 mm-thick parallel bars, covered with a wire mesh screen, with spaces 1 mm apart and habituated for approximately 30 minutes for 4 days. Mice were unrestrained, and were singly placed under an inverted wire mesh basket to allow for unrestricted air flow. All behavioral testing was performed during the first half of the light cycle in a sound, light, and temperature controlled room. The von Frey test utilizes a series of calibrated monofilaments, (2.83 – 4.31 log stimulus intensity; North Coast Medical, Morgan Hills, CA) applied randomly to the left and right plantar surface of the hindpaw for 3 seconds. Lifting, licking or shaking the paw was considered a response. For all behavioral testing, threshold assessment was performed in a blinded fashion by J.L.W.

4.2.4 Chronic constriction injury (CCI) surgery

Following BL behavioral assessment, the surgical procedure for chronic constriction of the sciatic nerve was completed as previously described [216], but modified for mouse [305, 306]. Briefly, in isoflurane- (induction 5% vol. followed

by 2.0% in oxygen) anesthetized mice, the mid- to lower back and the dorsal left thigh shaved and cleaned with 75% ethanol. Using aseptic procedures, the sciatic nerve was carefully isolated, and loosely ligated with 3 segments of 5-0 chromic gut sutures (Ethicon, Somerville, NJ). Sham surgery was identical to CCI surgery but without the loose nerve ligation. The overlying muscle was sutured closed with (1) 4-0 sterile silk suture (Ethicon, Somerville, NJ), and animals recovered from anesthesia within approximately 5 minutes. Animal placement into either CCI or sham surgical groups was randomly assigned.

4.2.5 Acute intrathecal injection

In mice with intrathecal injections, all drugs were administered via acute i.t. catheter placement. Injections were performed via a lumbar puncture in between L5-L6. Briefly, an 'injection catheter' made from a 27-gauge needle with the plastic hub removed was fitted into polyethylene (PE) 20 tubing, and the needle portion of another 27-gauge needle was inserted at the other end, with the hub of this needle connected to a 10 µl Hamilton syringe, closely resembling the 'injection catheter' previously described [202, 217, 226, 297]. Using prior publications as a guideline, a dose of 5 µg AM1710 [300] or 3 µg of the selective CB_2R antagonist, AM630 [307] was used. Drug or equivolume vehicle was drawn into the injection catheter, and the tip of the 27-gauge needle was gently inserted in between L5-L6. During this time, light leg twitching and a tail flick was typically observed indicating successful i.t. catheter placement. Drug or vehicle was injected during a 5 second interval. Drug treatment was randomly assigned to

animals. Upon completion of injection, the 27-gauge needle was removed. A 100% motor recovery rate was observed from this injection procedure.

4.2.6 Acute intraperitoneal injection

An acute IP injection of either AM1710 or equivolume vehicle was used, in CCI-induced neuropathic mice or sham-operated non-neuropathic mice. Prior reports [176] indicate an efficacious dose of 25 mg/kg/ ml (5 mg/ kg) AM1710, which was administered in these studies.

4.2.7 Immunohistochemical procedures from CCI-treated mice

Following behavioral assessment, animals were overdosed with an intraperitoneal injection sodium phenobarbital (Sleepaway, Fort Dodge Animal Health, Fort Dodge, IA), then perfused transcardially with saline followed by 4% paraformaldehyde. Whole vertebral columns with intact spinal cords (cervical 2 through sacral 1 spinal column segments) were removed, and underwent overnight fixation in 4% paraformaldehyde at 4°C. This tissue collection approach ensured that all relevant anatomical components, including the cervical, thorasic, and lumbosacral spinal cord, DRG, and overlying meninges, were intact within the vertebral column, allowing important spatial relationships to remain for examining corresponding functional interactions at individual and specific spinal cord levels. All specimens underwent EDTA (Sigma Aldrich, St. Louis, MO) decalcification for approximately 2 weeks, and spinal cord sections were subsequently paraffin processed and embedded in Paraplast Plus Embedding Media (McCormick Scientific, St. Louis, MO) as previously described [218, 300,

301, 308]. Adjacent tissue sections (7 µm) were mounted on Superfrost Plus slides (VWR, Radnor, PA), and allowed to adhere to slides overnight at 40°C, followed by deparaffinization, and rehydration via descending alcohols to PBS (1X, pH 7.4). Sections were then processed with microwave antigen retrieval procedures (citrate buffer pH 6.0, or tris-based buffer, pH 9.0; BioCare Medical, Concord, CA).

Slides were incubated with 5% normal donkey serum (NDS), in PBS (pH 7.4) for 2 hours, followed by overnight primary antibody incubation in a humidity chamber at 3° C. Slides underwent secondary antibody incubation for 2 hours in a humidity chamber at room temperature, rinsed in PBS, and then coverslipped with Vectashield containing the nuclear stain 4',6-diamidino-2-phenylindole (DAPI) (Vector Labs, Burlingame, CA). All antibody methods were as previously described [300, 301]. For the detection of MCP-1/CCL2 an Armenian hamster anti-rat monoclonal antibody was used (clone 2H5, cat. # NB100-78196, Novus Biologicals, Littleton, CO), with a primary antibody dilution of 1:100, and detected with a Donkey- anti-hamster FITC tagged secondary antibody (Jackson Immunoresearch, (West Grove, PA).

4.2.8 Immunohistochemical spectral image analysis

All images of the spinal cord dorsal horn, overlying meninges and DRGs were captured by a Nikon inverted fluorescent microscope (Melville, NY), at 20x magnification, with a Nuance Spectral Camera (Cambridge Research & Instrumentation, Woburn, MA), as previously described [300, 301]. Briefly,

utilizing the Nuance computer software, the fluorescent wavelength emission spectra range was initially determined for each fluorophore utilized in the detection of the primary antibody of interest (DAPI, 488 nm +/- 10nm; FITC, 575 nm +/- 5nm; Rhodamine Red 600 nm+/- 5nm) by using a control slide with only a drop of the pure fluorophore. The fluorescent intensity threshold for each protein marker was determined by the user finding the most appropriate threshold that captures the specific FITC or Rhodamine Red staining for each protein marker within a tissue (e.g., dorsal horn spinal cord or DRG). Once the optimal level of fluorescent threshold was determined for a particular protein marker, this level was held consistent throughout all of the treatment groups for the image analysis within each protein marker of interest. These steps were followed by software conversion allowing fluorescent wavelength intensity for each fluorophore to be converted to a numerical value.

Primary antibody staining procedures remained consistent to minimize intensity variations of each fluorophore (FITC or Rhodamine Red) used to detect the different primary antibodies of interest. To ensure that fluorophore binding was not impeded through possible steric hindrance of other proximal fluorophores, sections were labeled for only one cellular marker of interest on a slide.

The average count of fluorescent emission intensity per second exposure, per mm^2 is the analyzed value that we report here. That is, fluorescent intensity average count/second/mm^2, which takes into account the density as well as the intensity of the fluorophore detected. A total of 4 sections per animal (N=3) were

randomly selected and analyzed in this manner. By applying this novel method of data acquisition and analysis, experimenter bias is eliminated, yielding greater consistency and objectivity to fluorescent quantification.

4.2.9 RAW264.7 cell culture, AM1710 incubation, and Lipopolysaccharide stimulation

The mouse macrophage-like RAW 264.7 cells were obtained from American Type Culture Collection (cat# TIB-71; ATCC Manassas, VA) and cultured in Dulbecco's Modified Eagle's Medium (Sigma-Aldrich, St. Louis, MO) supplemented with 10% heat-inactivated fetal bovine serum and 100 U/ml penicillin and 100 µg/ml streptomycin (Gibco-Life Technologies, Grand Island, NY) at 37°C under humidified 5% CO2 atmosphere. Cells were seeded at 150,000 cells/mL in 24 well plates and grown overnight. The following day, cells were treated with 0 (no treatment control), 10 pg/mL, 1 ng/mL, 10 ng/mL, and 100 ng/mL AM1710 for 10 minutes without any other treatment, or 4 hours after 10 minutes exposure to the gram negative cell wall protein lipopolysaccharide (LPS) at the concentration of 500 ng/mL, (E. coli #055:B5, Sigma Aldrich, St. Louis, MO). Cells were washed with fresh media after treatments and incubated for 4 or 24 hours followed by collection of supernatants and cells for RNA (4 hours post treatment) or total cellular protein (24 hours post treatment). All treatments were conducted in quadruplicates and extracellular proteins (supernatants) or total cell lysates were used for protein as outlined below.

4.2.10 Cell culture protein quantification by ELISA

RAW 264.7 treated cell supernatants (50 µL) or 10 ug total cellular protein in quadruplicates were collected separately into tubes and flash frozen in liquid nitrogen. Tubes were then stored at -80*C until assayed for extracellular or intracellular protein quantification. ELISA procedures were performed for IL-10, and TNF-α, according to manufacturer's instructions (R&D Systems, Minneapolis, MN, USA).

4.2.11 Data analysis

Psychometric behavioral analysis was performed as previously described [221] to compute the log stiffness that would have resulted in the 50% paw withdrawal rate. Briefly, thresholds were estimated by fitting a Gaussian integral psychometric function to the observed withdrawal rates for each of the tested von Frey hairs, using a maximum-likelihood fitting method [90]. For behavioral statistical analysis to assess the presence of allodynia, a 1-way ANOVA was used at BL, and a 2-way repeated measures ANOVA was used at 3 and 10 days after CCI/sham surgery in CCI-related experiments. All other data analysis was performed using a one-way ANOVA. A p-value of <0.05 was considered statistically significant. The computer program GraphPad Prism version 4.03 (GraphPad Software Inc., San Diego, CA) was used in all statistical analyses. All data is expressed as mean +/- SEM. For post hoc analysis Bonferroni's test was performed.

4.3 Results

4.3.1 CB_1R KO Mice display similar allodynia profiles to their WT and Het littermates

The functional knockout of the CB_1R produced no overt changes in the bilateral allodynia profiles obtained with CCI. Prior to surgical manipulation, all groups exhibited similar bilateral (ipsilateral and contralateral) BL behavioral thresholds (ANOVA, $F_{(5,40)}$ =1.661; p=0.1693 ANOVA, $F_{(5,40)}$ =1.659; p=0.1697, respectively), (Figure 4.1 A,B). Following CCI, clear bilateral allodynia developed regardless of the CB_1R genetic profile by Day 3 compared to sham-operated mice (ANOVA, $F_{(17,72)}$ =9.755; p<0.0001 ANOVA, $F_{(17,72)}$ =20.09; p<0.0001, respectively). Bilateral allodynia remained reliable until Day 27 post surgical manipulation, when allodynia started to spontaneously resolve (ANOVA, $F_{(77,395)}$ =2.956; p<0.0001 ANOVA, $F_{(77,395)}$ =5.483; p<0.0001, respectively). All groups of sham-operated mice exhibited thresholds similar to baseline responses.

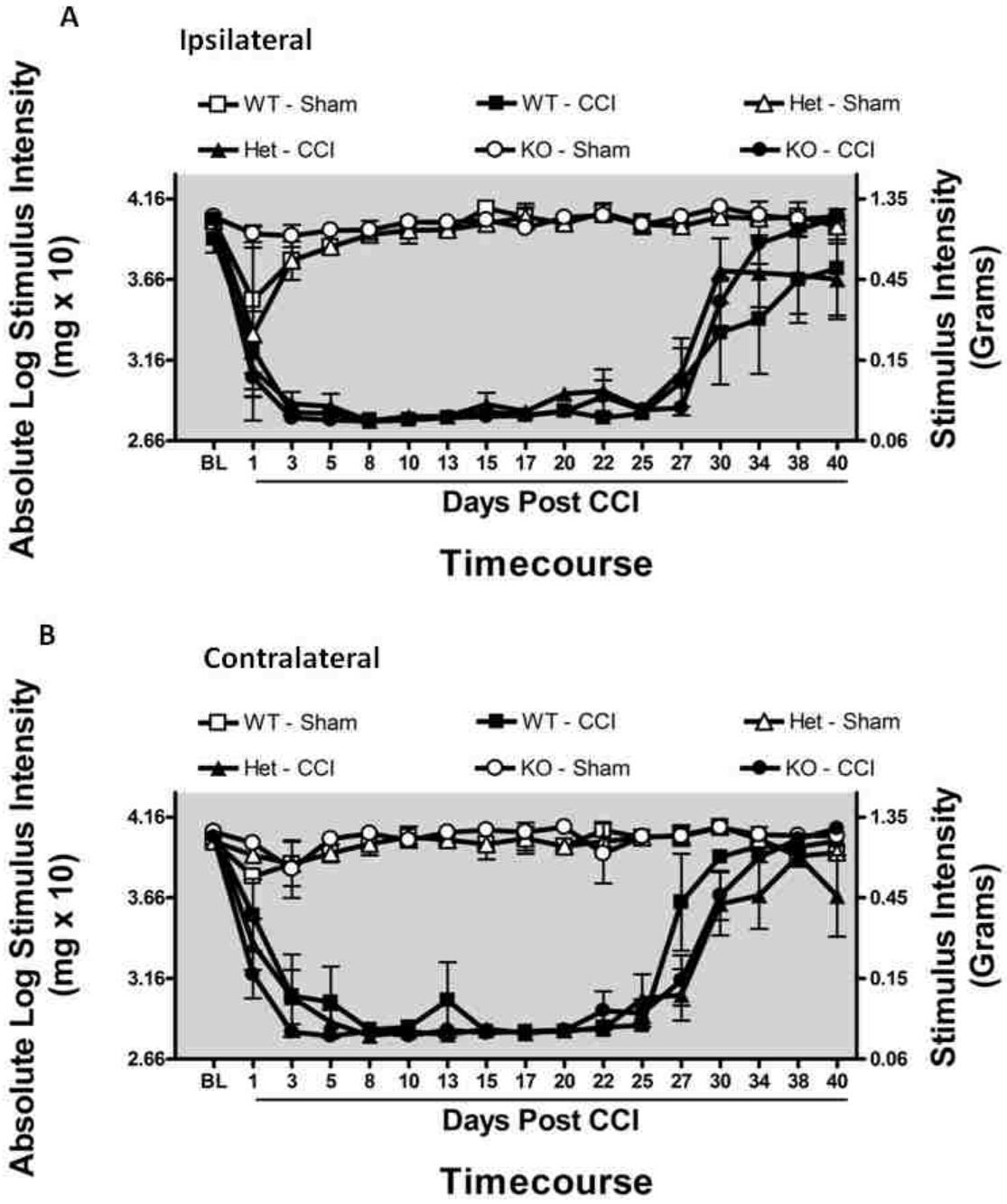

Figure 4.1 Characterization of length and severity of bilateral allodynia in CB_1R KO, Het and WT mice.

Characterization of length and severity of bilateral allodynia in CB_1R KO, Het and WT mice. **A**, **B,** Mice develop and maintain CCI-induced allodynia regardless of functional CB_1R copy number. Before surgical manipulation, all experimental groups exhibited similar ipsilateral and contralateral BL thresholds. CCI surgery produced significant bilateral allodynia at day 3 post CCI through day 27 post CCI compared to sham-treated animals.

4.3.2 Intrathecal injection of AM1710 reverses CCI-induced allodynia independently of actions due to the CB_1R and is dependent on CB_2R actions

The CB_2R cannabilactone agonist, AM1710, reversed allodynia produced by CCI. Pilot experiments determined i.t. administration of 5 µg AM1710 produced maximal behavioral pain reversal by 1.5 hours, with allodynia fully returning by 5 hours after drug administration (data not shown). Prior to surgical manipulation, all groups exhibited similar bilateral (ipsilateral and contralateral) BL behavioral thresholds (ANOVA, $F_{(8,52)}$ =1.199; p=0.3214 ANOVA, $F_{(8,52)}$ =1.172; p=0.3369, respectively), (Figure 4.2 A,B). Following CCI, clear bilateral allodynia developed by Day 5 and 12 compared to sham-operated mice (ANOVA, $F_{(15,89)}$ =137.4; p<0.0.0001 ANOVA, $F_{(15,89)}$ =207.3; p<0.0001, respectively). On Day 12, following i.t. AM1710 injection in sham-operated mice, AM1710 did not alter normal sensory threshold responses to light touch, as well as throughout the entire timecourse. However, in mice with CCI, i.t. AM1710 produced reversal from allodynia, with maximal efficacy observed at 2 hr following injection in CB_1R wildtype (WT), heterozygous (Het) or homozygous gene deleted knockout (KO) mice. Neuropathic mice lacking functional CB_1Rs and pretreated intrathecally 30 minutes in advance with the selective CB_2R antagonist AM630 failed to behaviorally reverse from allodynia when treated with i.t. AM1710, and revealed response thresholds similar to control mice with CCI (ANOVA, $F_{(3,19)}$ =0.9822; p=0.3918 ANOVA, $F_{(3,19)}$ =1.729; p=0.2029, respectively), (Figure 4.2 C,D).

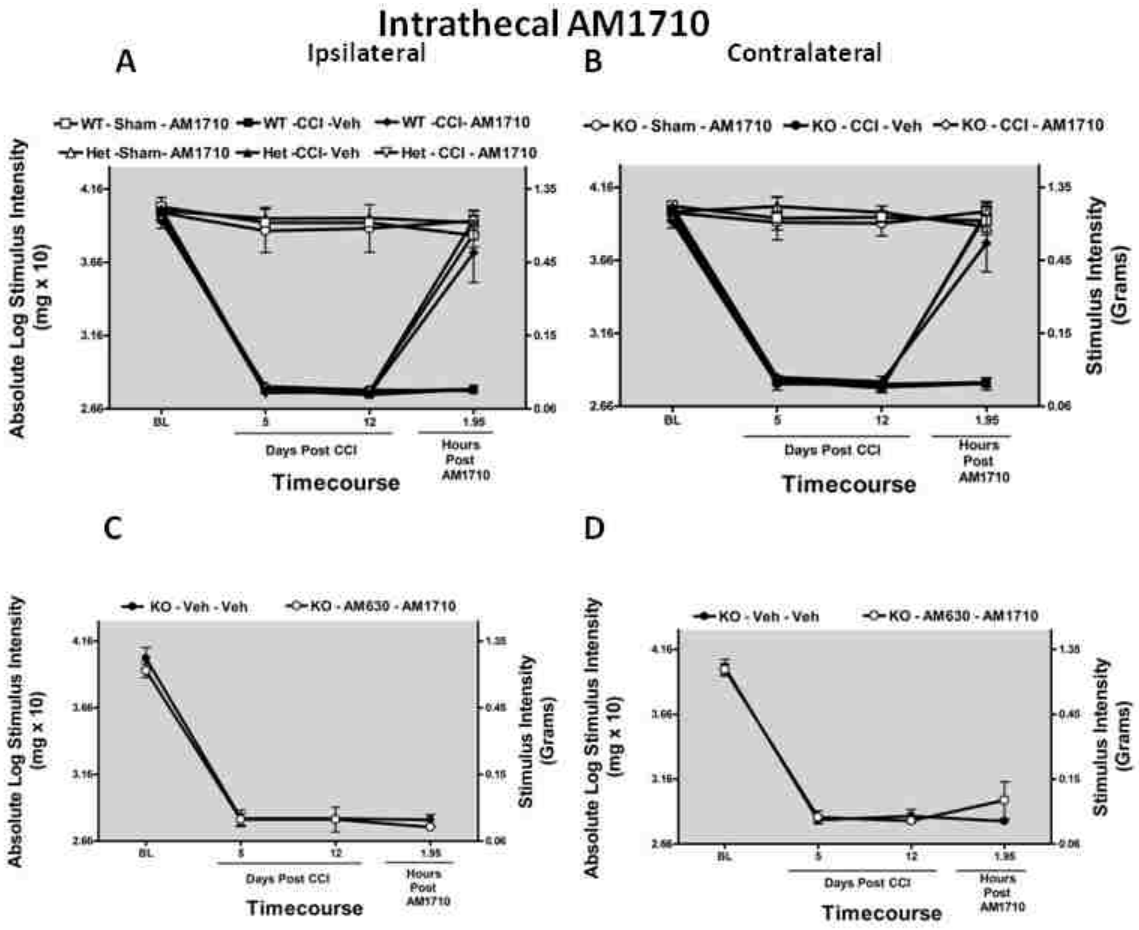

Figure 4.2 Intrathecal AM1710, a cannabinoid 2 receptor agonist reverses CCI-induced allodynia in a CB_2R dependent manner.

Intrathecal AM1710, a cannabinoid 2 receptor agonist reverses CCI-induced allodynia in a CB_2R dependent manner. **A**, **B**, AM1710 reverses CCI-induced allodynia independent of CB_1R actions. Before surgical manipulation, all experimental groups exhibited similar ipsilateral and contralateral BL thresholds and CCI surgery produced significant bilateral allodynia at days 5 and 12 following injury compared to sham-treated animals. Responses from AM1710 (5 µg) maximally reversed CCI-induced allodynia at ~2 hours after intrathecal administration. **C**, **D,** Intrathecal pre-treatment with the CB_2R selective antagonist AM630 30 minutes before i.t. administration of AM1710 blocks the anti-allodynia effects of AM1710 in CB_1R KO mice.

4.3.3 Immunohistochemical analysis of spinal cord dorsal horn and DRG cytokines from mice receiving i.t. AM1710

Bilateral IL-10 (IR) in both the ipsilateral and contralateral spinal cord dorsal horn is dramatically decreased in CCI-induced neuropathic mice compared to sham-treated mice (CB_1R WT, Het or KO), (Figure 4.3 A, Supplemental Figure A-3 A, respectively). While not significant, a trend is observed of increased IL-10 IR in

CB_1R Het or KO mice compared to CB_1R WT. However, treatment with AM1710 increased IL-10 IR bilaterally, with levels similar to those found in non-neuropathic controls (ANOVA, $F_{(8,26)}$ =16.55; $p<0.0001$ ANOVA, $F_{(8,26)}$ =5.756; $p=0.0010$, respectively). Fluorescent images of ipsilateral dorsal horn spinal cord from wild type mice with either sham treatment with i.t. AM1710 (Figure 4.3 B), CCI treatment with i.t. vehicle (Figure 4.3 C), or with AM1710 (Figure 4.3 D) corresponding to the quantitative image analysis data are presented.

Similarly, bilateral IL-10 IR in corresponding ipsilateral and contralateral DRG is dramatically decreased bilaterally in CCI-induced neuropathic mice (CB_1R WT, Het, or KO) compared to sham-treated mice (CB_1R WT, Het or KO), (Figure 4.3 E, Supplemental Figure A-3 B, respectively). Interestingly, a similar DRG trend, as seen in the dorsal horn of the spinal cord, was additionally observed with regard to IL-10 IR increases in neuropathic CB_1R Het and KO, in comparision to CB_1R WT mice. However, treatment with AM1710 significantly increased IL-10 IR bilaterally, to control levels of non-neuropathic mice (ANOVA, $F_{(8,26)}$ =15.59; $p<0.0001$ ANOVA, $F_{(8,26)}$ =6.605; $p=0.0004$, respectively).

For IL-1β IR analysis, compared to non-neuropathic sham-operated mice (CB_1R WT Het KO) given i.t. AM1710, CCI-induced a robust bilateral increase in IL-1β IR within the dorsal horn of the spinal cord in control injected animals (Figure 4.3 F, Supplemental Figure A-3 C, respectively). Conversely, i.t. administration of AM1710 completely suppressed increased dorsal horn IL-1β IR within 2 hours of administration of the drug (ANOVA, $F_{(8,26)}$ =22.94; $p<0.0001$ ANOVA, $F_{(8,26)}$

=21.56; p<0.0001, respectively). Representative fluorescent images are of sham-treated mice with i.t. AM1710 (Figure 4.3 G), CCI-treated rats with i.t. vehicle (Figure 4.3 H), or CCI treated-rats with AM1710 injection (Figure 4.3 I) that correspond to data examined by microscopy analysis.

In corresponding DRG, bilateral IL-1β immunoreactivity (IR) is additionally increased in CCI-induced neuropathic mice compared to sham-treated mice (Figure 4.3 J, Supplemental Figure A-3 D, respectively). However, 2 hours after treatment with AM1710 suppressed IR increases in IL-1β were observed (ANOVA, $F_{(8,26)}$ =14.40; p<0.0001 ANOVA, $F_{(8,26)}$ =16.17; p<0.0001, respectively).

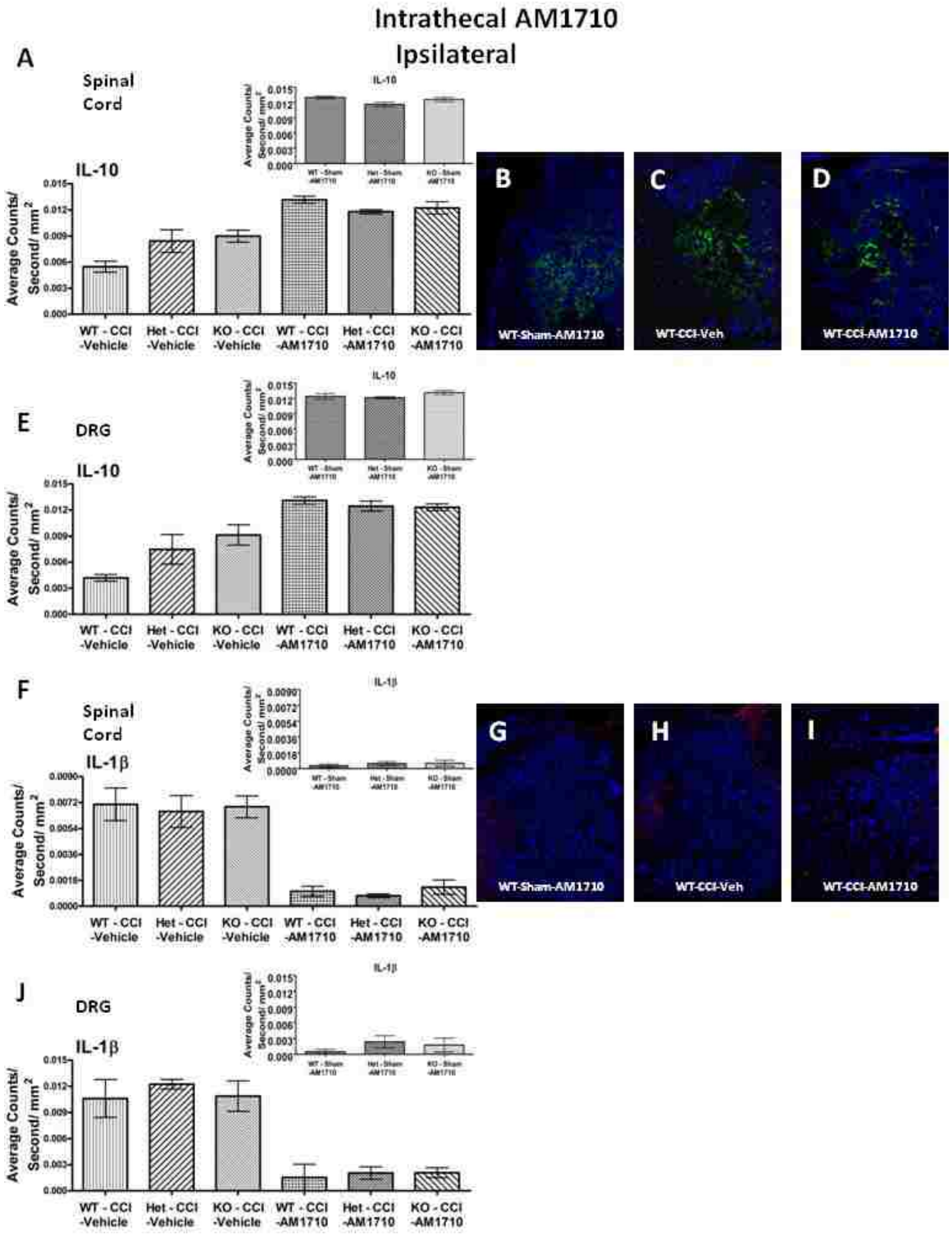

Figure 4.3 Ipsilateral immunofluorescent intensity quantification cytokines

Ipsilateral immunofluorescent intensity quantification from 7 µm thick sections of dorsal horn spinal cord and corresponding DRG from behaviorally verified CB_1R KO, Het, WT mice, following i.t. vehicle or AM1710. **A,** IL-10 expression in dorsal horn spinal cord was decreased in CCI-treated mice that received i.t. vehicle compared to control sham-treated mice given AM1710,

while IL-10 IR recovered to sham levels in CCI neuropathic mice given i.t. AM1710. **B**, **C**, **D**, Representative spectrally unmixed images at 20x magnification of IL-10 fluorescent labeling (green) with DAPI nuclear stain (blue) in dorsal horn spinal cord. In all images the scale bar is equal to 50 µm. **E,** IL-10 expression in DRG was decreased in CCI-treated mice that received i.t. vehicle compared to control sham-treated mice given AM1710, while IL-10 IR recovered to sham levels in CCI neuropathic mice given i.t. AM1710. **F**, Compared to sham controls, IL-1β expression was increased in the dorsal horn spinal cord of CCI-treated animals given i.t. vehicle of AM1710. However, i.t. AM1710 in CCI-treated mice robustly suppressed increases in IL-1β IR. **G**, **H**, **I**, Representative spectrally unmixed images at 20x magnification of IL-1β fluorescent labeling (red) with DAPI nuclear stain (blue) in dorsal horn spinal cord. **J**, Compared to sham controls, IL-1β expression was increased in the DRG of CCI-treated animals given i.t. vehicle of AM1710. However, i.t. AM1710 in CCI-treated mice robustly suppressed increases in IL-1β IR.

4.3.4 Intraperitoneal injection of AM1710 reverses CCI-induced allodynia in CB_1R knockout mice

In pilot studies we examined an AM1710 i.p. dose of 25 mg/kg/ ml based on prior reports [176]. This dose of AM1710 was sufficient in reversing bilateral allodynia with maximal reversal occurring at 0.5 hours that continued to 1 hour after administration, with the anti-allodynic effects gone by 2 hours (data not shown). Prior to surgical manipulation, all groups exhibited similar bilateral (ipsilateral and contralateral) BL behavioral thresholds (ANOVA, $F_{(8,52)}$ =2.085; p=0.0574 ANOVA, $F_{(8,52)}$ =1.341; p=0.2486, respectively), (Figure 4.4 A,B). Clear bilateral allodynia developed by Day 5 through 12 in all CCI treated mice compared to sham-operated mice (ANOVA, $F_{(15,89)}$ =182.4; p<0.0001 ANOVA, $F_{(15,89)}$ =143.5; p<0.0001, respectively). On Day 12, following i.p. AM1710 injection in sham-operated mice, AM1710 did not alter normal sensory threshold responses to light touch. However, in mice with CCI, i.p. AM1710 produced reversal from allodynia, regardless of the CB_1R copy number.

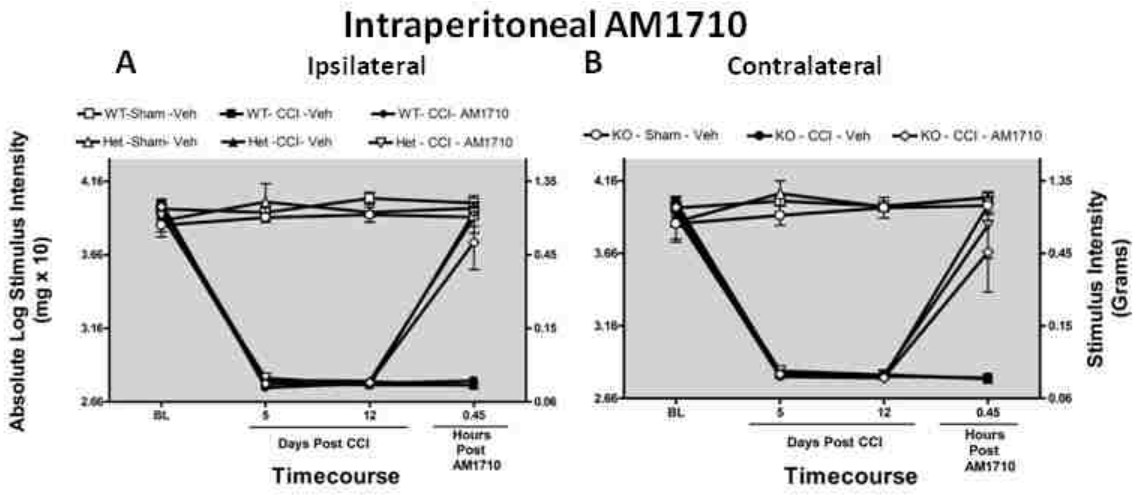

Figure 4.4 Intraperitoneal AM1710, a cannabinoid 2 receptor agonist reverses CCI-induced allodynia in a CB_1R independent manner.

Intraperitoneal AM1710, a cannabinoid 2 receptor agonist reverses CCI-induced allodynia in a CB_1R independent manner. **A**, **B**, AM1710 reverses CCI-induced allodynia independent of CB_1R actions. Before surgical manipulation, all experimental groups exhibited similar ipsilateral and contralateral BL thresholds and CCI surgery produced significant bilateral allodynia at days 5 and 12 following injury compared to sham-treated animals. Responses from AM1710 (25 mg/kg/ml) maximally reversed CCI-induced allodynia at ~ 30 minutes after intraperitoneal administration.

4.3.5 Immunohistochemical analysis of spinal cord dorsal horn and DRG IL-10, IL-1β and microglial Iba-1

Bilateral IL-10 IR in the spinal cord dorsal horn is dramatically decreased in CCI-induced neuropathic mice compared to sham-treated mice (ANOVA, $F_{(8,26)}$ =6.211; p=0.0006 ANOVA, $F_{(8,26)}$ =6.810; p=0.0004, respectively), (Figure 4.5 A,Supplemental Figure A-4 A, respectively). Surprisingly, treatment with i.p. AM1710 did not alter spinal IL-10 IR. As observed previously, a trend for increased spinal IL-10 in CCI-treated Het and KO mice when compared to WT mice persisted in this data set.

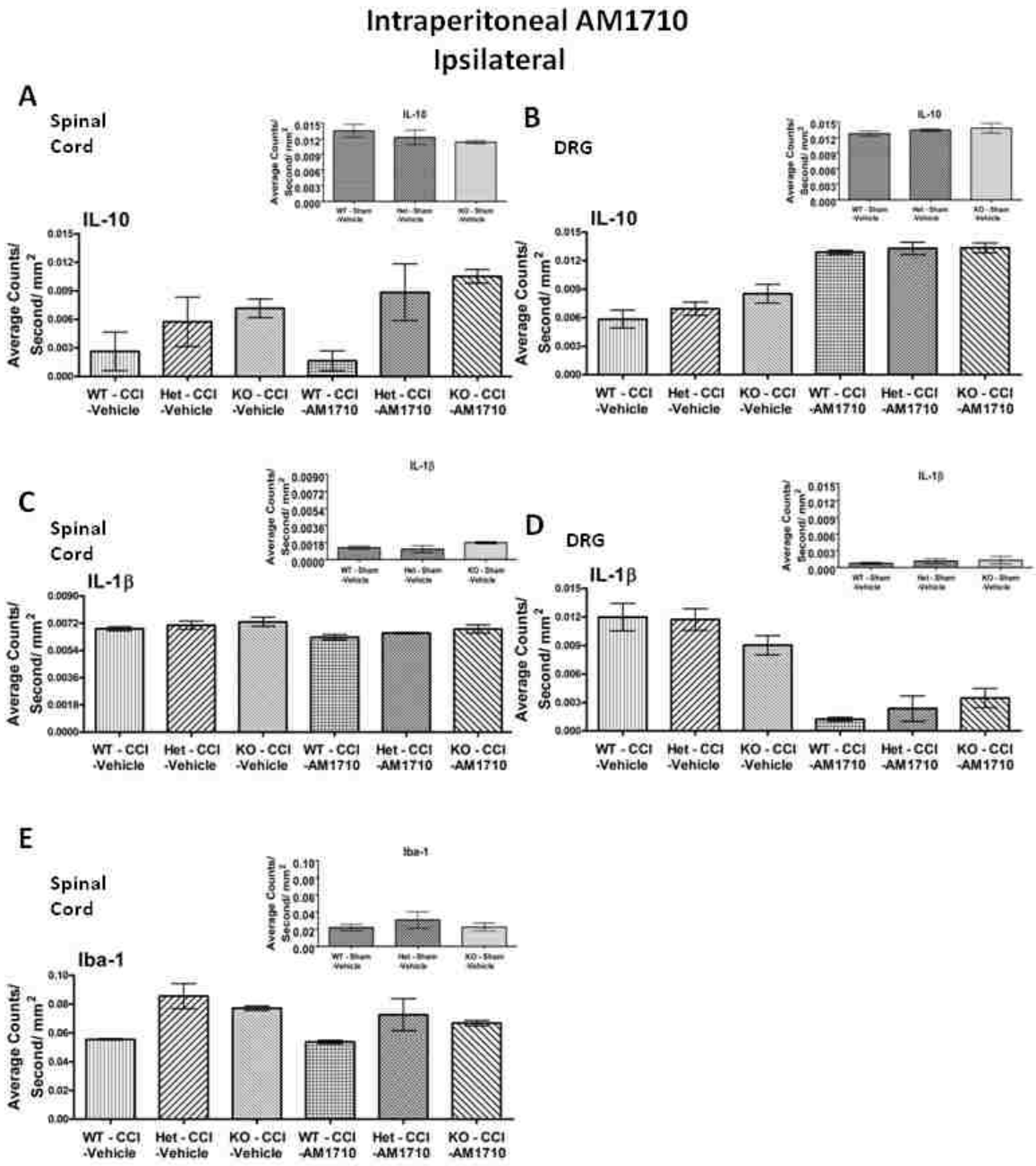

Figure 4.5 Ipsilateral immunofluorescent intensity quantification

Ipsilateral immunofluorescent intensity quantification from 7 µm thick sections of dorsal horn spinal cord and corresponding DRG from behaviorally verified CB_1R KO, Het, WT mice, following i.p. vehicle or AM1710. **A,** IL-10 expression in dorsal horn spinal cord was decreased in CCI-treated mice that received i.p. vehicle compared to control sham-treated mice given AM1710, and IL-10 IR remained unchanged at neuropathic levels in CCI neuropathic mice given i.p. AM1710. **B,** IL-10 expression in DRG was decreased in CCI-treated mice that received i.p. vehicle compared to control sham-treated mice given AM1710, while IL-10 IR recovered to sham levels in CCI neuropathic mice given i.p. AM1710. **C**, Compared to sham controls, IL-1β expression was increased in the dorsal horn spinal cord of CCI-treated animals given i.p. vehicle of AM1710. Intraperitoneal AM1710 in CCI-treated mice did not alter increases in IL-1β IR. **D**, Compared to sham controls, IL-1β expression was increased in the DRG of CCI-treated animals given i.p.

vehicle of AM1710. However, i.p. AM1710 in CCI-treated mice robustly suppressed increases in IL-1β IR. **E,** Iba-1 IR expression increased within the ipsilateral dorsal horn of the spinal cord following CCI manipulations compared to control sham treatment, irrespective of i.p. vehicle or AM1710.

While bilateral IL-10 IR in corresponding DRG is diminished in CCI-induced neuropathic mice (WT, Het, KO) compared to sham-treated mice (Figure 4.5 B, Supplemental Figure A-4 B, respectively), treatment with i.p. AM1710 raised IL-10 IR bilaterally. These levels were similar to those found in non-neuropathic sham mice (ANOVA, $F_{(8,26)}$ =20.80; p<0.0001 ANOVA, $F_{(8,26)}$ =11.31; p<0.0001, respectively).

IL-1β IR analysis, compared to non-neuropathic sham-operated mice given i.p. vehicle, revealed that CCI-induced neuropathy produced a bilateral increase in IL-1β IR within the dorsal horn spinal cord in i.p. vehicle injected animals (ANOVA, $F_{(8,26)}$ =145.2; p<0.0001 ANOVA, $F_{(8,26)}$ =172.3; p<0.0001, respectively) (Figure 4.5 C, Supplemental Figure A-3 C, respectively). Surpisingly, i.p. administration of AM1710 did not alter dorsal horn IL-1β IR in mice (CB_1R WT, Het, KO) reversed from allodynia.

Supporting the previous data, bilateral IL-1β immunoreactivity (IR) in corresponding DRG is again increased in CCI-induced neuropathic mice (CB_1R WT, Het, KO) compared to sham-treated mice (Figure 4.5 M, Supplemental Figure A-4 D, respectively). Treatment with i.p. AM1710 suppress IL-1β IR with bilateral effects resulting in levels comparible to non-neuropathic controls (ANOVA, $F_{(8,26)}$ =25.30; p<0.0001 ANOVA, $F_{(8,26)}$ =11.08; p<0.0001, respectively). Non-neuropathic sham-operated animals (CB_1R WT, Het and KO

mice) given i.p. vehicle exhibited similar Iba-1 IR levels. Iba-1 is a marker for altered microglial activity, and increased dorsal horn Iba-1 IR in CCI-treated mice during AM1710-induced reversal from allodynia remained unchanged compared to CCI-treated treated mice with ongoing allodynia (ANOVA, $F_{(8,26)}$ =15.37; p<0.0001 ANOVA, $F_{(8,26)}$ =8.777; p=0.0001, respectively), (Figure 4.5 E, Supplemental Figure A-4 E, respectively). Similarly, while non-neuropathic sham-operated animals given i.p. vehicle exhibited similar GFAP IR levels, a marker for altered astrocyte activity, AM1710 did not modify the observed increased dorsal horn GFAP IR in CCI-treated mice during AM1710-induced reversal from allodynia compared to CCI-treated treated mice with ongoing allodynia (data not shown).

4.3.6 Immunohistochemical analysis of MCP-1 in DRG and dorsal horn spinal cord

Bilateral MCP-1 IR in corresponding DRG is dramatically increased in CCI-induced neuropathic mice (WT, Het, KO) compared to sham-treated mice receiving i.p. vehicle (Figure 4.6 A, Supplemental Figure A-5 A, respectively). However, treatment with i.p. AM1710 significantly decreased MCP-1 IR bilaterally, with levels similar to non-neuropathic controls (ANOVA, $F_{(8,26)}$ =13.39; p<0.0001 ANOVA, $F_{(8,26)}$ =7.566; p=0.0006, respectively). Peripheral administration of AM1710 (i.p.) leads to profound suppression of vehicle-treated MCP-1 in the DRG, with a modest reduction in MCP-1 in the spinal cord. Like peripheral administration, i.t. AM1710 results in dramatically reduced MCP-1 IR in DRG. However, unlike i.p. administration of AM1710, i.t. injection substantially

suppresses MCP-1 IR in the spinal cord of neuropathic rats. In DRG, bilateral MCP-1 IR is dramatically increased in CCI-induced neuropathic mice (WT, Het, KO) receiving i.t. vehicle compared to sham-treated mice (WT, Het, KO) with i.t. AM1710 (Figure 4.6 B, Supplemental Figure A-5 B, respectively). Treatment with AM1710 reduced MCP-1 IR bilaterally (ANOVA, $F_{(8,26)}$ =4.677; p=0.0032 ANOVA, $F_{(8,26)}$ =8.242; p=0.0001, respectively).

CCI-induced neuropathy, in all mice (WT, Het, KO), produced a robust bilateral increase in MCP-1 IR within the spinal cord dorsal horn when compared to sham control mice (WT, Het, KO), (Figure 4.6 C, Supplemental Figure A-5 C, respectively). Unlike the unremarkable actions of i.p. AM1710 on dorsal horn spinal cord levels of either IL-10 or IL-1β IR, i.p. administration of AM1710 decreased dorsal horn MCP-1 IR within 30 minutes. (ANOVA, $F_{(8,26)}$ =27.94; p<0.0001 ANOVA, $F_{(8,26)}$ =21.29; p<0.0001, respectively). A similar overall effect on MCP-1 IR was observed with i.t. AM1710. Compared to non-neuropathic sham-operated mice (WT, Het, KO) given i.t. AM1710, CCI-induced neuropathy produced reliable bilateral increases in MCP-1 IR within the dorsal horn, independently of genetic copy number of CB_1R (Figure 4.6 D, Supplemental Figure A-5 D, respectively). Meanwhile, i.t. administration of AM1710 completely suppressed increased dorsal horn MCP-1 IR (ANOVA, $F_{(8,26)}$ =11.46; p<0.0001 ANOVA, $F_{(8,26)}$ =7.243; p=0.0003, respectively).

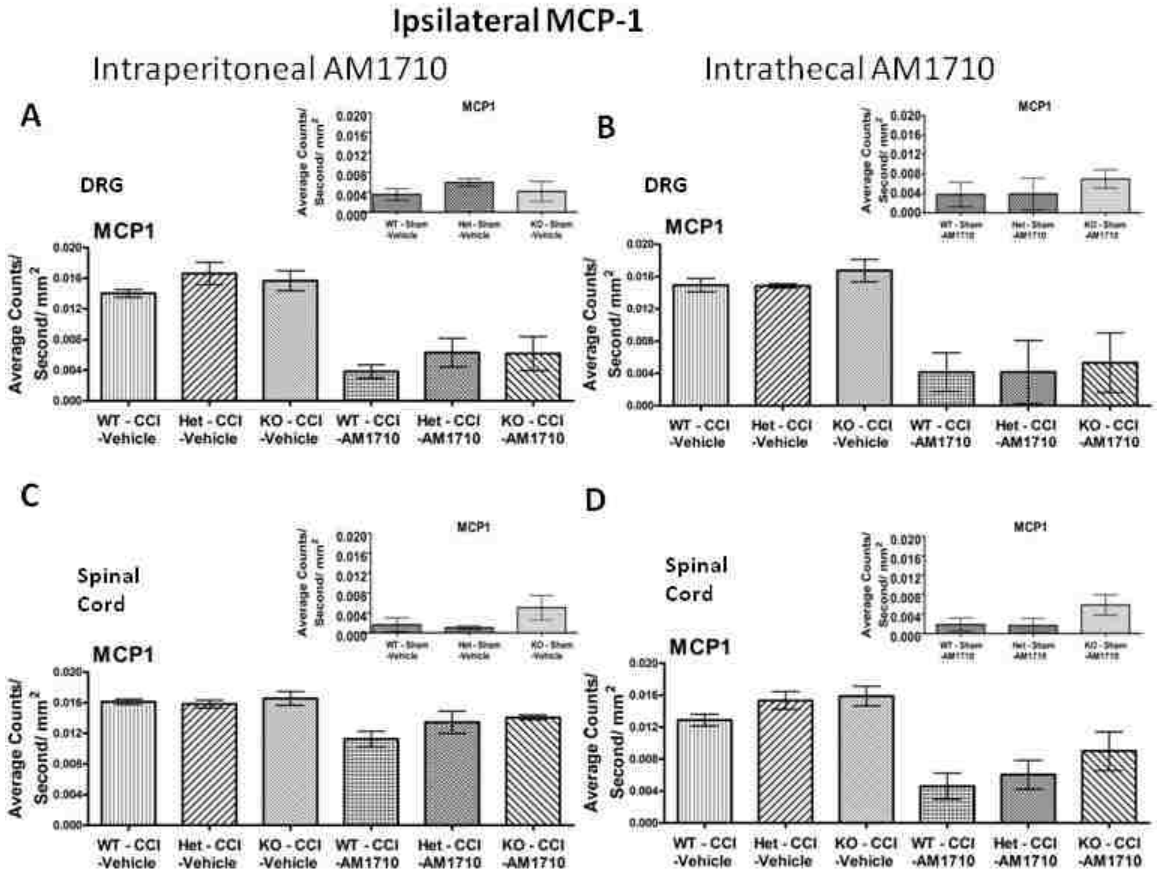

Figure 4.6 Ipsilateral immunofluorescent intensity quantification MCP1

Ipsilateral immunofluorescent intensity quantification of DRG and spinal cord dorsal horn reveals both i.p. and i.t. AM1710 administration reduces the expression of the chemokine MCP-1. **A**, **B**, Compared to control mice, DRG MCP-1 IR expression was increased in CCI-treated neuropathic mice that received either i.p. or i.t vehicle of AM1710, while DRG MCP-1 IR in CCI-treated mice given either i.p. or i.t. AM1710 was substantially reduced. All sections were 7 µm in thickness. **C**, **D**, Compared to control mice, dorsal horn spinal cord MCP-1 IR expression was increased in CCI-treated neuropathic mice that received either i.p. or i.t vehicle of AM1710, while dorsal horn spinal cord MCP-1 IR in CCI-treated mice given either i.p. or i.t. AM1710 was substantially reduced. All sections were 7 µm in thickness.

4.3.7 AM1710 abolishes Lipopolysaccharide effects in RAW264.7 Cells

Macrophage like RAW264.7 cells were were stimulated with 500 ng of the gram negative bacteria cell wall protein lipopolysaccharide (LPS) for 10 minutes, and then treated with either 10 ng AM1710, 100 ng AM1710 or equivolume vehicle for 10 minutes, 30 minutes or 1 hour. Compared to the no treatment controls, LPS stimulation produced a robust increase of both IL-10 and TNF-α protein in cell

supernatants (ANOVA, $F_{(7,31)}$ =95.89; p<0.0001 ANOVA, $F_{(7,31)}$ =654.3; p<0.0001, respectively), (Figure 4.7 A, B, respectively). At both doses, and all sampled timepoints, AM1710 was able to abolish LPS stimulated protein production, back to basal levels.

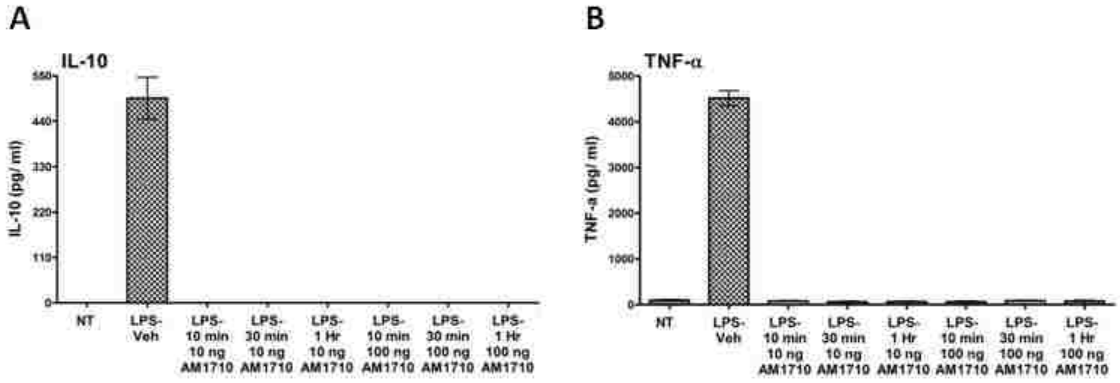

Figure 4.7 Alone AM1710 abolishes Lipopolysaccharide effects in RAW264.7 cells.

Alone AM1710 abolishes Lipopolysaccharide effects in RAW264.7 cells. **A, B,** LPS stimulation of RAW264.7 cells produced robust increases in both IL-10 and TNF-α protein, and AM1710 treatment dramatically diminished both proteins back to basal levels.

4.4 Discussion

Together these data support an anti-inflammatory mechanism of AM1710 that is selective for the CB_2R, and is not reliant on actions of CB_1R. AM1710 in a cell culture model of macrophage stimulation dramatically modulated both the pro- and anti-inflammatory cytokines TNF-α and IL-10 to unstimulated basal levels. Peripheral or peri-spinal (i.t.) administration of AM1710 markedly reduced elevated MCP-1 IR, in both spinal cord and DRG. Interestingly, although i.p. AM1710 produced robust behavioral reversal of allodynia within 30 minutes of administration, yet changes in IL-1β and IL-10 IR were only observed in the DRG, not spinal cord. In all groups of mice peri-spinal delivered AM1710

produced changes in both spinal cord as well as DRG, with corresponding relief from allodynia in IL-10, IL-1β, as well as MCP-1. The CB_1R reduced copy number did not alter MCP-1 or IL-1β IR. We characterized the length and severity of CCI-induced neuropathy in CB_1R KO, Het, and WT mice on a CD1 genetic background. Clear bilateral allodynia persisted for approximately 30 days regardless of CB_1R genetic deletion. These data are the first demonstration evaluating the severity and duration of allodynia due to CCI in CB_1R knockout and heterozygous mice. However, several models of neuropathic pain have been used to examine the role of CB_1R in other pain models, as discussed below.

4.4.1 The role of CB_1R in neuropathic pain

The finding of a behavioral lack of effect on chronic pain symptoms with respect to the CB_1R copy number in CB_1R KO mice may be specific to allodynia. The observation that CB_1R knockout mice display similar severity and duration of allodynia compared to their heterozygous and wild type litermates was not expected based on prior evidence [309-311]. Previous reports detail pharmacological blockade of CB_1R with the selective CB_1R antagonist Rhimanobant/SR141716/AM251 has an effect on reversing allodynia. In rats given oral doses of AM251, the compound reversed CCI-induced allodynia [310]. In separate studies, AM251 attenuated mechanical allodynia in diabetic mice [309]. Additionally, acute i.t. delivery of AM251, in a dose-dependent manner, reversed formalin induced pain [311]. Allodynia vs. other measures of sensory responses like hyperalgesia, may be less sensitive to the genetic deletion of CB_1R. CCI-treated CB_1R KO and WT mice both developed the same levels of

thermal hyperalgesia [310]. KO mice with sciatic nerve ligation (SNL) developed unilateral allodynia that was comparable to WT littermates, and allodynic behavior between groups was nearly identical through the measured timecourse [312]. These data suggest that under WT conditions antagonism of CB_1R is conducive for anti-allodynia. However, in CB_1R KO mice, there must be compensatory mechanisms that allow for allodynia to be produced to levels corresponding to WT mice.

4.4.2 Specificity of AM1710's behavioral and cytokine effects

To verify the spinal CB_2R actions of AM1710 following pain reversal, we examined the effects of i.t. AM1710 in mice with a CB_1R genetic deletion, compared to heterozygous and wildtype littermates. Furthermore, pre-treatment with AM630, a selective CB_2R antagonist, in CB_1R KO mice with CCI, blocked the effects of AM1710. This provides further *in vivo* evidence that AM1710 acts on CB_2R to suppress allodynia. In support of work in rats [300], intrathecal AM1710 reset both spinal and DRG levels of IL-10 and IL-1β IR to basal levels in neuropathic mice in the presence of behavioral reversal, independent of CB_1R.

To verify the peripheral CB_2R actions of AM1710 to produce anti-allodynia we examined AM1710 given i.p. in CB_1R knockout mice. Again, we compared the behavioral outcomes to CB_1R heterozygous and wild type mice with CCI, and found that the activation of the CB1R is not necessary for the anti-allodynia effects of AM1710. Further, peripheral AM1710 produced changes in only DRG IL-10 and IL-1β at an early 30 minute timepoint. These data support prior findings

that detail that AM1710 does not effectively cross the blood brain barrier, and effects of i.p. AM1710 are fast acting (<30 min after administration) [176]. Peripheral AM1710 may act at either nociceptive terminals and/or nociceptors neuronal cell bodies within the DRG. These data additionally support that CB_2R may be found on peripheral nerve terminals, especially under neuropathic conditions [313]. Although not significantly different, the CB_1R KO displayed the least amount of reversal. In support of peripherally restricted actions of i.p. AM1710, we show robust effects at the level of the DRG on both IL-10 and IL-1β IR. Additionally, reduced IL-10 and increased IL-1β IR as well as glial GFAP and IBA-1 IR, persisted in the spinal cord concurrent with acute relief from allodynia, which suggests that spinal mechanisms do not necessarily drive acute neuropathic pain. No change in spinal IL-1β and IL-10 following i.p. AM1710 suggest that the spinal changes of cytokine expression requires additional time to catch up following DRG alterations. These short term effects, with allodynia returning by 2 hours after i.p. administration, could be due to clearance of AM1710 from peripheral circulation to unmodified IL-10 levels in the spinal cord.

4.4.3 Separation of spinal and DRG mechanisms in neuropathic pain

Very few publications have looked at dorsal horn spinal cord changes with a peripheral injection, or DRG changes with an intrathecal injection [300, 301]. Here, the reported anatomically distinct protein profiles have not been widely examined. Both spinal cord and DRG IR are altered with an i.t. injection. However, following i.p. injection only, DRG at a 30 minute timepoint, reveal IL-10 and IL-1β IR changes that correspond to allodynia reversal. It may be under

these conditions that an existing and dynamic neuron to glial component is important in mediating acute actions.

4.4.4 Role of MCP-1 in neuropathic pain

The chemokine MCP-1 is known to be released by neurons in the dorsal horn of the spinal cord, is bound by its receptor, CCR2, found on immune cells (macrophage and microglia), and resulting CCR2 signaling cascades are characterized to attract monocyte-derived cells to areas of tissue injury and insult. MCP-1 regulation is highly dynamic, and is well characterized to be upregulated in spinal and DRG neuronal cell bodies in numerous animal models of neuropathic pain [49, 78, 79, 294, 295, 314-318] as well as in spinal astrocytes [33]. These data support prior reports demonstrating increased MCP-1 expression in both spinal cord superficial nociceptive neurons as well as interneurons, astrocytes and DRG nociceptive neuronal cell bodies with CCI-induced neuropathy [33, 49, 318-322]. However, we have extended the findings of these prior reports and show dynamic regulation of MCP-1 with either i.p. or i.t. administration of the anti-inflammatory CB_2R agonist AM1710. I.t. AM1710 led to a significant decrease of MCP-1 in both the spinal cord and DRG. I.p. AM1710 led to decreases in not only DRG MCP-1 IR, but also in dorsal horn spinal cord MCP-1 IR. This early alteration of spinal MCP-1 after peripheral administration of AM1710 suggests that it may be the driving factor regulating neuropathic pain.

Indeed, under pathological conditions it has been found that the actions of CCR2, due to MCP-1 binding on either resident spinal microglia or infiltrating bone

marrow microglia is sufficent for the development of neuropathic pain behaviors after peripheral nerve ligation [318]. Pharmacological suppression of MCP-1 under neuropathic conditions blocks the development of pain [323]. Additionally, overexpression of MCP-1 was capable of producing allodynia in otherwise naïve animals [324]. It has been shown that release of MCP-1 leads directly to the upregulation of IL-1β [323]. One critical factor in controlling neuropathic pain may be increased MCP-1 actions Importantly, CB_2R agonists may participate in regulating MCP-1 mediated pain.

4.4.5 Constitutive CB_1R modulation of inflammatory factors

The endocannabinoid system is emerging as a critical mediator of inflammation and pain signaling. Activation of the CB_1R can produce pain relief in animal models of pain, which may have inflammatory components, and as such blocking the actions of the CB_1R to mediate pain may seem counter-intuitive. However, anti-inflammatory actions are well known to facilitate eduring pain relief, and blocking CB_1R may prove to enhance anti-inflammation. Here, under inflammatory neuropathic conditions, the functional deletion of CB_1R produces increases of the anti-inflammatory cytokine IL-10 over wild-type in both spinal cord and DRG tissue, in the presence of stable allodynia.

Evidence exists that antagonism of CB_1R, or reducing the effects of constitutive CB_1R, may be beneficial in lowering pro-inflammatory factors. Chronic oral administration of AM251 reduces CCI-induced increases in prostaglandin in blood, nitric oxide in sciatic nerve, and spinal TNF-α to basal levels [310]. In

another study, chronic oral treatment with AM251 lowered the amount of spinal TNF-α in streptozotocin-induced diabetes [325]. Several reports show decreased TNF-α and IL-1β following LPS administration in rats when rats were treated with AM251 [326, 327].

We propose an endocannabinoid mediated form of neuroprotection. Normal, constitutive actions of CB_1R on nerve terminals under neuropathic pain/inflammatory conditions may serve to be neuroprotective [261, 284, 299, 328]. However, with this vital component of the endocannabinoid system removed, as in CB_1R knockout mice, neurons no longer have the same supported protection. Microglia may compensate, thereby becoming activated upon insult, as presented in the spectral analysis data of Iba-1 IR. This increased activation did not increase pro-inflammatory IL-1β IR, but increased IR of the neuroprotective cytokine, IL-10 [227]. Although speculative, the current findings may be due to higher endocannabinoid ligand binding to the CB_2R expressed on microglia.

An inverse role for CB_1R and IL-10 expression can be made from prior literature where studies pharmacologically block the CB_1R. Adipocites from obese Zucker rats treated for 3 weeks with AM251 had lower TNF-α and correspondingly higher IL-10 levels [329]. Additionally, AM251, when given peripherally or spinally in mice, lowered circulating pro-inflammatory cytokines with increased IL-10 [330, 331]. Given this evidence, there may be additional therapeutic, anti-inflammatory

synergism with the administration of CB_1R antagonists coupled with CB_2R agonists [332].

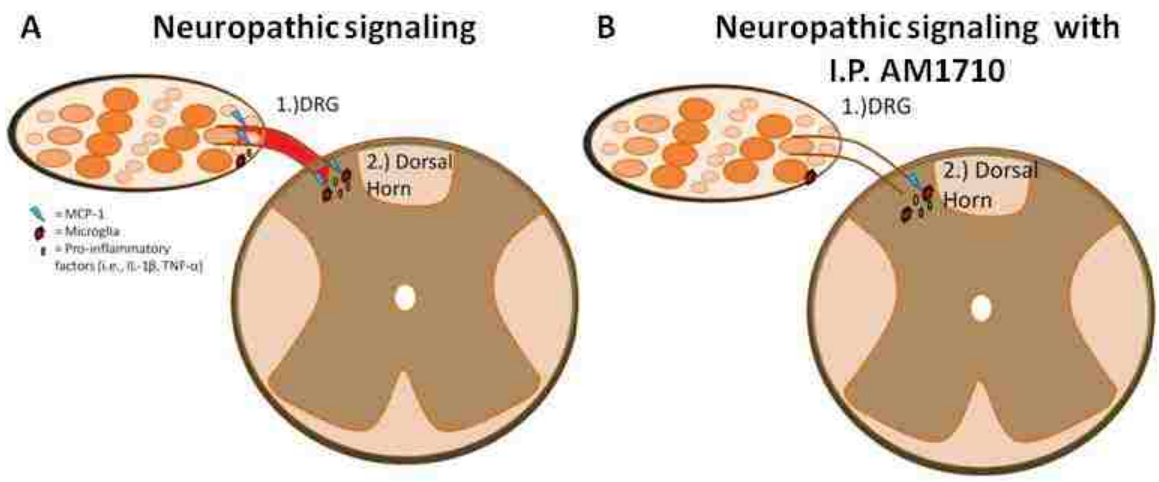

Figure 4.8 Diagram of proposed DRG and dorsal horn spinal cord interplay in the regulation and maintenance of neuropathic pain.

Diagram of proposed DRG and dorsal horn spinal cord interplay in the regulation and maintenance of neuropathic pain. **A,** Under neuropathic conditions increases in both spinal and DRG MCP-1 (blue lightening bolt) from neurons leads to glial activation (red many sided polygon), and upregulation of pro-inflammatory factors (yellow oval), such as the pro-inflammatory cytokines IL-1β and TNF-α. Further, this cycle is continued by steady aberrant pain signaling from the DRG into the dorsal horn spinal cord (red trace from DRG to spinal cord). **B,** During acute peripheral pain relief, such as with i.p. AM1710, decreased DRG pro-inflammatory factors and MCP-1 are observed, leading to abolished pain signaling to the dorsal horn spinal cord. This in turn lowers neuronal production of spinal MCP-1. However, due to the acute mechanisms at play, lower spinal MCP-1 does not immediately translate to diminished glial pro-inflammatory signaling. This allows for aberrant chronic pain signaling to be rapidly re-instated once peripheral drug effects start to wear away.

4.4.6 Spinal CB_2R agonists as attractive therapeutics

Both i.p. and i.t. AM1710 administration is effective in reversing CCI-induced neuropathy independent of CB_1R actions. However, i.p. injection produced a more transient reversal from allodynia than spinal injection, and supports that spinal administration of CB_2R agonists may be more efficacious in long term pain control. This may be due to opponent systems at play with an i.p. injection that an i.t. injection does not encounter. I.p. injection of AM1710 is able to produce acute pain relief, but does not cross the blood brain barrier, and therefore, must be circulated through the periphery to ultimately reach sites of action, such as

peripheral nerve terminals, and does not produce spinal protein changes in either IL-10 or IL-1β.

Importantly, it has been shown that under pathological pain there is increased MCP-1 expression in neuronal cell bodies within the DRG, which correspond to abbarent pain singaling into the superficial laminae within the dorsal horn spinal cord. This elevated DRG MCP-1 is typically observed with elevated levels of DRG IL-1β, and influx of monocytes into the DRG. The primary nerve afferents located within the spinal cord dorsal horn superficial lamina pre-synaptically release MCP-1 upon repeated and sustained abberent pain signaling input from the DRG. Astrocytes additionally release MCP-1 under pathological conditions [33]. As in the DRG, this elevated MCP-1 is typically observed with elevated levels of spinal IL-1β and activated microglia (Figure 4.8, A). These spinal proteins have been shown to be critical in the mediation of enduring chronic pain relief. However, in the absence of alterations of either cytokine in the spinal cord, we show that IR levels of both proteins are reset to basal levels in DRG, and a reduction in both spinal and DRG MCP-1 IR. Further these restricted changes were sufficient to produce acute (approximately 1 hour) allodynia reversal. Acute pain relief may require glial alterations leading to changes in pain processing at either the spinal cord, or the DRG. Although actions in the DRG may produce initial pain reversal, it is not sufficient to diminish ongoing chronic glial inflammatory events within the spinal cord, and thus ultimately spinally driven pain signaling is unmasked and pathological pain signaling is re-established (Figure 4.8, B). Therefore, targeting the spinal cord may be necessary to produce

long term relief from chronic pain. AM1710, as well as other CB_2R selective compounds, has the ability to produce a robust anti-inflammatory effect and holds promise for the treatment of neuropathic pain.

5. Discussion

5.1 The endocannabinoid system in chronic pain

The bioavailability of endocannabinoids such as anandamide and 2-AG in neurons and microglia [8, 92] are primarily controlled through enzymatic metabolism by FAAH and MAGL [140, 142, 234]. Increased endocannabinoid expression and activity in regions such as the spinal cord are characterized to inhibit pain-like behaviors in rats [208, 258]. The enzyme, MAGL, has been identified on presynaptic axon terminals in brain, suggesting it can terminate 2-AG activity following ligand-receptor internalization by presynaptic neurons [141, 143]. The current studies reported in this thesis supports, but is not limited to, the presynaptic localization of MAGL because MAGL immunofluorescent levels were dramatically increased by neuropathy in the superficial dorsal horn of the spinal cord where afferent nociceptive fiber terminals communicate to pain processing neurons. These data extend prior reports by showing a strong decrease in spinal MAGL immunoreactivity (IR) following either i.t. AM1241 or AM1710 that is concurrent with complete reversal of allodynia. Indeed, MAGL inhibitors decrease allodynia in CCI-induced neuropathic mice [151], resulting in an increase in 2-AG accumulation that is widely characterized to produce analgesia [153]. Microglia also produce and release 2-AG, and MAGL activity has been described in microglia [145]. In support of these prior reports, studies presented in this dissertation (Chapter 3) reveals MAGL staining colocalized with Iba-1 positive microglia in spinal parenchyma and infiltrating monocytes within spinal meninges.

Surprisingly, an unremarkable minor increase of FAAH was observed following CCI-neuropathy compared to sham controls, and these levels remained unchanged following either i.t. AM1241 or AM1710 injection. As such, it is not clear from these data whether FAAH plays an important role in chronic pain produced by CCI-peripheral neuropathy given these levels remained unchanged during pain reversal. However, only a single biochemical marker was used to ascertain FAAH expression levels. Further, activity of FAAH may not be reflected in its levels of expression. The data presented here as part of my dissertation represents the only known reports addressing pain suppression concurrent with spinal modulation of endocannabinoid degradative enzymes following treatment with CB_2R agonists under neuropathic conditions.

5.2 Chronic Pain and Cannabinoid 2 Receptor Agonists

The effects of two structurally distinct CB_2R agonists, AM1241 and AM1710, on chronic bilateral allodynia produced by unilateral sciatic nerve CCI was examined in this body of work. The pattern of bilateral allodynia reported here in both mice and rats supports a number of prior reports demonstrating a similar behavioral pattern from CCI [200, 201, 203, 217, 237-239]. Bilateral biochemical changes in the spinal cord and the DRG have been examined that may, in part, characterize underlying contralateral allodynia from CCI. These studies reported bilateral increases in neuronal Fos protein [241], TNF-α protein [191], and IL-6 mRNA expression [239]. Additionally, very recent reports have demonstrated increases in unilateral spinal IL-1β mRNA expression [242], or increased IL-1β spinal IHC IR [243] following unilateral sciatic nerve ligation or transection. Further, the

endogenous IL-1β receptor antagonist, IL-1RA, contributes to the anti-inflammatory effects of activated CB_2 receptors [244]. Here I have presented evidence that both CB_2R agonists, AM1241 and AM1710 produced robust bilateral reversal from allodynia in a dose-dependent manner that may act via anti-inflammatory mechanisms. This will be discussed in greater detail below. I additionally investigated intraperitoneal drug efficacy of AM1710 and discovered that the compound's anti-allodynia and anti-inflammatory effects were not reliant on CB_1R actions. While prior reports show that peripheral administration of either AM1241 or AM1710 suppresses pathological pain induced by numerous methods, [176, 182, 198, 199, 209], such as peripheral neuropathy induced by spinal nerve ligation [182, 211] and cancer chemotherapeutic agents [176, 177, 198, 210], the current results extend these findings by showing that peri-spinal (intrathecal; i.t.) AM1241 or AM1710 injection acts to reverse CCI-induced allodynia. Intrathecal efficacy of AM1710 was not dependent on spinal CB_1R mechanisms. Importantly, neither i.t. AM1241 nor AM1710 themselves did not alter normal baseline (BL) sensory threshold responses at any dose, which is distinct from reports showing an anti-nociceptive action at peripheral nerve terminals following peripheral administration of AM1241 or AM1710 that produced increased BL sensory thresholds [165, 175, 176, 197].

5.2.1 Dorsal horn spinal cord and dorsal root ganglia IL-10

This thesis presents evidence for distinct profiles of anti-inflammatory cytokine protein expression patterns in the dorsal horn of the spinal cord and DRG. In both the dorsal horn and DRG of neuropathic rats and mice, bilateral IL-10 IR

was significantly lower compared to non-neuropathic rats and mice. While a reduction of peripheral nerve or DRG IL-10 mRNA or protein has been reported [74, 191, 236], to date, no prior reports have demonstrated decreased dorsal horn IL-10 IR in adult mice or rats during chronic allodynia from peripheral neuropathy.

5.2.2 Glial, cytokine and p38MAPK alterations in dorsal root ganglia

DRG satellite cells form a distinct sheath that completely surround sensory neurons, and together with the neuron, create a discrete morphological [71] and a functional unit [69]. Satellite DRG glia have gained increasing recognition for altering nociceptive transmission by expressing and responding to several proinflammatory cytokines including IL-1β [69, 72]. Proinflammatory factors examined in this thesis include IL-1β to provide a characterization of the anti-inflammatory effects of CB_2R agonists. In addition to IL-1β, the mitogen-activated protein kinase (MAPK) family consists of three major members that includes p38, contributes to pain sensitization following peripheral nerve injury [27, 34, 192, 195, 232, 245-248] via the actions of spinal IL-1β and other proinflammatory cytokines [249, 250]. These cytokines produce changes at the levels of both the dorsal horn spinal cord and the dorsal root ganglion, which are critical for chronic pain processing. Indeed, IL-1β rapidly activates DRG nociceptive cells in a p38MAPK-dependent manner [80]. The data in this thesis supports these reports, as increased expression of p-p38MAPK and IL-1β, in addition to GFAP, were present in the DRG of neuropathic animals. The corresponding L4-L5 DRG immunofluorescent analysis from neuropathic rats and mice revealed similar

changes in protein expression patterns. However, bilateral rat DRG changes were observed only with GFAP IR. This difference may be due to a higher sensitivity in the contralateral side of mice compared to rats as a consequence of the immune stimulus from CCI surgery. The data presented here support these prior reports in that increased p-p38MAPK IR is present in the DRG in neuropathic rats. In addition, allodynia and increased protein levels of DRG IL-1β following spinal immune activation (i.t. HIV-1 gp120) was completely prevented by i.t. AM1710 pretreatment, as measured by quantitative ELISA protein analysis. Thus immunofluorescent quantitative IL-1β changes observed from DRG in CCI neuropathic animals using IHC procedures is supported. These data extend prior reports that CB_2R agonists act in a general anti-inflammatory manner by identifying specific *in vivo* DRG changes of elevated IL-10 with concurrently diminished IL-1β.

5.2.3 Alterations in dorsal horn spinal cord

In dorsal horn spinal cord, greater bilateral astrocyte GFAP and microglial Iba-1 IR levels were quantified in neuropathic mice and rats, compared to non-neuropathic controls. Additionally, increased bilateral p-p38MAPK was assessed only in neuropathic rats. Further, an increase in unilateral spinal IL-1β IR was measured on the side ipsilateral to CCI in rats, and a bilateral increase in spinal IL-1β IR was measured in mice. However, following an i.t. AM1241 or AM1710 injection, not only was behavioral allodynia reversed, but IL-10 and IL-1β IR levels were similar to those observed in non-neuropathic animals.

Increased microglial and astocytic glial markers in the spinal cord dorsal horn in neuropathic rats and mice, as assessed by immunofluorescent detection, was detected supporting prior reports [251, 252]. Dorsal horn spinal cord astrocyte and microglial responses are recognized to participate in pathological pain found with a variety of animal models via the actions of p-p38MAPK and IL-1β [24, 194, 253].

CB_2R mRNA and immunohistochemically identified protein expression is present mostly in spinal microglia [93, 94, 135, 139, 212]. CB_2Rs in the CNS have been identified mostly on microglia [94], and prior studies reported decreased microglial activation following i.t. administration of CB_2R agonists [94, 131, 139]. Studies examining spinal cords of transgenic CB_2R knock-out mice exposed to partial sciatic nerve injury with concurrent neuropathic pain-like behaviors [93] also revealed increased bilateral dorsal horn microglial activation compared to wild-type controls. These results suggest that CB_2Rs play a regulatory role in microglial activation during peripheral neuropathic conditions. However, here I have shown that neither i.t. AM1241 nor AM1710 inhibits dorsal spinal microglial activation, as assessed by Iba-1 staining, despite full behavioral reversal of CCI-induced allodynia. Upregulation of Iba-1 is widely known to indicate active microglia [57, 255, 256]. Other markers for activated microglia include the CD11b/CD18 [268], or translocator protein (TSPO), formerly known as the peripheral benzodiazepine receptor [276] preferentially expressed in CNS macrophage/microglia. The differences in the data results from prior reports may be that these compounds act by inhibiting general spinal proinflammatory

processes while leaving microglial function intact. Importantly, increased expression of microglial Iba-1 is indicative of ongoing microglial activity, but cannot distinguish anti-inflammatory vs. proinflammatory phenotypes. Thus, it is possible that the increased microglial Iba-1 reported here may be a consequence of increased IL-10 and/or MAP-phosphatase production, which are negative regulators to several proinflammatory MAPKs [91]. This notion is supported by a prior *in vitro* study that demonstrated CB_2R ligands enhance IL-10 release from immune stimulated macrophages [257]. However, interpretations of these results are limited, given only a single microglial marker was used to examine microglial activation. Microglia are also well characterized to become activated in a proinflammatory manner due to abberant neuronal signaling under pathological conditions.

5.3 Neuron to glia link – MCP-1

The chemokine MCP-1/CCL2 is known to be released by neurons, and binds its receptor, CCR2, found on immune cells, microglia, and possibly GABAergic spinal neurons [321], and CCL2 is characterized to attract monocyte-derived cells to areas of tissue injury and insult. Its regulation is highly dynamic, and is well characterized to be upregulated in spinal and DRG neuronal cell bodies in numerous animal models of neuropathic pain [49, 78, 79, 294, 295, 314-318]. Either pharmacological or genetic suppression of MCP-1's actions under neuropathic conditions blocks the development of pain [315, 318]. We confirm prior reports demonstrating increased MCP-1 expression in both spinal cord and DRG with CCI-induced neuropathy. We show dynamic regulation of MCP-1 with

either i.p. or i.t. administration of the anti-inflammatory CB_2R agonist AM1710. I.t. AM1710 led to a significant decrease of MCP-1 in both the spinal cord and DRG neurons. I.p. AM1710 led to decreases in not only DRG MCP-1 IR, but also dorsal horn spinal cord MCP-1 IR. This early alteration of spinal MCP-1 after peripheral administration of AM1710 suggests that it may an initial driving factor regulating neuropathic pain as previously demonstrated [49, 318-322]. It has been shown that release of MCP-1 leads directly to the upregulation of IL-1β [323]. One critical factor in controlling neuropathic pain may be diminished MCP-1. Furthermore, the ability to decrease MCP-1 may be neuroprotective, as increases in MCP-1 are found in neurodegenerative diseases, such as multiple sclerosis and ALS [333].

5.4 Constitutive CB_1R modulation of inflammatory factors and a neuroprotectve endocannabinoid mechanism

As previously discussed, activation of the CB_1R on neurons is well characterized to produce relief from pathological pain signaling. Although counter-intuitive, given activation of CB_1R can produce pain relief, blocking CB_1R may prove to enhance anti-inflammation. Here, under inflammatory neuropathic conditions, the functional deletion of CB_1R produces increases of the anti-inflammatory cytokine IL-10 compared to wild-type in both spinal cord and DRG tissue, in the presence of stable allodynia. These data suggest that constitutive CB_1R expression may suppress IL-10 expression. Indeed, evidence exists that antagonism of CB_1R, or reducing the effects of constitutive CB_1R, may be beneficial in lowering pro-inflammatory factors. Chronic oral administration of AM251 reset CCI-induced

increases in inflammatory prostaglandin in blood, nitric oxide in sciatic nerve, and spinal TNF-α to basal levels [310]. In another study, chronic oral treatment with AM251 lowered the amount of spinal TNF-α in streptozotocin-induced diabetes, an inflammatory pain condition following induction of type II diabetes in rats [325]. Several reports show decreased TNF-α and IL-1β in an *in vivo* LPS inflammatory rat model whereby rats were treated with AM251 [326, 327]. Thus, in combination, these reports suggest reducing CB_1R may lead to anti-inflammatory conditions.

Constitutive actions of CB_1R on nerve terminals under neuropathic pain/inflammatory conditions may serve to be neuroprotective [261, 284, 299, 328]. However, with this vital component of the endocannabinoid system removed, as in CB_1R knockout mice, neurons are no longer protected under inflammatory conditions. Under these altered conditions, microglia may compensate, becoming more activated upon insult, as seen in the present spectral analysis data of Iba-1 IR. This increased activation did not increase pro-inflammatory IL-1β IR, but increased IR of the neuroprotective cytokine, IL-10. Although speculative, the current findings may be due to endocannabinoid binding to the CB_2R, presumably on microglia, as the CB_1R is removed.

5.5 Clinical

CB_2R agonists are emerging as favorable therapeutics over CB_1R for the treatment of chronic pain, as these compounds produce relief from pain symptoms without the commonly reported CB_1R-related side-effects, like

catalepsy and motor ataxia. CB_2R agonists may exert their actions independently from μ-opioid receptor actions, and no evidence currently exists related to the development of tolerance or addiction following CB_2R agonist administration. While CB_2R agonists appear to be highly promising as a new avenue for pain therapeutics, the actual direct CNS and DRG effects of CB_2R agonists on the endocannabinoid system are largely unknown. In addition, the CNS role in pain modulation of the endocannabinoid system is itself not fully understood.

My dissertation research has added to this understanding. Although both CB_2R agonist compounds, AM1710 and AM1241, exhibited behavioral effects which occurred within a relatively short therapeutic half-life (~3 hours and ~1.5 hours, respectively in rats), these data reveal crucial findings which may support the development of longer lasting, 'next generation' CB_2R agonists to produce therapeutic pain control. An advantage of a short therapeutic half-life is the capability to tightly regulate drug loading doses and potential unwanted side-effects. Oral formulations easily allow for repeated dosing at discrete intervals. Additionally, a short half-life for i.t. efficacy localized to the spinal cord may be advantageous as it may remain localized to spinal canal, avoiding potential whole body global inhibition of important immune function. Prior reports together with the data presented here support that the actions of both AM1710 and AM1241 are highly effective to control pathological pain when delivered either peripherally or by i.t. administration. Additionally, this report supports that pathological pain states, which can include contralateral allodynia ("mirror image" body part) is mediated by significant shifts in ipsilateral and contralateral pro- and anti-

inflammatory spinal cord cytokine milieu, as well as shifts in p38MAPK, MCP-1 and the endocannabinoid degradative enzyme, MAGL. The implication of these results is that compounds capable of acting on cytokines in the CNS, or specifically on corresponding DRG can therapeutically control clinically relevant centrally and peripherally mediated pathological pain conditions.

Although speculative, spinal CB_2R activation in humans may be necessary to reverse ongoing chronic pathological pain. This approach would preferentially target pathologically activated glia which are critical modulators of chronic neuropathic pain. Targeting glial cells including microglial cytokines, using CB_2R ligands may hold the key to unlocking an efficacious treatment for chronic pain patients.

5.6 Experimental Limitations

Chronic pain is a complex disease and is comprised of both a physiological and emotional component. As such, there are multiple alterations in sensory perceptions that change behavioral outcomes. Here I only tested one behavioral measure of chronic pain, allodynia. Therefore, the behavioral results discussed may not fully reflect behavioral outcomes of other tests commonly used to assess chronic pain symptoms in animals. Other reasonable animal behavioral tests that could have been performed include, but are not limited to: Hargreave's test/ Hot plate test, for heightened nociceptive responses. Although not necessarily indicative of pathological pain, depression, or depressive-like outcomes are often correlated to chronic pain conditions. Additionally, the forced swim test could

have been applied to examine depressive-like behavioral outcomes. However, the von Frey test is very reliable, and the results obtained and described here did not contain ambiguity regarding the effects of the compounds tested.

Additionally, I relied heavily on the use of novel spectral microscopy quantitation for much of my protein analysis work. It must be acknowledged that this method is only semi-quantitative, as I do not measure the florescent intensity output to any known protein concentration curve. These measurements do not provide the actual concentration of the proteins tested in the sample, rather the ability to say that one tissue sample has more protein than another. The other alternative protein quantitation methods that could have been employed here are either ELISA or Western Blot protein analysis. However, both of these methods rely on the grinding of tissue, which eliminates the ability to spatially observe the expression of a given protein within the tissue directly involved in an analysis. Further, I am able to discern ipsilateral vs. contralateral spinal cord dorsal horn, and as reported, the ipsilateral meningeal layer of the spinal cord dorsal horn (Chapter 3). This ability to distinguish and quantify discrete anatomical protein changes would be very difficult to reproducibly achieve with the human error associated with dissection techniques, for either ELISA or Western blot analysis.

5.7 Future Directions

It has been found that both endocannabinoids and CB_2R agonists can bind to the ligand-gated ion channel TRPV-1 [235]. TRPV-1 belongs to the family of transient receptor potential (TRP) ionic channel family, which includes TRPV-1,

TRPV-2, TRPV-4, TRPM-8 and TRPA-1 that are expressed by nociceptors. When activated, these channels are known to generate an inward flow of cations, such as Ca^{2+}. TRPV-1's are widely characterized in the periphery on nociceptive (C and Aδ fiber) nerve terminals within the skin, and cell bodies in DRG, and within the CNS [235, 334]. Activation is known to occur under noxious chemical stimulation, such as with capsaicin, the active ingredient in chili peppers, forskolin, and mustard seed oil [335]. When these compounds bind to and activate the TRPV-1, this inward flow of Ca^{2+} depolarizes neuronal signaling, leading to stimulus transduction ultimately producing the sensation of burning pain via the pain signaling pathway previously described [335]. Cross-talk also exists within the TRPV family, and it is known that activation of a TRPV-1 can not only desensitize itself, but also neighboring TRP's. It has been speculated that CB_2R agonists at least in part, exert its actions as a weak agonist for the TRPV-1 receptors generating small inward currents and Ca^{2+} accumulation. Consequently, threshold levels to produce action potentials in nociceptors are not generated [235, 336]. By potentially acting weakly as a TRPV-1 agonist, it has been speculated that CB_2R agonists are able to "desensitize" the receptor without producing pain [235, 336]. Indeed, *in vitro*, it has been demonstrated that if a TRPV-1 is bound by a CB_2R agonist, a reduction in Ca^{2+} signaling events can occur [336]. However, no report clearly demonstrates that CB_2R agonists act via TRPV-1 *in vivo*. With the use of TRPV-1 knockout mice, my future research will examine whether TRPV-1 is required for the *in vivo* efficacy of the CB_2R selective agonist AM1710. I will additionally verify wether glial activation profiles, cytokine

and chemokine expression are altered in the absence of TRPV-1 (TRPV-1 knockout mice).

6. References

1. Centers for Disease Control and Prevention, *Health, United States, 2006, With Special Feature on Pain.* 2006, Centers for Disease Control and Prevention's (CDC) National Center for Health Statistics. p. 559.

2. Argoff, C.E., et al., *Diabetic peripheral neuropathic pain: clinical and quality-of-life issues.* Mayo Clin Proc, 2006. **81**(4 Suppl): p. S3-11.

3. Christo, P.J. and D. Mazloomdoost, *Cancer pain and analgesia.* Ann N Y Acad Sci, 2008. **1138**: p. 278-98.

4. Douglas, C., J.A. Wollin, and C. Windsor, *Illness and demographic correlates of chronic pain among a community-based sample of people with multiple sclerosis.* Arch Phys Med Rehabil, 2008. **89**(10): p. 1923-32.

5. Russell, A.S., *Quality-of-life assessment in rheumatoid arthritis.* Pharmacoeconomics, 2008. **26**(10): p. 831-46.

6. Winter, Y., et al., *Health-related quality of life in ALS, myasthenia gravis and facioscapulohumeral muscular dystrophy.* J Neurol, 2010. **257**(9): p. 1473-81.

7. Guindon, J. and A.G. Hohmann, *Cannabinoid CB2 receptors: a therapeutic target for the treatment of inflammatory and neuropathic pain.* Br J Pharmacol, 2008. **153**(2): p. 319-34.

8. Stella, N., *Endocannabinoid signaling in microglial cells.* Neuropharmacology, 2009. **56 Suppl 1**: p. 244-53.

9. Craig, A.D., *Distribution of brainstem projections from spinal lamina I neurons in the cat and the monkey.* J Comp Neurol, 1995. **361**(2): p. 225-48.

10. Villanueva, L. and J.F. Bernard, *The multiplicity of ascending pain pathways.*, in *Handbook of behavioral state control: cellular and molecular mechanisms*, R. Lydic and H.A. Baghdoyan, Editors. 1999, CRC: Boca Raton, FL. p. 569-585.

11. Willis, W.D. and R.E. Coggeshall, *Sensory Mechanisms of the Spinal Cord*. 2nd Ed ed. 1991, New York: Plenum Press.

12. Berthele, A., et al., *Distribution and developmental changes in metabotropic glutamate receptor messenger RNA expression in the rat lumbar spinal cord.* Brain Res Dev Brain Res, 1999. **112**(1): p. 39-53.

13. Lawson, S.N., B.A. Crepps, and E.R. Perl, *Relationship of substance P to afferent characteristics of dorsal root ganglion neurones in guinea-pig.* J Physiol, 1997. **505 (Pt 1)**: p. 177-91.

14. Hunt, S.P. and P.W. Mantyh, *The molecular dynamics of pain control.* Nat Rev Neurosci, 2001. **2**(2): p. 83-91.

15. Costigan, M., J. Scholz, and C.J. Woolf, *Neuropathic pain: a maladaptive response of the nervous system to damage.* Annu Rev Neurosci, 2009. **32**: p. 1-32.

16. Woolf, G. and M.W. Salter, *Neuronal plasticity: increasing the gain in pain.* Science, 2000. **288**: p. 1765-1769.

17. Cook, A.J., et al., *Dynamic receptive field plasticity in rat spinal cord dorsal horn following C-primary afferent input.* Nature, 1987. **325**(7000): p. 151-3.

18. Wall, P.D. and C.J. Woolf, *The brief and the prolonged facilitatory effects of unmyelinated afferent input on the rat spinal cord are independently influenced by peripheral nerve section.* Neuroscience, 1986. **17**(4): p. 1199-205.

19. Baumbauer, K.M., E.E. Young, and R.L. Joynes, *Pain and learning in a spinal system: contradictory outcomes from common origins.* Brain Res Rev, 2009. **61**(2): p. 124-43.

20. Luo, C., et al., *Activity-dependent potentiation of calcium signals in spinal sensory networks in inflammatory pain states.* Pain, 2008. **140**(2): p. 358-67.

21. Ossipov, M.H., et al., *Spinal and supraspinal mechanisms of neuropathic pain.* Ann N Y Acad Sci, 2000. **909**: p. 12-24.

22. Ji, R.R. and C.J. Woolf, *Neuronal plasticity and signal transduction in nociceptive neurons: implications for the initiation and maintenance of pathological pain.* Neurobiol Dis, 2001. **8**(1): p. 1-10.

23. Simone, D.A., et al., *Sensitization of cat dorsal horn neurons to innocuous mechanical stimulation after intradermal injection of capsaicin.* Brain Res, 1989. **486**(1): p. 185-9.

24. DeLeo, J.A., L.S. Sorkin, and L.R. Watkins, eds. *Immune and Glial Regulation of Pain*. 2007, IASP Press: Seattle.

25. De Leo, J.A., V.L. Tawfik, and M.L. LaCroix-Fralish, *The tetrapartite synapse: Path to CNS sensitization and chronic pain.* Pain, 2006. **122**: p. 17-21.

26. Hashizume, H., et al., *Spinal glial activation and cytokine expression after lumbar root injury in the rat.* Spine, 2000. **25**: p. 1206-1217.

27. Ji, R.R., et al., *MAP kinase and pain.* Brain Res Rev, 2009. **60**(1): p. 135-48.

28. Ledeboer, A., et al., *Involvement of spinal cord nuclear factor kappaB activation in rat models of proinflammatory cytokine-mediated pain facilitation.* Eur J Neurosci, 2005. **22**: p. 1977-86.

29. Milligan, E.D. and L.R. Watkins, *Pathological and protective roles of glia in chronic pain.* Nat Rev Neurosci, 2009. **10**(1): p. 23-36.

30. Watkins, L.R., et al., *Norman Cousins Lecture. Glia as the "bad guys": implications for improving clinical pain control and the clinical utility of opioids.* Brain Behav Immun, 2007. **21**(2): p. 131-46.

31. Ji, R.R. and G. Strichartz, *Cell signaling and the genesis of neuropathic pain.* Sci STKE, 2004. **2004**(252): p. reE14.

32. White, J.P., et al., *Extracellular signal-regulated kinases in pain of peripheral origin.* Eur J Pharmacol, 2011. **650**(1): p. 8-17.

33. Gao, Y.J., et al., *JNK-induced MCP-1 production in spinal cord astrocytes contributes to central sensitization and neuropathic pain.* J Neurosci, 2009. **29**(13): p. 4096-108.

34. Jin, S.X., et al., *p38 mitogen-activated protein kinase is activated after a spinal nerve ligation in spinal cord microglia and dorsal root ganglion neurons and contributes to the generation of neuropathic pain.* J Neurosci, 2003. **23**(10): p. 4017-22.

35. Katsura, H., et al., *Activation of Src-family kinases in spinal microglia contributes to mechanical hypersensitivity after nerve injury.* J Neurosci, 2006. **26**(34): p. 8680-90.

36. Wen, Y.R., et al., *Activation of p38 mitogen-activated protein kinase in spinal microglia contributes to incision-induced mechanical allodynia.* Anesthesiology, 2009. **110**(1): p. 155-65.

37. Zhuang, Z.Y., et al., *A peptide c-Jun N-terminal kinase (JNK) inhibitor blocks mechanical allodynia after spinal nerve ligation: respective roles of JNK activation in primary sensory neurons and spinal astrocytes for neuropathic pain development and maintenance.* J Neurosci, 2006. **26**(13): p. 3551-60.

38. Choi, J.I., et al., *Peripheral inflammation induces tumor necrosis factor dependent AMPA receptor trafficking and Akt phosphorylation in spinal cord in addition to pain behavior.* Pain, 2010. **149**(2): p. 243-53.

39. White, F.A., S.K. bhangoo, and R.D. Miller, *Chemokines: Integrators of pain and inflammation.* Nature Rev, 2005. **4**: p. 834-844.

40. Willis, C.L. and T.P. Davis, *Chronic inflammatory pain and the neurovascular unit: a central role for glia in maintaining BBB integrity?* Curr Pharm Des, 2008. **14**(16): p. 1625-43.

41. Bhat, N.R., et al., *Extracellular signal-regulated kinase and p38 subgroups of mitogen-activated protein kinases regulate inducible nitric oxide synthase and tumor necrosis factor-alpha gene expression in endotoxin-stimulated primary glial cultures.* J Neurosci, 1998. **18**(5): p. 1633-41.

42. Levy, D., A. Hoke, and D.W. Zochodne, *Local expression of inducible nitric oxide synthase in an animal model of neuropathic pain.* Neurosci Lett, 1999. **260**(3): p. 207-9.

43. Levy, D. and D.W. Zochodne, *NO pain: potential roles of nitric oxide in neuropathic pain.* Pain Pract, 2004. **4**(1): p. 11-8.

44. Meller, S.T. and G.F. Gebhart, *Nitric oxide (NO) and nociceptive processing in the spinal cord.* Pain, 1993. **52**(2): p. 127-36.

45. Kato, T. and S. Kitagawa, *Regulation of neutrophil functions by proinflammatory cytokines.* Int J Hematol, 2006. **84**(3): p. 205-9.

46. Cavaillon, J.M. and D. Annane, *Compartmentalization of the inflammatory response in sepsis and SIRS.* J Endotoxin Res, 2006. **12**(3): p. 151-70.

47. Leon, B. and C. Ardavin, *Monocyte-derived dendritic cells in innate and adaptive immunity.* Immunol Cell Biol, 2008. **86**(4): p. 320-4.

48. Simmonds, R.E. and B.M. Foxwell, *Signalling, inflammation and arthritis: NF-kappaB and its relevance to arthritis and inflammation.* Rheumatology (Oxford), 2008. **47**(5): p. 584-90.

49. White, F.A., et al., *Excitatory monocyte chemoattractant protein-1 signaling is up-regulated in sensory neurons after chronic compression of the dorsal root ganglion.* Proc Natl Acad Sci U S A, 2005. **102**(39): p. 14092-7.

50. Pekny, M. and M. Pekna, *Astrocyte intermediate filaments in CNS pathologies and regeneration.* J Pathol, 2004. **204**(4): p. 428-37.

51. Eng, L.F., R.S. Ghirnikar, and Y.L. Lee, *Glial fibrillary acidic protein: GFAP-thirty-one years (1969-2000).* Neurochem Res, 2000. **25**(9-10): p. 1439-51.

52. Echeverry, S., X.Q. Shi, and J. Zhang, *Characterization of cell proliferation in rat spinal cord following peripheral nerve injury and the relationship with neuropathic pain.* Pain, 2008. **135**(1-2): p. 37-47.

53. Mika, J., et al., *Differential activation of spinal microglial and astroglial cells in a mouse model of peripheral neuropathic pain.* Eur J Pharmacol, 2009. **623**(1-3): p. 65-72.

54. Imai, Y., et al., *A novel gene iba1 in the major histocompatibility complex class III region encoding an EF hand protein expressed in a monocytic lineage.* Biochem Biophys Res Commun, 1996. **224**(3): p. 855-62.

55. McKay, S.M., et al., *Distinct types of microglial activation in white and grey matter of rat lumbosacral cord after mid-thoracic spinal transection.* J Neuropathol Exp Neurol, 2007. **66**(8): p. 698-710.

56. Mori, I., et al., *Upregulated expression of Iba1 molecules in the central nervous system of mice in response to neurovirulent influenza A virus infection.* Microbiol Immunol, 2000. **44**(8): p. 729-35.

57. Ohsawa, K., et al., *Involvement of Iba1 in membrane ruffling and phagocytosis of macrophages/microglia.* J Cell Sci, 2000. **113 (Pt 17)**: p. 3073-84.

58. Moestrup, S.K. and H.J. Moller, *CD163: a regulated hemoglobin scavenger receptor with a role in the anti-inflammatory response.* Ann Med, 2004. **36**(5): p. 347-54.

59. Porcheray, F., et al., *Macrophage activation switching: an asset for the resolution of inflammation.* Clin Exp Immunol, 2005. **142**(3): p. 481-9.

60. Yiangou, Y., et al., *COX-2, CB2 and P2X7-immunoreactivities are increased in activated microglial cells/macrophages of multiple sclerosis and amyotrophic lateral sclerosis spinal cord.* BMC Neurol, 2006. **6**: p. 12.

61. Yu, W.R., et al., *Human neuropathological and animal model evidence supporting a role for Fas-mediated apoptosis and inflammation in cervical spondylotic myelopathy.* Brain, 2011. **134**(Pt 5): p. 1277-92.

62. Horvath, R.J., et al., *Morphine tolerance attenuates the resolution of postoperative pain and enhances spinal microglial p38 and extracellular receptor kinase phosphorylation.* Neuroscience. **169**(2): p. 843-54.

63. Alkaitis, M.S., et al., *Evidence for a role of endocannabinoids, astrocytes and p38 phosphorylation in the resolution of postoperative pain.* PLoS One, 2010. **5**(5): p. e10891.

64. Ponomarev, E.D., et al., *CNS-derived interleukin-4 is essential for the regulation of autoimmune inflammation and induces a state of alternative activation in microglial cells.* J Neurosci, 2007. **27**(40): p. 10714-21.

65. Wu, Z., J. Zhang, and H. Nakanishi, *Leptomeningeal cells activate microglia and astrocytes to induce IL-10 production by releasing pro-inflammatory cytokines during systemic inflammation.* J Neuroimmunol, 2005. **167**(1-2): p. 90-8.

66. Kunori, S., et al., *A novel role of prostaglandin E2 in neuropathic pain: blockade of microglial migration in the spinal cord.* Glia, 2011. **59**(2): p. 208-18.

67. Wieseler-Frank, J., et al., *A novel immune-to-CNS communication pathway: cells of the meninges surrounding the spinal cord CSF space produce proinflammatory cytokines in response to an inflammatory stimulus.* Brain Behav Immun, 2007. **21**(5): p. 711-8.

68. Rice, T., et al., *Characterization of the early neuroinflammation after spinal cord injury in mice.* J Neuropathol Exp Neurol, 2007. **66**(3): p. 184-95.

69. Takeda, M., M. Takahashi, and S. Matsumoto, *Contribution of the activation of satellite glia in sensory ganglia to pathological pain.* Neurosci Biobehav Rev, 2009. **33**(6): p. 784-92.

70. Otoshi, K., et al., *The reactions of glial cells and endoneurial macrophages in the dorsal root ganglion and their contribution to pain-related behavior after application of nucleus pulposus onto the nerve root in rats.* Spine (Phila Pa 1976), 2010. **35**(3): p. 264-71.

71. Hanani, M., *Satellite glial cells in sensory ganglia: from form to function.* Brain Res Brain Res Rev, 2005. **48**(3): p. 457-76.

72. Takeda, M., M. Takahashi, and S. Matsumoto, *Contribution of activated interleukin receptors in trigeminal ganglion neurons to hyperalgesia via satellite glial interleukin-1beta paracrine mechanism.* Brain Behav Immun, 2008. **22**(7): p. 1016-23.

73. Skoff, A.M., C. Zhao, and J.E. Adler, *Interleukin-1alpha regulates substance P expression and release in adult sensory neurons.* Exp Neurol, 2009. **217**(2): p. 395-400.

74. Jancalek, R., et al., *Bilateral changes of TNF-alpha and IL-10 protein in the lumbar and cervical dorsal root ganglia following a unilateral chronic*

constriction injury of the sciatic nerve. J Neuroinflammation, 2010. **7**: p. 11.

75. Dubovy, P., et al., *Increased invasion of ED-1 positive macrophages in both ipsi- and contralateral dorsal root ganglia following unilateral nerve injuries.* Neurosci Lett, 2007. **427**(2): p. 88-93.

76. Hu, P., et al., *Immune cell involvement in dorsal root ganglia and spinal cord after chronic constriction or transection of the rat sciatic nerve.* Brain Behav Immun, 2007. **21**(5): p. 599-616.

77. Hu, P. and E.M. McLachlan, *Macrophage and lymphocyte invasion of dorsal root ganglia after peripheral nerve lesions in the rat.* Neuroscience, 2002. **112**(1): p. 23-38.

78. Bhangoo, S., et al., *Delayed functional expression of neuronal chemokine receptors following focal nerve demyelination in the rat: a mechanism for the development of chronic sensitization of peripheral nociceptors.* Mol Pain, 2007. **3**: p. 38.

79. Jung, H., et al., *Monocyte chemoattractant protein-1 functions as a neuromodulator in dorsal root ganglia neurons.* J Neurochem, 2008. **104**(1): p. 254-63.

80. Binshtok, A.M., et al., *Nociceptors are interleukin-1beta sensors.* J Neurosci, 2008. **28**(52): p. 14062-73.

81. Copray, J.C., et al., *Expression of interleukin-1 beta in rat dorsal root ganglia.* J Neuroimmunol, 2001. **118**(2): p. 203-11.

82. Obreja, O., et al., *IL-1 beta potentiates heat-activated currents in rat sensory neurons: involvement of IL-1RI, tyrosine kinase, and protein kinase C.* FASEB J, 2002. **16**(12): p. 1497-503.

83. Inoue, A., et al., *Interleukin-1beta induces substance P release from primary afferent neurons through the cyclooxygenase-2 system.* Journal of Neurochemistry, 1999. **73**: p. 2206-2213.

84. Ji, R.R., et al., *p38 MAPK activation by NGF in primary sensory neurons after inflammation increases TRPV1 levels and maintains heat hyperalgesia.* Neuron, 2002. **36**(1): p. 57-68.

85. Xu, J.T., et al., *p38 activation in uninjured primary afferent neurons and in spinal microglia contributes to the development of neuropathic pain induced by selective motor fiber injury.* Exp Neurol, 2007. **204**(1): p. 355-65.

86. Watkins, L.R. and S.F. Maier, *Targeting glia to control clinical pain: An idea whose time has come.* Drug Discovery Today: Therapeutic Strategies, 2004.

87. Ledeboer, A., et al., *Minocycline attenuates mechanical allodynia and proinflammatory cytokine expression in rat models of pain facilitation.* Pain, 2005. **115**: p. 71-83.

88. Liu, C.C., et al., *Prevention of paclitaxel-induced allodynia by minocycline: Effect on loss of peripheral nerve fibers and infiltration of macrophages in rats.* Mol Pain, 2010. **6**: p. 76.

89. Chang, Y.W. and S.G. Waxman, *Minocycline attenuates mechanical allodynia and central sensitization following peripheral second-degree burn injury.* J Pain, 2010. **11**(11): p. 1146-54.

90. Giuliani, F., W. Hader, and V.W. Yong, *Minocycline attenuates T cell and microglia activity to impair cytokine production in T cell-microglia interaction.* J Leukoc Biol, 2005. **78**(1): p. 135-43.

91. Romero-Sandoval, E.A., et al., *Cannabinoid receptor type 2 activation induces a microglial anti-inflammatory phenotype and reduces migration via MKP induction and ERK dephosphorylation.* Mol Pain, 2009. **5**: p. 25.

92. Walter, L., et al., *Nonpsychotropic cannabinoid receptors regulate microglial cell migration.* J Neurosci, 2003. **23**(4): p. 1398-405.

93. Racz, I., et al., *Crucial role of CB(2) cannabinoid receptor in the regulation of central immune responses during neuropathic pain.* J Neurosci, 2008. **28**(46): p. 12125-35.

94. Romero-Sandoval, A., N. Nutile-McMenemy, and J.A. DeLeo, *Spinal microglial and perivascular cell cannabinoid receptor type 2 activation reduces behavioral hypersensitivity without tolerance after peripheral nerve injury.* Anesthesiology, 2008. **108**(4): p. 722-34.

95. Calignano, A., et al., *Control of pain initiation by endogenous cannabinoids.* Nature, 1998. **394**(6690): p. 277-81.

96. Richardson, J.D., L. Aanonsen, and K.M. Hargreaves, *Antihyperalgesic effects of spinal cannabinoids.* Eur J Pharmacol, 1998. **345**(2): p. 145-53.

97. Richardson, J.D., S. Kilo, and K.M. Hargreaves, *Cannabinoids reduce hyperalgesia and inflammation via interaction with peripheral CB1 receptors.* Pain, 1998. **75**(1): p. 111-9.

98. Moriconi, A., et al., *GPR55: Current knowledge and future perspectives of a purported "Type-3" cannabinoid receptor.* Curr Med Chem, 2010. **17**(14): p. 1411-29.

99. Johns, D.G., et al., *The novel endocannabinoid receptor GPR55 is activated by atypical cannabinoids but does not mediate their vasodilator effects.* Br J Pharmacol, 2007. **152**(5): p. 825-31.

100. Lauckner, J.E., et al., *GPR55 is a cannabinoid receptor that increases intracellular calcium and inhibits M current.* Proc Natl Acad Sci U S A, 2008. **105**(7): p. 2699-704.

101. Oka, S., et al., *Identification of GPR55 as a lysophosphatidylinositol receptor.* Biochem Biophys Res Commun, 2007. **362**(4): p. 928-34.

102. Ryberg, E., et al., *The orphan receptor GPR55 is a novel cannabinoid receptor.* Br J Pharmacol, 2007. **152**(7): p. 1092-101.

103. Kotsikorou, E., et al., *Lipid bilayer molecular dynamics study of lipid-derived agonists of the putative cannabinoid receptor, GPR55.* Chem Phys Lipids, 2011. **164**(2): p. 131-43.

104. Sharir, H. and M.E. Abood, *Pharmacological characterization of GPR55, a putative cannabinoid receptor.* Pharmacol Ther, 2010. **126**(3): p. 301-13.

105. Staton, P.C., et al., *The putative cannabinoid receptor GPR55 plays a role in mechanical hyperalgesia associated with inflammatory and neuropathic pain.* Pain, 2008. **139**(1): p. 225-36.

106. Howlett, A.C., *Cannabinoid receptor signaling.* Handb Exp Pharmacol, 2005(168): p. 53-79.

107. Mitrirattanakul, S., et al., *Site-specific increases in peripheral cannabinoid receptors and their endogenous ligands in a model of neuropathic pain.* Pain, 2006. **126**(1-3): p. 102-14.

108. Svizenska, I., P. Dubovy, and A. Sulcova, *Cannabinoid receptors 1 and 2 (CB1 and CB2), their distribution, ligands and functional involvement in nervous system structures--a short review.* Pharmacol Biochem Behav, 2008. **90**(4): p. 501-11.

109. Munro, S., K.L. Thomas, and M. Abu-Shaar, *Molecular characterization of a peripheral receptor for cannabinoids.* Nature, 1993. **365**(6441): p. 61-5.

110. Bouaboula, M., et al., *Cannabinoid-receptor expression in human leukocytes.* Eur J Biochem, 1993. **214**(1): p. 173-80.

111. Galiegue, S., et al., *Expression of central and peripheral cannabinoid receptors in human immune tissues and leukocyte subpopulations.* Eur J Biochem, 1995. **232**(1): p. 54-61.

112. Bouaboula, M., et al., *Signaling pathway associated with stimulation of CB2 peripheral cannabinoid receptor. Involvement of both mitogen-activated protein kinase and induction of Krox-24 expression.* Eur J Biochem, 1996. **237**(3): p. 704-11.

113. Slipetz, D.M., et al., *Activation of the human peripheral cannabinoid receptor results in inhibition of adenylyl cyclase.* Mol Pharmacol, 1995. **48**(2): p. 352-61.

114. Bidaut-Russell, M., W.A. Devane, and A.C. Howlett, *Cannabinoid receptors and modulation of cyclic AMP accumulation in the rat brain.* J Neurochem, 1990. **55**(1): p. 21-6.

115. Howlett, A.C., *Cannabinoid inhibition of adenylate cyclase. Biochemistry of the response in neuroblastoma cell membranes.* Mol Pharmacol, 1985. **27**(4): p. 429-36.

116. Mackie, K. and B. Hille, *Cannabinoids inhibit N-type calcium channels in neuroblastoma-glioma cells.* Proc Natl Acad Sci U S A, 1992. **89**(9): p. 3825-9.

117. Liu, J., et al., *Functional CB1 cannabinoid receptors in human vascular endothelial cells.* Biochem J, 2000. **346 Pt 3**: p. 835-40.

118. Rueda, D., et al., *The CB(1) cannabinoid receptor is coupled to the activation of c-Jun N-terminal kinase.* Mol Pharmacol, 2000. **58**(4): p. 814-20.

119. Jen, T.Y., G.A. Hughes, and H. Smith, *Total synthesis of delta 8-(delta 1(6))-tetrahydrocannabinol, a biologically active constituent of hashish (marijuana).* J Am Chem Soc, 1967. **89**(17): p. 4551-2.

120. Mechoulam, R. and Y. Gaoni, *A Total Synthesis of Dl-Delta-1-Tetrahydrocannabinol, the Active Constituent of Hashish.* J Am Chem Soc, 1965. **87**: p. 3273-5.

121. Mechoulam, R. and Y. Gaoni, *Hashish. IV. The isolation and structure of cannabinolic cannabidiolic and cannabigerolic acids.* Tetrahedron, 1965. **21**(5): p. 1223-9.

122. Blair, R.E., et al., *Prolonged exposure to WIN55,212-2 causes downregulation of the CB1 receptor and the development of tolerance to its anticonvulsant effects in the hippocampal neuronal culture model of acquired epilepsy.* Neuropharmacology, 2009. **57**(3): p. 208-18.

123. Howlett, A.C., *Pharmacology of cannabinoid receptors.* Annu Rev Pharmacol Toxicol, 1995. **35**: p. 607-34.

124. Goonawardena, A.V., G. Riedel, and R.E. Hampson, *Cannabinoids alter spontaneous firing, bursting, and cell synchrony of hippocampal principal cells.* Hippocampus, 2010.

125. Chanda, P.K., et al., *Monoacylglycerol lipase activity is a critical modulator of the tone and integrity of the endocannabinoid system.* Mol Pharmacol, 2010. **78**(6): p. 996-1003.

126. Hayakawa, K., et al., *Cannabidiol potentiates pharmacological effects of Delta(9)-tetrahydrocannabinol via CB(1) receptor-dependent mechanism.* Brain Res, 2008. **1188**: p. 157-64.

127. Schlosburg, J.E., et al., *Chronic monoacylglycerol lipase blockade causes functional antagonism of the endocannabinoid system.* Nat Neurosci, 2010. **13**(9): p. 1113-9.

128. Hampson, R.E. and S.A. Deadwyler, *Cannabinoids reveal the necessity of hippocampal neural encoding for short-term memory in rats.* J Neurosci, 2000. **20**(23): p. 8932-42.

129. Robinson, L., et al., *Hippocampal endocannabinoids inhibit spatial learning and limit spatial memory in rats.* Psychopharmacology (Berl), 2008. **198**(4): p. 551-63.

130. Pertwee, R.G., *The diverse CB1 and CB2 receptor pharmacology of three plant cannabinoids: delta9-tetrahydrocannabinol, cannabidiol and delta9-tetrahydrocannabivarin.* Br J Pharmacol, 2008. **153**(2): p. 199-215.

131. Toth, C.C., et al., *Cannabinoid-mediated modulation of neuropathic pain and microglial accumulation in a model of murine type I diabetic peripheral neuropathic pain.* Mol Pain, 2010. **6**: p. 16.

132. Chopra, K., et al., *Sesamol suppresses neuro-inflammatory cascade in experimental model of diabetic neuropathy.* J Pain, 2010. **11**(10): p. 950-7.

133. Dogrul, A., et al., *Systemic and spinal administration of etanercept, a tumor necrosis factor alpha inhibitor, blocks tactile allodynia in diabetic mice.* Acta Diabetol, 2010.

134. Talbot, S., et al., *Key role for spinal dorsal horn microglial kinin B1 receptor in early diabetic pain neuropathy.* J Neuroinflammation, 2010. **7**(1): p. 36.

135. Zhang, J., et al., *Induction of CB2 receptor expression in the rat spinal cord of neuropathic but not inflammatory chronic pain models.* Eur J Neurosci, 2003. **17**(12): p. 2750-4.

136. Carlisle, S.J., et al., *Differential expression of the CB2 cannabinoid receptor by rodent macrophages and macrophage-like cells in relation to cell activation.* Int Immunopharmacol, 2002. **2**(1): p. 69-82.

137. Liu, Q.R., et al., *Species differences in cannabinoid receptor 2 (CNR2 gene): identification of novel human and rodent CB2 isoforms, differential tissue expression and regulation by cannabinoid receptor ligands.* Genes Brain Behav, 2009. **8**(5): p. 519-30.

138. Wotherspoon, G., et al., *Peripheral nerve injury induces cannabinoid receptor 2 protein expression in rat sensory neurons.* Neuroscience, 2005. **135**(1): p. 235-45.

139. Romero-Sandoval, A. and J.C. Eisenach, *Spinal cannabinoid receptor type 2 activation reduces hypersensitivity and spinal cord glial activation after paw incision.* Anesthesiology, 2007. **106**(4): p. 787-94.

140. Blankmann, J.l., G.M. Simon, and B.F. Cravatt, *A comprehensive profile of brain enzymes that hydrolyze the endocannabinoid 2-arachidonoylglycerol.* Chem Biol, 2007. **14**: p. 1347-1356.

141. Gulyas, A.I., et al., *Segregation of two endocannabinoid-hydrolyzing enzymes into pre- and postsynaptic compartments in the rat hippocampus, cerebellum and amygdala.* Eur J Neurosci, 2004. **20**(2): p. 441-58.

142. McKinney, M.K. and B.F. Cravatt, *Structure and function of fatty acid amide hydrolase.* Annu Rev Biochem, 2005. **74**: p. 411-432.

143. Dinh, T.P., T.F. Freund, and D. Piomelli, *A role for monoglyceride lipase in 2-arachidonoylglycerol inactivation.* Chem Phys Lipids, 2002. **121**(1-2): p. 149-58.

144. Witting, A., et al., *P2X7 receptors control 2-arachidonoylglycerol production by microglial cells.* Proc Natl Acad Sci U S A, 2004. **101**(9): p. 3214-9.

145. Muccioli, G.G., et al., *Identification of a novel endocannabinoid-hydrolyzing enzyme expressed by microglial cells.* J Neurosci, 2007. **27**(11): p. 2883-9.

146. Lever, I.J., et al., *Localization of the endocannabinoid-degrading enzyme fatty acid amide hydrolase in rat dorsal root ganglion cells and its*

regulation after peripheral nerve injury. J Neurosci, 2009. **29**(12): p. 3766-80.

147. Horvath, G., et al., *The role of TRPV1 receptors in the antinociceptive effect of anandamide at spinal level.* Pain, 2008. **134**(3): p. 277-84.

148. Guindon, J., J. Desroches, and P. Beaulieu, *The antinociceptive effects of intraplantar injections of 2-arachidonoyl glycerol are mediated by cannabinoid CB2 receptors.* Br J Pharmacol, 2007. **150**(6): p. 693-701.

149. Guindon, J., et al., *Peripheral antinociceptive effects of inhibitors of monoacylglycerol lipase in a rat model of inflammatory pain.* Br J Pharmacol, 2010.

150. Potenzieri, C., T.S. Brink, and D.A. Simone, *Excitation of cutaneous C nociceptors by intraplantar administration of anandamide.* Brain Res, 2009. **1268**: p. 38-47.

151. Kinsey, S.G., et al., *Blockade of endocannabinoid-degrading enzymes attenuates neuropathic pain.* J Pharmacol Exp Ther, 2009. **330**(3): p. 902-910.

152. Long, J.Z., et al., *Dual blockade of FAAH and MAGL identifies behavioral processes regulated by endocannabinoid crosstalk in vivo.* Proc Natl Acad Sci U S A, 2009. **106**(48): p. 20270-20275.

153. Sagar, D.R., et al., *Dynamic regulation of the endocannabinoid system: implications for analgesia.* Mol Pain, 2009. **5**: p. 59.

154. Piomelli, D., *The molecular logic of endocannabinoid signalling.* Nat Rev Neurosci, 2003. **4**(11): p. 873-84.

155. Beltramo, M., *Cannabinoid type 2 receptor as a target for chronic - pain.* Mini Rev Med Chem, 2009. **9**(1): p. 11-25.

156. Thakur, G.A., et al., *Latest advances in cannabinoid receptor agonists.* Expert Opin Ther Pat, 2009. **19**(12): p. 1647-73.

157. Huang, S.M., et al., *Identification of a new class of molecules, the arachidonyl amino acids, and characterization of one member that inhibits pain.* J Biol Chem, 2001. **276**(46): p. 42639-44.

158. Showalter, V.M., et al., *Evaluation of binding in a transfected cell line expressing a peripheral cannabinoid receptor (CB2): identification of cannabinoid receptor subtype selective ligands.* J Pharmacol Exp Ther, 1996. **278**(3): p. 989-99.

159. Keyse, S.M., *Dual-specificity MAP kinase phosphatases (MKPs) and cancer.* Cancer Metastasis Rev, 2008. **27**(2): p. 253-61.

160. Mukherjee, S., et al., *Species comparison and pharmacological characterization of rat and human CB2 cannabinoid receptors.* Eur J Pharmacol, 2004. **505**(1-3): p. 1-9.

161. Yao, B.B., et al., *In vitro pharmacological characterization of AM1241: a protean agonist at the cannabinoid CB2 receptor?* Br J Pharmacol, 2006. **149**(2): p. 145-54.

162. Lozano-Ondoua, A.N., et al., *A cannabinoid 2 receptor agonist attenuates bone cancer-induced pain and bone loss.* Life Sci, 2010. **86**(17-18): p. 646-53.

163. Curto-Reyes, V., et al., *Spinal and peripheral analgesic effects of the CB2 cannabinoid receptor agonist AM1241 in two models of bone cancer-induced pain.* Br J Pharmacol, 2010. **160**(3): p. 561-73.

164. Ibrahim, M.M., et al., *CB2 cannabinoid receptor activation produces antinociception by stimulating peripheral release of endogenous opioids.* Proc Natl Acad Sci U S A, 2005. **102**(8): p. 3093-8.

165. Rahn, E.J., et al., *Antinociceptive effects of racemic AM1241 and its chirally synthesized enantiomers: lack of dependence upon opioid receptor activation.* AAPS J, 2010. **12**(2): p. 147-57.

166. Hsieh, G.C., et al., *Central and peripheral sites of action for CB receptor mediated analgesic activity in chronic inflammatory and neuropathic pain models in rats.* Br J Pharmacol, 2011. **162**(2): p. 428-40.

167. Wilkerson, J.L., et al. *Cannabinoid 2 Receptor (CB2R) Selective Agonists Given Intrathecally Reverse Chronic Constriction Injury (CCI)-Induced Allodynia in Society for Neuroscience*. 2009. Chicago, IL.

168. Wilkerson, J.L., et al. *Selective cannabinoid receptor 2 (CB2) agonists administered intrathecally act as indirect agonists to differentially alter p38 MAPK production in the spinal cord and dorsal root ganglion in neuropathic rats* in *Society of Neuroscience*. 2010. San Diego.

169. Leichsenring, A., et al., *Analgesic and antiinflammatory effects of cannabinoid receptor agonists in a rat model of neuropathic pain.* Naunyn Schmiedebergs Arch Pharmacol, 2009. **379**(6): p. 627-36.

170. Valenzano, K.J., et al., *Pharmacological and pharmacokinetic characterization of the cannabinoid receptor 2 agonist, GW405833, utilizing rodent models of acute and chronic pain, anxiety, ataxia and catalepsy.* Neuropharmacology, 2005. **48**(5): p. 658-72.

171. Hu, B., et al., *Depression-like behaviour in rats with mononeuropathy is reduced by the CB2-selective agonist GW405833.* Pain, 2009. **143**(3): p. 206-12.

172. Schuelert, N., et al., *Paradoxical effects of the cannabinoid CB2 receptor agonist GW405833 on rat osteoarthritic knee joint pain.* Osteoarthritis Cartilage, 2010. **18**(11): p. 1536-43.

173. Alawi, K. and J. Keeble, *The paradoxical role of the transient receptor potential vanilloid 1 receptor in inflammation.* Pharmacol Ther, 2010. **125**(2): p. 181-95.

174. Hagenacker, T., D. Ledwig, and D. Busselberg, *Feedback mechanisms in the regulation of intracellular calcium ([Ca2+]i) in the peripheral nociceptive system: role of TRPV-1 and pain related receptors.* Cell Calcium, 2008. **43**(3): p. 215-27.

175. Khanolkar, A.D., et al., *Cannabilactones: a novel class of CB2 selective agonists with peripheral analgesic activity.* J Med Chem, 2007. **50**(26): p. 6493-500.

176. Rahn, E.J., et al., *Pharmacological characterization of AM1710, a putative cannabinoid CB(2) agonist from the cannabilactone class: Antinociception without central nervous system side-effects.* Pharmacol Biochem Behav, 2011. **98**(4): p. 493-502.

177. Rahn, E.J., et al. *Prophylactic treatment with cannabinoids suppresses the development of neuropathic nociception resulting from treatment with the chemotherapeutic agent paclitaxel in rats* in *Society for Neuroscience*. 2010. San Diego, CA.

178. Luongo, L., et al., *1-(2',4'-dichlorophenyl)-6-methyl-N-cyclohexylamine-1,4-dihydroindeno[1,2- c]pyrazole-3-carboxamide, a novel CB2 agonist, alleviates neuropathic pain through functional microglial changes in mice.* Neurobiol Dis, 2010. **37**(1): p. 177-85.

179. Xu, J.J., et al., *Pharmacological characterization of a novel cannabinoid ligand, MDA19, for treatment of neuropathic pain.* Anesth Analg, 2010. **111**(1): p. 99-109.

180. Frost, J.M., et al., *Indol-3-yl-tetramethylcyclopropyl ketones: effects of indole ring substitution on CB2 cannabinoid receptor activity.* J Med Chem, 2008. **51**(6): p. 1904-12.

181. Yao, B.B., et al., *In vitro and in vivo characterization of A-796260: a selective cannabinoid CB2 receptor agonist exhibiting analgesic activity in rodent pain models.* Br J Pharmacol, 2008. **153**(2): p. 390-401.

182. Yao, B.B., et al., *Characterization of a cannabinoid CB2 receptor-selective agonist, A-836339 [2,2,3,3-tetramethyl-cyclopropanecarboxylic acid [3-(2-methoxy-ethyl)-4,5-dimethyl-3H-thiazol-(2Z)-ylidene]-amide], using in vitro pharmacological assays, in vivo pain models, and pharmacological magnetic resonance imaging.* J Pharmacol Exp Ther, 2009. **328**(1): p. 141-51.

183. Kinsey, S.G., et al., *The CB(2) cannabinoid receptor-selective agonist O-3223 reduces pain and inflammation without apparent cannabinoid behavioral effects.* Neuropharmacology, 2010.

184. Ohta, H., et al., *Imine derivatives as new potent and selective CB2 cannabinoid receptor agonists with an analgesic action.* Bioorg Med Chem, 2008. **16**(3): p. 1111-24.

185. Gardin, A., et al., *Cannabinoid receptor agonist 13, a novel cannabinoid agonist: first in human pharmacokinetics and safety.* Drug Metab Dispos, 2009. **37**(4): p. 827-33.

186. Hosking, R.D. and J.P. Zajicek, *Therapeutic potential of cannabis in pain medicine.* Br J Anaesth, 2008. **101**(1): p. 59-68.

187. Bar-Joseph, A.F., G.; Richstein, A.; Dar, D. E.; Amselem, S.; Bar-Ilan, A.; Avidor, B.; Yacovan, A.; Meilin, S.; Weksler, A.; Berckovitch, Y. *PRS-211,375, a novel selective CB2 receptor agonist, demonstrates analgesic activity in several animal models. Program No. 909.05. 2003 Neuroscience Meeting Planner. New Orleans, LA: Society for Neuroscience, 2003. Online.* 2003.

188. Bar-Joseph, A.M., S.; Eliav, E.; Weksler, A.; Berckovitch, Y ; Richstein, A.; Avraham, A.; Efroni, G.; Yehezkel, L.; Yacovan, A.; Avidor, B.; David, P., *PRS-211,375, a novel CB2 selective cannabinoid receptor agonist demonstrates analgesic activity in two neuropathic pain models. Program No. 225.12. 2004 Neuroscience Meeting Planner. San Diego, CA: Society for Neuroscience, 2004. Online.* 2004.

189. Giblin, G.M., et al., *Discovery of 2-[(2,4-dichlorophenyl)amino]-N-[(tetrahydro- 2H-pyran-4-yl)methyl]-4-(trifluoromethyl)- 5-pyrimidinecarboxamide, a selective CB2 receptor agonist for the treatment of inflammatory pain.* J Med Chem, 2007. **50**(11): p. 2597-600.

190. Watkins, L.R., et al., *"Listening" and "talking" to neurons: implications of immune activation for pain control and increasing the efficacy of opioids.* Brain Res Rev, 2007. **56**(1): p. 148-69.

191. Schafers, M., et al., *Selective increase of tumour necrosis factor-alpha in injured and spared myelinated primary afferents after chronic constrictive injury of rat sciatic nerve.* Eur J Neurosci, 2003. **17**(4): p. 791-804.

192. Svensson, C.I., et al., *Spinal p38beta isoform mediates tissue injury-induced hyperalgesia and spinal sensitization.* J Neurochem, 2005. **92**: p. 1508-1520.

193. Boyle, D.L., et al., *Regulation of peripheral inflammation by spinal p38 MAP kinase in rats.* PLoS Med, 2006. **3**(9): p. e338.

194. Ji, R.R. and M.R. Suter, *p38 MAPK, microglial signaling, and neuropathic pain.* Mol Pain, 2007. **3**: p. 33.

195. Sorkin, L., et al., *Spinal p38 mitogen-activated protein kinase mediates allodynia induced by first-degree burn in the rat.* J Neurosci Res, 2009. **87**(4): p. 948-55.

196. Holguin, A., et al., *HIV-1 gp120 stimulates proinflammatory cytokine-mediated pain facilitation via activation of nitric oxide synthase-I (nNOS).* Pain, 2004. **110**: p. 517-530.

197. Ibrahim, M.M., et al., *CB2 cannabinoid receptor mediation of antinociception.* Pain, 2006. **122**(1-2): p. 36-42.

198. Rahn, E.J., et al., *Selective activation of cannabinoid CB2 receptors suppresses neuropathic nociception induced by treatment with the chemotherapeutic agent paclitaxel in rats.* J Pharmacol Exp Ther, 2008. **327**(2): p. 584-91.

199. Beltramo, M., et al., *CB2 receptor-mediated antihyperalgesia: possible direct involvement of neural mechanisms.* Eur J Neurosci, 2006. **23**(6): p. 1530-8.

200. Paulson, P.E., K.L. Casey, and T.J. Morrow, *Long-term changes in behavior and regional cerebral blood flow associated with painful peripheral mononeuropathy in the rat.* Pain, 2002. **95**: p. 31-40.

201. Paulson, P.E., T.J. Morrow, and K.L. Casey, *Bilateral behavioral and regional cerebral blood flow changes during painful peripheral mononeuropathy in the rat.* Pain, 2000. **84**: p. 233-245.

202. Beutler, A.S., et al., *Intrathecal gene transger by adeno-associated virus for pain.* Current Opinion in Molecular therapeutics, 2005. **7**(5): p. 431-39.

203. Loram, L.C., et al., *Enduring reversal of neuropathic pain by a single intrathecal injection of adenosine 2A receptor agonists: a novel therapy for neuropathic pain.* J Neurosci, 2009. **29**(44): p. 14015-25.

204. Milligan, E.D., et al., *Repeated intrathecal injections of plasmid DNA encoding interleukin-10 produce prolonged reversal of neuropathic pain.* Pain, 2006. **126**: p. 294-308.

205. Milligan, E.M., et al., *Glially driven enhancement of pain and its control by anti-inflammatory cytokines*, in *Immune and Glial Regulation of Pain*, J.A. De Leo, L.S. Sorkin, and L.R. Watkins, Editors. 2007, IASP Press: Seattle.

206. Schoeniger-Skinner, D.K., et al., *Interleukin-6 mediates low-threshold mechanical allodynia induced by intrathecal HIV-1 envelope glycoprotein gp120.* Brain Behav Immun, 2007. **21**(5): p. 660-7.

207. Abraham, K.E., D. McMillen, and K.L. Brewer, *The effects of endogenous interleukin-10 on gray matter damage and pain behaviors following excitotoxic spinal cord injury in the mouse.* Neurosci., 2004. **124**: p. 945-922.

208. Kinsey, S.G., et al., *Fatty acid amide hydrolase and monoacylglycerol lipase inhibitors produce anti-allodynic effects in mice through distinct cannabinoid receptor mechanisms.* J Pain, 2010. **11**(12): p. 1420-8.

209. Nackley, A.G., et al., *Activation of cannabinoid CB2 receptors suppresses C-fiber responses and windup in spinal wide dynamic range neurons in the absence and presence of inflammation.* J Neurophysiol, 2004. **92**(6): p. 3562-74.

210. Rahn, E.J., A. Makriyannis, and A.G. Hohmann, *Activation of cannabinoid CB1 and CB2 receptors suppresses neuropathic nociception evoked by the chemotherapeutic agent vincristine in rats.* Br J Pharmacol, 2007. **152**(5): p. 765-77.

211. Ibrahim, M.M., et al., *Activation of CB2 cannabinoid receptors by AM1241 inhibits experimental neuropathic pain: pain inhibition by receptors not present in the CNS.* Proc Natl Acad Sci U S A, 2003. **100**(18): p. 10529-33.

212. Cabral, G.A., et al., *CB2 receptors in the brain: role in central immune function.* Br J Pharmacol, 2008. **153**(2): p. 240-51.

213. Ehrhart, J., et al., *Stimulation of cannabinoid receptor 2 (CB2) suppresses microglial activation.* J Neuroinflammation, 2005. **2**: p. 29.

214. Chaplan, S.R., et al., *Quantitative assessment of tactile allodynia in the rat paw.* J. Neurosci. Meth., 1994. **53**: p. 55-63.

215. Milligan, E.D., et al., *Thermal hyperalgesia and mechanical allodynia produced by intrathecal administration of the Human Immunodeficiency Virus-1 (HIV-1) envelope glycoprotein, gp120.* Brain Res., 2000. **861**: p. 105-116.

216. Bennett, G.J. and K.Y. Xie, *A peripheral mononeuropathy in rat that produces disorders of pain sensation like those seen in man.* Pain, 1988. **33**: p. 87-107.

217. Milligan, E.D., et al., *Controlling neuropathic pain by adeno-associated virus driven production of the anti-inflammatory cytokine, interleukin-10.* Molecular Pain, 2005. **1**: p. 9-22.

218. Wallace, J.A., et al., *Tyrosine hydroxylase-containing neurons in the spinal cord of the chicken. I. Development and analysis of catecholamine synthesis capabilities.* Cell Mol Neurobiol, 1996. **16**(6): p. 625-48.

219. Mansfield, J.R., C. Hoyt, and R.M. Levenson, *Visualization of microscopy-based spectral imaging data from multi-label tissue sections.* Curr Protoc Mol Biol, 2008. **Chapter 14**: p. Unit 14 19.

220. Mahad, D.J., et al., *Detection of cytochrome c oxidase activity and mitochondrial proteins in single cells.* J Neurosci Methods, 2009. **184**(2): p. 310-9.

221. Treutwein, B. and H. Strasburger, *Fitting the psychometric function.* Percept Psychophys, 1999. **61**(1): p. 87-106.

222. Andres, C., et al., *Quantitative automated microscopy (QuAM) elucidates growth factor specific signalling in pain sensitization.* Mol Pain, 2010. **6**: p. 98.

223. Racz, I., et al., *Interferon-gamma is a critical modulator of CB(2) cannabinoid receptor signaling during neuropathic pain.* J Neurosci, 2008a. **28**(46): p. 12136-45.

224. Plunkett, J.A., et al., *Effects of interleukin-10 (IL-10) on pain behavior and gene expression following excitotoxic spinal cord injury in the rat.* Exper. Neurol., 2001. **168**: p. 144-154.

225. Ledeboer, A., et al. *Paclitaxel-induced mechanical allodynia in rats is inhibited by spinal delivery of plasmid DNA encoding interleukin-10*. in *Proceedings of the 11th World Congress on Pain,*. 2006. Sydney, Australia: International Association for the Study of Pain.

226. Milligan, E.D., et al., *Controlling pathological pain by adenovirally driven spinal production of the anti-inflammatory cytokine, Interleukin-10.* European Journal Neuroscience, 2005. **21**: p. 2136-2148.

227. Sloane, E., et al., *Anti-inflammatory cytokine gene therapy decreases sensory and motor dysfunction in experimental Multiple Sclerosis: MOG-EAE behavioral and anatomical symptom treatment with cytokine gene therapy.* Brain Behav Immun, 2009. **23**(1): p. 92-100.

228. Sloane, E.M., et al., *Immunological priming potentiates non-viral anti-inflammatory gene therapy treatment of neuropathic pain.* Gene Therapy, 2009(1): p. 1-13.

229. Soderquist, R.G., et al., *PEGylation of interleukin-10 for the mitigation of enhanced pain states.* Experimental Neurology, 2009. **submitted**.

230. Soderquist, R.G., et al., *Release of plasmid DNA-encoding IL-10 from PLGA microparticles facilitates long-term reversal of neuropathic pain following a single intrathecal administration.* Pharm Res, 2010. **27**(5): p. 841-54.

231. Amiji, M.M., *Polymeric Gene Delivery: Principles and Applications*. 2005, Boca Raton: CRC Press.

232. Suter, M.R., et al., *Large A-fiber activity is required for microglial proliferation and p38 MAPK activation in the spinal cord: different effects of resiniferatoxin and bupivacaine on spinal microglial changes after spared nerve injury.* Mol Pain, 2009. **5**: p. 53.

233. Tsuda, M., K. Inoue, and M.W. Salter, *Neuropathic pain and spinal microglia: a big problem from molecules in 'small' glia.* Trends in Neuroscience, 2005. **28**: p. 101-107.

234. Basavarajappa, B.S., *Critical enzymes involved in endocannabinoid metabolism.* Protein Pept Lett, 2007. **14**(3): p. 237-46.

235. Akopian, A.N., et al., *Cannabinoids desensitize capsaicin and mustard oil responses in sensory neurons via TRPA1 activation.* J Neurosci, 2008. **28**(5): p. 1064-75.

236. Jancalek, R., et al., *Bilateral changes of IL-10 protein in lumbar and cervical dorsal root ganglia following proximal and distal chronic constriction injury of peripheral nerve.* Neurosci Lett, 2011. **501**(2): p. 86-91.

237. Spataro, L.E., et al., *Spinal gap junctions: potential involvement in pain facilitation.* J Pain, 2004. **5**(7): p. 392-405.

238. Bessiere, B., et al., *A single nitrous oxide (N2O) exposure leads to persistent alleviation of neuropathic pain in rats.* J Pain. **11**(1): p. 13-23.

239. Dubovy, P., et al., *Satellite glial cells express IL-6 and corresponding signal-transducing receptors in the dorsal root ganglia of rat neuropathic pain model.* Neuron Glia Biol. **6**(1): p. 73-83.

240. Leiphart, J.W., C.V. Dills, and R.M. Levy, *Decreased spinal alpha2a- and alpha2c-adrenergic receptor subtype mRNA in a rat model of neuropathic pain.* Neurosci Lett, 2003. **349**(1): p. 5-8.

241. Ro, L.S., et al., *Territorial and extra-territorial distribution of Fos protein in the lumbar spinal dorsal horn neurons in rats with chronic constriction nerve injuries.* Brain Res, 2004. **1004**(1-2): p. 177-87.

242. Shi, X.Q., et al., *Statins alleviate experimental nerve injury-induced neuropathic pain.* Pain. **152**(5): p. 1033-43.

243. Siniscalco, D., et al., *Long-lasting effects of human mesenchymal stem cell systemic administration on pain-like behaviors, cellular, and biomolecular modifications in neuropathic mice.* Front Integr Neurosci. **5**: p. 79.

244. Molina-Holgado, F., et al., *Endogenous interleukin-1 receptor antagonist mediates anti-inflammatory and neuroprotective actions of cannabinoids in neurons and glia.* J Neurosci, 2003. **23**(16): p. 6470-4.

245. Svensson, C.I., et al., *Activation of p38 MAP Kinase in spinal microglia is a critical link in inflammation induced spinal pain processing.* J Neurochem, 2003. **in press**.

246. Svensson, C.I., et al., *Spinal blockade of TNF blocks spinal nerve ligation-induced increases in spinal P-p38.* Neurosci Lett, 2005. **379**(3): p. 209-13.

247. Zhuang, Z.Y., et al., *ERK is sequentially activated in neurons, microglia, and astrocytes by spinal nerve ligation and contributes to mechanical allodynia in this neuropathic pain model.* Pain, 2005. **114**(1-2): p. 149-59.

248. Zhuang, Z.-Y., et al., *Role of the CX3CR1/p38 MAPK pathway in spinal microglia for the development of neuropathic pain following nerve injury-induced cleavage of fractalkine.* Brain Behav Immun., 2007. **21**(5): p. 642-651.

249. Liu, Y.L., et al., *Tumor necrosis factor-alpha induces long-term potentiation of C-fiber evoked field potentials in spinal dorsal horn in rats with nerve injury: the role of NF-kappa B, JNK and p38 MAPK.* Neuropharmacology, 2007. **52**(3): p. 708-15.

250. Kawasaki, Y., et al., *Cytokine mechanisms of central sensitization: Distinct and overlapping role of interleukin-1b, interleukin-6, and tumor necrosis factor-a in regulating syntapic and neuronal activity in the superficial spinal cord.* J Neurosci, 2008. **28**(20): p. 5189-5194.

251. Obata, H., et al., *Activation of astrocytes in the spinal cord contributes to the development of bilateral allodynia after peripheral nerve injury in rats.* Brain Res, 2010. **1363**: p. 72-80.

252. Schreiber, K.L., A.J. Beitz, and G.L. Wilcox, *Activation of spinal microglia in a murine model of peripheral inflammation-induced, long-lasting contralateral allodynia.* Neurosci Lett, 2008. **440**(1): p. 63-7.

253. Scholz, J. and C.J. Woolf, *The neuropathic pain triad: neurons, immune cells, and glia.* Nat Neuroscience, 2007. **10**(11): p. 1361-68.

254. Romero-Sandoval, E.A., R.J. Horvath, and J.A. Deleo, *Neuroimmune interactions and pain: Focus on glial-modulating targets.* Curr Opin Investig Drugs, 2008. **9**(7): p. 726-34.

255. Ibrahim, A.S., et al., *Genistein attenuates retinal inflammation associated with diabetes by targeting of microglial activation.* Mol Vis, 2010. **16**: p. 2033-42.

256. Kraft, A.D., et al., *Activated microglia proliferate at neurites of mutant huntingtin-expressing neurons.* Neurobiol Aging, 2011.

257. Correa, F., et al., *Activation of cannabinoid CB2 receptor negatively regulates IL-12p40 production in murine macrophages: role of IL-10 and ERK1/2 kinase signaling.* Br J Pharmacol, 2005. **145**(4): p. 441-8.

258. Martin, W.J., C.M. Loo, and A.I. Basbaum, *Spinal cannabinoids are anti-allodynic in rats with persistent inflammation.* Pain, 1999. **82**(2): p. 199-205.

259. Choi, S. and W.J. Friedman, *Inflammatory cytokines IL-1beta and TNF-alpha regulate p75NTR expression in CNS neurons and astrocytes by distinct cell-type-specific signalling mechanisms.* ASN Neuro, 2009. **1**(2).

260. Martin, A., et al., *Evaluation of the PBR/TSPO radioligand [(18)F]DPA-714 in a rat model of focal cerebral ischemia.* J Cereb Blood Flow Metab, 2010. **30**(1): p. 230-41.

261. Ahmed, M.M., et al., *Cannabinoid subtype-2 receptors modulate the antihyperalgesic effect of WIN 55,212-2 in rats with neuropathic spinal cord injury pain.* Spine J, 2010. **10**(12): p. 1049-54.

262. Watkins, L.R., et al., *The "toll" of opioid-induced glial activation: improving the clinical efficacy of opioids by targeting glia.* Trends Pharmacol Sci, 2009. **30**(11): p. 581-91.

263. Siemionow, K., et al., *The effects of inflammation on glial fibrillary acidic protein expression in satellite cells of the dorsal root ganglion.* Spine (Phila Pa 1976), 2009. **34**(16): p. 1631-7.

264. Haddad, J.J., N.E. Saade, and B. Safieh-Garabedian, *Interleukin-10 and the regulation of mitogen-activated protein kinases: are these signalling modules targets for the anti-inflammatory action of this cytokine?* Cell Signal, 2003. **15**(3): p. 255-67.

265. Milligan, E.D., et al., *An initial investigation of spinal mechanisms underlying pain enhancement induced by fractalkine, a neuronally released chemokine.* Eur J Neurosci, 2005. **22**: p. 2775-2782.

266. Sacerdote, P., et al., *In vivo and in vitro treatment with the synthetic cannabinoid CP55, 940 decreases the in vitro migration of macrophages in the rat: involvement of both CB1 and CB2 receptors.* J Neuroimmunol, 2000. **109**(2): p. 155-63.

267. Banerjee, A. and S. Gerondakis, *Coordinating TLR-activated signaling pathways in cells of the immune system.* Immunol Cell Biol, 2007. **85**(6): p. 420-4.

268. Milligan, E.D., et al., *Intrathecal HIV-1 envelope glycoprotein gp120 induces enhanced pain states mediated by spinal cord proinflammatory cytokines.* J Neurosci, 2001. **21**(8): p. 2808-19.

269. Milligan, E.D., et al., *A method for increasing the viability of the external portion of lumbar catheters placed in the spinal subarachnoid space of rats.* J Neurosci Methods, 1999. **90**(1): p. 81-6.

270. Tsuda, M., et al., *JAK-STAT3 pathway regulates spinal astrocyte proliferation and neuropathic pain maintenance in rats.* Brain. **134**(Pt 4): p. 1127-39.

271. Obata, K., et al., *Role of mitogen-activated protein kinase activation in injured and intact primary afferent neurons for mechanical and heat hypersensitivity after spinal nerve ligation.* J Neurosci, 2004. **24**(45): p. 10211-22.

272. Gao, Y.J. and R.R. Ji, *Targeting astrocyte signaling for chronic pain.* Neurotherapeutics, 2010. **7**(4): p. 482-93.

273. Kim, D.S., et al., *Profiling of dynamically changed gene expression in dorsal root ganglia post peripheral nerve injury and a critical role of injury-induced glial fibrillary acidic protein in maintenance of pain behaviors [corrected].* Pain, 2009. **143**(1-2): p. 114-22.

274. Ahmed, Z., et al., *Actin-binding proteins coronin-1a and IBA-1 are effective microglial markers for immunohistochemistry.* J Histochem Cytochem, 2007. **55**(7): p. 687-700.

275. Kanazawa, H., et al., *Macrophage/microglia-specific protein Iba1 enhances membrane ruffling and Rac activation via phospholipase C-gamma -dependent pathway.* J Biol Chem, 2002. **277**(22): p. 20026-32.

276. Chauveau, F., et al., *Nuclear imaging of neuroinflammation: a comprehensive review of [11C]PK11195 challengers.* Eur J Nucl Med Mol Imaging, 2008. **35**(12): p. 2304-19.

277. Moore, K.W., et al., *Interleukin-10 and the interleukin-10 receptor.* Annu Rev Immunol, 2001. **19**: p. 683-765.

278. Milligan, E.D., et al., *Systemic administration of CNI-1493, a p38 mitogen-activated protein kinase inhibitor, blocks intrathecal human immunodeficiency virus-1 gp120-induced enhanced pain states in rats.* J Pain, 2001b. **2**(6): p. 326-333.

279. White, F.A., H. Jung, and R.J. Miller, *Chemokines and the pathophysiology of neuropathic pain.* Proc Natl Acad Sci U S A, 2007. **104**(51): p. 20151-8.

280. McMahon, S.B., W.B.J. Cafferty, and F. Marchand, *Immune and glial cell factors as pain mediators and modulators.* Experimental Neurology, 2005. **192**: p. 444-462.

281. Inoue, K., *The function of microglia through purinergic receptors: Neuropathic pain and cytokine release*

Pharmacology and Therapeutics, 2006. **109**: p. 210 – 226.

282. Watkins, L.R., E.D. Milligan, and S.F. Maier, *Glial activation: a driving force for pathological pain.* Trends in Neuroscience, 2001. **24**: p. 450-455.

283. Son, Y., et al., *Mitogen-Activated Protein Kinases and Reactive Oxygen Species: How Can ROS Activate MAPK Pathways?* J Signal Transduct. **2011**: p. 792639.

284. Eljaschewitsch, E., et al., *The endocannabinoid anandamide protects neurons during CNS inflammation by induction of MKP-1 in microglial cells.* Neuron, 2006. **49**(1): p. 67-79.

285. van Noort, J.M., *Stress proteins in CNS inflammation.* J Pathol, 2008. **214**(2): p. 267-75.

286. Alpini, G. and S. Demorrow, *Changes in the endocannabinoid system may give insight into new and effective treatments for cancer.* Vitam Horm, 2009. **81**: p. 469-85.

287. Goldsmith, M., et al., *Synergistic IL-10 induction by LPS and the ceramide-1-phosphate analog PCERA-1 is mediated by the cAMP and p38 MAP kinase pathways.* Mol Immunol, 2009. **46**(10): p. 1979-87.

288. Goldsmith, M., et al., *A ceramide-1-phosphate analogue, PCERA-1, simultaneously suppresses tumour necrosis factor-alpha and induces interleukin-10 production in activated macrophages.* Immunology, 2009. **127**(1): p. 103-15.

289. Agrawal, S. and E.R. Kandimalla, *Synthetic agonists of Toll-like receptors 7, 8 and 9.* Biochem Soc Trans, 2007. **35**(Pt 6): p. 1461-7.

290. DeLeo, J.A. and R.W. Colburn, *Proinflammatory cytokines and glial cells: Their role in neuropathic pain*, in *Cytokines and Pain*, L.R. Watkins and S.F. Maier, Editors. 1999, Birkhauser: Basel. p. 159-182.

291. Benveniste, E.N., *Intracellular signaling cascades in glia*, in *Immune and Glial Regulation of Pain*, J.A. DeLeo, L.S. Sorkin, and L.R. Watkins, Editors. 2007, IASP Press: Seattle. p. 43-63.

292. Milligan, E.D., et al., *Spinal glia and proinflammatory cytokines mediate mirror-image neuropathic pain in rats.* J Neuroscience, 2003. **23**: p. 1026-1040.

293. Abdallah, B., et al., *A powerful nonviral vector for In Vivo gene transfer into the adult mammalian brain: Polyethylenimine.* Human Gene Therapy, 1996. **7**: p. 1947-1954.

294. Hu, J.H., et al., *Involvement of spinal monocyte chemoattractant protein-1 (MCP-1) in cancer-induced bone pain in rats.* Neurosci Lett. **517**(1): p. 60-3.

295. Jeon, S.M., K.M. Lee, and H.J. Cho, *Expression of monocyte chemoattractant protein-1 in rat dorsal root ganglia and spinal cord in experimental models of neuropathic pain.* Brain Res, 2009. **1251**: p. 103-11.

296. Ledeboer, A.M., et al., *Intrathecal interleukin-10 gene therapy attenuates paclitaxel-induced mechanical allodynia and proinflammatory cytokine expression in dorsal root ganglia in rats.* Brain Behavior and Immunity, 2007. **21**(5): p. 686-698.

297. Milligan, E.D., et al., *Intrathecal polymer-based interleukin-10* gene delivery for neuropathic pain.* Neuron Glia Biology, 2006. **2**: p. 293-308.

298. Salio, C., et al., *Pre- and postsynaptic localizations of the CB1 cannabinoid receptor in the dorsal horn of the rat spinal cord.* Neuroscience, 2002. **110**(4): p. 755-64.

299. Maresz, K., et al., *Direct suppression of CNS autoimmune inflammation via the cannabinoid receptor CB1 on neurons and CB2 on autoreactive T cells.* Nat Med, 2007. **13**(4): p. 492-7.

300. Wilkerson, J.L., et al., *Intrathecal cannabilactone CB(2)R agonist, AM1710, controls pathological pain and restores basal cytokine levels.* Pain. **153**(5): p. 1091-106.

301. Wilkerson, J.L., et al., *Immunofluorescent spectral analysis reveals the intrathecal cannabinoid agonist, AM1241, produces spinal anti-inflammatory cytokine responses in neuropathic rats exhibiting relief from allodynia.* Brain Behav. **2**(2): p. 155-77.

302. Yamamoto, W., T. Mikami, and H. Iwamura, *Involvement of central cannabinoid CB2 receptor in reducing mechanical allodynia in a mouse model of neuropathic pain.* Eur J Pharmacol, 2008. **583**(1): p. 56-61.

303. Ledent, C., et al., *Unresponsiveness to cannabinoids and reduced addictive effects of opiates in CB1 receptor knockout mice.* Science, 1999. **283**(5400): p. 401-4.

304. Wilkerson, J., Alberti, L., Wallace, J., Kerwin, A., Dengler, E., Bowman, B., Platero, P., Thakur, G., Makriyannis, A., Ledent, C., and E. Milligan *Selective cannabinoid receptor 2 (CB2R) agonist AM1710 acts independently of cannabinoid receptor 1 (CB1R) responses in neuropathic CB1R -/- mice.* J Pain, 2012. **13**(4, Supplement 1).

305. Murphy, P.G., et al., *Endogenous interleukin-6 contributes to hypersensitivity to cutaneous stimuli and changes in neuropeptides associated with chronic nerve constriction in mice.* Eur J Neurosci, 1999. **11**(7): p. 2243-53.

306. Ramer, M.S., G.D. French, and M.A. Bisby, *Wallerian degeneration is required for both neuropathic pain and sympathetic sprouting into the DRG.* Pain, 1997. **72**(1-2): p. 71-8.

307. Gu, X., et al., *Intrathecal administration of the cannabinoid 2 receptor agonist JWH015 can attenuate cancer pain and decrease mRNA expression of the 2B subunit of N-methyl-D-aspartic acid.* Anesth Analg. **113**(2): p. 405-11.

308. Dworkin, R.H., et al., *Pharmacologic management of neuropathic pain: evidence-based recommendations.* Pain, 2007. **132**(3): p. 237-51.

309. Comelli, F., et al., *Rimonabant, a cannabinoid CB1 receptor antagonist, attenuates mechanical allodynia and counteracts oxidative stress and nerve growth factor deficit in diabetic mice.* Eur J Pharmacol. **637**(1-3): p. 62-9.

310. Costa, B., et al., *Effect of the cannabinoid CB1 receptor antagonist, SR141716, on nociceptive response and nerve demyelination in rodents with chronic constriction injury of the sciatic nerve.* Pain, 2005. **116**(1-2): p. 52-61.

311. Naderi, N., et al., *The interaction between intrathecal administration of low doses of palmitoylethanolamide and AM251 in formalin-induced pain related behavior and spinal cord IL1-beta expression in rats.* Neurochem Res. **37**(4): p. 778-85.

312. Castane, A., et al., *Development and expression of neuropathic pain in CB1 knockout mice.* Neuropharmacology, 2006. **50**(1): p. 111-22.

313. Kress, M. and R. Kuner, *Mode of action of cannabinoids on nociceptive nerve endings.* Exp Brain Res, 2009. **196**(1): p. 79-88.

314. Dansereau, M.A., et al., *Spinal CCL2 pronociceptive action is no longer effective in CCR2 receptor antagonist-treated rats.* J Neurochem, 2008. **106**(2): p. 757-69.

315. Echeverry, S., et al., *Peripheral Nerve Injury Alters Blood-Spinal Cord Barrier Functional and Molecular Integrity through a Selective Inflammatory Pathway.* J Neurosci, 2011. **31**(30): p. 10819-28.

316. Morin, N., et al., *Neutrophils invade lumbar dorsal root ganglia after chronic constriction injury of the sciatic nerve.* J Neuroimmunol, 2007. **184**(1-2): p. 164-71.

317. Zhang, J. and Y. De Koninck, *Spatial and temporal relationship between monocyte chemoattractant protein-1 expression and spinal glial activation following peripheral nerve injury.* J Neurochem, 2006. **97**(3): p. 772-83.

318. Zhang, J., et al., *Expression of CCR2 in both resident and bone marrow-derived microglia plays a critical role in neuropathic pain.* J Neurosci, 2007. **27**(45): p. 12396-406.

319. Jung, H., et al., *Visualization of chemokine receptor activation in transgenic mice reveals peripheral activation of CCR2 receptors in states of neuropathic pain.* J Neurosci, 2009. **29**(25): p. 8051-62.

320. Tanaka, T., et al., *Enhanced production of monocyte chemoattractant protein-1 in the dorsal root ganglia in a rat model of neuropathic pain:*

possible involvement in the development of neuropathic pain. Neurosci Res, 2004. **48**(4): p. 463-9.

321. Gosselin, R.D., et al., *Constitutive expression of CCR2 chemokine receptor and inhibition by MCP-1/CCL2 of GABA-induced currents in spinal cord neurones.* J Neurochem, 2005. **95**(4): p. 1023-34.

322. Thacker, M.A., et al., *CCL2 is a key mediator of microglia activation in neuropathic pain states.* Eur J Pain, 2009. **13**(3): p. 263-72.

323. Old, E.A. and M. Malcangio, *Chemokine mediated neuron-glia communication and aberrant signalling in neuropathic pain states.* Curr Opin Pharmacol. **12**(1): p. 67-73.

324. Menetski, J., et al., *Mice overexpressing chemokine ligand 2 (CCL2) in astrocytes display enhanced nociceptive responses.* Neuroscience, 2007. **149**(3): p. 706-14.

325. Liu, W.J., et al., *Effect of rimonabant, the cannabinoid CB1 receptor antagonist, on peripheral nerve in streptozotocin-induced diabetic rat.* Eur J Pharmacol. **637**(1-3): p. 70-6.

326. Roche, M., et al., *In vivo modulation of LPS-induced alterations in brain and peripheral cytokines and HPA axis activity by cannabinoids.* J Neuroimmunol, 2006. **181**(1-2): p. 57-67.

327. Roche, M., et al., *Augmentation of endogenous cannabinoid tone modulates lipopolysaccharide-induced alterations in circulating cytokine levels in rats.* Immunology, 2008. **125**(2): p. 263-71.

328. Pacher, P. and G. Hasko, *Endocannabinoids and cannabinoid receptors in ischaemia-reperfusion injury and preconditioning.* Br J Pharmacol, 2008. **153**(2): p. 252-62.

329. Miranville, A., et al., *Reversal of inflammation-induced impairment of glucose uptake in adipocytes by direct effect of CB1 antagonism on adipose tissue macrophages.* Obesity (Silver Spring). **18**(12): p. 2247-54.

330. Smith, S.R., C. Terminelli, and G. Denhardt, *Modulation of cytokine responses in Corynebacterium parvum-primed endotoxemic mice by centrally administered cannabinoid ligands.* Eur J Pharmacol, 2001. **425**(1): p. 73-83.

331. Smith, S.R., C. Terminelli, and G. Denhardt, *Effects of cannabinoid receptor agonist and antagonist ligands on production of inflammatory cytokines and anti-inflammatory interleukin-10 in endotoxemic mice.* J Pharmacol Exp Ther, 2000. **293**(1): p. 136-50.

332. Zhang, M., et al., *Modulation of the balance between cannabinoid CB(1) and CB(2) receptor activation during cerebral ischemic/reperfusion injury.* Neuroscience, 2008. **152**(3): p. 753-60.

333. Brohede, U., et al., *Sustained release from mesoporous nanoparticles: evaluation of structural properties associated with release rate.* Curr Drug Deliv, 2008. **5**(3): p. 177-85.

334. Barbara, G., et al., *T-type calcium channel inhibition underlies the analgesic effects of the endogenous lipoamino acids.* J Neurosci, 2009. **29**(42): p. 13106-14.

335. Bianchi, B.R., et al., *Modulation of human TRPV1 receptor activity by extracellular protons and host cell expression system.* Eur J Pharmacol, 2006. **537**(1-3): p. 20-30.

336. Akopian, A.N., et al., *Role of ionotropic cannabinoid receptors in peripheral antinociception and antihyperalgesia.* Trends Pharmacol Sci, 2009. **30**(2): p. 79-84.

Appendix A: Supplemental Figures

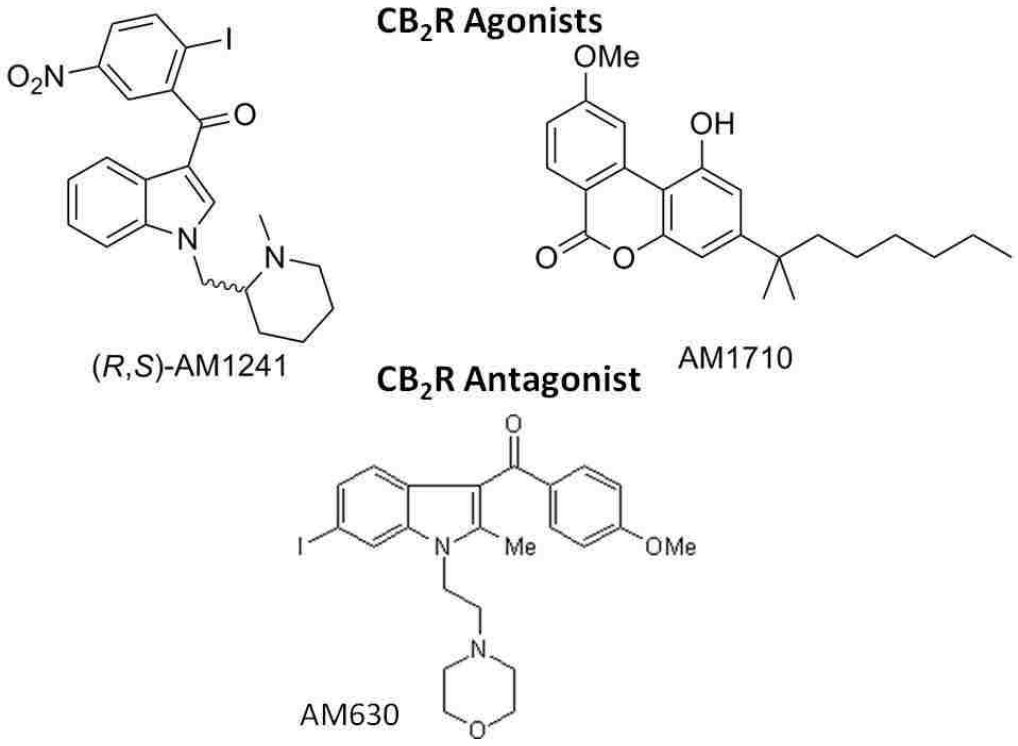

Supplemental Figure A.1

Chemical structures of CB_2R agonists and antagonist utilized in all experiments.

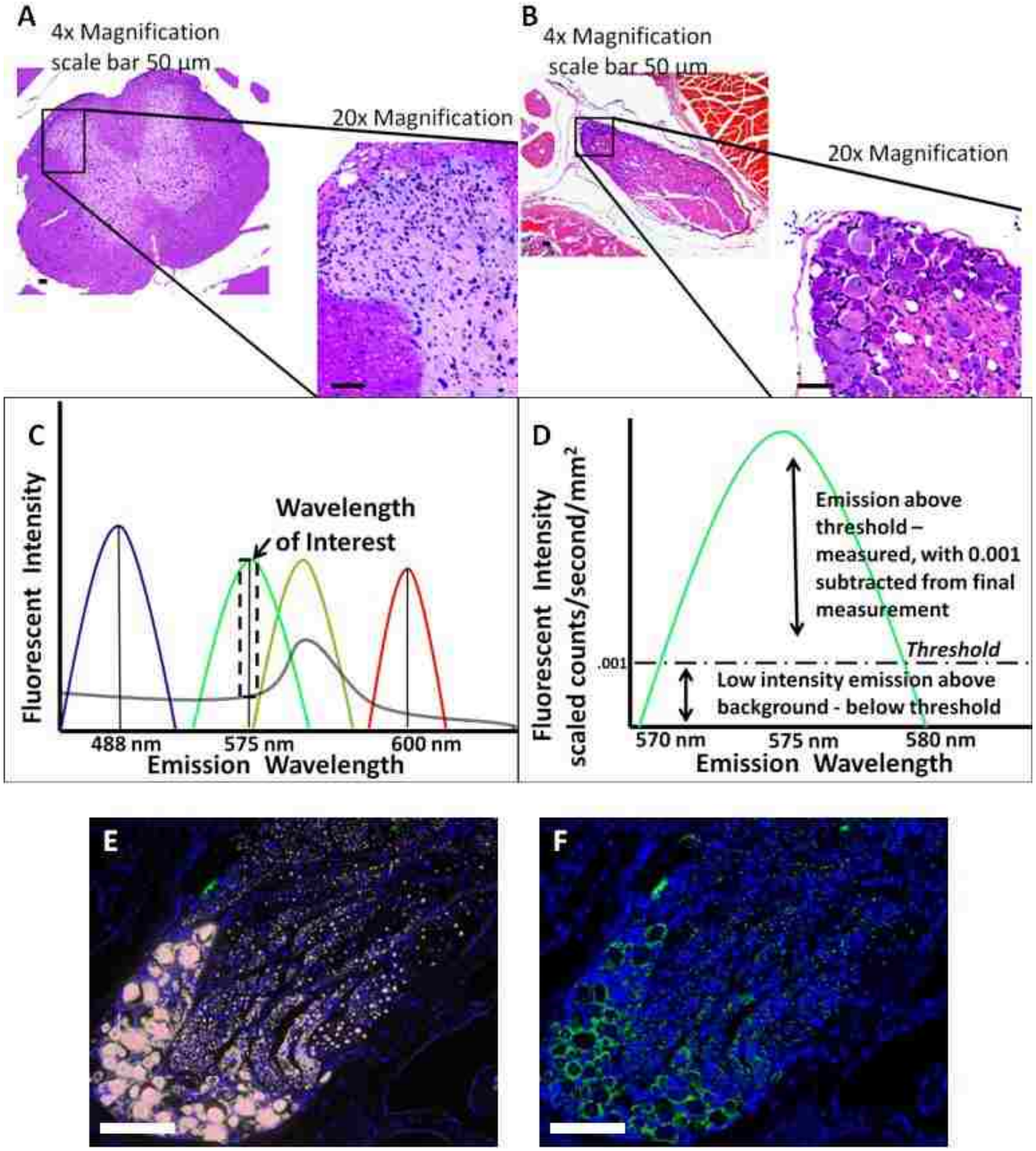

Supplemental Figure A.2

Anatomical location of images acquired and spectral analysis allows for discrete fluorescence signal detection and analysis. **A**, Hematoxylin and eosin staining of the dorsal horn of the spinal cord and **B**, dorsal root ganglion (area within black box) is displayed in context to relevant anatomical structures (the entire spinal cord and partial cauda equina, respectively)at 4x magnification, and then at 20x magnification. **C**, Representative fluorescent emission for DAPI (blue) FITC (light green), GFP (dark green) Rhodamine Red (red) and autofluorescence (double black). Selection of narrow fluorescent peak emission bands (dotted black box around FITC wavelength) allows for analysis of only FITC signal, without autoflourescent or GFP signal contaminating fluorescent analysis. **D**, Representative fluorescent emission threshold level of FITC defined and expanded from dotted black box in **A**, with the fluorescent threshold of intensity set (dashed black line), above autofluorescent levels. **E,** Representative spectral image of dorsal

root ganglion as stained for IL-10 (green), with autofluorescent signal defined in pink. **F**, Same image in **E**, with autofluorescent signal removed. In all images the scale bar is equal to 50 µm.

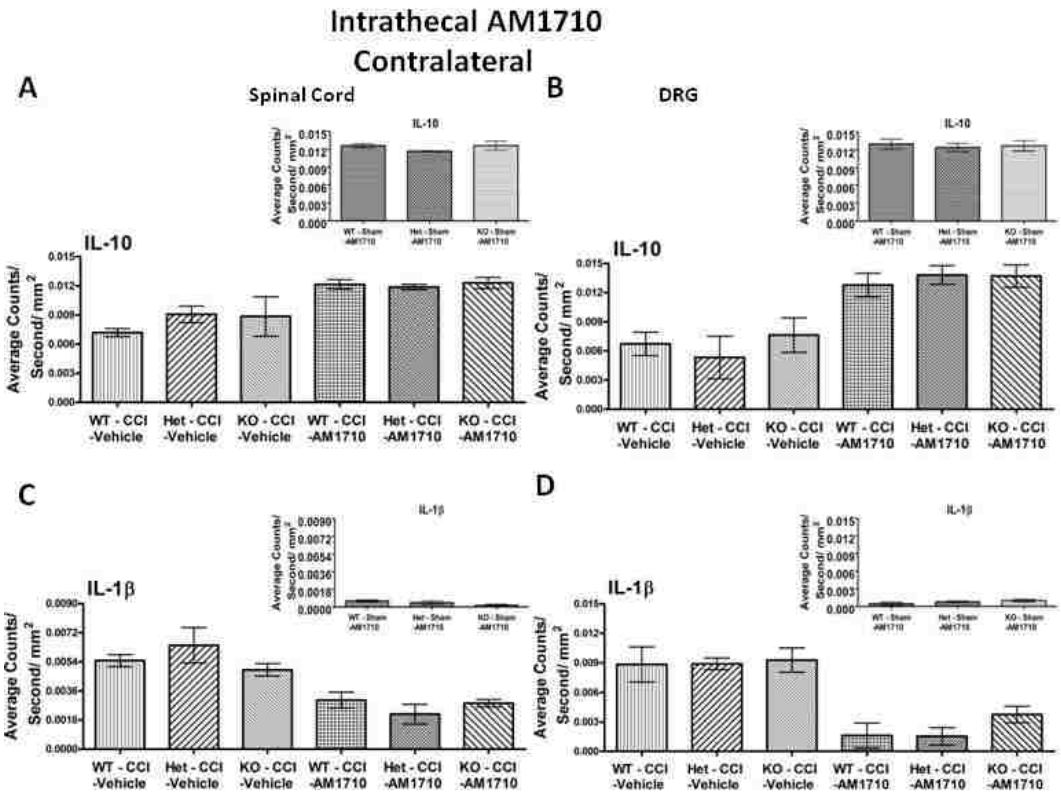

Supplemental Figure A.3

Contralateral immunofluorescent intensity quantification from 7 µm thick sections of dorsal horn spinal cord and corresponding DRG from behaviorally verified CB_1R KO, Het, WT mice, following i.t. vehicle or AM1710. **A,** IL-10 expression in contralateral dorsal horn spinal cord was decreased in CCI-treated mice that received i.t. vehicle compared to control sham-treated mice given AM1710, while IL-10 IR recovered to sham levels in CCI neuropathic mice given i.t. AM1710. **B,** Contralateral IL-10 expression in DRG was decreased in CCI-treated mice that received i.t. vehicle compared to control sham-treated mice given AM1710, while IL-10 IR recovered to sham levels in CCI neuropathic mice given i.t. AM1710. **C**, Compared to sham controls, IL-1β expression was increased in the contralateral dorsal horn spinal cord of CCI-treated animals given i.t. vehicle of AM1710. However, i.t. AM1710 in CCI-treated mice robustly suppressed increases in IL-1β IR. **D**, Compared to sham controls, IL-1β expression was increased in the contralateral DRG of CCI-treated animals given i.t. vehicle of AM1710. However, i.t. AM1710 in CCI-treated mice robustly suppressed increases in IL-1β IR.

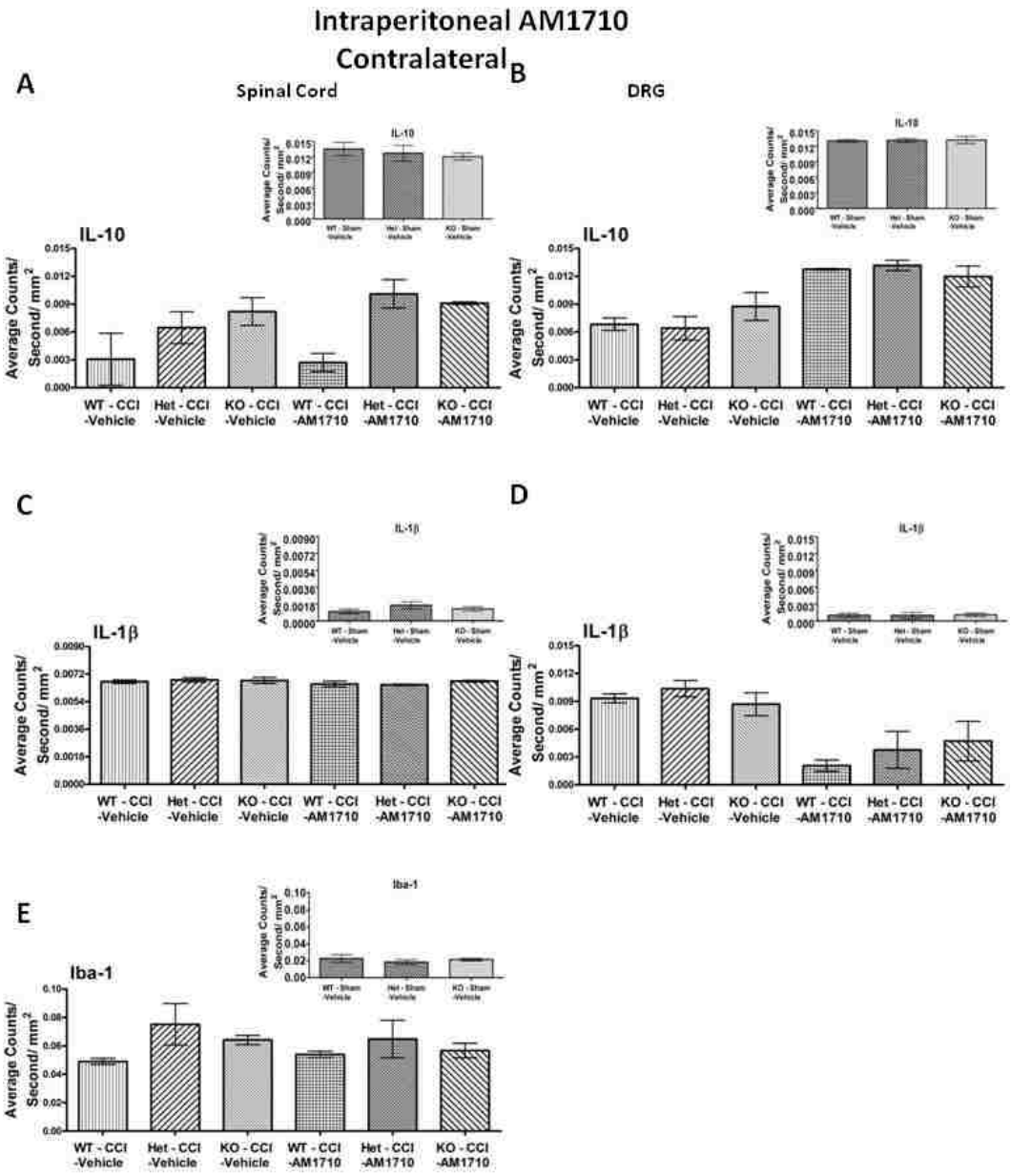

Supplemental Figure A.4

Contralateral immunofluorescent intensity quantification from 7 µm thick sections of dorsal horn spinal cord and corresponding DRG from behaviorally verified CB_1R KO, Het, WT mice, following i.p. vehicle or AM1710. **A,** IL-10 expression in contralateral dorsal horn spinal cord was decreased in CCI-treated mice that received i.p. vehicle compared to control sham-treated mice given AM1710, and IL-10 IR remained unchanged at neuropathic levels in CCI neuropathic mice given i.p. AM1710. **B,** IL-10 expression in contralateral DRG was decreased in CCI-treated mice that received i.p. vehicle compared to control sham-treated mice given AM1710, while IL-10 IR recovered to sham levels in CCI neuropathic mice given i.p. AM1710. **C**, Compared to sham controls, IL-1β expression was increased in the contralateral dorsal horn spinal cord of CCI-treated animals given i.p. vehicle of AM1710. Intraperitoneal AM1710 in CCI-treated mice did not alter increases in IL-1β IR. **D**, Compared to sham controls, IL-1β expression was increased in the contralateral DRG of CCI-treated animals given i.p. vehicle of AM1710. However, i.p. AM1710 in CCI-treated mice robustly suppressed increases in IL-1β IR.

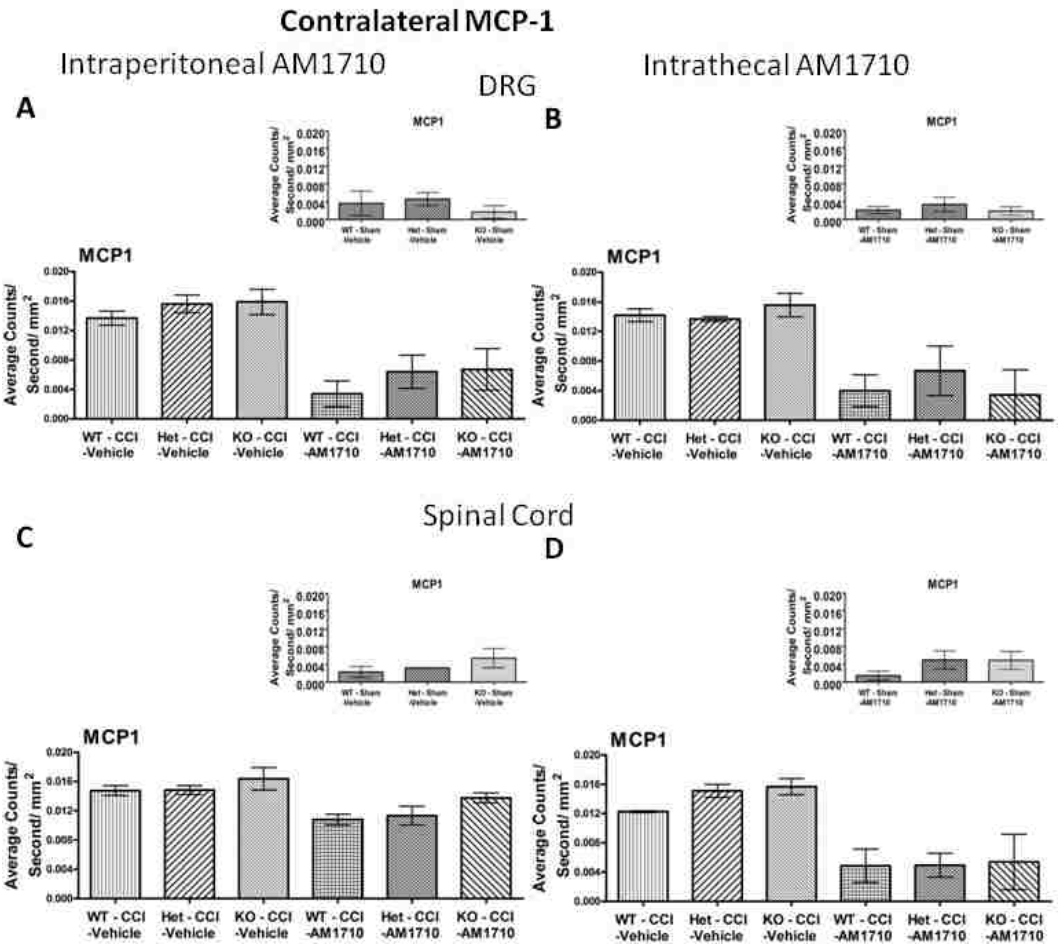

Supplemental Figure A.5

Contralateral immunofluorescent intensity quantification of DRG and spinal cord dorsal horn reveals both i.p. and i.t. AM1710 administration reduces the expression of the chemokine MCP-1. **A**, **B**, Compared to control mice, contralateral DRG MCP-1 IR expression was increased in CCI-treated neuropathic mice that received either i.p. or i.t vehicle of AM1710, while DRG MCP-1 IR in CCI-treated mice given either i.p. or i.t. AM1710 was substantially reduced. All sections were 7 □m in thickness. **C**, **D**, Compared to control mice, contralateral dorsal horn spinal cord MCP-1 IR expression was increased in CCI-treated neuropathic mice that received either i.p. or i.t vehicle of AM1710, while dorsal horn spinal cord MCP-1 IR in CCI-treated mice given either i.p. or i.t. AM1710 was substantially reduced.